Dissecting the regulation of entry into gametogenesis in budding yeast

Janis Tam

University College London

and

The Francis Crick Institute

PhD Supervisor: Dr Folkert van Werven

A thesis submitted for the degree of

Doctor of Philosophy

University College London

February 2020

Declaration

I, Janis Tam, confirm that the work presented in this thesis is my own. Where information has been derived from other sources, I confirm that this has been indicated in the thesis.

Abstract

Cells fate choices are governed by a multitude of signalling pathways during development. Environmental and internal cues converge onto important developmental genes that control transcriptional networks and in turn dictate cell fate outcomes. In budding yeast *Saccharomyces cerevisiae*, nutrient and mating type signals regulate the expression of a developmental gene called *IME1*. Upon nutrient starvation, *IME1* is expressed and diploid cells are induced to enter a conserved cell differentiation programme known as sporulation or gametogenesis. During sporulation, meiotic cell divisions take place to generate four haploid spores. How nutrient signals modulate the expression of *IME1* was unknown. In this thesis, I demonstrate that nutrient signals regulate repression of *IME1* transcription. Glucose and rich nutrients including nitrogen compounds control the binding of an array of at least nine sequence-specific transcription factors to the *IME1* promoter. The transcription factors in turn recruit Tup1-Cyc8, a conserved transcriptional repressor complex to inhibit *IME1* transcription. Importantly, Tup1-Cyc8 is heavily involved in the repression of *IME1* transcription, given that *IME1* is fully de-repressed when Tup1-Cyc8 is depleted. I find that three transcription factors, Yap6, Sok2, and Phd1, play significant roles in mediating Tup1-Cyc8 repression of the *IME1* promoter. Remarkably, *IME1* transcription is highly responsive to changes in nutrient availability. I show that the *IME1* promoter is poised for activation under Tup1-Cyc8 repression. Furthermore, *IME1* transcription is rapidly activated when Tup1-Cyc8 is lost. My findings present a model of how complex signals regulate developmental genes at the transcriptional level to control cell fate decisions in eukaryotes.

Impact Statement

Developmental decisions are tightly regulated by signalling cues in eukaryotes. Throughout development, cells respond to distinct signals and undergo cell differentiation programmes to establish cell identity. Importantly, genes that dictate cell fate decisions during development must be carefully controlled, given that untimely expression can result in detrimental outcomes such as aneuploidy and cancer. In this thesis, I investigated how signal inputs modulate cell fate outcomes by studying initiation of meiosis, an important developmental decision in budding yeast. My findings demonstrate that nutrient signals regulate transcriptional repression of *IME1*, a crucial gene that governs entry into meiosis. Distinct nutrient signals mediate association of multiple transcription factors to the *IME1* promoter, and in turn modulate recruitment of the Tup1-Cyc8 repressor complex. The results presented in my thesis provide a framework of how complex signals are integrated to control the expression of important developmental genes in eukaryotes.

IME1 was first discovered in 1988 and plays a pivotal role in governing entry into meiosis in yeast. Since then many studies have emerged to dissect how nutrient signals regulate *IME1* promoter activity to control *IME1* transcription. Although Tup1-Cyc8 was recognised to be a regulator of *IME1* transcription, how Tup1-Cyc8 integrates nutrient signals and represses *IME1* transcription was unknown. Furthermore, there was limited information on which sequence elements in the *IME1* promoter respond to nutrient cues. In this thesis, I present novel findings that pinpoint how nutrient signals are integrated at the *IME1* promoter. I deciphered the role of Tup1-Cyc8 in regulating *IME1* transcription, and determined how distinct nutrient signals regulate recruitment of Tup1-Cyc8 to the *IME1* promoter. Moreover, I characterised seven short sequence motifs in the *IME1* promoter that respond to nutrient availability in the environment. I also identified a list of novel *IME1* regulators that can be examined in future studies.

Tup1-Cyc8 is a well-established repressor complex in yeast with conserved functional homologues found in other eukaryotes (e.g. Groucho in *Drosophila*, TLE1 in human). How Tup1-Cyc8 represses its target genes has been the subject of

investigation for decades. In this thesis, I propose a Tup1-Cyc8 repression model that exhibits similarities but is distinct from previous models. My findings demonstrate that Tup1-Cyc8 interacts with a distinct set of transcription factors to inhibit promoter-bound transcriptional activators. My model postulates that Tup1-Cyc8 induces loss of activation, which counters traditional views that Tup1-Cyc8 establishes repressive promoter structure to block transcriptional activity. In addition, I found that Tup1-Cyc8 binding enhances the responsiveness of *IME1* transcription to changes in nutrient availability, and thus my data provide insights into how gene expression plasticity can be regulated at the transcriptional level in all eukaryotic cells.

My results and conclusions in this thesis will be published in an editorial journal to facilitate dissemination of my research findings. Our publication entitled "Regulated repression, and not activation, governs the cell fate promoter controlling yeast meiosis" is currently in revision and can be found on the bioRxiv server (doi: https://doi.org/10.1101/2020.01.13.904912). My findings will be of broad interest to research fields including transcriptional regulation and developmental decisions.

Acknowledgement

My PhD training has been an invaluable experience. I would like to express my sincere gratitude to my PhD supervisor, Dr Folkert van Werven. I am very grateful for the opportunity to become a member of the Cell Fate and Gene Regulation Laboratory for the past four years. Thank you very much for your guidance, support, and patience – without which this thesis would not be made possible.

Next, I would like to extend my gratitude to all members of the Cell Fate and Gene Regulation Laboratory, past and present. I would like to thank Fabien Moretto, Radhika Warrier, Dora Sideri, Minghao Chia, Andrew Wu, Imke Ensinck, Alice Rossi, Luc Costello Heaven, and Jessie Beck for making our lab a wonderful place to work in. Stay in touch and I hope our paths will cross again in the future.

My thesis committee has provided me with tremendous help throughout my PhD training. I would like to thank Professor Rob de Bruin, Dr Nate Goehring, and Dr Jacky Hayles for their advice and encouragement.

I would like to acknowledge and express my appreciation to the Science Technology Platforms (STPs) and Laboratory Infrastructure teams at the Francis Crick Institute, including the Fermentation, Genomics Equipment Park, Light Microscopy, Proteomics, Glasswash, and Media Preparation facilities. I would especially like to thank Deborah Aubyn, Matt Renshaw, and David Frith for dedicating their time to help with my research questions.

Finally, I would like to thank my parents for their unfailing love, support, and care. Thanks to Ryan Wong for always being there and for being a constant source of joy and reassurance. A big thank you to all my friends for standing by me, believing in me, and giving me strength.

This PhD project was supported by the Francis Crick Institute (FC001203), which is core funded by Cancer Research UK (FC001203), the UK Medical Research Council (FC001203), and the Wellcome Trust (FC001203).

Table of Contents

Table of figures

List of tables

Abbreviations

1NM-PP1	4-Amino-1-*tert*-butyl-3-(1'-naphthylmethyl)pyrazolo[3,4-d]pyrimidine
3-IAA	Indole-3-acetic acid
Ac	Histone acetylation
AID	Auxin-induced degron
AMP	Adenosine monophosphate
APSES	Transcription regulator helix-turn-helix, APSES-type DNA-binding domain
ATF/CREB	Activating transcription factors/cyclic AMP response element binding
ATP	Adenosine triphosphate
bp	Base pair
BYTA	Buffered, yeast extract, tryptone, acetate medium
bZIP	Basic leucine zipper domain
C. glabrata	*Candida glabrata*
C2H2 ZF	Cys2His2-fold zinc finger
cAMP	Cyclic AMP
cDNA	Complementary DNA
ChIP	Chromatin immunoprecipitation
ChIP-chip	Chromatin immunoprecipitation with DNA microarray
ChIP-seq	Chromatin immunoprecipitation with sequencing
CRE	Cyclic AMP responsive element
CREB	Cyclic AMP responsive element binding
CSM	Complete supplement mixture
DAPI	4',6-diamidino-2-phenylindole
DMSO	Dimethyl sulphoxide
DNA	Deoxyribonucleic acid
FKBP	FK506-binding protein
G_0	Quiescence
Glc	Glucose
HA tag	Haemagglutinin tag
HAT	Histone acetyltransferase
HDAC	Histone deacetylase

His	Histidine (or histidine auxotrophic marker)
HSF	Heat shock factor-type
IREu	*IME1* repeated element upstream
Kan	Kanamycin (or kanamycin-resistance cassette)
kb	Kilobase
kDa	Kilodalton
MAPK	Mitogen-activated protein kinase
*MAT***a**	Mating type **a**
*MAT*α	Mating type α
MNase	Micrococcal nuclease
MNase-seq	Micrococcal nuclease sequencing
mRNA	Messenger RNA
MSE	Middle sporulation element
Nat	Nourseothricin (or nourseothricin-resistance cassette)
NuRD	Nucleosome remodelling deacetylase
OD_{600}	Optical density at wavelength = 600 nm
ORF	Open reading frame
PBS	Phosphate buffered saline
PCR	Polymerase chain reaction
PKA	Protein kinase A
PolyQ	Polyglutamine
PONDR	Predictor Of Naturally Disordered Regions
PVDF	Polyvinylidene difluoride
qPCR	Quantitative polymerase chain reaction
RasGAP	Ras GTPase activating proteins
RasGEF	Ras GDP exchange factor
RNA	Ribonucleic acid
RRE1	RME1-response element 1
RT-qPCR	Reverse transcription with quantitative polymerase chain reaction
S. cerevisiae	*Saccharomyces cerevisiae*
SC	Synthetic complete medium
SDS-PAGE	Sodium dodecyl sulphate-polyacrylamide gel electrophoresis
SEM	Standard error of mean

sfGFP	Superfolder green fluorescent protein
smFISH	Single molecule RNA fluorescence *in situ* hybridisation
SPO	Sporulation medium
STRE	Stress response element
SUMO	Small ubiquitin-like modifier
SV40NLS	Simian virus 40 nuclear localisation signal
TA	Transcriptional activator
TF	Transcription factor
TOR	Target of rapamycin
TORC1	Target of rapamycin complex 1
TPR	Tetratricopeptide repeat
TR	Transcriptional repressor
Trp	Tryptophan (or tryptophan auxotrophic marker)
UAS	Upstream activation sequence
Ura	Uracil
URS	Upstream repressing sequence
URS1	Upstream repressor site 1
UTR	Untranslated region
WT	Wild-type
Yap	Yeast Activator Proteins
YeTFaSCo	Yeast Transcription Factor Specificity Compendium
YP	Yeast extract, peptone medium
YPD	Yeast extract, peptone, dextrose medium
YPD (E)	Exponential growth phase in YPD medium
YPD (S)	Cells grown to saturation in YPD medium
YRE-A	Yap response element adjacent

Chapter 1. Introduction

1.1 Developmental transcription factors integrate multiple signals to determine cell fate outcome

All organisms are made up of specialised cell types. Throughout development, cells need to make an important developmental decision – whether to differentiate into another cell type or not. This decision is controlled by signalling cues that arise from internal and extracellular stimuli. Such signals typically converge onto developmental transcription factors, which govern transcriptional networks required to complete multiple cell differentiation processes. How signal inputs control a cell fate outcome is an important question in biology. In this thesis, I will explore this question by studying the transcriptional regulation of a developmental transcription factor in budding yeast.

Budding yeast cells make specific cell fate choices to adapt to the constantly changing environment. Upon nutrient deprivation, yeast cells undergo a specialised cell differentiation programme called sporulation or gametogenesis during which cells undertake meiotic divisions. The signalling cues that determine whether sporulation takes place or not in yeast are integrated by a single gene called *IME1*, which encodes a transcriptional activator that is crucial to initiate entry into meiosis. Given its pivotal role in reprogramming cell fate in yeast, *IME1* must be carefully controlled to ensure that the transcriptional activator is timely and faithfully expressed to induce the onset of meiosis only when cells are starved. Yet, how nutrient signalling cues regulate *IME1* in yeast to control entry into meiosis in yeast is unclear.

1.2 General mechanisms of eukaryotic gene activation

The central dogma of molecular biology indicates that a gene is expressed when genetic information is transferred to messenger RNA (mRNA) through a process called transcription (Crick, 1970). The sequential information in mRNA is further translated into proteins which regulate various cellular processes and responses (Crick, 1970). Hence, during development, genes that encode crucial regulatory transcription factors such as *IME1* must become transcriptionally active. Conversely, the expression of these genes should be tightly repressed when the developmental signals are absent. In eukaryotes, gene expression is controlled and fine-tuned by multiple layers of transcriptional regulation. Importantly, transcriptional regulation is dictated by the non-coding DNA sequence that is immediately upstream of the gene known as the gene promoter. The promoter plays a fundamental role in activating gene transcription as it recruits RNA polymerase, the key player that transcribes genetic information into mRNA, close to the transcription start site of the gene (Kanhere and Bansal, 2005). Eukaryotic gene promoters contain core promoter elements that are sufficient to initiate basal levels of RNA polymerase II-mediated transcription in *in vitro* conditions (Roeder, 1996). The TATA box is a well-characterised core element that is present in metazoan genes and approximately 20% of yeast genes (Venters and Pugh, 2009). In metazoans, TATA boxes are located at 25 to 30 base pairs (bp) upstream of the transcription start site. Compared to metazoans, yeast TATA boxes are found slightly more upstream as they are located at 30 to 60 bp from the transcription start site (Venters and Pugh, 2009). The TATA box directs transcription by interacting with TBP (TATA-binding protein) through minor groove contacts (Roeder, 1996). The binding of TBP induces DNA to kink and leads to the recruitment of multiple general transcription factors and RNA polymerase II to form the pre-intiation complex (Roeder, 1996). The kinase activity of the general transcription factor TFIIH (Kin28 in yeast) phosphorylates the C-terminal domain of RNA polymerase II at the Ser5 position, and thereby initiates RNA polymerase II to transcribe through the coding region (reviewed in Phatnani and Greenleaf, 2006).

In addition to the core promoter elements, the upstream non-coding regions of eukaryotic genes also consist of gene-specific regulatory elements that fine-tune the

expression of individual genes in response to specific signals. These regulatory sequences are found in *cis* to the core promoter and can influence the level of gene transcription. In metazoans, regulatory sequences known as enhancers promote transcriptional activation of target genes. Enhancers are located from 100 bp to millions of base pairs from target genes and chromatin looping may be required to bring enhancers and promoters into proximity (Mora et al., 2016). In yeast, gene expression is controlled by regulatory sequences that are commonly found between 100 and 500 bp upstream of the start codon (Harbison et al., 2004). Upstream regulatory sequences that upregulate and downregulate transcription are called upstream activating sequences (UAS) and upstream repressing sequences (URS), respectively (Venters and Pugh, 2009). How do these *cis*-regulatory sequences adjust the level of transcription in response to internal and environmental signals? *Cis*-regulatory sequences contain specific DNA motifs that are recognised by sequence-specific transcription factors. Such transcription factors act as regulators that activate or repress gene transcription depending on the genomic context and the co-regulators they interact with (Venters and Pugh, 2009). First, transcription factors may recruit ATP-dependent chromatin remodelling complexes to alter the promoter architecture. ATP-dependent chromatin remodellers are categorised into four sub-families based on sequence similarities: ISWI (imitation switch), CHD (chromodomain helicase DNA-binding), SWI/SNF (switch/sucrose non-fermentable), and INO80 (reviewed in Clapier et al., 2017, Venters and Pugh, 2009). Notably, the catalytic subunits of these remodellers possess ATPase activities, which generate energy via ATP hydrolysis and drive DNA translocation when bound to chromatin. As a result, the interactions between histone proteins and DNA are disrupted and the histone positions are shifted relative to DNA (Clapier et al., 2017). The action of chromatin remodellers, such as that of the SWI/SNF sub-family facilitates nucleosome repositioning and eviction (Clapier et al., 2017), and thereby promotes the accessibility of gene promoters to activators and the transcriptional machinery. Furthermore, chromatin remodellers that belong to the INO80 sub-family mediates histone variant exchange to expel H2A.Z histone proteins (Htz1 in yeast) from coding regions during transcriptional activation (Brahma et al., 2017, Papamichos-Chronakis et al., 2011). Second, sequence-specific transcription factors may recruit histone modifying enzymes that catalyse post-translational modifications on histone proteins. Histones can be post-translationally modified by acetylation,

phosphorylation, methylation, deamination, glycosylation, ADP ribosylation, ubiquitylation, and sumoylation (Bannister and Kouzarides, 2011). Histone modifications such as acetylation and methylation can alter chromatin structure at gene promoters and thereby regulate gene transcription. Histone acetylation is facilitated by histone acetyltransferases (HATs) and removed by histone deacetylases (HDACs) at the lysine side chains (Bannister and Kouzarides, 2011). Histone hyperacetylation is generally associated with less stable nucleosomes, higher DNA exposure, and thus more accessible chromatin structures (reviewed in Barnes et al., 2019). In addition, gene transcription is regulated by acetylation of lysine at specific sites. For example, acetylation of lysine 9 in histone H3 (H3K9) and H3K14 are correlated with active transcription start sites and transcriptional rates genome-wide in yeast (Pokholok et al., 2005). Similarly, histone methylation is catalysed and removed by methyltransferases and demethylases respectively and regulates gene expression depending on the specific site modified (Hyun et al., 2017). In yeast, dimethylation of H3K4 in coding regions is found in transcriptionally active coding regions, while H3K79 methylation can be involved in gene activation or silencing (Bernstein et al., 2002, Farooq et al., 2016). Methylated lysines on histone proteins can also be recognised by effector proteins with methyl-lysine-binding motifs, such as the WD40, PHD, and chromo domains (reviewed in Hyun et al., 2017). Remarkably, changes in histone methylation marks are correlated with the phosphorylation status of the RNA polymerase II C-terminal domain, suggesting that the transcriptional machinery may communicate with chromatin marks (reviewed in Venters and Pugh, 2009). Third, transcription factors can compete to bind to specific DNA motifs in the *cis*-regulatory sequences. Under activating conditions, transcriptional activators may replace repressors at the *cis*-regulatory sequences due to changes in cellular levels of the transcription factors. Furthermore, changes in internal and/or external signals may affect the binding specificity of gene regulators through regulating multiple transcription factors. Sequence-specific transcription factors can bind to DNA in a co-operative manner to enhance their DNA-binding specificity (reviewed in Lelli et al., 2012). Transcription factors may demonstrate classical co-operativity or latent specificity in which protein-protein interactions between transcription factors direct the complex to specific binding sites (Lelli et al., 2012). Moreover, binding of transcription factors can affect the accessibility of chromatin at the gene promoter. In the collaborative competition model, binding of

the first transcription factor alters the position of nucleosomes and allows the second transcription factor to bind to a neighbouring site (Lelli et al., 2012). Finally, the transcription factor binding motif can play an active role in gene regulation by inducing conformational changes in the bound transcription factor. As a result, different co-acitvator or co-repressor complexes are recruited to regulate gene transcription (Lelli et al., 2012). Taken together, the interplay between the *cis*-regulatory sequences and sequence-specific transcription factors governs gene expression.

1.3 Budding yeast as a model organism

Budding yeast *Saccharomyces cerevisiae* is a model organism that is widely used for studying basic molecular and cellular mechanisms. Budding yeast is a single cell eukaryotic fungus that provides numerous advantages to work with in the laboratory. Firstly, budding yeast is a tractable microorganism that can be easily maintained in the laboratory using growth media. Under optimal growth conditions, yeast cells grow rapidly and the doubling time is around 90 minutes per cycle. Furthermore, budding yeast has a well annotated genome and is also genetically amenable. Many genetic tools are available to study the functions of genes in budding yeast. For example, genes can be mutated or tagged rapidly using the one-step PCR protocol (Longtine et al., 1998). In addition, yeast genes can be directly fused with sequence encoding fluorescent protein to produce a recombinant protein that consists of the protein of interest tagged with a fluorescent protein (Duina et al., 2014). Fluorescently labelled protein can be directly visualised by microscopy to study the expression and sub-cellular localisation of the protein of interest. RNA transcripts can also be directly visualised by single molecule RNA fluorescence *in situ* hybridisation in yeast cells. Given that budding yeast cells are small and have a cell diameter of approximately 5µm (Duina et al., 2014), it is possible to observe and quantify the transcripts of interest present in the entire cell by obtaining z-stack images containing multiple optical slices.

As a eukaryote, budding yeast contains membrane-bound organelles and conserved cellular components that can be exploited to explore cellular mechanisms, such as DNA damage, autophagy, transcription, and genome organisation. In 1996, budding yeast became the first eukaryotic organism with the whole genome completely sequenced by the collaborative efforts of various research groups across the world (Goffeau et al., 1996). Comparison between yeast and human genomes revealed that 20% of yeast genes have human orthologues, and 87% of yeast protein domains can be found in human (Peterson et al., 2013). Many yeast genes were reported to share similar functions with their human counterparts that display sequence similarities (Kachroo et al., 2015). Furthermore, budding yeast can be used to model mutations in human proteins as 29% of yeast protein mutations can be found in human proteins with the same domains (Peterson et al., 2013). The

conservation of protein functions between yeast and human has facilitated discoveries of the molecular mechanisms underpinning prion disease, neurodegenerative disease, ageing, and cancer in humans (Liebman and Chernoff, 2012, Miller-Fleming et al., 2008, Denoth Lippuner et al., 2014, Simon et al., 2000, Coelho et al., 2019).

The budding yeast genome encodes 5885 protein-coding open reading frames (ORF) in 12,068 kilobases (kb) (Goffeau et al., 1996), which translates into one protein-coding ORF per ~2 kb. The biological functions of approximately 85% of the protein-coding genes in budding yeast have been determined since the completion of the genome (Botstein and Fink, 2011). The compactness of the budding yeast genome is remarkable when compared to other genomes. For example, in the fission yeast and *C. elegans* genomes, one protein-coding ORF is predicted in every ~3 kb and ~5 kb (Wood et al., 2002, The C. elegans Sequencing Consortium, 1998). On average, each budding yeast ORF is 1450 base pairs (bp) in length, with intergenic regions that are 309 bp upstream and 163 bp downstream of the ORF (Dujon, 1996). Introns are rare in budding yeast genes as they only exist in around 4% of protein-coding genes (Goffeau et al., 1996). While the budding yeast genome was being assembled after the completion of sequencing, it was discovered that a whole genome duplication occurred in an ancestor of budding yeast (Wolfe, 2015). As a consequence, 551 genes have been duplicated in the genome, representing 19.6% of genes in budding yeast (Byrne and Wolfe, 2005). The duplicated genes and their protein products are known as paralogues. Paralogues are related in coding sequence and synteny but can have diversified functions in budding yeast.

1.4 Sexual life cycle of budding yeast

Budding yeast cells can stably exist in haploid or diploid state. Under nutrient-rich conditions, both haploid and diploid yeast cells can proliferate asexually by budding (Figure 1). During budding, a daughter cell “buds” from the mother cell and eventually separates from the mother cell by mitotic cell division. Haploid cells express a single mating type locus (*MAT*). Depending on which allele of mating type locus is expressed, haploid cells can be either mating type **a** (*MAT***a**) or α (*MAT*α). The *MAT* locus in haploid cells can undergo gene conversion that converts cells to the other mating type. Haploid cells release pheromones that are unique to their mating types (**a**-factor or α-factor). When haploid cells of opposite mating types are in proximity to each other, they respond to the pheromones and initiate mating (Figure 1). The two haploid cells fuse and form a diploid cell (*MAT***a**/α) that inherits both sets of chromosomes from the parents. When nutrients including glucose and nitrogen compounds are absent, cells stop dividing their chromosomes by mitosis and enters a conserved cell differentiation programme called sporulation or gametogenesis (Figure 1). Diploid cell that expresses both mating type loci undergoes sexual reproduction, during which the homologous chromosomes in the mother cell are segregated by meiosis. Meiosis is a specialised cell division that is conserved throughout eukaryotes, and is a critical process to generate haploid gametes from diploid cells to increase the genetic variation within a cell population. Meiosis is characterised by a number of stages that result in the production of four haploid spores at the end of the process. First, DNA is replicated once in the diploid cell, followed by one round of nuclear division that segregates the homologous chromosomes (meiosis I). A second round of nuclear division follows (meiosis II) to separate the sister chromatids. Comparison of meiosis between budding yeast and higher eukaryotes revealed that the process is highly conserved in terms of molecular processes and cytological structures (Loidl, 2000). In budding yeast, the outcome of meiotic divisions is four haploid spores, each enveloped in a thick spore wall that are packaged into a tetrahedral ascus. The thick, stress-resistant coat surrounding the spores ensures that the haploid progenies are protected from nutrient starvation and propagate only when the environmental conditions become optimal for growth.

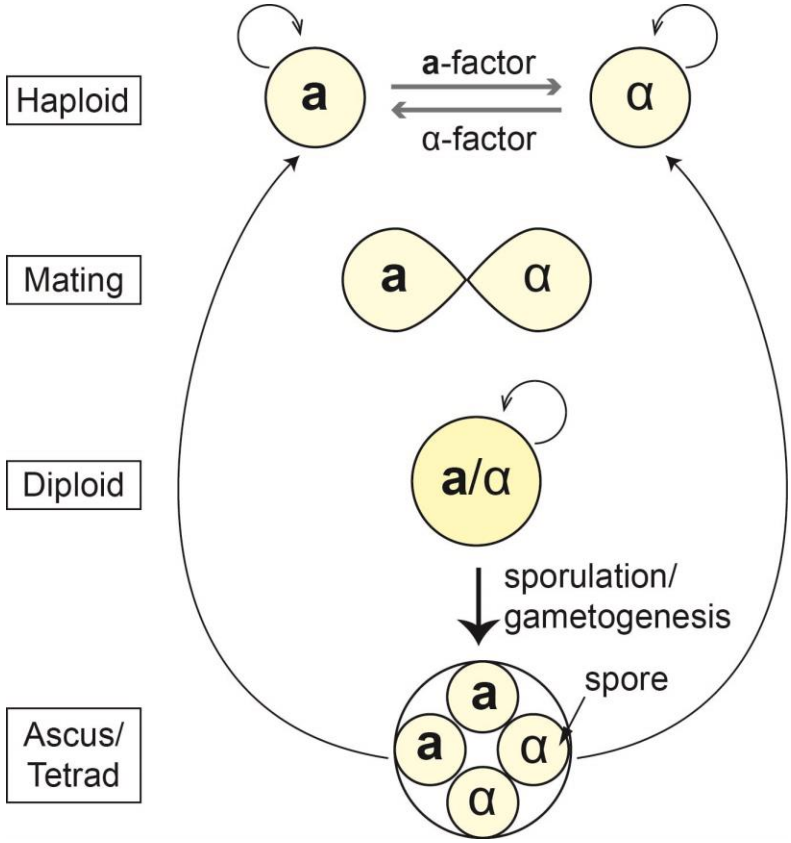

Figure 1. Budding yeast life cycle (adapted from (Herskowitz, 1988)).
Budding yeast cells can exist in haploid and diploid states. When nutrients are ample, yeast cells can propagate by mitotic cell division (budding). Haploid cells of opposite mating type (*MAT***a** and *MAT*α) can fuse to make a diploid cell (*MAT***a**/α). Under nutrient deprivation, the diploid cell undergoes sporulation or gametogenesis, during which meiosis takes place to produce four haploid spores. Half of the haploid progenies is *MAT***a** and the other half is *MAT*α.

1.5 Cell fates of budding yeast

In response to signalling changes within the cell and in the surrounding environment, budding yeast is capable of undergoing cell fate transitions to develop specialised types of cells that can better adapt to the new environment. Mating is one type of fate decisions made by haploid cells only (Figure 2). Haploid cells release pheromones that are detected by the Ste2 and Ste3 receptors on the surface of *MAT***a** and *MAT*α cells (Merlini et al., 2013). Pheromone binding activates the MAPK (mitogen-activated protein kinase) pathway, and in turn switches on mating-specific genes to induce cell cycle arrest and morphological changes that direct cells towards their mating partners.

Many cell fate choices in budding yeast are influenced by the availability of nutrients in the growth environment. When nitrogen compounds and glucose, the preferred carbon source are present in the medium, cells ferment glucose to produce energy by glycolysis. Under this optimal growth condition, budding yeast cells choose to proliferate rapidly by budding (Figure 2). At this stage, cells are known to be undergoing vegetative growth. During fermentation, ethanol, a non-fermentable carbon source is produced as a result of the glycolytic process. As glucose eventually becomes exhausted in the growth medium, a metabolic switch known as diauxic shift takes place. Yeast cells continue to divide by budding, but a non-fermentable carbon source (e.g. ethanol, acetate, glycerol) is utilised by respiration. Post-diauxic growth is characterised by slower cell division that lasts until the non-fermentable carbon source is fully utilised. Eventually, cells are grown to a saturation state, and a fate transition takes place from mitotic cell division to stationary phase or quiescence (G_0) (Figure 2). Quiescent budding yeast cells become dormant, non-dividing, and develop thicker cell walls. To optimise survival, cells utilise internal nutrient storage sources and increase autophagy (An et al., 2014). Quiescent cells are also characterised by their compact genomes, which is related to the enhanced binding of linker histone Hho1 (Piñon, 1978, Schäfer et al., 2008, Takeshige et al., 1992, de Nobel et al., 2000). At this stage, the topological organisation of the budding yeast genome is significantly reprogrammed (Rutledge et al., 2015).

Nutrient starvation also triggers other types of cell fate transitions in budding yeast. In the presence of high glucose and low nitrogen, yeast cells that co-express *MAT***a** and *MAT*α (*MAT***a**/α) exhibit pseudohyphal or filamentous growth (Madhani, 2000) (Figure 2). Pseudohyphal growth is resulted from the activation of two Ras-dependent signalling pathways, MAPK and cAMP/PKA (cyclic AMP/protein kinase A) (Stanhill et al., 1999, Rupp et al., 1999). During pseudohyphal growth, cells alter their bud sites and form chains of long, thin cells as a means to forage for new nitrogen sources (Gimeno et al., 1992). Notably, pseudohyphal growth driven by nitrogen starvation is distinct from filamental growth caused by alcohol stress or slow cell cycle progression (Lorenz et al., 2000, Hollenhorst et al., 2000, Jiang and Kang, 2003). Finally, when glucose and nitrogen compounds are both limiting in the environment, *MAT***a**/α cells enter sporulation to generate haploid spores by meiosis, which are protected from environmental stress until growth conditions become optimal again (Figure 2).

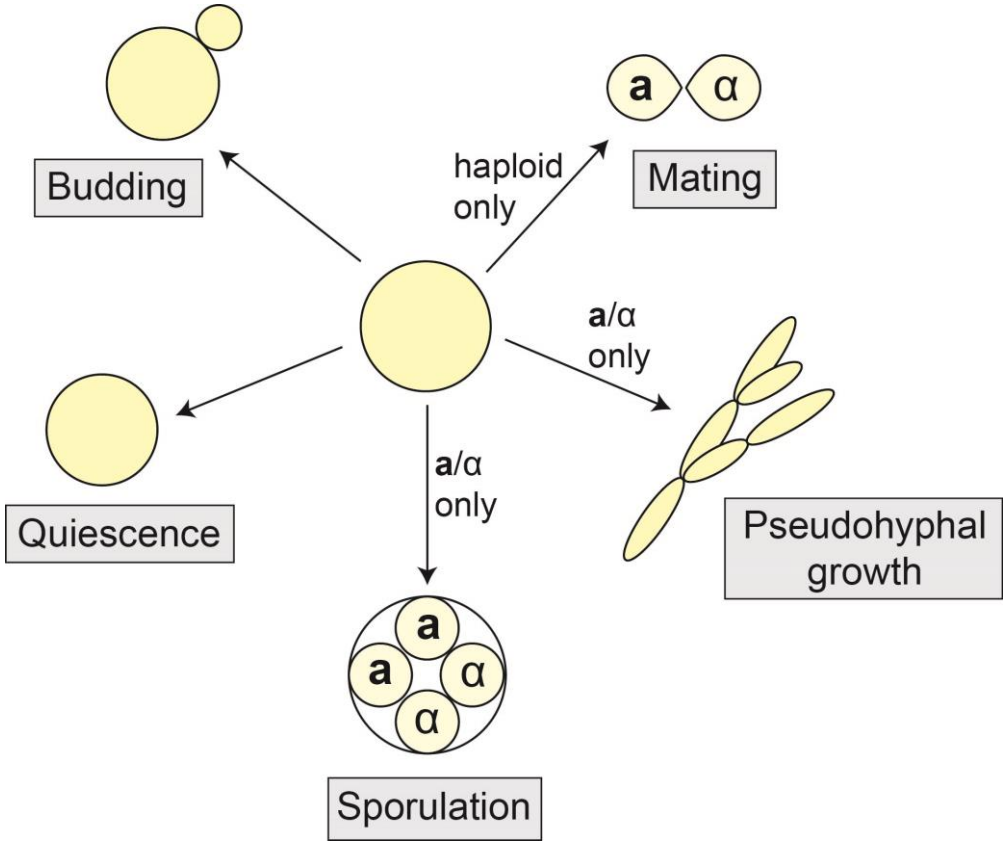

Figure 2. Different signals direct yeast cells to enter different cell fates (adapted from (Ahmadpour et al., 2014)).

Yeast cells undergo morphological changes to adapt to the changing environment. Haploid and diploid yeast cells divide by budding in nutrient-rich conditions. Haploid cells of opposite mating types elongate towards each other to mate. Changes in nutrient availability also prompt cells to transit into different cell types. Under nitrogen deprivation, cells expressing both *MAT***a** and *MAT*α (*MAT***a**/α) form pseudohyphae to forage for nitrogen sources. When both glucose and nitrogen are absent, cells enter a dormant stage called quiescence. Prolonged nutrient starvation induces *MAT***a**/α cells to undergo sporulation to produce stress-resistant spores.

1.6 Entry into meiosis in yeast is tightly regulated by mating type signals, nutrients, and respiration

Entry into meiosis during sporulation is a highly co-ordinated cell fate transition. The decision of whether or not to initiate meiosis is tightly governed by a multitude of intrinsic signals and environmental cues (Figure 3). These signals ensure that meiosis only occurs when all conditions are satisfied. In order to initiate meiosis in yeast, cells must express both *MAT***a** and *MAT*α mating types. In wild-type yeast, cells that express *MAT***a**/α mating types are typically diploid. Haploid and diploid cells expressing only a single mating type cannot enter meiosis. Strikingly, engineered haploid cells harbouring both mating types can initiate meiosis, but results in meiotic catastrophe due to lack of homologous chromosomes (Wagstaff et al., 1982). Next, nutrients including glucose and nitrogen compounds must be absent from the growth medium. Nutrient starvation is a critical signal that ensures cells do not undertake the sporulation programme when growth or other morphological changes may occur. When nutrients become depleted, G1 cyclins and the cyclin-dependent kinase Cdc28 are downregulated (van Werven and Amon, 2011). This ensures that cells quit the vegetative cell cycle when meiosis is initiated. Expression of Cln3, a key G1 cyclin represses entry into meiosis (Nakazawa et al., 2010). Furthermore, respiration needs to take place, meaning that cells must have functional mitochondria and a non-fermentable carbon source needs to be present. When glucose is exhausted or absent in the environment, cells utilise non-fermentable carbon sources to produce energy by respiration. During sporulation, extensive transcriptional changes take place that induce cells to undergo a series of processes, including meiosis I and II, spore formation, and spore maturation. Active respiration is likely required to provide energy that is necessary for cells to complete the sporulation programme. Cells with compromised mitochondrial activity do not undertake meiosis (Jambhekar and Amon, 2008, Weidberg et al., 2016).

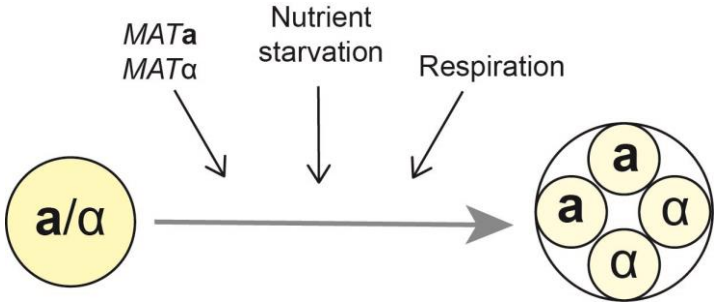

Figure 3. Initiation of yeast meiosis is controlled by multiple signals.
Entry into meiosis in yeast is governed by three distinct signals: cell mating type, nutrients, and respiration. In order to initiate meiosis, yeast cells must respire, have *MAT***a**/α mating types, and nutrients including glucose and nitrogen compounds must be absent from the surrounding environment.

In the laboratory, we can study separate events in the sporulation programme by synchronising cells to initiate meiosis. This is achieved by growing cells in growth media that provide distinct nutrient conditions. These nutrient conditions allow cells to grow rapidly at first, then rich nutrients are eventually depleted and a non-fermentable carbon source is provided to promote respiration (Figure 4). Typically, yeast cells are grown in a rich medium (YPD) that supplies ample glucose and rich nutrients including nitrogen compounds. When saturation is reached in the YPD medium, cells are transferred to a pre-sporulation medium (BYTA) that contains rich nutrients including nitrogen compounds, but not glucose. In addition, the pre-sporulation medium provides acetate, a non-fermentable carbon source that encourages cells to respire. Subsequently, cells are shifted to the sporulation medium (SPO), in which rich nutrients including nitrogen compounds are also removed. Acetate is provided in the sporulation medium to support respiration. Additionally, pH is maintained in the sporulation medium as yeast sporulation prefers to take place at pH 7.3 (Freese et al., 1982).

Further protocols have been developed based on the sporulation induction procedure to synchronise cells at particular stages in the sporulation programme. These methods involve creating roadblocks in the sporulation programme and subsequently releasing cells from the roadblocks. Such protocols are typically used for sequencing and genomic analyses for pinpointing changes specific to a certain

stage in sporulation. For example, pre-meiotic DNA replication and the meiotic divisions can be synchronised by controlling the expression of *IME1*, which encodes a key transcription factor that activates the meiotic programme in yeast (Chia and van Werven, 2016). Furthermore, yeast cells can be arrested after pre-meiotic DNA replication by deleting *NDT80*, a gene expressed during the sporulation programme that commits cells to complete meiosis and sporulation (Xu et al., 1995). Cells with *ndt80*Δ can return to vegetative growth after initiation of meiosis, allowing cell responses to re-exposure of nutrients to be examined (Winter, 2012).

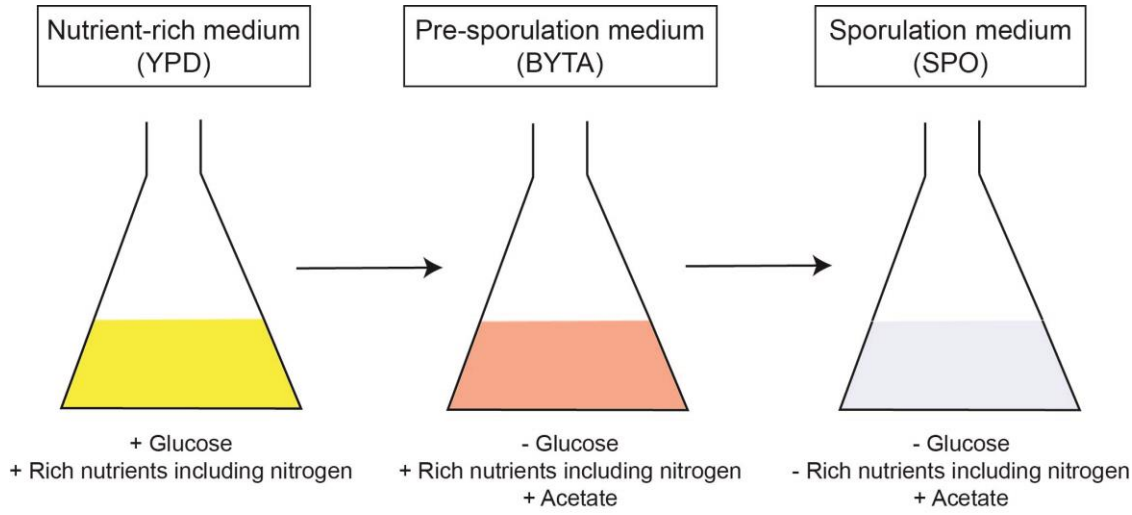

Figure 4. Laboratory procedure to induce yeast meiosis synchronously.
In the laboratory, we employ growth media that provide distinct nutrient conditions to synchronise entry into meiosis in yeast. To induce sporulation, yeast cells are first grown in rich medium providing glucose and nitrogen compounds. Next, cells are starved by subsequently removing glucose and nitrogen while acetate is provided.

In budding yeast, multiple layers of regulation restrict only cells that have met all the conditions outlined in Figure 3 to initiate meiosis. These strict conditions prevent de-regulation of meiosis genes, which often has deleterious effects on yeast cells. One example is the mis-regulation of *SPO13*, a gene that is normally expressed during yeast meiosis. Spo13 plays an important role in regulating proper nuclear divisions during meiosis. However, when expressed in cells undergoing mitosis, Spo13 causes cell cycle arrest (McCarroll and Esposito, 1994). Similar effects have also been observed in fission yeast. Fission yeast cells undergo mating and meiosis when nutrients, especially nitrogen compounds are limiting in the

environment (Yamamoto, 1996). In fission yeast, entry into meiosis is also governed by a multitude of signals including mating pheromone signalling, cyclic AMP (cAMP)-dependent protein kinase signalling, and respiration (Yamamoto, 1996, van Werven and Amon, 2011). Ectopic expression of meiosis-specific proteins during mitosis causes chromosomal defects in fission yeast cells. For example, mis-expression of the meiosis-specific spliced form of Crs1 cyclin in vegetative cells leads to cell cycle arrest and abnormal chromosomal segregation (Averbeck et al., 2005). Furthermore, overexpression of Rec8, a meiotic cohesion induces chromosomal mis-segregation and results in uniparental disomy in the progenies (Folco et al., 2017). Regulation of entry into meiosis in yeast parallels the tight control of germ cell fate decision in mammals. In mammalian cells, aberrant expression of meiosis-specific factors is highly detrimental and has major clinical implications. One example is Aurora-C, a serine/threonine kinase that is expressed during spermatogenesis and oogenesis. Overexpression of Aurora-C in mouse fibroblast cells was reported to induce aberrant cell divisions and multi-nucleation (Khan et al., 2011). Furthermore, Aurora-C overexpression has been linked to cancer in mouse and human cells (Khan et al., 2011, Tsou et al., 2011). Another example is a group of proteins known as cancer/testis antigens in humans. Cancer/testis antigens normally localise to the male germline and are involved in processes such as chromosome pairing in sperm cells (Türeci et al., 1998). Yet many cancer/testis antigens are also expressed as immunogenic proteins in a range of malignant tumours (Kalejs and Erenpreisa, 2005). Finally, mis-regulation of *Stra8*, a transcriptional activator that induces gonadal gells to undergo meiosis, has been implicated in lymphoma (Gantchev et al., 2019). These examples illustrate the importance that meiosis-specific genes must be tightly controlled and timely expressed in all eukaryotic cells.

1.7 Expression of meiotic genes is highly regulated throughout the sporulation programme

How do multiple signals converge to drive entry into meiosis in budding yeast? The key decision maker in this cell fate commitment is the transcription factor Ime1 (inducer of meiosis 1). *IME1* was first cloned and identified as an inducer of meiosis in a study published in 1988 (Kassir et al., 1988). *IME1* is expressed during the early stages of sporulation. Expression level of *IME1* rises to a maximum between 4 to 6 hours after sporulation induction, and declines thereafter (Kassir et al., 1988). Cells are unable to undergo meiosis when the *IME1* gene is disrupted (Kassir et al., 1988). Importantly, *IME1* plays a fundamental role in integrating the upstream signals to dictate whether meiosis should be initiated or not. *IME1* expression is regulated by mating type signals, nutrient availability, and respiration. Transcription of *IME1* occurs only in cells that express both *MAT***a** and *MAT*α, and when glucose and nitrogen compounds are absent. Furthermore, cells must also be respiring to induce *IME1* transcription.

IME1 transcription activates the meiotic programme in yeast, which is characterised by a complex gene regulatory network and large scale transcriptome reprogramming. DNA microarray data revealed that more than 1000 of approximately 6200 protein-coding genes are differentially expressed during yeast meiosis (Chu et al., 1998). The number of genes that are upregulated and downregulated during yeast meiosis are almost equal (Chu et al., 1998). Meiotic genes are expressed in waves as they are involved in different stages of the differentiation programme (Figure 5). Based on the timing of expression, meiotic genes are roughly divided into three classes – early, middle, and late genes. *IME1* encodes a key transcription factor that activates early meiotic gene expression and thereby induces the initiation of the meiotic programme. Hence, the regulation of *IME1* transcription determines whether or not the cell is committed to undergo meiotic cell divisions and spore formation (Figure 5). The majority of early meiotic genes are characterised by the presence of a URS1 (upstream repressor site 1) motif (GGCGGC) in their upstream untranslated regions (Chu et al., 1998). The URS1 site is commonly found in the upstream sequences of many yeast genes, and is also widespread in the upstream regulatory regions of other eukaryotes (Sumrada and Cooper, 1987). Ume6, a zinc

cluster repressor, binds to the URS1 motifs of the early meiotic genes and represses their expression by directing Rpd3 histone deacetylase to the promoters (Strich et al., 1994, Lardenois et al., 2015). Under sporulation inducing conditions, the key inducer of meiosis *IME1* is expressed. Meanwhile, Ume6 and URS1 motifs switch into positive regulators in an *IME1*-dependent manner. When *IME1* is expressed, Ume6 converts into an activating protein (Bowdish et al., 1995). Furthermore, URS1 sites become activating sequences that activate the expression of early meiotic genes (Bowdish et al., 1995, Gailus-Durner et al., 1997). The key player in this switch is Rim11, a kinase that is normally repressed by glucose via cAMP/PKA phosphorylation (Rubin-Bejerano et al., 2004). When glucose is limiting, Rim11 becomes active and phosphorylates a domain in the Ime1 protein. The phosphorylation event facilitates interaction between Ime1 and Ume6 (Rubin-Bejerano et al., 2004, Rubin-Bejerano et al., 1996). The Rim15 kinase is also involved in promoting Ime1-Ume6 interaction but its role is less clear (Vershon and Pierce, 2000). Ime1 is a transcriptional activator that does not have a DNA-binding motif. By dimerising with Ume6, Ime1 can be guided to the URS1 sequences and promote transcriptional activation of early meiotic genes.

One of the early meiotic genes activated by Ime1 via the URS1 sequence is *IME2*, which encodes a meiosis-specific serine/threonine kinase. Ime2 has two important functions during the progression of meiosis (Figure 5). First, Ime2 activity facilitates pre-meiotic DNA replication and recombination that occurs downstream of Ime1 in meiosis (Clifford et al., 2004). In the absence of Ime1, Ime2 permits expression of meiotic genes, suggesting that Ime2 functions downstream of Ime1 (Mitchell et al., 1990). Furthermore, *IME2* disruption delays the expression of meiotic genes even when *IME1* is expressed (Mitchell et al., 1990). Second, Ime2 negatively regulates Ime1 expression by interacting with Ime1. Ime2 kinase activity was shown to phosphorylate Ime1 *in vitro*, which may direct Ime1 to protein degradation (Guttmann-Raviv et al., 2002). In the absence of Ime2, *IME1* mRNA and protein levels accumulate (Mitchell et al., 1990, Guttmann-Raviv et al., 2002, Shefer-Vaida et al., 1995). Thus, Ime2 negatively feeds back to Ime1 and ensures that Ime1 expression is transient during yeast meiosis.

In addition, Ime2 also leads to the activation of Ndt80 (Sopko et al., 2002), a transcription factor that activates the middle meiotic genes (Chu and Herskowitz, 1998) (Figure 5). Ndt80 is a transcription factor expressed during the prophase of meiosis I (prophase I) and is required for cells to exit prophase to carry out nuclear division (Xu et al., 1995). Ndt80 establishes the commitment point in yeast meiosis. Cells that constantly express Ndt80 enter the meiotic programme irreversibly, while disruption of *NDT80* permits cells to return to vegetative growth (Tsuchiya et al., 2014, Xu et al., 1995). Ndt80 recognises a DNA sequence known as the MSE (middle sporulation element) motif (YGNCACAAAA) (reviewed in Winter, 2012). The MSE motif is found in the upstream regions of 70% of the middle meiotic genes expressed between 2 and 5 hours after sporulation induction (Chu et al., 1998). Ndt80 also promotes its own transcription via a positive feedback loop to reinforce its expression during meiosis (Tsuchiya et al., 2014). Expression of middle meiotic genes induce cells to undergo meiotic divisions and form spores. Eventually, the late meiotic genes are activated to promote spore maturation.

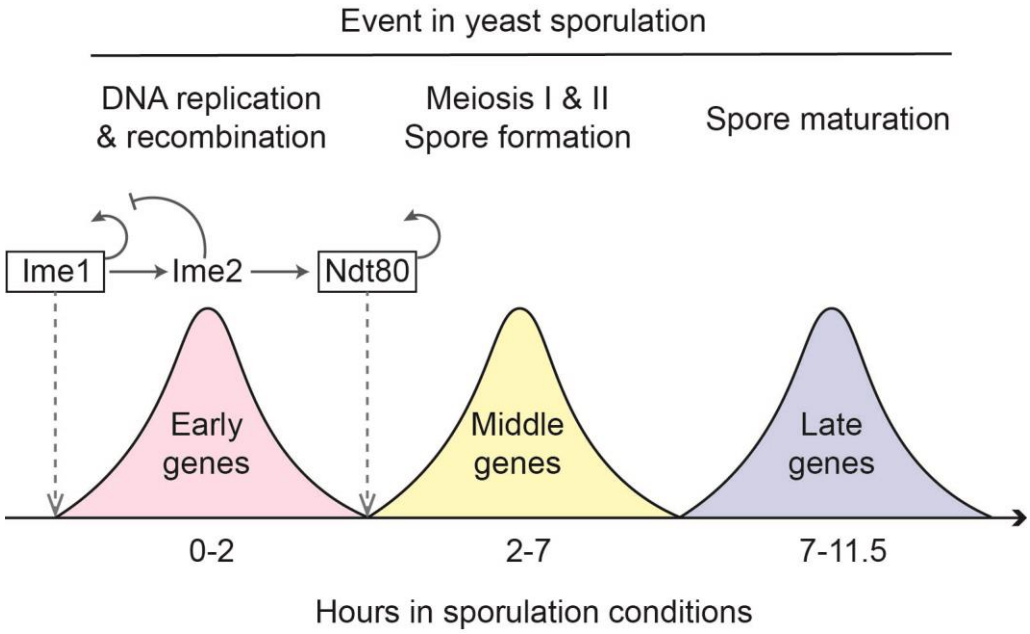

Figure 5. Yeast sporulation requires cascades of meiotic gene activation (Chu et al., 1998, Gurevich and Kassir, 2010).

The meiotic programme in yeast is specified by the expression of early, middle, and late meiotic genes. Several key players regulate proper entry and progression of meiosis. Ime1 is the key transcription factor that governs initiation of the meiotic programme. When Ime1 is expressed, the transcription factor activates the early meiotic genes with Ume6 and reinforces its own expression via a positive feedback loop (discussed below). Ime2, a meiosis-specific protein kinase activates Ndt80 and negatively feeds back on Ime1 activity. Ndt80 expression defines the commitment point in yeast meiosis. Once Ndt80 is expressed, the middle and late genes are subsequently activated to complete the sporulation programme. Ndt80 also promotes its own expression via a positive feedback loop. These key players are essential for regulating meiosis in yeast by controlling expression of meiotic genes at different stages.

1.8 The *IME1* promoter acts as a signal integrator to control entry into meiosis in yeast

IME1 is a gene that governs entry into meiosis and serves as a gatekeeper of a major developmental decision in yeast. Multiple signalling pathways govern transcription of *IME1* such that meiotic entry is limited to cells that are starved, respiring, and express *MAT***a**/α mating type loci. Overexpression of *IME1* can override the control by these signalling pathways, and forces cells to initiate meiosis under suboptimal or unsuitable conditions. In vegetative cells growing on acetate, *IME1* overexpression induces expression of meiotic genes that are normally undetected in wild-type cells (Smith et al., 1990). Diploid cells that are starved of amino acids enter and complete meiosis when *IME1* is overexpressed (Smith et al., 1990). Ectopic *IME1* expression also initiates meiosis in cells with incorrect mating types. For example, *IME1* expression induces diploid cells with *MAT***a**/**a** mating type to sporulate (Smith et al., 1990). Furthermore, *IME1* expression induces haploid cells expressing both *MAT***a** and *MAT*α to initiate meiosis (Mitchell and Bowdish, 1992). Yet, overexpressing *IME1* in haploid cells is lethal when cells enter meiosis I, as segregation of homologous chromosomes cannot occur. Consequently, cells become inviable likely due to double-strand breaks in DNA (Mitchell and Bowdish, 1992). In addition, *IME1* overexpression can bypass the requirement for respiration to induce meiosis (Honigberg and Purnapatre, 2003). Taken together, *IME1* expression is co-regulated by mating type, nutrient, and respiration signals. Notably, genes that have major roles in controlling cell fate decisions are commonly regulated by a multitude of intrinsic and environmental signals. One example is STRA8 (stimulated by retinoic acid 8), a transcriptional activator that is responsible for initiating meiosis during spermatogenesis and oogenesis in mammalian cells (Anderson et al., 2008, Tedesco et al., 2009). To ensure timely expression of *Stra8*, an intrinsic meiotic competence factor called *Dazl* must be present in cell (Lin et al., 2008). In addition, retinoic acid acts as an extracellular signalling molecule to activate the expression of *Stra8* by binding to specific nuclear hormone receptors (Ma et al., 2018). STRA8 in turn initiates meiosis by altering the expression of genes that are involved in meiosis (Ma et al., 2018). *IME1* and *Stra8* demonstrate that multiple signals regulate developmental genes at the transcriptional level in different organisms to ensure that they are expressed timely in cells.

How do multiple layers of signals arising from different origins regulate *IME1* transcription? The key to this question lies in the unusually large promoter of *IME1*, which is more than 2.3 kb in length. The *IME1* promoter consists of three putative TATA boxes, annotated between 158 to 353 bp upstream of the *IME1* ORF (Sagee et al., 1998). In line with the mapped TATA boxes, transcription of *IME1* was found to be initiated at 229 bp upstream of the *IME1* start codon (Sherman et al., 1993). Importantly, the *IME1* promoter integrates the signals controlling entry into meiosis, including signals derived from mating type of the cell, nutrient availability, and respiration (Figure 6). When the cell is starved, respiring, and expresses *MAT***a**/α mating type loci, the *IME1* promoter becomes transcriptionally active and *IME1* is expressed. High expression level of *IME1* prompts the cell to initiate the meiotic programme and complete sporulation. Hence, the *IME1* promoter is key to convert multiple signals into a binary cell decision – whether or not the cell undergoes sporulation. The large *IME1* upstream region is known to be organised with *cis*-regulatory elements that modulate *IME1* transcription. Studies have demonstrated that the *IME1* promoter is decorated with both activating and repressive transcriptional elements that respond to different signalling pathways (Figure 6). For example, a 21 bp region that is close to 2 kb upstream of the ORF mediates *IME1* repression in cells with incorrect mating types (Covitz and Mitchell, 1993). This region was later found to recruit Rme1, a transcription factor that inhibits *IME1* transcription in cells with single or the same mating types (discussed below). The *IME1* promoter also contains regulatory elements that respond to nutrients. In a study published in 1995, Shefer-Vaida and co-workers examined the transcriptional activity of various parts of the *IME1* promoter using a β-galactosidase reporter assay (Shefer-Vaida et al., 1995). Two upstream activation sequences (UAS) were identified at the *IME1* promoter which, when fused to non-meiotic gene without any UAS, elicited the same expression pattern as *IME1* in nitrogen-deprived condition (Shefer-Vaida et al., 1995). Furthermore, Sagee et al. identified five regulatory elements in the *IME1* promoter between 621 and 1369 bp upstream of the ORF (Sagee et al., 1998). One of the elements, IREu (*IME1* repeated element upstream) was reported to be an activating element that is repressed by glucose in nutrient-rich conditions (Sagee et al., 1998). Until more recently, the *IME1* promoter was predicted to be regulated by a large number of transcription factors (Kahana et al., 2010). In this study, putative regulators of the *IME1* promoter were predicted using chromatin immunoprecipitation

with DNA microarray (ChIP-chip) datasets, consensus transcription factor binding motifs in the *IME1* promoter, and sequence conservation in other *Saccharomyces sensu stricto* species such as *Saccharomyces paradoxus* and *Saccharomyces bayanos* (Kahana et al., 2010). These studies on the *IME1* promoter illustrate that the upstream regulatory region of *IME1* is enriched with regulatory elements that integrate signals from multiple pathways to control *IME1* transcription. How signals arising from the mating type, respiration, and nutrient pathways converge onto the *IME1* promoter will be discussed in the next sections (1.9, 1.10, 1.11).

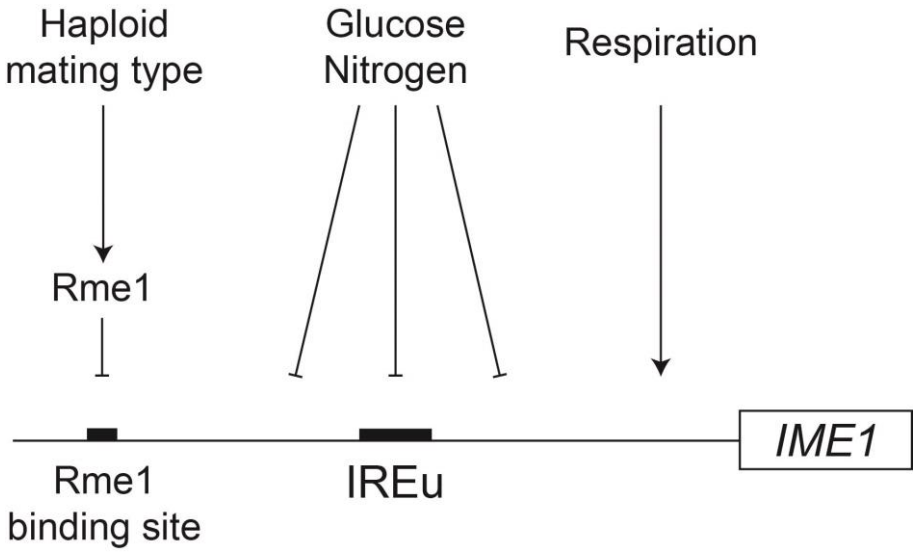

Figure 6. The *IME1* promoter integrates multiple signals to control entry into meiosis (adapted from (Honigberg and Purnapatre, 2003, van Werven and Amon, 2011)).

Schematic diagram representing the signals that regulate *IME1* promoter activity. Mating type signals converge onto a transcription factor, Rme1 that binds to approximately 2 kb upstream of the *IME1* ORF. Nutrient signals regulate multiple response elements in the *IME1* promoter. Glucose represses an activating element known as IREu located between 1122 to 1153 bp upstream of the *IME1* start codon. Respiration also plays roles in regulating *IME1* transcription. Multiple pathways ensure that *IME1* is transcribed only under conditions appropriate for entry into meiosis.

1.9 Mating type control of the *IME1* promoter

In yeast, co-expression of *MAT***a** and *MAT*α mating type loci is a pre-requisite for *IME1* transcription and entry into meiosis. *IME1* transcription occurs in cells with *MAT***a**/α mating type (Kassir et al., 1988). In contrast, *IME1* does not transcribe in haploid cells with single mating type, or diploid cells with *MAT***a**/**a** or *MAT*α/α mating types (Covitz and Mitchell, 1993, Kassir et al., 1988). The mechanism by which signals arising from the mating type loci communicate with the *IME1* promoter has been elucidated. In cells with single or the same mating type loci, a Cys2His2 zinc finger transcription factor called Rme1 (regulator of meiosis 1) is produced (Covitz et al., 1991). Disruption of *RME1* permits diploid cells expressing the same mating type loci to undergo meiosis, thus Rme1 represses meiosis in cells with inappropriate mating types (Rine et al., 1981). Rme1 was shown to bind at the RRE1 (RME1-response element 1) motif located at approximately 2 kb upstream of the *IME1* ORF (Covitz and Mitchell, 1993) (Figure 7). Instead of directly repressing the transcription of *IME1*, Rme1 acts as a transcriptional activator when bound to the RRE1 motif (Covitz and Mitchell, 1993). Binding of Rme1 at the *IME1* promoter stimulates transcription of a long non-coding RNA known as *IRT1* (van Werven et al., 2012) (Figure 7). *IRT1* is exclusively produced in cells expressing only one or the same mating type loci, but not in *MAT***a**/α cells. As *IRT1* transcription advances through the upstream regulatory region of *IME1* towards the ORF, a repressed chromatin state is established in the *IME1* promoter. This is achieved by the combined actions of nucleosome re-organisation, deposition of H3K4me2 and H3K36me methylation marks, and interaction with histone deacetylases (van Werven et al., 2012). As a result, *IME1* transcription is inhibited in cells with single or the same mating type loci. In *MAT***a**/α cells, **a**1 and α2 proteins are produced from the mating type loci and form a heterodimer. The **a**1-α2 heterodimer binds to the upstream region of *RME1* and represses *RME1* transcription, likely through the action of the Tup1-Cyc8 repressor complex (Covitz et al., 1991, Mathias et al., 2004). Therefore, very low levels of Rme1 are available in *MAT***a**/α cells to activate *IRT1* transcription.

In addition to *IRT1*, a second long non-coding transcript called *IRT2* is produced just upstream of *IRT1* in *MAT***a**/α cells (Figure 7). *IRT2* transcription is activated by the binding of Ume6-Ime1 to a sequence motif 90 bp upstream of *IRT2*

(Moretto et al., 2018). The sequence of *IRT2* overlaps with the Rme1 binding sites in the *IME1* promoter. When *IRT2* is transcribed in *MAT***a**/α cells, nucleosomes are deposited at the same time which generates a compact chromatin environment around the Rme1 binding sites (Moretto et al., 2018). The local chromatin changes induced by *IRT2* transcription displace Rme1 from the *IME1* promoter, and thereby silence *IRT1* and promote *IME1* transcription (Figure 7). Ime1 expression, in turn, activates *IRT2* transcription. Thus, Ime1 reinforces its own transcription in *MAT***a**/α cells by forming a positive feedback loop with *IRT2* and *IRT1*.

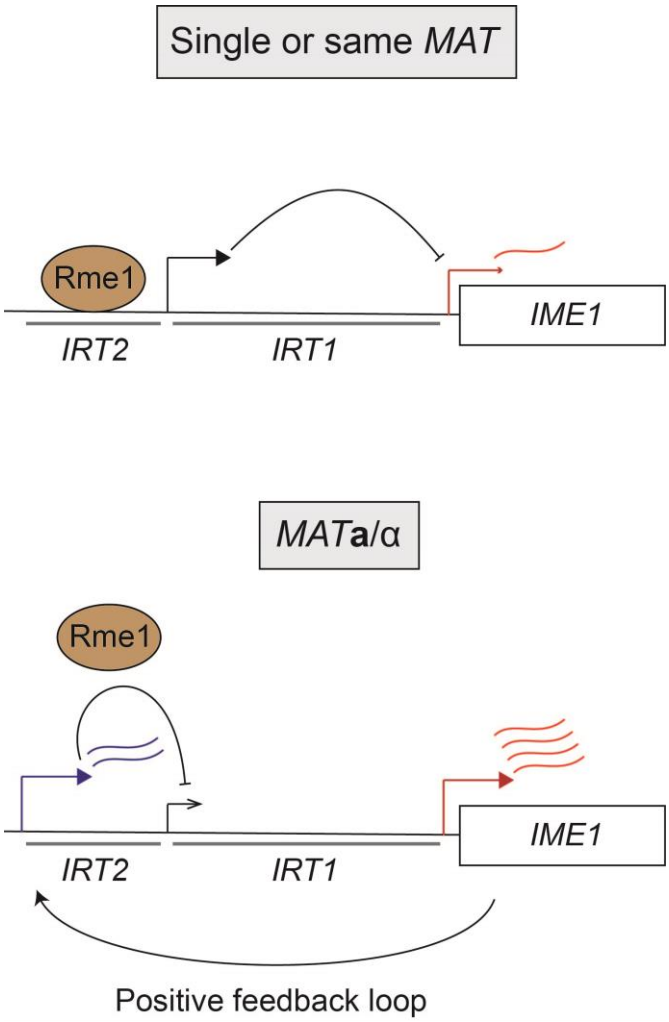

Figure 7. *IME1* promotes its own transcription via a positive feedback loop involving *IRT1* and *IRT2* in *MAT*a/α cells (adapted from (Moretto et al., 2018)).
In cells expressing a single or the same mating type loci, the lack of **a**1-α2 repressor allows Rme1 to express and bind to the *IME1* promoter. Rme1 binding triggers *IRT1*

transcription, which represses *IME1* promoter activity *in cis*. In *MAT***a**/α cells, the **a**1-α2 repressor prevents Rme1 production and thereby prevents *IRT1* transcription. The *IME1* promoter becomes active and *IME1* is transcribed. The Ime1 protein partners with Ume6, and binds to a site that is 2 kb upstream of the ORF. Ime1-Ume6 activates transcription of *IRT2*, which in turn displaces any Rme1 bound in the promoter and ensures *IRT1* transcription is tightly repressed. Thus, *IRT2* promotes *IME1* transcription.

In eukaryotes, meiosis is a conserved cell differentiation programme that produces gametes or spores containing half the DNA content of the parent cell. Hence, meiosis is often referred to as a reduction division process. Diploid yeast cells normally express both *MAT***a** and *MAT*α mating types. *IME1* is transcribed only when both mating type loci are present, perhaps because the mating type signals indicate that the cell is diploid and thus have sufficient DNA content to undergo meiosis. In other organisms, correct chromosome number is also a requirement for initiation and completion of meiosis. For example, ectopic expression of meiotic activator Mei3 in haploid fission yeast cells is sufficient to initiate meiosis, but eventually leads to meiotic catastrophe (Wang et al., 1998). Furthermore, engineered *Arabidopsis suecica* plants with double chromosomal content also displayed meiotic abnormalities and chromosomal fragmentation in cells (Madlung et al., 2005). Therefore, mating type control of *IME1* transcription may parallel mechanisms in other eukaryotes that prevent meiosis from occurring when cells contain incorrect number of chromosomes.

1.10 Respiration is required for *IME1* transcription

Respiration is a requirement for entry into meiosis in budding yeast. In order to initiate meiosis, a non-fermentable carbon source such as acetate must be present. In addition, cells must also have functional mitochondria that can utilise the non-fermentable carbon source to produce energy by respiration. Interestingly, the non-fermentable carbon source and mitochondrial activity are important for different stages of meiosis in yeast. The non-fermentable carbon source is required for pre-meiotic DNA replication and recombination to take place prior to prophase I, but is no longer needed beyond prophase I (Jambhekar and Amon, 2008). Conversely, mitochondrial competence is required for meiotic divisions to take place beyond prophase I (Jambhekar and Amon, 2008).

IME1 expression is modulated by respiration at the protein level. Specifically, Ime1 expression is sensitive to mitochondrial activity, and not the non-fermentable carbon source (Jambhekar and Amon, 2008). Ime1 is significantly downregulated when cytochrome c oxidase/Complex IV, a crucial enzyme in the electron transfer chain, is defective or inhibited (Jambhekar and Amon, 2008). In contrast, absence of acetate does not affect Ime1 expression, suggesting that the non-fermentable carbon source is involved in other aspects of meiosis initiation (Jambhekar and Amon, 2008). In addition, mitochondrial activity also regulates *IME1* transcription. Chemical inhibition of different components required for mitochondrial activity, such as cytochrome c reductase, ATP synthase, and proton gradient, was found to severely affect *IME1* transcription (Weidberg et al., 2016).

Respiration has been suggested to regulate *IME1* transcription by altering the extracellular pH. Respiration is known to have an effect on the environmental pH, which in turn regulates cell growth and survival (summarised in Baron et al., 2013). When a non-fermentable carbon source is utilised for growth, cells alkalinise the growth medium and an alkaline stress is imposed on cells. In response to the alkaline stress, cells reduce their growth rate and optimise survival. Rim101, a Cys2His2 zinc finger transcriptional repressor, is activated in response to medium alkalinisation by a C-terminal proteolytic cleavage (Futai et al., 1999). The activation of Rim101 triggers signalling cascades and cellular responses that enable cells to adapt to the

alkaline stress. Rim101 has been implicated in regulating *IME1* transcription. In *rim101*Δ cells, *IME1* fails to accumulate in sporulation conditions (Su and Mitchell, 1993). Furthermore, induced expression of *IME1* rescues the sporulation defect in *rim101*Δ cells (Su and Mitchell, 1993). More recently, Rim101 was proposed to regulate *IME1* transcription by directly mediating signals from the electron transfer chain to the *IME1* promoter (Zhao et al., 2018). Ndi1, a component of Complex I in the respiratory chain, promotes Rim101 expression. Rim101 in turn represses transcription of *SMP1*, which encodes a MADS-box transcription factor that binds to the *IME1* promoter and represses its activity (Zhao et al., 2018). Nevertheless, *IME1* transcription defects are less severe in *rim101*Δ cells, compared to cells with dysfunctional mitochondria (Jambhekar and Amon, 2008). Therefore, respiration also regulates *IME1* transcription via a Rim101-independent pathway.

In mitochondria, respiration takes place to convert organic compounds into energy in the form of adenosine triphosphate (ATP) for various cell processes, including gene transcription. Although mitochondrial activity has been established to regulate *IME1* transcription, it is still unclear whether respiration targets the *IME1* promoter specifically or affects transcriptional efficiency in a global fashion. The Ndi1-Rim101-Smp1 pathway discussed above suggests that mitochondrial activity targets the *IME1* promoter to regulate *IME1* transcription. Some studies showed that *IME1* transcription defects in respiration-deficient cells are not related to energy levels. For example, the intracellular ATP concentrations in cells with different defects in the electron transport chain were found to be comparable to wild-type cells in sporulation conditions (Zhao et al., 2018). Furthermore, providing respiration-deficient cells with glucose as an alternative energy source cannot rescue *IME1* transcription (Jambhekar and Amon, 2008). These observations support that *IME1* transcription is regulated by a specific signalling pathway mediated by respiration, rather than consuming energy produced by respiration. Meanwhile, other studies have suggested that respiration acts as an energy provider for *IME1* transcription. Previous work found that *IME1* transcription can be rescued in respiration-deficient strains in the presence of glucose when the Ras/PKA and TORC1 pathways are inhibited (Weidberg et al., 2016). In addition, *IME1* cannot be expressed from inducible promoter under sporulation conditions in respiration-deficient cells (Weidberg et al., 2016). These data indicate that respiration does not target the *IME1*

promoter, and the role of respiration can be substituted by glycolysis. Taken together, current studies have presented contradictory views on the role of respiration in regulating *IME1* transcription. While some evidence suggests that respiration provides energy for *IME1* transcription, other studies have proposed that respiration targets *IME1* transcription through regulating specific regulatory proteins such as Rim101 and Smp1. Further studies are required to decipher whether respiration defects result in global loss of transcription or specific effects on *IME1* transcription, or both.

1.11 Glucose and nitrogen regulate the *IME1* promoter through the Ras/PKA and TORC1 pathways

Initiation of meiosis in yeast is strictly limited to cells that experience nutrient starvation. In early studies, nitrogen starvation was proposed to initiate meiosis in budding yeast. Studies found that the presence of ammonium ions, a nitrogen source utilised by budding yeast, inhibits entry into meiosis (Fowell, 1969, Miller, 1957). In 1982, the nutrient requirements for yeast meiosis became better defined by a study published by Freese and co-workers (Freese et al., 1982). As described in this study, cells were exposed to multiple types of nutrient starvation and it was found that depletion of nitrogen, carbon, or phosphate compounds is sufficient to induce meiosis in yeast (Freese et al., 1982). Importantly, the preferred carbon source glucose must be absent from the growth medium for meiosis to take place. In addition, a slowly metabolising nitrogen compound such as phenylalanine also encourages initiation of meiosis (Freese et al., 1982). Thus, yeast cells undertake meiosis when glucose and good nitrogen sources are absent, but nutrient signals also need to be partially active to provide energy for the completion of meiosis.

IME1 transcription is sensitive to nutrient availability in the growth medium. The presence of glucose represses *IME1* transcription (Kassir et al., 1988). When a non-fermentable carbon source such as acetate is present, *IME1* transcription is weakly activated. In the absence of glucose and nitrogen compounds, *IME1* transcription is strongly activated and *IME1* is expressed at high levels (Kassir et al., 1988). Thus, *IME1* transcription is repressed by glucose and nitrogen compounds in rich growth medium. Glucose and nitrogen compounds activate the Ras/PKA (protein kinase A) and TORC1 (target of rapamycin complex 1) signalling pathways, which converge onto the *IME1* promoter to modulate *IME1* transcription. The Ras/PKA and TORC1 signalling pathways are conserved nutrient-sensing pathways that modulate various cell responses, such as stimulating cell growth and regulating stress responses (Sapio et al., 2014, Smith et al., 1998, Loewith and Hall, 2011). Mis-regulation of Ras/PKA and TORC1 signalling has been implicated in cancer formation in humans (Sapio et al., 2014, Xie et al., 2016).

In budding yeast, Ras/PKA pathway and Gpr1-Gpa2-Rgs2 GPCR system are the two major glucose sensing and signalling pathways (reviewed in Conrad et al., 2014). The Ras/PKA pathway senses intracellular glucose, while the Gpr1-Gpa2-Rgs2 system detects extracellular glucose. Notably, signals from both systems converge onto the adenylate cyclase, which converts ATP into the secondary messenger cyclic AMP (cAMP). Thus, cAMP plays a significant role in mediating the upstream glucose signals to modulate cell responses. In the Ras/PKA signalling system, glucose derivatives from glycolysis stimulates the highly conserved Ras small G proteins that are tethered to the plasma membrane (Conrad et al., 2014). Ras proteins are encoded by *RAS1* and *RAS2* in yeast. The activity of the Ras proteins is modulated by three proteins, GTPase activating proteins (RasGAP) Ira1 and Ira2, and GDP exchange factor (RasGEF) Cdc25 (Broach and Deschenes, 1990). Like all G proteins, Ras proteins are active in GTP-bound form and inactive in GDP-bound form. Ras activation is facilitated by Cdc25, which replaces the bound GDP with GTP. Cdc25 was suggested to induce post-translational modification of Ras, which contributes to the nucleotide exchange event. Ira1 and Ira2 inactivate Ras proteins by stimulating the intrinsic GTPase activity in Ras and thereby promoting hydrolysis of GTP (reviewed in Santangelo, 2006). The active Ras proteins in turn stimulate the adenylate cyclase at the plasma membrane, encoded by the *CYR1* gene, to produce cAMP. cAMP then binds to PKA and switches on its activity. PKA is a heterotetrameric complex with two catalytic kinase subunits (Tpk1/Tpk2/Tpk3) and two regulatory subunits (Bcy1) (Conrad et al., 2014). When cAMP binds to the regulatory Bcy1 subunits of the PKA tetramer, the active catalytic Tpk kinase subunits are released (reviewed in Santangelo, 2006). These active PKA subunits phosphorylate downstream effector proteins, and eventually trigger transcriptional changes that turn into cell responses. Although glucose has been recognised as the major trigger of the Ras/PKA pathway, other nutrients can also modulate PKA activity. These nutrients, including phosphate, amino acids, and ammonium ions bind to specific nutrient receptors in the plasma membrane and activate the PKA pathway. The signalling pathways by which these nutrients trigger PKA activity are cAMP-independent, and the mechanistic details are still largely unknown (Conrad et al., 2014). The PKA pathway plays an important role in regulating many stress responses and morphological changes in yeast, such as quiescence and pseudohyphal differentiation (Gray et al., 2004, Tamaki, 2007). Two

paralogous zinc finger transcription factors, Msn2 and Msn4, mediate many stress responses that are regulated by the PKA pathway (Smith et al., 1998). It is worth mentioning that cAMP, the secondary messenger in the PKA pathway, can also regulate gene transcription through the CREB (cyclic AMP responsive element binding) transcription factors. CREB transcription factors recognise the CRE (cyclic AMP responsive element) motif in gene promoters. Upon phosphorylation by kinases such as PKA, CREB transcription factors are activated to modulate gene transcription (Shaywitz and Greenberg, 1999).

The TOR (target of rapamycin) signalling pathways were first discovered in budding yeast as targets of rapamycin, a drug with immunosuppressant and anti-tumour properties (Xie et al., 2016). The core player of these pathways is a serine/threonine enzyme known as Tor, which is encoded by two genes *TOR1* and *TOR2* in yeast (reviewed in Loewith and Hall, 2011). Tor1 and Tor2 belong to the PI kinase-related protein kinase family and are paralogues that share 67% amino acid sequence similarity. The two proteins have similar domain structures that contain HEAT repeats at the N-termini, followed by the FAT domain, FRB domain, kinase domain, and finally the FATC domain at the C-termini. Notably, rapamycin targets Tor by forming a complex with its FRB domain and another protein, FKBP (FK506-binding protein) that is encoded by *FPR1* in yeast (Heitman et al., 1991). Tor1 or Tor2 proteins can form two distinct complexes, known as TORC1 (TOR complex 1) and TORC2. TORC1 and TORC2 are different in terms of subunit composition and complex conformation, so that only TORC1 is sensitive to rapamycin treatment as one of the subunits in TORC2 shields the Tor2 domain targeted by rapamycin (Loewith et al., 2002). In addition, TORC1 and TORC2 play different cellular functions. TORC2 is tethered to the plasma membrane and is mainly involved in regulating plasma membrane homeostasis and actin cytoskeleton in yeast (reviewed in Roelants et al., 2017). Conversely, the TORC1 pathway responds to a variety of nutrient and stress signals, including carbon and nitrogen sources, phosphate, caffeine, and various stresses (salt, oxidative, temperature) (reviewed in Loewith and Hall, 2011). In yeast, the TORC1 pathway is primarily activated by nitrogen compounds. Nutrient signals converge onto the Gtr1-Gtr2 heterodimer, which is tethered to the membrane of the yeast vacuole by the EGO complex. The Gtr1-Gtr2 heterodimer is converted into an active conformation by loading Gtr1 with GTP and

Gtr2 with GDP. The active heterodimer binds to the Kog1 subunit of TORC1, and thereby activates the complex (reviewed in González and Hall, 2017). Additionally, TORC1 can also function in a second pathway that is independent of the Gtr proteins (Stracka et al., 2014). One of the well characterised substrates of TORC1 is the Sch9 protein kinase, of which the phosphorylation status is sensitive to the nutrients present in the environment (Loewith and Hall, 2011). TORC1 is known to repress a large set of genes in the presence of amino acids and other nitrogen sources, which is often referred to as nitrogen catabolite repressible genes (Godard et al., 2007). TORC1 activity was demonstrated to inhibit nitrogen and carbon repressible genes by phosphorylating and sequestering transcriptional activators into the cytosol (Beck and Hall, 1999).

TORC1 signalling pathway represses *IME1* transcription in nutrient-rich medium. Treating yeast cells with rapamycin in nutrient-rich medium promotes *IME1* transcription and spore formation 48 hours after rapamycin treatment (Jambhekar and Amon, 2008). However, the percentage of spore formation induced by TORC1 inhibition is much lower than that observed in sporulation conditions, suggesting that other nutrient signalling pathways are also involved in repressing *IME1* expression. Past studies proposed that the PKA pathway also represses *IME1* transcription in nutrient-rich condition. Stress-response genes repressed by the PKA pathway, such as *TPS1* that encodes a trehalose-6-P synthase, may be required for inducing *IME1* transcription (Honigberg and Purnapatre, 2003). Furthermore, the *IME1* promoter may be directly repressed by the PKA pathway. In the presence of glucose, Sok2, a transcriptional repressor activated by PKA phosphorylation, negatively regulates activity of the IREu element in the *IME1* promoter (Shenhar and Kassir, 2001) (Figure 6). In addition, the IREu element also resembles a STRE (stress response element) sequence, which is a characterised binding site of Msn2 and Msn4 (Sagee et al., 1998). These observations suggest that Msn2 and Msn4 may play roles in activating *IME1* when the PKA pathway becomes inactive. Notably, more recent work demonstrated that nutrient repression of *IME1* transcription is mediated via only the Ras/PKA and TORC1 pathways (Weidberg et al., 2016). In this work, PKA activity was investigated using an analogue-sensitive version of PKA, which was inhibited by the addition of the ATP analogue 1NM-PP1. Inhibition of PKA completely removes glucose repression of *IME1* transcription (Weidberg et al., 2016). Importantly,

inhibition of Ras/PKA and TORC1 pathways leads to full de-repression of *IME1* transcription in the presence of glucose and nitrogen compounds. *IME1* transcript levels were found to mimic that in sporulation conditions, and almost all cells undergo meiosis 24 hours after PKA and TORC1 inhibition (Weidberg et al., 2016). Moreover, partial TORC1 activity is required for efficient *IME1* transcription (Weidberg et al., 2016). Given that meiosis is an energy-consuming process, it is possible that the remnant TORC1 activity serves as a nutrient sensor to detect the presence of an energy source that could support the meiotic programme to completion. In addition to controlling *IME1* transcription, PKA and TORC1 pathways also play roles in regulating the Ime1 protein to ensure successful entry into meiosis. Inhibition of the TORC1 pathway using rapamycin was reported to re-localise Ime1 into the nucleus and increase Ime1 half-life (Colomina et al., 2003). As discussed above in section 1.7, Rim11 and Rim15 are crucial for Ime1 activity by inducing interaction between Ime1 and Ume6 when meiosis is initiated. Previous study suggested that Ime1 phosphorylation mediated by Rim11 is inhibited by the PKA pathway (Rubin-Bejerano et al., 2004). Furthermore, Rim15 acts immediately downstream of the PKA pathway and integrates signals from multiple nutrient signalling pathways, including TORC1 (Swinnen et al., 2006). Thus, downregulation of PKA and TORC1 signals may promote Ime1 expression and nuclear activity in nutrient-poor conditions. Taken together, PKA and TORC1 pathways play pivotal roles in governing entry into meiosis by dictating *IME1* transcription and modulating Ime1 expression and activity. The multifaceted regulation of *IME1* by PKA and TORC1 ensures that entry into meiosis occurs only when rich nutrients are absent from the environment.

It is worth mentioning that Snf1, a glucose-sensitive pathway was also proposed to regulate *IME1* transcription (Honigberg and Lee, 1998). Snf1 kinase is an AMP-activated serine/threonine kinase that is de-repressed upon glucose limitation. Previous study showed that *IME1* transcription is significantly downregulated in sporulation conditions when Snf1 kinase is deleted (Honigberg and Lee, 1998). Furthermore, deleting Snf1 affects downstream processes in yeast meiosis including failure to induce *IME2* transcripts, reduced DNA replication and recombination, and impeded chromosome segregation during meiosis I (Honigberg and Lee, 1998). Nutrient signalling pathways are known to cross-talk with other pathways by regulating the same components in the signalling network. In yeast,

PKA and Snf1 pathways share common downstream targets and cross-talks between the two pathways have been described. For example, Snf1 phosphorylates the adenylate cyclase and modulates intracellular cAMP levels (Nicastro et al., 2015). Hence, PKA and Snf1 may converge onto common signalling nodes to regulate *IME1* transcription, but the molecular mechanism remains to be investigated.

How do PKA and TORC1 signalling pathways govern *IME1* transcription? The key factor that integrates the PKA and TORC1 signals at the *IME1* promoter is Tup1-Cyc8, a conserved transcriptional repressor complex in budding yeast (Figure 8). The structure, functions, and modes of action of the Tup1-Cyc8 complex will be further discussed in the next section (1.12). Tup1-Cyc8 was discovered to be a negative regulator of *IME1* transcription from a genetic screen, in which mutations of *TUP1* and *CYC8* led to de-repression of *IME1* under repressive conditions (Mizuno et al., 1998). *IME1* repression mediated by Tup1-Cyc8 is independent of Rme1 repression induced by mating type control. In addition, Tup1-Cyc8 directly interacts with the *IME1* promoter to modulate *IME1* expression (Mizuno et al., 1998). Recent work has demonstrated that Tup1 binds to the *IME1* promoter from 750 to 1400 bp upstream of the *IME1* ORF in nutrient-rich condition (Weidberg et al., 2016). Notably, Tup1 binding is mediated by signals from the PKA and TORC1 pathways, suggesting that Tup1-Cyc8 integrates nutrient signals to repress *IME1* transcription. Furthermore, Tup1-Cyc8 has been proven to be a crucial nutrient-sensitive regulator of *IME1*, since depletion of Tup1 leads to full de-repression of *IME1* transcription in the presence of glucose and nitrogen compounds (Weidberg et al., 2016). In conclusion, rich nutrients activate the PKA and TORC1 pathways, which in turn recruit the Tup1-Cyc8 repressor complex to the *IME1* promoter (Figure 8). Tup1-Cyc8 exerts repression at the *IME1* promoter and inhibits *IME1* transcription in the presence of glucose and nitrogen compounds. Thus, cells do not initiate entry into meiosis. When nutrients become depleted, Tup1-Cyc8 dissociates from the *IME1* promoter due to downregulated PKA and TORC1 signals. *IME1* transcription is de-repressed, and cells initiate entry into meiosis.

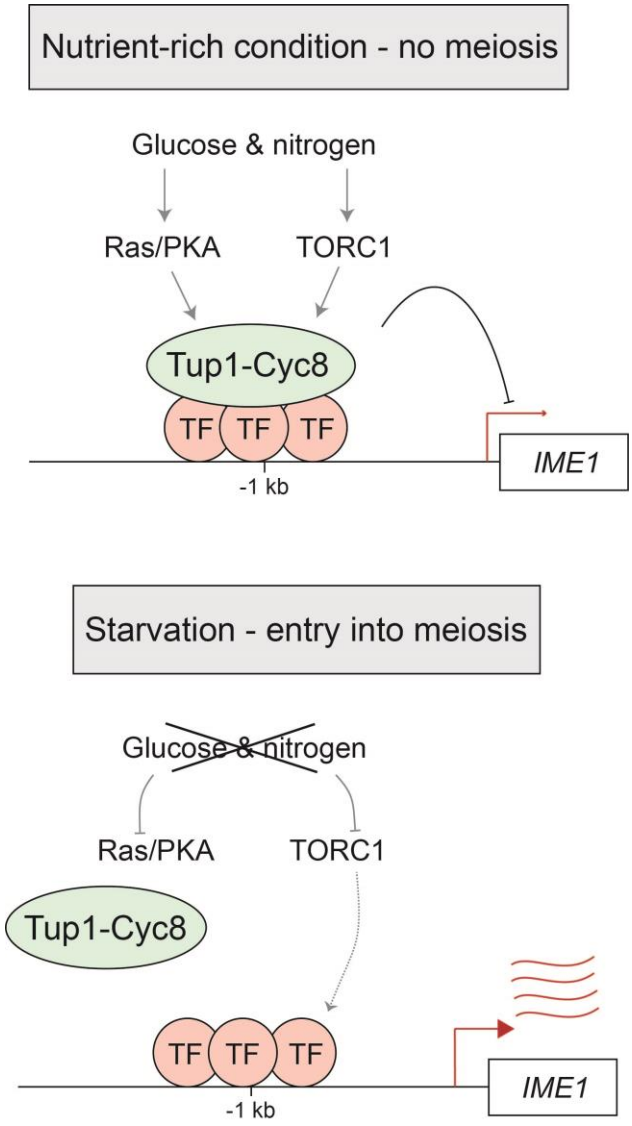

Figure 8. Nutrient repression of *IME1* transcription is mediated by PKA and TORC1 signalling pathways via the Tup1-Cyc8 repressor complex.

In nutrient-rich conditions, glucose and nitrogen compounds activate the PKA and TORC1 signalling pathways. These signals recruit Tup1-Cyc8 to the *IME1* promoter to repress *IME1* transcription. Conversely, when glucose and nitrogen compounds are absent, PKA and TORC1 are downregulated. Tup1-Cyc8 leaves the *IME1* promoter and *IME1* transcription is de-repressed. Partial TORC1 activity is also required for *IME1* induction. TF = Tup1-Cyc8 recruiting transcription factor.

1.12 Tup1-Cyc8 is a global transcriptional repressor complex conserved in eukaryotes

Tup1-Cyc8 is a conserved global transcriptional repressor complex in yeast. Tup1-Cyc8 regulates more than 150 genes with diverse functions, which account for 3% of total genes in yeast (reviewed in Smith and Johnson, 2000). The majority of Tup1-Cyc8 targets are genes that regulate stress responses, glucose repression, and genes that are mating type-specific. Tup1 and Cyc8 (also known as Ssn6) play distinct functions in the repressor complex: Cyc8 mediates recruitment of the complex to the target promoters, whereas Tup1 confers transcriptional repression activity of the complex. Several lines of experimental evidence support that Tup1 is the repressor, and Cyc8 is the mediator. First, deletion of Cyc8 removes Tup1 binding at the gene promoter, but not vice versa. Deletion of either Tup1 or Cyc8 leads to de-repression of the target gene (Fleming et al., 2014). Second, gene repression is impaired when Tup1 is deleted, even though Cyc8 is recruited to the promoter (Keleher et al., 1992). Third, artificially tethering Tup1 to gene promoter using a LexA DNA-binding domain is sufficient to repress gene transcription without Cyc8 (Tzamarias and Struhl, 1994).

The Tup1 repressor is highly similar to repressors of the Groucho/TLE family including the TLE1 repressor in human, Groucho in *Drosophila*, Unc-37 in *C. elegans*, and Tup11 and Tup12 in fission yeast (Fagerström-Billai and Wright, 2005, Smith and Johnson, 2000). Tup1 is considered to be a functional homologue of Groucho/TLE repressors. Tup1 and Groucho/TLE repressors both possess intrinsic repressor activity. Furthermore, Tup1 and Groucho/TLE repressors are structurally similar and are characterised by a WD40 repeat structure in their C-termini (reviewed in Fisher and Caudy, 1998). Similar to Tup1, Groucho/TLE repressors do not bind to DNA directly but interact with DNA-binding transcription factors at the target regions (Jennings and Ish-Horowicz, 2008). In mammalian cells, yeast Cyc8 can interact with the TLE1 repressor and mediate transcriptional repression (Grbavec et al., 1999). However, Tup1 was not classified as a member of the Groucho/TLE family since there are also differences in protein domains and repression mechanisms (Fisher and Caudy, 1998). Tup1 and Groucho/TLE repressors play fundamental roles in regulating developmental programmes in eukaryotes. In budding yeast, the Tup1-

Cyc8 repressor complex regulates various signalling pathways that control processes including mating type specification, DNA damage, glucose repression, flocculation, and stress responses. Deleting either or both Tup1 and Cyc8 causes severe phenotypes such as slow growth, loss of mating in haploid cells, and poor sporulation (Smith and Johnson, 2000). In *Drosophila*, the Groucho repressor establishes proper body patterning and neural tube development in the embryo (Muhr et al., 2001, Goldstein et al., 1999). Furthermore, the human TLE1 repressor is highly expressed in the post-natal brain, and a single nucleotide mutation in TLE1 results in postnatal microcephaly (Cavallin et al., 2018).

Structural domains of the Tup1-Cyc8 complex

In budding yeast, Tup1 and Cyc8 interact with each other to form a complex that targets genes for transcriptional repression (Williams et al., 1991). The active form of the Tup1-Cyc8 complex is composed of four Tup1 subunits and one Cyc8 subunit, yielding a large macromolecular complex (Varanasi et al., 1996). The Tup1 tetramer is constructed from a dimer of Tup1 dimers, which in turn interact with Cyc8 (Matsumura et al., 2012). Furthermore, the Tup1-Cyc8 complex is assumed to adopt an elongated conformation, as it gives an over-estimated mass on non-denaturing gels (Redd et al., 1997). Both Tup1 and Cyc8 proteins contain distinct domains that are important for their functions in the complex.

Tup1 is encoded by 713 amino acids and is approximately 78 kDa in size (Redd et al., 1997, Tartas et al., 2017) (Figure 9). The first 72 amino acids at the N-terminus of Tup1 forms the domain that interacts with Cyc8, as shown by two hybrid assays (Tzamarias and Struhl, 1994, Tartas et al., 2017). The repression domain of Tup1 is located next to the Cyc8 interaction domain from amino acids 72 to 200 (Tzamarias and Struhl, 1994). The repression domain of Tup1 interacts with the N-terminal tails of H3 and H4 histone proteins. Disrupting the interactions between Tup1 and the histone proteins impairs the repressor activity of Tup1 (Edmondson et al., 1996). The C-terminus of the Tup1 protein encodes seven WD40 repeats, with each repeat containing approximately 42 to 43 residues that terminates with a tryptophan-aspartic acid (WD) dipeptide (van der Voorn and Ploegh, 1992). X-ray crystallography data

of the β-subunit of G proteins showed that WD40 repeats fold into a β propeller structure (Chen and Courey, 2000), which likely serves as a receptor domain that interacts with other proteins. For example, the WD40 β propeller can act as a protein scaffold that bind to peptide sequences present in a wide range of transcriptional repressors (Jennings et al., 2006). The WD40 repeats in the Tup1 repressor are involved in regulating a subset of Tup1-Cyc8 targets. Specifically, the Tup1 β propeller modulates mating type and DNA damage genes, but is not necessary for repressing glucose-repressible and oxygen stress-inducible genes (Tzamarias and Struhl, 1995). In some cases, the WD40 β propeller in Tup1 also serves as a protein scaffold that interacts with DNA-binding proteins, such as the α2 repressor (Komachi et al., 1994).

Cyc8, the partner of Tup1, is encoded by 966 amino acids and is approximately 107 kDa in size (Redd et al., 1997, Tartas et al., 2017) (Figure 9). The Cyc8 protein possesses 10 tandem repeats of the tetratricopeptide (TPR) motif that is each encoded by 34 amino acids (Tartas et al., 2017). Each TPR motif contributes a basic helix-turn-helix fold (Zeytuni and Zarivach, 2012), and together the TPR repeats build a protein surface that mediates interactions with other proteins or ligands. The TPR domain of Cyc8 is responsible for interacting with Tup1 and DNA-binding transcription factors (Tzamarias and Struhl, 1995). The first three TPR repeats close to the N-terminus mediate hydrophobic interactions with Tup1, where a leucine residue at amino acid position 62 is important for this interaction (Matsumura et al., 2012). The first TPR1 motif, in particular, plays important roles in mediating interaction between Tup1 and Cyc8. Tup1 only interacts with Cyc8 if the TPR1 motif is structurally intact and is properly aligned relative to TPR2 and TPR3 (Gounalaki et al., 2000). The remaining seven TPR repeats in Cyc8 interact with DNA-binding transcription factors that regulate various pathways such as flocculation, oxidative stress, and DNA damage (Tzamarias and Struhl, 1995). Furthermore, a polyglutamine (polyQ) tract is present at the N-terminus of Cyc8 from amino acids 1 to 46 (Tartas et al., 2017). The polyQ domain in Cyc8 maintains proper interaction between Tup1 and Cyc8, as disruption of this domain causes self-association of Cyc8 and impairs its ability to interact with Tup1 (Tartas et al., 2017). In summary, Tup1 and Cyc8 protein domains mediate protein-protein interactions with each other, and link the Tup1-Cyc8 complex to DNA-binding proteins. By interacting with DNA-

binding proteins at different promoters, Tup1-Cyc8 can mediate transcriptional repression of different targets.

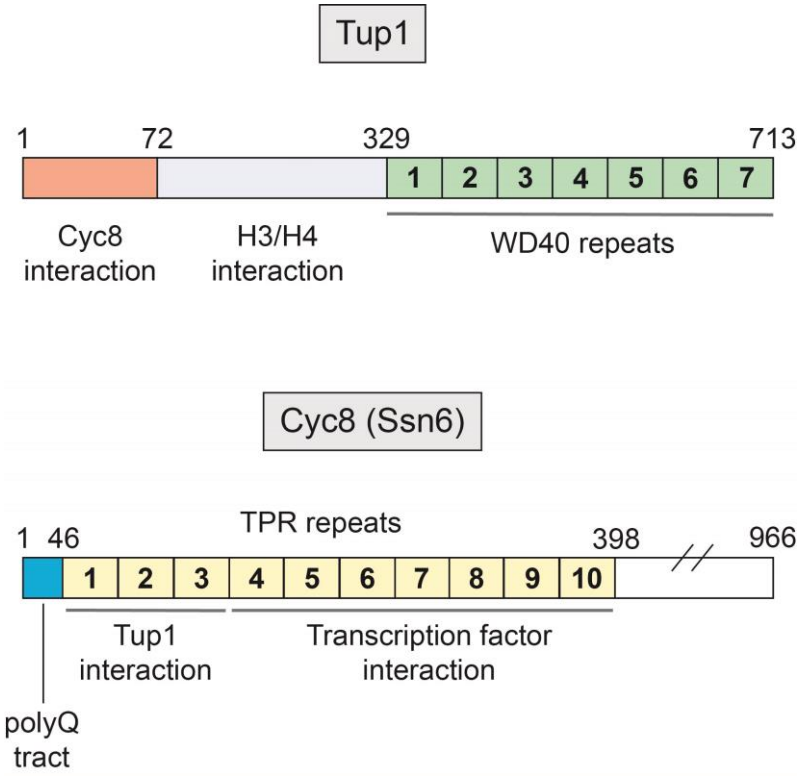

Figure 9. Protein domains in Tup1 and Cyc8 and their functions (adapted from (Matsumura et al., 2012, Tartas et al., 2017)).

Tup1-Cyc8 associates with promoter-bound transcription factors

Tup1-Cyc8 is recruited to the upstream regulatory regions of its target genes to mediate transcriptional repression. The Tup1-Cyc8 complex has no DNA-binding specificity and does not bind directly to DNA. In order to interact with gene promoters, Tup1-Cyc8 associates with promoter-bound transcription factors via protein-protein interactions (Figure 10). It is generally accepted that Cyc8 interacts with the DNA-binding transcription factors using its tandem TPR repeats (Smith et al., 1995). For some promoters, Tup1 can also interact with the transcription factors via the C-terminal WD40 β propeller structure (Komachi et al., 1994, Komachi and Johnson, 1997). Transcription factors that recruit Tup1-Cyc8 are important in mediating repression of the target genes. Mutations or truncations of Tup1-Cyc8 interacting

transcription factors result in loss of Tup1 binding even when the transcription factors remain bound to the promoters (Hall and Johnson, 1987, Komachi et al., 1994). In addition, transcriptional repression mediated by Tup1-Cyc8 is lost when the binding motif of the interacting transcription factor is removed (Keleher et al., 1992).

Transcription factors are known to dynamically interact with the upstream regulatory regions of genes. Transcription factors that recruit Tup1-Cyc8 control gene expression by binding and dissociating from the target promoters under specified conditions. Tup1-Cyc8 interacts with a large set of transcription factors that do not share apparent sequence similarities. Hence, Tup1-Cyc8 has the ability to regulate diverse gene promoters that are very different from each other. The transcription factor that recruits Tup1-Cyc8 is specific to the pathway that regulates the gene, so Tup1-Cyc8 can selectively interact with subsets of gene promoters under distinct conditions. Previous studies have identified some of the transcription factors that recruit Tup1-Cyc8 to gene promoters (Figure 10). One of the best studied examples is the α2 repressor. Tup1-Cyc8 interacts with the α2 repressor to suppress mating type-specific genes in both haploid and diploid cells. In haploid cells with *MAT*α mating type, α2 forms a heterodimer with a SRF1-like protein called Mcm1, and directs Tup1-Cyc8 to repress genes that are only expressed in cells with *MAT***a** mating type (Keleher et al., 1992, Keleher et al., 1988). Alternatively, in diploid cells that express both *MAT***a** and *MAT*α loci, α2 protein partners with **a**1 and guides Tup1-Cyc8 to haploid-specific genes, such as *RME1* (Goutte and Johnson, 1988, Covitz et al., 1991). Another well-known example is Mig1, a Cys2His2 zinc finger transcription factor that mediates glucose repression by recruiting the Tup1-Cyc8 complex (Trumbly, 1992). However, more than 40% of Tup1 target sites are not bound by known Tup1 recruiting transcription factors (Hanlon et al., 2011). Comparisons of ChIP-chip datasets and *tup1*Δ expression data uncovered novel transcription factors that likely recruit Tup1-Cyc8 to the target promoters. Further co-immunoprecipitation experiments showed that a subset of these transcription factors, including Yap6, Cin5, Phd1, and Skn7, physically interact with the Tup1-Cyc8 complex (Hanlon et al., 2011). Another transcription factor, Sok2, also scored highly as a potential Tup1-Cyc8 interacting transcription factor. Whether these transcription factors direct Tup1-Cyc8 to gene promoters remains to be investigated.

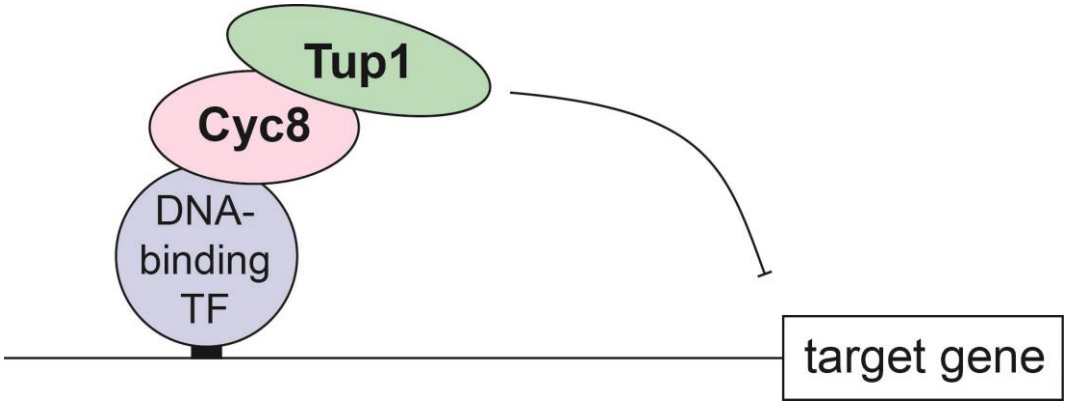

Tup1-Cyc8 gene targets	DNA-binding transcription factor(s)
MAT **a**-specific genes	α2 and Mcm1
Haploid-specific genes	**a**1 and α2
Glucose-repressible genes	Mig1
DNA damage-inducible genes	Crt1
Hypoxic genes	Rox1/Mot3
Starch degrading enzymes	Nrg1
Osmotic stress-inducible genes	Sko1
Flocculation genes	Flo1

Figure 10. Tup1-Cyc8 associates with gene promoters by interacting with promoter-bound transcription factors (adapted from (Smith and Johnson, 2000)). Tup1-Cyc8 does not bind directly to DNA. Tup1-Cyc8 is recruited to gene promoters by interacting with promoter-bound transcription factors. Typically, Cyc8 mediates protein-protein interaction between Tup1 and the transcription factor, while Tup1 exerts transcriptional repression. The transcription factor that recruits Tup1-Cyc8 to the promoter depends on the signalling pathway. Some of the transcription factors that recruit Tup1-Cyc8 to pathway-specific gene sets have been identified and are listed in the table. TF = transcription factor.

Mechanisms of transcriptional repression mediated by Tup1-Cyc8

Multiple mechanisms have been proposed for how Tup1-Cyc8 represses gene transcription. One of the mechanisms involves re-organisation and stabilisation of nucleosomes at gene promoters (model 1 in Figure 11). Previous work on the *STE6* promoter demonstrated that Tup1 binds to nucleosomes in a ratio of 2:1 to organise promoter structure (Ducker and Simpson, 2000). Tup1 stabilises nucleosomes at the -1 and -2 positions at the target promoters, likely as a means to block transcriptional activators from binding (Rizzo et al., 2011). The chromatin remodelling activity of Tup1 involves Isw2, an ATP-dependent chromatin remodelling enzyme that was found to modulate half of Tup1-remodelled genes (Rizzo et al., 2011). Tup1 may also induce the binding of a low occupancy nucleosome, called the P nucleosome between nucleosomes at -1 and +1 positions (Chen et al., 2013). When Tup1 is depleted, an expanded nucleosome-depleted region is formed near the transcription start site of Tup1-bound promoters by shifting nucleosomes apart and reducing nucleosome occupancy (Rizzo et al., 2011). It is worth noting that Tup1 also has a role in incorporating histone variants into chromatin, such as at the *GAL1* promoter. Tup1 inserts Htz1 (H2AZ) at the nucleosome that overlaps with the transcription start site in the *GAL1* promoter, and thereby establishes transcriptional memory and enables faster re-activation by RNA Polymerase II and the Mediator (Sood et al., 2017, Gligoris et al., 2007).

In addition, Tup1-Cyc8 represses its bound promoters by promoting histone deacetylation (model 2 in Figure 11). Tup1 interacts with the N-terminals of H3 and H4 histone proteins in multiple acetylation states (Edmondson et al., 1996). Tup1 preferentially associates with monoacetylated H3 proteins, while it is also able to bind H4 proteins with no acetylation, monoacetylation, and diacetylations (Edmondson et al., 1996). Many studies have reported that Tup1 recruits histone deacetylases (HDACs) to establish repressive chromatin structure around the target promoter. HDACs regulate gene transcription by opposing the action of another group of enzymes known as histone acetyltransferases (HATs). HATs interact with the N-terminal tails of histones and modify them by transferring an acetyl group to the side chains of lysine residues. This abolishes the positive charge of the lysine residues and thus reduce the interactions between the negatively charged DNA and histone

proteins (Bannister and Kouzarides, 2011). As a result, the chromatin structure becomes loose and open, which allows the transcriptional machinery to bind and initiate gene transcription (Barnes et al., 2005). Conversely, HDACs catalyse lysine de-acetylation reactions, therefore histone proteins re-gain positive charges and chromatin structure transforms into a compact, repressed state (Bannister and Kouzarides, 2011). HDACs can act globally and can also be recruited to target the upstream repressive sequences in gene promoters by specific repressor proteins (Kurdistani and Grunstein, 2003) such as Tup1. Tup1 physically interacts with multiple HDACs, including Class I HDACs Rpd3, Hos1, and Hos2 (Watson et al., 2000, Davie et al., 2003) and Class II HDAC Hda1 (Wu et al., 2001). In the absence of Tup1 or the recruited HDACs, H3 and H4 histone proteins are highly acetylated (Wu et al., 2001, Edmondson et al., 1996, Watson et al., 2000). Importantly, when HDACs are deleted, Tup1 targets are de-repressed as a consequence of increased H3 and H4 acetylation (Watson et al., 2000, Wu et al., 2001, Fleming et al., 2014). Given that Tup1 binds strongly to hypoacetylated histones, histone deacetylation is also a means by which Tup1-Cyc8 reinforces its own recruitment (Wu et al., 2001, Edmondson et al., 1996). Interestingly, Rpd3 and Hos2 can also interact with the TPR repeats of Cyc8 independent of Tup1, implying that Cyc8 may possess some extent of repressor activity (Davie et al., 2003). Notably, Tup1-Cyc8 target genes are repressed by different combinations of HDACs. For example, the flocculation gene *FLO1* is repressed by Rpd3 and Hda1 (Fleming et al., 2014), whereas *SUC2*, a glucose repressible gene required for sucrose utilisation, is repressed by Rpd3, Hos1, and Hos2 (Watson et al., 2000).

Apart from establishing repressive chromatin structure, Tup1-Cyc8 can inhibit transcription by directly interfering with the transcriptional machinery (model 3 in Figure 11). In eukaryotic transcription, the Mediator complex, as part of the RNA polymerase II holoenzyme, regulates transcription by forming a bridge between transcriptional activators and the RNA polymerase II. Several lines of evidence support that Tup1-Cyc8 interacts with the RNA polymerase II holoenzyme. First, Tup1-Cyc8 physically interacts with various subunits of the holoenzyme, such as the Hrs1 (or Pgd1) subunit of the Mediator complex, and the Srb10 (or Ssn3) subunit that phosphorylates the C-terminal domain of RNA polymerase II (Papamichos-Chronakis et al., 2000, Zaman et al., 2001). Second, transcriptional repression

mediated by Tup1-Cyc8 is relieved when the holoenzyme subunits, such as Srb10, Srb11, and Tsf3 (or Sin4) are lost (Zaman et al., 2001, Carlson, 1997, Wahi and Johnson, 1995, Chen et al., 1993). Third, the binding of Tup1 obstructs recruitment of the TATA-binding protein and RNA polymerase II to gene promoters (Kuras and Struhl, 1999, Mennella et al., 2003, Zaman et al., 2001). Thus, Tup1 prevents formation of the pre-initiation complex and blocks transcription. Fourth, Tup1-Cyc8 can inhibit transcription on a basal promoter containing only the TATA box, suggesting that Tup1-Cyc8 is able to repress basal transcription (Tzamarias and Struhl, 1994). Tup1-Cyc8 is also sufficient to repress basal transcription in an *in vitro* system (Herschbach et al., 1994). Finally, artificially tethering the RNA polymerase II holoenzyme to a Tup1-Cyc8 bound promoter is sufficient to bypass transcriptional repression (Papamichos-Chronakis et al., 2000).

Given that many Tup1-Cyc8 targets are involved in stress responses, Tup1-Cyc8 bound genes must be able to express quickly under certain environments. How do the target genes of Tup1-Cyc8 become activated swiftly under activating conditions? Multiple models have proposed that relieving Tup1-Cyc8 repression also induces transcriptional activation at the same time. These models indicate that Tup1-Cyc8 compromises activator functions under repressive conditions, or directly switch into an activator under activating conditions. In the first model, Tup1-Cyc8 limits the accessibility of transcription activators at the gene promoters (model 4 in Figure 11). When the targets genes are required to be activated, Tup1-Cyc8 dissociates from the promoters and allows transcriptional activators to bind. One example that supports this model is the *HO* promoter. The *HO* gene is expressed in haploid cells, but not in diploid cells due to Tup1-Cyc8 repression. In haploid cells, the transcriptional activator Swi5 is detected at the *HO* promoter at the anaphase stage of the cell cycle. Yet, when Tup1 is bound, Swi5 is absent at the promoter suggesting that Tup1-Cyc8 blocks transcriptional activator recruitment (Mathias et al., 2004). The second model indicates that Tup1-Cyc8 transforms into a transcriptional activator under activating conditions (model 5 in Figure 11). Multiple studies have demonstrated that transcriptional activation of Tup1-Cyc8 targets also requires the presence of Tup1 and Cyc8 (Tanaka and Mukai, 2015, Conlan et al., 1999, Proft and Struhl, 2002). In addition, Tup1-Cyc8 was shown to mediate recruitment of the SAGA

and Swi/Snf complexes to gene promoter under activating conditions (Proft and Struhl, 2002).

Tup1-Cyc8 has also been suggested to repress gene transcription by inhibiting promoter-bound transcriptional activators (model 6 in Figure 11). *In vivo* footprinting data of a Tup1-repressed promoter revealed that the transcriptional activator Gal4 is bound to its binding site when the promoter is repressed (Redd et al., 1996). More recently, Wong and Struhl proposed that the transcription factors that recruit Tup1-Cyc8 to gene promoters can activate transcription (Wong and Struhl, 2011). In this work, several lines of evidence suggested that Tup1 prevents bound transcription factors from activating transcription. Firstly, Tup1 blocks the recruitment of SAGA catalytic subunit Gcn5, histone remodelling proteins Snf2 and Sth1, and Mediator subunit Gal11, which are required for full de-repression of the target promoters. Next, transcriptional repression mediated by Tup1 precedes nucleosome deposition at multiple promoters, but occurs at around the same time as dissociation of the Mediator and nucleosome remodelling protein. These data indicate that repressed chromatin is not a pre-requisite for Tup1 repression. In addition, transcriptional activator Gcn4 is able to associate with Tup1-bound promoters next to the Tup1 binding site, suggesting that Tup1 does not block recruitment of transcriptional activators. Notably, Gcn4 binding is unchanged after Tup1 dissociation, thus Tup1 binding does not affect recruitment of transcriptional activators. Tup1 may prevent transcriptional activators from recruiting the Swi/Snf, SAGA, and Mediator complexes, as analysis of chromatin immunoprecipitation with sequencing (ChIP-seq) data showed that Tup1 shares the same binding site with subunits of these complexes. Importantly, Tup1 can interact with the activation domains of transcriptional activators *in vivo*. Taken together, the Wong & Struhl model states that Tup1 interacts with the activation domains of transcription factors, and thereby masks their activation potential (Wong and Struhl, 2011). Consequently, the transcription factors cannot recruit transcriptional co-activator complexes and transcription activation is inhibited.

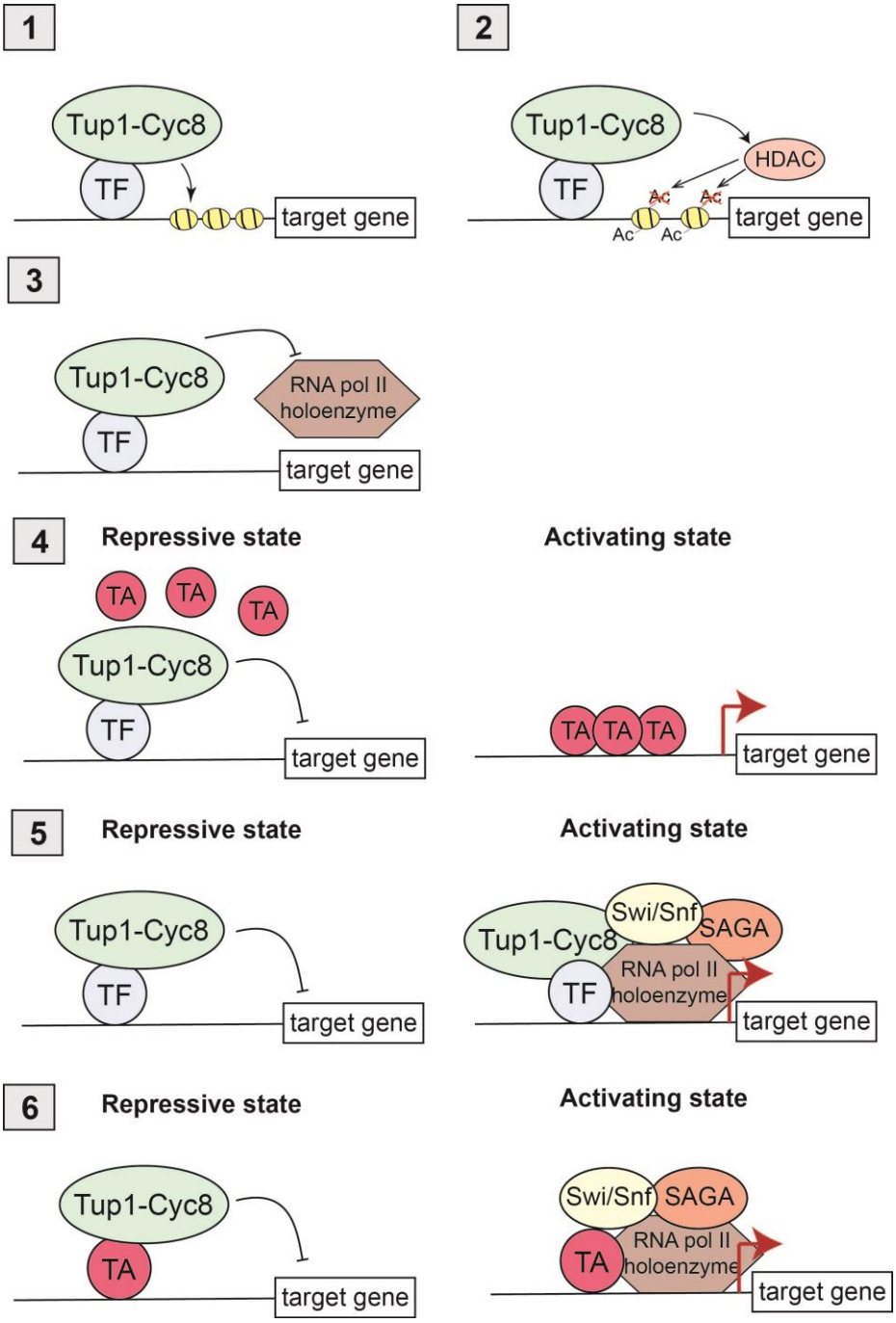

Figure 11. Tup1-Cyc8 represses its target genes via various mechanisms.

Tup1-Cyc8 targets are repressed by one or a combination of multiple different mechanisms. 1) Tup1 stabilises and repositions nucleosomes to limit promoter accessibility to transcriptional activators and RNA polymerase II machinery. 2) Tup1 recruits histone deacetylases to deacetylate H3 and H4 histones. 3) Tup1 directly interferes with the transcription machinery. 4) Tup1 occupies the transcription activator sites in the promoter. Under activating conditions, the Tup1-Cyc8 complex is displaced

by transcriptional activators that induce transcription. 5) Tup1 plays dual functions in transcriptional regulation. Tup1-Cyc8 acts as a transcriptional repressor, and can also transform into a transcriptional activator by recruiting the Swi/Snf and SAGA complexes to the promoter under activating conditions (adapted from (Proft and Struhl, 2002)). 6) Tup1 represses gene transcription by blocking the activation domains of the recruiting transcription factors. Under activating conditions, Tup1-Cyc8 dissociates from the transcription factors and thus reveals the activation domains. The transcriptional activators recruit co-activator complexes and induce gene transcription. TF = Tup1-Cyc8 recruiting transcription factor(s), HDAC = histone deacetylase, Ac = H3/H4 acetylation, TA = transcriptional activator.

How Tup1-Cyc8 represses *IME1* transcription is unknown. Several observations in the literature have provided clues on how Tup1-Cyc8 may inhibit activity of the *IME1* promoter. First, analysis of genome-wide micrococcal nuclease sequencing (MNase-seq) data revealed that Tup1 may play a role in nucleosome positioning and stabilisation at the *IME1* promoter (Weidberg et al., 2016, Rizzo et al., 2011). Second, Tup1-Cyc8 is unlikely to transform into an *IME1* activator upon nutrient starvation, since Tup1 dissociates from the *IME1* promoter when the PKA and TORC1 pathways are inhibited (Weidberg et al., 2016). Third, Tup1-Cyc8 binding likely inhibits transcriptional activation of *IME1*. Previous study demonstrated that the *IME1* promoter regions that mediate Tup1 repression and *IME1* activation are in close proximity to each other (Mizuno et al., 1998). In addition, Pog1, a known transcriptional activator of *IME1*, binds to the *IME1* promoter under starvation conditions at the same regions where Tup1 binds (van Werven et al., 2012, Weidberg et al., 2016). Sequence analysis of the *IME1* promoter also showed that the Tup1-bound region is overlaid with putative binding sites of transcriptional activators, such as Gcn4 and Dal82 (Kahana et al., 2010). I speculated that Tup1-Cyc8 is the major repressor of *IME1* transcription in nutrient-rich conditions primarily by inhibiting transcriptional activation. Understanding how Tup1-Cyc8 regulates *IME1* transcription may be key to understand how nutrient signals are co-ordinated to control meiotic entry in yeast.

1.13 Detecting interactions between transcription factors and the *IME1* promoter by chromatin immunoprecipitation (ChIP)

The general repressor complex Tup1-Cyc8 associates with its target gene promoters via interacting with transcription factors that recognise specific DNA sequences in the promoters. To investigate how Tup1-Cyc8 complex regulates *IME1* transcription, it is essential to understand how Tup1-Cyc8 interacts with the *IME1* promoter. Hence, it is critical to identify the transcription factors that can interact with Tup1-Cyc8 and bind to specific DNA sequences in the *IME1* promoter. In this thesis, I employed the chromatin immunoprecipitation (ChIP) technique to screen for transcription factors that are likely to contribute to Tup1-Cyc8 recruitment at the *IME1* promoter. In addition, ChIP analyses were performed to measure the binding of Tup1-Cyc8 and candidate transcription factors at the *IME1* promoter in various nutrient conditions in order to examine whether their binding depends on the presence of certain nutrients.

Chromatin immunoprecipitation (ChIP) is a molecular biology technique that is widely used to examine interaction between a protein of interest and DNA. Basic procedures of ChIP assays emerged in studies published around 40 years ago, which described the use of formaldehyde and UV light as crosslinking reagents to examine protein-chromatin interactions in calf thymus nuclear extract and bacteria respectively (Jackson, 1978, Gilmour and Lis, 1984). Crosslinking is the first step of the ChIP technique that is required to fix and stabilise protein-DNA complexes in cells. During this step, crosslinking reagents induce chemical reactions to occur between protein and DNA such that the protein binding sites can be purified and examined at a later step. Formaldehyde is a common crosslinking reagent that couples protein to DNA by inducing two subsequent nucleophilic attacks between the two species (Hoffman et al., 2015). Formaldehyde crosslinking is often favoured compared to other crosslinking methods due to the possibility to reverse the crosslinks between protein and DNA by heat (Jackson, 1978, Hoffman et al., 2015). As demonstrated by a previous study, the reversal rate of formaldehyde-induced crosslinks is exponentially dependent on temperature (Kennedy-Darling and Smith, 2014). Moreover, formaldehyde crosslinking does not damage DNA (Celis et al., 1976). Therefore, DNA sequences can be recovered from protein-DNA complexes

by reverse crosslinking and identified directly by quantitative PCR (qPCR) or sequencing. Given that formaldehyde is the smallest aldehyde, formaldehyde triggers reactions between protein/DNA groups in proximity that are approximately 2Å apart (Solomon and Varshavsky, 1985, Quievryn and Zhitkovich, 2000). Hence, formaldehyde is more likely to capture close-range interactions compared to other reagents such as cisplatin, which has a crosslinking distance of 4Å (Spencer et al., 2003). However, there are also limitations in using formaldehyde crosslinking to detect interactions between protein and DNA. First, formaldehyde facilitates crosslinks between not only protein-DNA, but also protein-protein and protein-RNA interactions (Das et al., 2004, Hoffman et al., 2015). For this reason, it is difficult to differentiate whether the protein of interest interacts with chromatin directly or via another DNA-binding protein. Furthermore, incomplete RNase treatment may increase the level of background signals in the ChIP assay. Second, previous study reported that formaldehyde reacts with amino acid residues including tryptophan, histidine, glutamine, asparagine, arginine, and tyrosine (Metz et al., 2004). When formaldehyde is directly added to cell culture, it is possible that formaldehyde also reacts with amino acids present in the growth medium such as the YPD medium used in this thesis (Chapter 2: Table 1), resulting in lower protein-DNA crosslinking efficiency. Third, crosslinking conditions including formaldehyde concentration and duration must be carefully selected and controlled. Formaldehyde crosslinking typically takes place at a final formaldehyde concentration of ≤1% and crosslinking occurs within 30 minutes (Hoffman et al., 2015). Over-crosslinking results in inefficient chromatin fragmentation and loss of chromatin during the sonication and immunoprecipitation steps (Das et al., 2004). To prevent overfixation, quencher molecules such as glycine or Tris can be added to keep formaldehyde from further reacting with proteins (Hoffman et al., 2015).

Next, the crosslinked chromatin is extracted from the cell lysate and is subjected to fragmentation by sonication. The sonication step solubilises the chromatin by shearing chromatin into small fragments. Importantly, the level of chromatin fragmentation dictates how precisely the protein binding sites can be mapped in the genome. To efficiently pinpoint the locations of the protein binding sites, chromatin should be sheared to fragments that are 100 to 500 bp in length (Das et al., 2004). Previous study further suggested that sonicating chromatin

extensively to generate fragments that are 75 to 300 bp in length enhances enrichment of protein binding sites by reducing background ChIP signals (Fan et al., 2008). Sonication is commonly carried out in an ultrasonic bath such as Bioruptor Plus (Diagenode) used in this thesis. Recent study performed a comprehensive investigation into how the performance of water bath sonciator is affected by various sonication parameters (Pchelintsev et al., 2016). For the sonicator model tested, the authors reported that sonication energy was equally delivered to samples placed in different positions in the rotating carousel (Pchelintsev et al., 2016). In addition, the length of the ON/OFF cycle, the level of power outputs (low or high), and the SDS concentration in the sample buffer were found to have minimal effects on sonication efficiency. In contrast, the water level in the water bath should be maintained at the recommended level as slightly higher or lower levels had a substantial impact on the performance of the sonicator (Pchelintsev et al., 2016). Foaming of the sample buffer should also be prevented by keeping the samples on ice and adjusting the power output of the sonicator (Das et al., 2004). Finally, the sonication strength and duration should be adjusted and optimised based on the specific experimental conditions such as cell type, cell density, growth conditions, and the extent of crosslinking. To examine the efficiency of chromatin fragmentation, DNA should be reverse crosslinked and analysed by agarose gel electrophoresis (Pchelintsev et al., 2016, Das et al., 2004). It is worth noting that the sonication step leads to degradation of proteins that are at least 100 kilodaltons (kDa) in size, where larger proteins are subjected to more degardation (Pchelintsev et al., 2016). Hence, sonication may potentially reduce the immunoprecipitation efficiency of larger proteins of interest. To circumvent this issue, chromatin can be fragmented using a combination of brief sonication and benzonase digestion to maintain the integrity of the high molecular weight proteins (Pchelintsev et al., 2016).

Following sonication of the chromatin, the protein of interest is isolated along with its bound chromatin fragment in the immunoprecipitation step. During this step, the target protein is recognised by an antibody that is specific to the protein or the epitope tag that is attached to the protein. The antibody is directly conjugated to agarose beads, or coupled to beads coated with protein A or protein G to precipitate the protein-DNA complexes from the sample (Das et al., 2004). The specificity and efficiency of the antibody should be evaluated as it has a critical impact on the

enrichment of the protein binding sites. Serial dilution analysis can be performed to determine the efficiency of the antibody (Spencer et al., 2003). To assess antibody specificity, cell lysate with no target protein or no epitope attached to the protein should be included as negative control. Furthermore, non-specific protein-bead interactions can be minimised by washing beads with buffers that contain salt and detergent (Spencer et al., 2003). Immunoprecipitated protein-DNA complexes are subsequently subjected to reverse crosslinking and proteinase K is added to accelerate the isolation of DNA (Pchelintsev et al., 2016). The recovered DNA is purified and quantified by techniques such as Southern blotting, microarray, or PCR-based approaches like quantitative PCR (qPCR) (Das et al., 2004).

In this thesis, I performed ChIP analyses to investigate how Tup1-Cyc8 and multiple transcription factors interact with the *IME1* promoter to control *IME1* transcription under different nutrient conditions. The workflow of the ChIP assay protocol employed to investigate protein binding at the *IME1* promoter is summarised in Figure 12. Briefly, I attached DNA sequence encoding three copies of the V5 epitope to the 3' end of the ORF encoding the transcription factor of interest. Formaldehyde was added directly to cells expressing the epitope-tagged transcription factor to reversibly crosslink its interactions with the yeast genome. Subsequently, cells are lysed and the extracted chromatin was sheared by sonication. Immunoprecipitation of the target transcription factor was carried out using agarose beads that are covalently conjugated to an antibody that specifically recognises the V5 epitope. The agarose beads were washed extensively, and DNA was eluted by reverse crosslinking and proteinase K treatment. To detect and quantify the binding levels of the transcription factors at the *IME1* promoter, I analysed the eluted DNA by qPCR using primer pairs that amplify various regions in the *IME1* promoter (Chapter 3: Figure 13 and Supplementary table 3). Notably, I examined transcription factor binding at the *IME1* promoter in various nutrient conditions by crosslinking cells in different types of growth media. Nutrient-rich growth medium such as YPD contains large amounts of nitrogen compounds that may react with formaldehyde during the crosslinking step. To normalise the ChIP signals across all nutrient conditions, I used the signals detected at the silent mating type cassette *HMR* as an endogenous reference in my qPCR analyses. My ChIP data provide important insights into how nutrients recruit multiple redundant

transcription factors to mediate Tup1-Cyc8 binding at the *IME1* promoter, which in turn represses *IME1* transcription and meiotic entry in yeast.

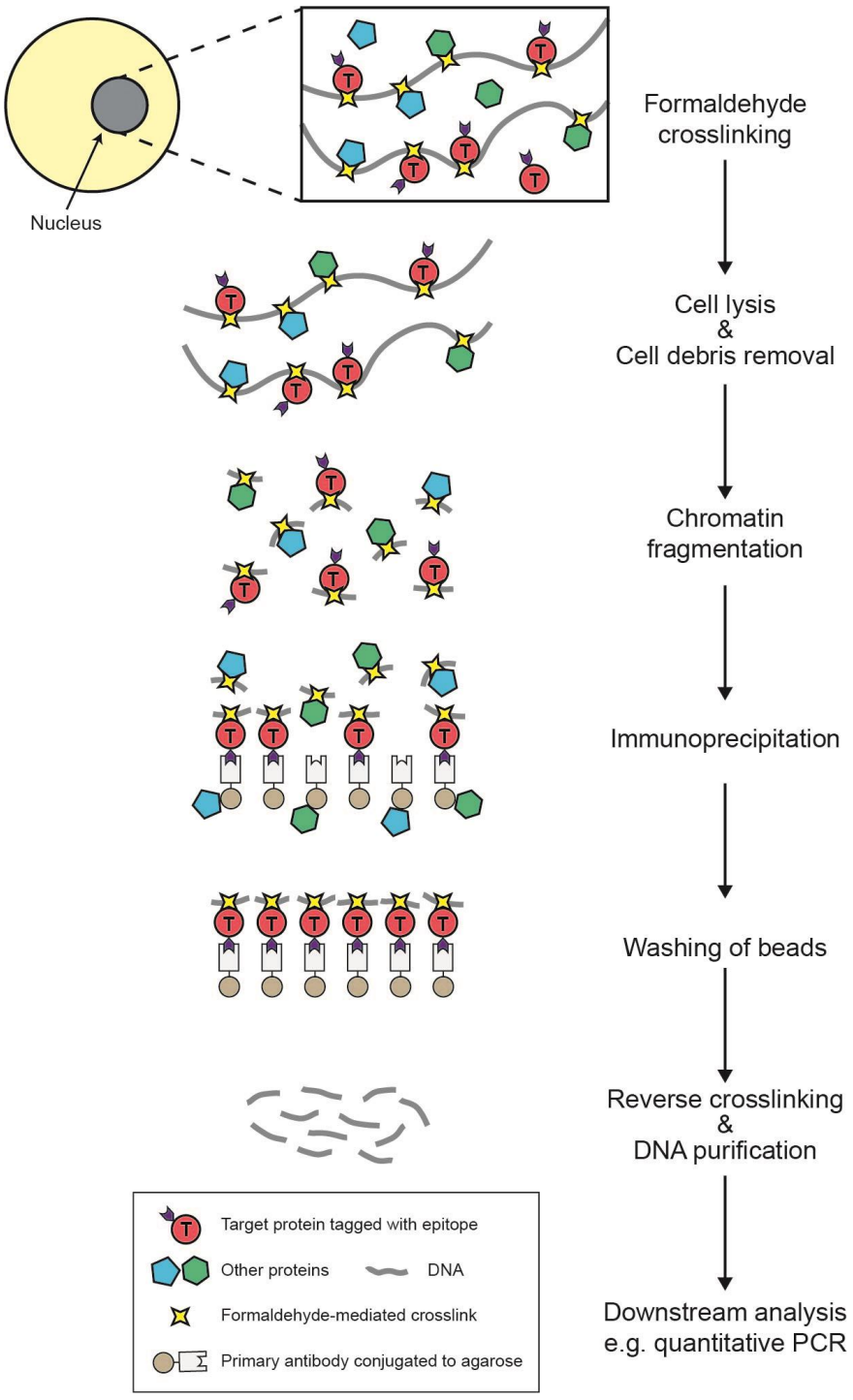

Figure 12. Workflow of the chromatin immunoprecipitation (ChIP) assay (adapted from (Spencer et al., 2003, Das et al., 2004)).

Schematic diagram representing the workflow of the ChIP protocol employed in this thesis. The protein of interest is tagged with specific epitope through genome editing. Formaldehyde is added directly to yeast culture to crosslink protein-DNA interactions. Next, cells are lysed and the majority of cell debris is removed by centrifugation. The cleared cell lysate is subjected to sonication to break chromatin into small fragments. To precipitate the target protein and its bound chromatin, primary antibody that is specific to the epitope tag and covalently linked to agarose is added to the sheared chromatin sample. The agarose beads are subsequently washed with buffers containing salt and detergent to minimise non-specific interactions. To elute DNA from the precipitated protein-DNA complexes, formaldehyde-induced crosslinks are reversed by heat and proteinase K is added to further release DNA by degrading the proteins. The eluted DNA is purified and analysed by qPCR to detect the level of protein binding at the *IME1* promoter and other target loci.

1.14 Objectives of this thesis

In this thesis, I set out to investigate how Tup1-Cyc8 controls *IME1* transcription by exploring several research questions. Firstly, I investigated how Tup1-Cyc8 represses the *IME1* promoter. I asked whether Tup1-Cyc8 primarily represses *IME1* transcription by inhibiting transcriptional activators in nutrient-rich condition. To study this question, I analysed the kinetics of *IME1* activation following the depletion of Tup1. I also investigated the contribution of other repression mechanisms, such as HDACs recruitment. Next, I examined how Tup1-Cyc8 is directed to the *IME1* promoter. Tup1-Cyc8 recruitment depends on interactions with DNA-binding transcription factors bound to the gene promoters. Thus, I set out to identify the transcription factors that interact with Tup1-Cyc8 at the *IME1* promoter. Furthermore, I investigated whether nutrient signals are mediated to Tup1-Cyc8 by modulating binding of the interacting transcription factors. Finally, I carried out functional analyses of multiple regions in the *IME1* promoter. I aimed to identify the sequence motifs that are sufficient to recruit Tup1-Cyc8 to the *IME1* promoter, and examine whether these sequence motifs are also important for *IME1* activation. Since Tup1-Cyc8 has been proposed to interact with the activation domains of its recruiting transcription factors, I also investigated whether the transcription factors that recruit Tup1-Cyc8 to the *IME1* promoter are also *IME1* activators.

The work presented in this thesis demonstrates how complex nutrients control binding of multiple transcription factors to regulate Tup1-Cyc8 repression of *IME1* transcription. Initiation of meiosis in yeast is a paradigm of how multiple signalling cues co-ordinate a developmental decision in eukaryotes. Hence, my findings provide a model of how transcriptional repression of a developmental regulator gene controls a fate decision in all eukaryotic cells.

Chapter 2. Materials & Methods

2.1 Yeast strains and plasmids

Saccharomyces cerevisiae with SK1 genetic background was employed for all experiments in this thesis. All experiments were carried out with diploid cells and the list of yeast strains described in this thesis can be found in Supplementary table 1. Gene deletions, *IME1* promoter truncations, and protein fusions were achieved by replacing the genes of interest with a selectable marker using the single step PCR-based gene modification protocol described in (Longtine et al., 1998). In this method, primers with homology to the target genomic locus were used to amplify a plasmid sequence encoding a selectable marker. Subsequently, the PCR fragment was used to substitute the target gene by homologous recombination during transformation. For endogenous gene tagging, primers with homology to the 3' end of the gene were used to amplify a plasmid sequence encoding the tag and a selectable marker. The PCR reactions were carried out using Ex Taq DNA polymerase (TaKaRa Bio) or KOD Hot Start DNA polymerase (Sigma-Aldrich) according to the manufacturers' instructions.

Transcription factor binding sites were predicted by scanning the *IME1* promoter with the curated transcription factor motifs in the YeTFaSCo database (de Boer and Hughes, 2012). Binding sites were predicted to have at least 75% of the maximum possible score, with the exception of Sut1 site which was predicted with a 70% threshold. The Sko1 site was manually labelled by scrutinising the *IME1* promoter region for sequences that resemble the consensus motif. The Nrg2 sites were manually labelled at the opposite strands of Nrg1 sites, given that the sequences also match the Nrg2 consensus motif. The Sfl1 sites were obtained from previous *IME1* promoter study (Kahana et al., 2010).

Construction of single-copy integration plasmids

List of single-copy integration plasmids used in this thesis can be found in Supplementary table 2. The vector backbone for constructing the single-copy integration plasmids in this thesis was derived from the single-copy integration

plasmid *pNH604* (Youk and Lim, 2014). The *pNH604* plasmid contained the 5'-untranslated region (UTR) and 3'-UTR of the *S. cerevisiae TRP1* gene. The sequence encoding Trp1 in *Candida glabrata*, which can be expressed in *S. cerevisiae* was present between the UTRs in the plasmid. The *pIME1-WT* (*pFW506*) plasmid was created by cloning the full length *IME1* promoter and *IME1* gene fused with *sfGFP* in the 5'-end (*pIME1-sfGFP-IME1*) into the *pNH604* plasmid. The *pIME1-sfGFP-IME1* fragment (~4.6 kb) was amplified from yeast cells expressing sfGFP-Ime1, and cloned into the *pNH604* plasmid at the NotI and BamHI sites by restriction digestion. Single-copy integration plasmids with transcription factor binding site mutations in the *IME1* promoter were derived from the *pIME1-WT* plasmid. To mutate transcription factor binding sites, DNA fragments that were 500 bp in length corresponding to 701 to 1100 bp upstream of the open reading frame (ORF) with binding site mutations were commercially synthesised (gBlocks Gene Fragments, Integrated DNA Technologies). The DNA fragment and the *pIME1-WT* plasmid were amplified by PCR and joined by Gibson assembly using the NEBuilder HiFi DNA Assembly Master Mix (New England BioLabs). The new plasmid sequences were verified by Sanger sequencing. The *pIME1-bs*∆ (*pFW575*) plasmid carried 103 mutated nucleotides to disrupt the Yap6, Sok2, Phd1, Mot3, Sko1, Nrg1, and Nrg2 binding sites (Supplementary figure 15). The *pIME1-bs*∆*yap6* (*pFW576*), *pIME1-bs*∆*sok2* (*pFW577*), *pIME1-bs*∆*phd1* (*pFW578*), *pIME1-bs*∆*nrg1* (*pFW600*), and *pIME1-bs*∆*sko1* (*pFW602*) plasmids were designed based on the promoter sequence in *pIME1-bs*∆ by replacing the mutated sites of Yap6, Sok2, Phd1, Nrg1/Nrg2, or Sko1 with the wild-type DNA motif sequences (Supplementary figure 16, Supplementary figure 17, Supplementary figure 18, Supplementary figure 19, Supplementary figure 20). The two Yap6 sites were studied separately by restoring the sequences from 837 to 844 bp and from 1006 to 1012 bp upstream of the ORF respectively in the *pIME1-bs*∆*1* (*pFW604*) and *pIME1-bs*∆*2* (*pFW606*) plasmids (Supplementary figure 21, Supplementary figure 22). Sok2 sites that match the MTGCA motif and AGGCAM motif (M represents A or C) were restored in the *pIME1-bs*∆*3* (*pFW608*) and *pIME1-bs*∆*4* (*pFW610*) plasmids respectively (Supplementary figure 23, Supplementary figure 24). The *pIME1-bs*∆*-spy* plasmid (*pFW669*) was designed based on the *pIME1-bs*∆ sequence with the Yap6 site from 837 to 844 bp upstream of the ORF and five Sok2/Phd1 sites matching the MTGCA motif restored (Supplementary figure 25). The *pIME1-spy*∆ plasmid (*pFW675*) contained mutated

nucleotides at the Yap6, Sok2, and Phd1 sites described for *pIME1-bsΔ-spy*, while other sequences remained wild-type (Supplementary figure 26). Plasmids were linearised with PmeI to release the *C. glabrata TRP1-pIME1-sfGFP-IME1* cassettes flanked by the 5' and 3' UTRs of *S. cerevisiae TRP1*. The constructs were transformed and integrated into the *TRP1* locus in yeast cells lacking endogenous *IME1* gene and promoter. Integration of the cassettes was verified by PCR with primers flanking the site of integration. Cells also expressed V5-tagged Tup1 to monitor Tup1 binding to the *IME1* promoter.

Yeast transformation

Yeast cells were transformed using the high efficiency protocol described in (Agatep et al., 1998). According to this protocol, yeast cells grown to mid-exponential phase in liquid culture were harvested and washed with 0.1M lithium acetate. After that, yeast cells were re-suspended in a mix containing 0.1M lithium acetate, 33.33% polyethylene glycol-3350, and 100 µg sonicated salmon sperm DNA (Agilent Technologies). The re-suspended cells were co-incubated with the transformation DNA (PCR fragment or digested plasmid DNA) at 30°C for 40 minutes and subjected to heat shock at 42°C for 20 minutes. Cells were pelleted, re-suspended in purified water, and spread onto agar plates. Transformed cells that were selected on an auxotrophic marker were plated directly onto synthetic complete agar medium without the amino acid produced by the auxotrophic marker. Transformed cells that were selected on an antibiotic resistance marker were first recovered on YPD medium overnight, and subsequently transferred onto YPD medium containing the antibiotic by replica plating.

Validation of gene modifications

Gene modifications were verified by PCR amplification of the genomic locus targeted for modification. The genomic DNA of yeast transformants were obtained using the "Smash and Grab" method. In this method, yeast cells were first re-suspended in a DNA breakage buffer containing 2% Triton X-100, 1% SDS, 100 mM sodium chloride, 10 mM Tris (pH8.0), and 1 mM EDTA. Next, equal volume of

phenol-chloroform-isoamyl alcohol (25:24:1) mixture (Fisher Scientific) was added and the cell mixture was subjected to mechanical breakage by 0.5 mm glass beads (BioSpec) on the Mini-Beadbeater-96 (BioSpec). The lysed cell mixture was centrifuged at high speed (≥ 13,200 r.p.m.) for at least five minutes to separate the liquid phases. To recover the genomic DNA, the top aqueous phase was transferred to 100% ethanol and the ethanol mixture was inverted multiple times to ensure that the contents were thoroughly mixed. The precipitated DNA was pelleted by centrifugation at high speed (≥ 13,200 r.p.m.) for at least five minutes. The DNA pellet was re-suspended in TE buffer with brief incubation at 37°C to dissolve the pellet. The extracted DNA was used as template for PCR reactions using primers that flank the sites of recombination. The PCR fragment size was determined by DNA gel electrophoresis. Additionally, protein fusions produced from endogenously tagged genes were also checked by western blotting and widefield microscopy. Positive yeast tranformants were streaked into single colonies, which were isolated and backcrossed with the wild-type strain or a previously backcrossed strain.

Diploid construction and tetrad dissection

Diploid yeast cells were generated by mixing populations of haploid *MAT***a** and *MAT*α cells on YPD agar plate. Mating between the haploid populations took place at 30°C for at least 6 hours. The mixed cell population was streaked onto YPD agar plate containing **a**-factor and α-factor to select for single colonies of diploid cells. The yeast clones isolated were examined under a light microscope to ensure that all cells were diploid.

To backcross yeast transformants and to construct yeast strains with multiple gene modifications, haploid *MAT***a** and *MAT*α cells were mated on YPD agar at 30°C for at least 6 hours. The cells were then transferred onto sporulation (SPO) agar medium and the plates were incubated at 30°C to induce diploid cells to sporulate. When tetrads were observed in the population, dissection was carried out to separate the progenies of the mated cells. Yeast cells were spheroplasted with 1 mg/mL Zymolyase-100T in 1M sorbitol at 37°C until the ascus wall was dissolved. The reaction was quenched by adding purified water to the digested cells and around

20µL of cell suspension was placed on an YPD plate. The spores in the tetrads were separated using a mechanical micromanipulator mounted on the Eclipse Ci upright microscope (Nikon). The plates were then incubated at 30°C to allow the colonies to grow out. The genotypes of the spores were scored by replica plating and cells with desired genotypes were selected.

2.2 Growth conditions and yeast media

Yeast cells were grown in YPD (yeast extract, peptone, dextrose) liquid or agar medium supplemented with tryptophan, uracil, and adenine at 30°C. Liquid cultures were agitated at 300 r.p.m. to facilitate aeration and to ensure homogenisation of the cultures. To obtain cells in exponential growth phase (YPD (E)), yeast culture was diluted to OD_{600} = 0.2 and cells were harvested after two to three duplications in cell density. To acquire cells grown to saturation (YPD (S)), yeast culture was diluted to OD_{600} = 0.2 and cells were yielded after 20 to 24 hours. To induce sporulation in liquid culture, cells were grown overnight to saturation in YPD and diluted to OD_{600} = 0.4 in the pre-sporulation medium BYTA (buffered, yeast extract, tryptone, acetate). BYTA medium provides acetate as a carbon source and induces cells to undergo respiration. After 16 to 18 hours in BYTA, cells were washed with purified water and re-suspended to OD_{600} = 1.8 in sporulation (SPO) medium. The SPO 0h samples were taken immediately after cells were shifted to SPO medium, and the SPO 4h samples were obtained four hours later. The YP + 0.05% Glc (YP without glucose) and SPO + 2% Glc (glucose-only) media were used to study responses to distinct nutrients in the rich medium in Figure 26 and Figure 36. Synthetic complete (SC) drop-out agar media were used to select for cells with auxotrophic markers, while YPD containing Nat (nourseothricin) and Kan (kanamycin) were used to select for cells with antibiotic resistance markers. All generated strains were saved as cell suspensions in sterile 15% glycerol at -80°C. The composition of all media used in this thesis are detailed in Table 1.

YPD	
Bacto Yeast extract (BD Biosciences)	1%
Bacto Peptone (BD Biosciences)	2%
Glucose	2%
Tryptophan	96 µg/mL
Uracil	24 µg/mL
Adenine	12 µg/mL
(YPD + Nat) Nourseothricin sulphate (BioVision)	0.1 mg/mL
(YPD + Kan) Geneticin G-418 Sulphate (Gibco)	0.2 mg/mL
SC-His (SC medium without histidine)	
Yeast Nitrogen Base w/o amino acids (BD Difco)	6.70%
Glucose	2%
CSM-His-Ura (MP Biomedicals)	0.075%
Uracil	60 µg/mL
SC-Trp (SC medium without tryptophan)	
Yeast Nitrogen Base w/o amino acids (BD Difco)	6.70%
Glucose	2%
CSM-Trp (MP Biomedicals)	0.074%
BYTA	
Bacto Yeast extract (BD Biosciences)	1%
Bacto Tryptone (BD Biosciences)	2%
Potassium acetate (Sigma Aldrich)	1%
Potassium phthalate monobasic (Sigma Aldrich)	50 mM
SPO	
Potassium acetate (Sigma Aldrich)	0.3%
Acetic acid	to pH 7.0
D-(+)-Raffinose pentahydrate (Sigma)	0.02%

YP + 0.05% Glc (YP only medium)	
Bacto Yeast extract (BD Biosciences)	1%
Bacto Peptone (BD Biosciences)	2%
Glucose	0.05%
Tryptophan	96 µg/mL
Uracil	24 µg/mL
Adenine	12 µg/mL
SPO + 2% Glc (glucose only medium)	
Potassium acetate (Sigma Aldrich)	0.3%
Acetic acid	to pH 7.0
D-(+)-Raffinose pentahydrate (Sigma)	0.02%
Glucose	2%

Table 1. Composition of yeast media used in this thesis.
The contents of the yeast media used in this thesis are listed in this table.

2.3 Return to growth in distinct nutrient conditions

The binding of Tup1 and other transcription factors to the *IME1* promoter under different nutrient conditions was examined in Figure 26 and Figure 36. For these experiments, yeast cells were grown to saturation in YPD and pre-sporulation medium following the standard sporulation protocol described in section 2.2. Subsequently, cells were shifted to four different types of media including sporulation medium (SPO), glucose only medium (SPO + 2% Glc), YP medium without glucose (YP + 0.05% Glc), and YPD medium (YP + 2% Glc). Yeast cells were harvested at the point of shift (SPO 0h) and after four hours (SPO 4h) for ChIP analyses.

2.4 Auxin-based degradation of Tup1 and Cyc8

The auxin-based degron system was used to study the effects of Tup1 and Cyc8 depletion (Nishimura et al., 2009). Tup1 and Cyc8 were C-terminally fused with the auxin-induced degron (AID) tag, which was comprised of three copies of the V5 epitope and the auxin-responsive protein IAA7 from *Arabidopsis thaliana*. The *Oryza sativa* TIR1 ligase (*osTIR1*) was also expressed under the *TEF1* promoter from a plasmid integrated at the *HIS3* locus (courtesy of Leon Chan) in the *TUP1-AID* and

CYC8-AID strains. To induce degradation of the AID-tagged proteins, 500 µM indole-3-acetic acid (3-IAA) (Aldrich) was added to exponentially growing yeast cell culture. As control, same volume of dimethyl sulphoxide (DMSO) was added to yeast cells. Cells were harvested at the indicated time points for ChIP, RT-qPCR, smFISH, and western blot analyses.

2.5 PKA and TORC1 inhibition

The analogue-sensitive *tpk1-as* strains were generated by creating a M164G point mutation in the Tpk1 subunit and ablating the redundant *TPK2* and *TPK3* genes (Weidberg et al., 2016). Yeast cells were grown to saturation in YPD medium and diluted to different densities in liquid culture due to the negative effects of PKA and TORC1 inhibition on cell growth. Untreated cells were diluted to OD_{600} = 0.1. To inhibit the PKA pathway, 5 µM of ATP analogue 1NM-PP1 (Calbiochem, Merck Millipore) was added to culture diluted to OD_{600} = 1. To inhibit the TORC1 pathway, 1 µg/mL rapamycin (Sigma) was added to culture diluted to OD_{600} = 0.5. Cells treated with both inhibitors were diluted to OD_{600} = 2. Yeast cultures were treated for 6 hours at 30°C, 300 r.p.m. and fixed with 5% trichloroacetic acid for western blotting.

2.6 Chromatin immunoprecipitation (ChIP)

Yeast cells were crosslinked with formaldehyde for 20 minutes at room temperature, and the reaction was quenched by the addition of 100mM glycine. The cells were pelleted by centrifugation at 3000 r.p.m. and washed once with FA lysis buffer (50 mM HEPES pH 7.5, 150 mM sodium chloride, 1 mM EDTA pH 7.6, 1% Triton X-100, 0.1% sodium deoxycholate, 0.1% SDS). The cell pellets were snap frozen in liquid nitrogen and stored at -80°C until they were processed. To prevent degradation of proteins during ChIP procedures, cOmplete Mini Protease Inhibitor Cocktail (Roche) was dissolved in FA lysis buffer and the buffer was pre-cooled on wet ice. Cell lysis of the frozen cell pellets was performed in cold FA lysis buffer with zirconia beads (BioSpec). Samples were homogenised using the Mini-Beadbeater-96 (BioSpec) on a pre-cooled tube block for 25 minutes. To protect cell contents from the heat generated by the homogeniser, tubes were placed onto a new pre-cooled

block after every five minutes of operation. The homogenised cells were first subjected to a round of low-speed (4000 r.p.m.) centrifugation at 4°C to remove unbroken cells and cell debris. Subsequently, the top fraction of the pellet and the supernatant were re-suspended and subjected to high-speed (13,000 r.p.m.) centrifugation at 4°C. The resulted pellet was re-suspended in cold FA lysis buffer. Chromatin was sheared by sonication using Bioruptor Plus (Diagenode) for nine cycles of 30s on, 30s off. Proteins harbouring V5 epitope tags were immunoprecipitated with anti-V5 agarose beads (Sigma-Aldrich) at room temperature for two hours with rotation. Following the immunoprecipitation step, the agarose beads were washed with FA lysis buffer, FA lysis buffer with 260mM sodium chloride, and a lithium chloride/detergent buffer (10 mM Tris pH 8, 250 mM lithium chloride, 0.5% NP-40, 0.5% sodium deoxycholate, 1 mM EDTA). DNA was reverse crosslinked in TE buffer with 1% SDS at 65°C, 500 r.p.m. overnight. Samples were then treated with 80 µg/mL proteinase K (Thermo Scientific) at 37°C for two hours and purified using the NucleoSpin Gel and PCR kit (Macherey-Nagel). The abundance of the target locus was determined by qPCR.

2.7 RNA isolation and reverse transcription

Yeast cells were pelleted by centrifugation and snap frozen in liquid nitrogen. Samples were stored at -80°C until they were processed. Total RNA was extracted from cells using the hot phenol method. TES buffer (10 mM Tris-HCl pH 7.5, 10 mM EDTA, 0.5% SDS) was added to cells with equal volume of acid-phenol:chloroform (Ambion). Samples were incubated at 65°C, 1400 r.p.m. for 45 minutes. Separation of the liquid phases was achieved by centrifugation (≥13,200 r.p.m.), and the top aqueous phase was transferred to 100% ethanol with 115 mM sodium acetate. Precipitation of RNA was allowed to take place overnight at -20°C. RNA was pelleted by high speed centrifugation, washed with 80% ethanol, and dissolved in DEPC-treated water at 37°C. Total RNA was purified using the NucleoSpin RNA kit (Macherey-Nagel) according to the manufacturer's instructions. The purification procedures included an rDNase digestion step to remove any residual genomic DNA in the samples. RNA concentrations were measured by the NanoDrop ND-1000 UV-Vis Spectrophotometer (Thermo Fisher Scientific). For reverse transcription, the

ProtoScript II First Strand cDNA Synthesis Kit (New England BioLabs) was used and 500 ng of RNA was provided as template in each reaction. The abundance of the target cDNA was determined by qPCR.

2.8 Quantitative PCR (qPCR)

qPCR reactions of ChIP and cDNA samples were performed with EXPRESS SYBR GreenER SuperMix (Thermo Fisher Scientific) or PowerUp SYBR Green Master Mix (Thermo Fisher Scientific). List of primers used in this thesis can be found in Supplementary table 3. Targets of interest were quantified by Applied Biosystems 7500 Fast Real-Time PCR System (Thermo Fisher Scientific), Applied Biosystems 7900HT Fast Real-Time PCR System (Thermo Fisher Scientific), or QuantStudio 12K Flex Real-Time PCR System (Thermo Fisher Scientific). Primer efficiency and linearity were examined by including a serial dilution (0.1, 0.01, 0.001, and 0.0001 times) of the standards as templates. The standard curve for each target was constructed by plotting the standard dilutions against their Ct values. The amount of targets present in each sample was calculated from the standard curves. For ChIP samples, input (no IP) samples were used as standards and signals were normalised over the silent mating type cassette *HMR*. In Supplementary figure 1, ChIP signals derived from the immunoprecipitated DNA samples were compared to that derived from the input samples and presented as percentage of the input signals. For cDNA samples, pooled cDNAs were used as standards and signals were normalised over actin *ACT1*.

2.9 Western blotting

Yeast cells were fixed with 5% trichloroacetic acid. Fixed cells were pelleted by centrifugation, washed with acetone and air dried in the fume hood for at least 90 minutes. Cells were lysed in protein breakage buffer (50 mM Tris at pH 7.5, 1 mM EDTA, 27.5 mM DTT) with 0.5 mm glass beads (BioSpec) on the Mini-Beadbeater-96 (BioSpec). Proteins were denatured in SDS loading buffer (62.5 mM Tris (pH 6.8), 2% β-mercaptoethanol, 10% glycerol, 3% SDS, and 0.017% Bromophenol Blue) at 100°C for 5 minutes. Total proteins were separated by SDS-PAGE in Tris-glycine

buffer (25 mM Tris base, 192 mM glycine, 0.1% SDS) and transferred onto PVDF membrane (Bio-Rad) by the semi-dry transfer or tank transfer method. Semi-dry transfer was carried out in the Trans-Blot SD Semi-Dry Transfer Cell (Bio-Rad) in which the sandwich was soaked in Tris-glycine semi-dry transfer buffer (48 mM Tris base, 39 mM glycine, 0.04% SDS, and 10% methanol). Tank transfer was performed in the Mini Trans-Blot Cell (Bio-Rad) in Tris-glycine wet transfer buffer (27.72 mM Tris base, 193.7 mM glycine, and 20% methanol) at 4°C with constant stirring of the buffer to reduce heat in the system. Membrane blocking was carried out in phosphate buffered saline (PBS) buffer containing 0.01% Tween-20, 1% milk and 1% bovine serum albumin for at least 45 minutes. V5 epitope-tagged proteins were detected using an anti-V5 antibody (Invitrogen, 1:2000, mouse). As loading control, Hxk1 proteins were detected using an anti-hexokinase antibody (Stratech Scientific, 1:2000, rabbit). The blots were incubated with the primary antibodies at 4°C overnight on a roller drum. Subsequently, the blots were washed with PBS buffer with 0.01% Tween-20. For secondary antibodies, IRDye 800CW (anti-mouse) and IRDye 680RD (anti-rabbit) (LI-COR) antibodies were added in 1:15000 dilutions. Images were acquired on the Odyssey CLx imaging system (LI-COR). Alternatively, HRP-conjugated anti-mouse and anti-rabbit secondary antibodies (GE Healthcare) were added in 1:8000 dilutions. ECL Prime (GE Healthcare) was added, and images were taken on Amersham Imager 600 (GE Healthcare). Protein signal quantification was carried out in the Image Studio Lite software (LI-COR) and Hxk1 levels were used to normalise protein signals.

2.10 Nuclei/DAPI counting

Yeast cells were harvested and fixed in 80% ethanol. Fixed cells were stained with 1 µg/mL 4',6-diamidino-2-phenylindole (DAPI) in PBS buffer to visualise the nuclei. Cells displaying two, three, or four DAPI masses were considered to have undergone meiosis, while meiosis did not take place in cells with one DAPI mass. At least 200 cells were assessed for each cell population. The percentage of population that underwent meiosis was calculated.

2.11 Single molecule RNA fluorescence *in situ* hybridisation (smFISH)

Yeast cells were fixed with formaldehyde at room temperature for 20 minutes on rotation. Subsequently, samples were placed on a roller drum overnight at 4°C. Yeast cells were pelleted at 3000 r.p.m. and washed twice with Buffer B (1.2M sorbitol, 0.1M potassium phosphate dibasic, pH 7.5). To spheroplast yeast cells, samples were treated with 40 µg/mL Zymolyase-100T (MP Biomedicals) and 57.2 mM β-mercaptoethanol in Buffer B at 30°C, 50 r.p.m. The progress of zymolyase digestion was constantly monitored under a microscope. For the smFISH experiments in this thesis, >90% yeast cells were spheoplasted after 20 to 25 minutes of zymolyase treatment. Spheroplasted cells were gently pelleted at 2000 r.p.m. and washed with Buffer B. Samples were centrifuged, re-suspended in 70% ethanol and incubated at room temperature for at least two hours. After that, ethanol was removed and cells were incubated in Wash Buffer (2xSSC, 10% formamide) at room temperature for at least 20 minutes. Cells were subsequently hybridised to fluorescently labelled smFISH probes in 1:1000 dilutions in Hybridisation Buffer (10% dextran, 2 mM vanadyl-ribonucleoside complex (New England BioLabs), 0.02% RNAse-free BSA, 1 mg/mL *E. coli* tRNA, 2xSSC, and 10% formamide). In this thesis, *IME1* transcripts were detected using a smFISH probe labelled with AF594 (Weidberg et al., 2016). As control, a Cy5-labelled probe directed to *ACT1* transcripts was also included (Weidberg et al., 2016). Probe hybridisation took place in darkness at 30°C for at least 16 hours. Hybridised cells were washed and stained with 1 µg/mL DAPI in Wash Buffer at 30°C for 30 minutes in darkness. Finally, samples were washed with Wash Buffer and re-suspended in 2xSSC buffer (Invitrogen).

Samples were imaged on the Eclipse Ti-E inverted microscope system (Nikon) using the 100x oil objective. To prevent sample bleaching, cells were centrifuged and re-suspended in anti-fade GLOX buffer described in (Raj et al., 2008) with 1% catalase (Sigma) and 1% glucose oxidase (Sigma) added. Images were acquired with the ORCA-FLASH 4.0 camera (Hamamatsu) using the NIS-elements software (Nikon). Cells were imaged at every 0.3µm along the z-axis using the built-in z-axis drive, and a total of 25 images were taken for each z-stack. Signals from all the planes were merged into a 2D image by applying maximum intensity z-projection in ImageJ (Schindelin et al., 2015). Only cells that displayed *ACT1* signals were

considered for *IME1* quantification using the StarSearch software (Levesque and Raj, http://rajlab.seas.upenn.edu/StarSearch/launch.html).

2.12 Fluorescence microscopy

For imaging of sfGFP-Ime1 in Figure 40, yeast cells were fixed with formaldehyde and re-suspended in a buffer containing 16.6 mM potassium phosphate monobasic, 83.4 mM potassium phosphate dibasic, and 1.2M sorbitol. The cellular localisation of Tup1-Cyc8 and other transcription factors was examined in Figure 16 and Figure 28 by tagging the proteins with mNeonGreen tagging cassettes (courtesy of Andreas Doncic) described in (Argüello-Miranda et al., 2018). Cells expressing mNeonGreen-tagged proteins also expressed a nuclear localisation signal derived from simian virus 40 with two copies of mCherry (2xmCherry-SV40NLS). Imaging was carried out using the same microscope and camera set up described for smFISH in 2.11. Signal quantification was carried out using the ImageJ software (Schindelin et al., 2015). Whole cell and nuclear mNeonGreen signals were quantified with the use of the nuclear marker (2xmCherry-SV40NLS). Signal from the cytosol was inferred from the difference between the whole cell signal and the nuclear signal.

2.13 Statistical analyses

Data statistics and statistical analyses were computed using GraphPad Prism version 8.2.0 for Windows, GraphPad Software, San Diego, California USA, www.graphpad.com. In Figure 18, Figure 40, and Figure 44, smFISH data were analysed using unpaired parametric two-tailed Welch's t-test with 95% confidence. P-values are indicated in the figures, where ns = non-significant, * = ≤ 0.05, ** = ≤ 0.01, and *** = ≤ 0.001.

Chapter 3. Tup1-Cyc8 is the major repressor of the *IME1* promoter in rich nutrients

Tup1-Cyc8 is a transcriptional repressor complex that is responsible for repressing a diversity of genes controlled by different signalling pathways. In nutrient-rich condition, Tup1 was found to interact with the upstream region regulating transcription of *IME1* at approximately 1000 base pairs (bp) upstream of the start codon (Weidberg et al., 2016). Yet, the importance of Tup1-Cyc8 in repressing *IME1* transcription and inhibiting entry into meiosis in the presence of nutrients was unknown. Tup1-Cyc8 is a well characterised transcriptional repressor complex. In *in vitro* conditions, Tup1 and Cyc8 subunits interact with each other to form a complex in a ratio of 4:1 (Williams et al., 1991, Varanasi et al., 1996). Most genes that are bound by either Tup1 or Cyc8 can be de-repressed when the other subunit of the Tup1-Cyc8 complex is lost, indicating that Tup1 and Cyc8 act together to repress gene targets (Chen et al., 2013). Previous study suggested Tup1 as a repressor of *IME1* transcription, but the role of Cyc8 had not been addressed (Weidberg et al., 2016). For this reason, I set out to investigate whether Cyc8 also targets the *IME1* promoter, and mediates repression of *IME1* transcription similar to Tup1.

Tup1-Cyc8 has been reported to mediate target gene repression by a number of different mechanisms. Tup1-Cyc8 can establish repressive chromatin structure at promoters by stabilising nucleosomes and recruiting histone deacetylases (HDACs) to histone proteins. Tup1-Cyc8 can also physically block the recruitment of transcription activators, or inhibit activators that are bound at the promoter under repressive conditions. Finally, Tup1-Cyc8 can directly interfere with the transcriptional machinery by interacting with TATA-binding proteins and the Mediator subunits of the RNA polymerase II holoenzyme. Different gene targets of Tup1-Cyc8 are repressed by one or a combination of these actions (Fleming et al., 2014, Zhang and Reese, 2004a, Watson et al., 2000). How Tup1-Cyc8 represses the *IME1* promoter was unclear. Analysis of genome-wide MNase-seq data showed that Tup1 deletion is correlated with decreased nucleosome occupancy at the *IME1* promoter (Rizzo et al., 2011, Weidberg et al., 2016). Thus, nucleosome stabilisation may

partially contribute to Tup1-mediated repression of *IME1*. Nevertheless, Tup1 can employ multiple mechanisms to repress the *IME1* promoter.

Here, I set out to investigate the relationship between Tup1-Cyc8 binding and *IME1* transcription. To understand the importance of Tup1-Cyc8 in *IME1* regulation, I examined how Tup1 or Cyc8 depletion may affect *IME1* repression in nutrient-rich condition. Furthermore, I assessed how rapidly *IME1* may be de-repressed when Tup1 is depleted in nutrient-rich condition. One of the mechanisms that Tup1-Cyc8 represses its targets is directly inhibiting transcriptional activation by blocking activator recruitment or functions. By following the kinetics of *IME1* activation after Tup1 depletion, I investigated whether *IME1* activators are possibly masked or blocked by Tup1-Cyc8. In addition, nutrient signals regulate the binding of Tup1-Cyc8 binding at the *IME1* promoter. In nutrient-depleted condition, Tup1 dissociates from the *IME1* promoter and thereby permits entry into meiosis (Weidberg et al., 2016). How nutrient signals regulate Tup1-Cyc8 binding at the *IME1* promoter was unknown. In this chapter, I examined how Tup1 and Cyc8 binding at the *IME1* promoter is altered in different growth stages. Since nutrient signals may drive changes in protein expression and cellular localisation, I asked whether protein levels and sub-cellular distributions of Tup1 and Cyc8 could have roles in regulating their binding at the *IME1* promoter. Finally, I explored whether HDACs are involved in *IME1* repression under nutrient-rich condition. The goals of these experiments were to delineate the role of Tup1-Cyc8 in regulating *IME1* expression, and provide insights into how Tup1-Cyc8 represses the *IME1* promoter in nutrient-rich condition.

3.1 Tup1 and Cyc8 associate with the *IME1* promoter in nutrient-rich conditions and dissociate when nutrients are depleted

In rich medium (YPD), Tup1 binding is detected from 750 to 1400 bp upstream of the *IME1* start codon (Weidberg et al., 2016). The binding of Tup1 is most intense at around 1000 bp upstream of the start codon. I hypothesised that if Tup1 and Cyc8 bind to the *IME1* promoter as a complex, then Cyc8 binding should also be detected at the *IME1* promoter and peak at 1000 bp upstream of the open reading frame (ORF). To examine whether Cyc8 binds to the *IME1* promoter, I attached three copies of the V5 epitope to the C-terminus of Cyc8 (Cyc8-V5) by endogenously fusing the DNA sequence encoding the V5 epitopes to the 3' end of the *CYC8* gene. I harvested cells carrying Cyc8-V5 during exponential growth (YPD (E)), when glucose and nitrogen compounds are the most abundant in the YPD medium. Cyc8 and its bound chromatin were purified by chromatin immunoprecipitation (ChIP), and its binding at the *IME1* promoter was quantified by quantitative PCR (qPCR).

In this thesis, I performed ChIP analyses to detect and quantify interactions between chromatin and chromatin-bound proteins, including Cyc8 in this experiment as well as Tup1 and various transcription factors in later sections and chapters. During the ChIP procedure, I crosslinked the protein-DNA complexes to stabilise the interactions by directly treating yeast cells with formaldehyde in growth media. In the laboratory, yeast cells normally grow and propagate in nutrient-rich YPD medium. To induce sporulation, cells were grown to saturation and subsequently shifted to acetate-containing BYTA medium to promote respiration. After reaching saturation in BYTA medium, cells were transferred to nutrient-deprived sporulation (SPO) medium in which cells starve and sporulate. Therefore, in order to compare the binding levels of chromatin-bound proteins at the *IME1* promoter at different stages of growth, I carried out formaldehyde crosslinking in media that contained different components and supplements (Chapter 2: Table 1). Notably, nutrient-rich YPD medium contains amino acids extracted from yeast extract and peptone, and is further supplemented with tryptophan, uracil, and adenine. In contrast, starvation-inducing SPO medium does not contain any amino acids in its contents (Chapter 2: Table 1). When formaldehyde is added to immobilise protein-DNA interactions, formaldehyde reacts with the thiol groups in the protein and crosslinks to amino acid

residues including tryptophan and histidine (Metz et al., 2004). It is possible that formaldehyde crosslinking is less efficient in nutrient-rich medium in some cases due to additional reactions with surrounding amino acids in the growth medium. To correct for the possible differences in crosslinking efficiency in YPD and SPO media, I normalised the ChIP signals detected at the *IME1* promoter over that at the silent mating type cassette *HMR*. Supplementary figure 1 presents Tup1 ChIP signals detected at the *IME1* promoter and at *HMR* in nutrient-rich condition as an example to demonstrate that the binding of Tup1 is specific to the *IME1* upstream region. In addition to crosslinking efficiency, this normalisation method also corrects for bead volume variation across the samples.

In this experiment, I used eight different primers that amplify different portions of the *IME1* promoter to determine where Cyc8 is bound most strongly (Figure 13A). Cyc8 was bound to the *IME1* promoter in nutrient-rich condition (Figure 13B). Importantly, Cyc8 binding spanned from 750 to 1400 bp upstream of the start codon, and peaked at -1000 bp. The binding pattern of Cyc8 at the *IME1* promoter is comparable to that of Tup1, suggesting that Tup1 and Cyc8 likely bind to the *IME1* promoter as a complex.

(A)

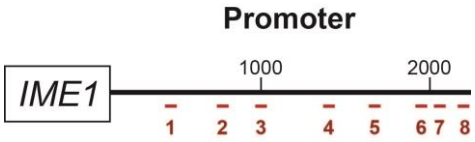

(B)

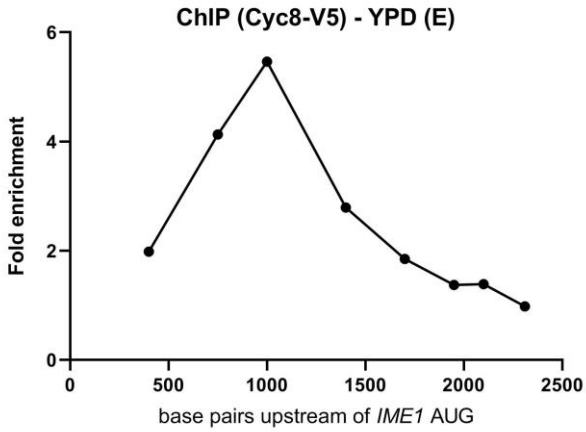

Figure 13. Cyc8 binds to the same region as Tup1 at the *IME1* promoter.

(A) Schematic representation of the qPCR primers used for scanning the *IME1* promoter. The primer pairs (red lines) amplify 400, 750, 1000, 1400, 1700, 1950, 2100, and 2310 bp upstream of the *IME1* start codon.

(B) ChIP-qPCR of V5 epitope-tagged Cyc8 (FW6381) in exponentially growing cells (YPD (E)) to scan for binding across the *IME1* promoter. Primer pairs shown in (A) were used for qPCR. ChIP signals were normalised over the silent mating type cassette *HMR*.

Next, I asked how the Tup1 and Cyc8 interactions with the *IME1* promoter respond to changes in nutrient availability in the surrounding environment. To study this question, I tagged Tup1 and Cyc8 with three copies of the V5 epitope (Tup1-V5 and Cyc8-V5) and measured their binding at the *IME1* promoter using ChIP-qPCR. The binding of Tup1 and Cyc8 was examined in various growth stages. In the laboratory, cells were grown in the YPD broth which provides rich glucose and nitrogen sources. In order to induce sporulation, cells were grown to saturation in YPD (20 to 24 hours) and transferred to a pre-sporulation medium that provides acetate as a carbon source. Subsequently, cells were shifted to the sporulation medium (SPO) containing no glucose or nitrogen compounds in which cells enter meiosis. To study different nutrient conditions, I monitored Tup1 and Cyc8 binding in exponentially growing cells (YPD (E)) and cells grown to saturation (YPD (S)) in YPD medium. I also sampled cells at 0 and 4 hours in sporulation medium (SPO 0h and SPO 4h) to represent conditions before and during meiotic entry. In this experiment, I only examined the region that is 1000 bp upstream of *IME1* (using primer pair 3 shown in Figure 13A) since Tup1 and Cyc8 primarily bind to this region.

Tup1 and Cyc8 both exhibited significant enrichment at the *IME1* promoter during exponential growth (Figure 14). This agrees with *IME1* being tightly repressed in exponentially growing cells. In cells grown to saturation and before meiotic entry (SPO 0h), Tup1 remained significantly bound to the promoter of *IME1*. Interestingly, Cyc8 binding at the *IME1* promoter decreased as cells were grown to saturation (Figure 14). When meiotic entry was induced in sporulation medium (SPO 4h), both Tup1 and Cyc8 were no longer detected at the *IME1* promoter. These data indicate that the occupancies of Tup1 and Cyc8 at the *IME1* upstream region are sensitive to

nutrient availability. There are similarities and differences between the binding patterns of Tup1 and Cyc8 in response to changes in the environment. Both Tup1 and Cyc8 associate with the *IME1* promoter in nutrient-rich condition, and dissociate when nutrients are depleted, suggesting that Tup1 and Cyc8 act together to repress *IME1* in the presence of nutrients. However, Cyc8 binding, but not Tup1 binding, was reduced in cells grown to saturation, indicating that the two subunits of the Tup1-Cyc8 complex may be differentially regulated by nutrients at the *IME1* promoter (discussed in section 7.6). Reduced cellular level of Cyc8 likely contributes to the loss of Cyc8 at the *IME1* promoter (Figure 15B). Given that Tup1 is able to interact with some DNA-binding transcription factors such as α2 protein without Cyc8 (Komachi et al., 1994), it is possible that Tup1 can directly interact with some of the recruiting transcription factors at the *IME1* promoter during saturated growth phase and prior to entry into meiosis. Further analyses are required to dissect whether Cyc8 interacts with the *IME1* promoter and represses *IME1* transcription when cells are grown to saturation. One simple experiment would be to deplete Cyc8 protein using the auxin-induced degron (AID) system (section 3.2) during the saturated growth phase and examine the effects on *IME1* transcription. If Cyc8 is required at the *IME1* promoter in saturated cells, Cyc8 depletion should lead to significant de-repression of *IME1* transcription. Conversely, if Cyc8 is no longer involved in *IME1* repression, Cyc8 depletion should have no effect on *IME1* transcription.

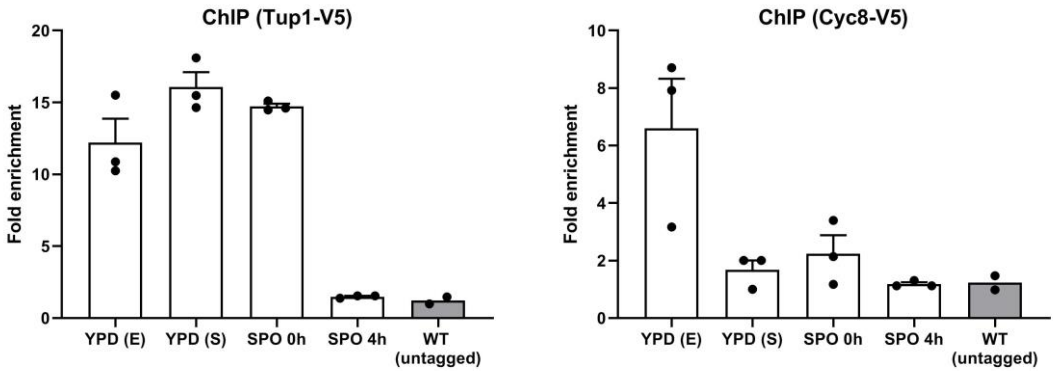

Figure 14. Tup1 and Cyc8 binding at the *IME1* promoter is sensitive to nutrients.
ChIP-qPCR of Tup1-V5 (FW3456) and Cyc8-V5 (FW6381) in exponentially growing cells (YPD (E)), cells grown to saturation (YPD (S)), prior to (SPO 0h) and during meiotic entry (SPO 4h). For qPCR, a primer pair that amplifies 1000 bp upstream of the *IME1* start codon was used. ChIP signals were normalised over the silent mating type cassette

HMR. As negative control, ChIP signals from exponentially growing wild-type untagged cells (FW1511) were included in the graphs. Bars represent mean (SEM) and dots indicate individual biological replicates.

Nutrient depletion might trigger protein degradation and cellular re-localisation. Therefore, loss of Tup1 and Cyc8 binding at the *IME1* promoter could be a result of reduced protein abundance or nuclear export. To investigate whether the removal of Tup1 and Cyc8 at the promoter is due to protein degradation, I performed western blotting on cells expressing Tup1-V5 and Cyc8-V5 at different growth stages as described for Figure 14. Tup1-V5 and Cyc8-V5 proteins were detected with an anti-V5 antibody, and their signals were normalised against hexokinase isoenzyme 1 (Hxk1) (Figure 15). In this thesis, Hxk1 was used as the loading control for western blots as it is strongly and stably expressed in various nutrient conditions. Furthermore, antibodies targeting Hxk1 were readily available in the laboratory. Yet, it is worth mentioning that Hxk1 expression level is sensitive to glucose signals. Previous study reported that the presence of glucose represses *HXK1* transcript level through inducing Hxk2 expression (Rodríguez et al., 2001). In line with their results, I also noted a mild increase in Hxk1 cellular expression when cells were shifted from exponential (YPD (E)) to saturated (YPD (S)) phase in my western blot data (Figure 15, Chapter 4: Figure 27). A similar increase in Hxk1 expression level was also observed when nutrient-sensitive PKA and/or TORC1 pathways were inhibited (Figure 37). For this reason, I would like to point out that the cellular expression levels in exponentially growing cells (YPD (E)) presented in Figure 15 and Chapter 4: Figure 27 may be slightly over-estimated due to lower Hxk1 levels. Nevertheless, there was little change in Hxk1 expression in cells grown to saturation (YPD (S)), prior to entry into meiosis (SPO 0h), and during entry into meiosis (SPO 4h) (Figure 15 and Chapter 4: Figure 27). Hence, it is valid to compare protein expression levels normalised to Hxk1 levels in cells during these stages.

From the western blot results, Tup1 expression in saturated cells, before and during meiotic entry was comparable to that in exponential growth (Figure 15A). These observations suggest that protein abundance is not the reason for the loss of Tup1 binding at the *IME1* promoter when nutrients are depleted. Conversely, Cyc8 expression was drastically reduced in cells grown to saturation, and remained low

before and during meiotic entry (Figure 15B). The western blot quantification data for Cyc8 strongly align with its ChIP profile at the *IME1* promoter (Figure 14 and Figure 15B). Thus, Cyc8 occupancy at the *IME1* promoter may be regulated by protein expression. Nevertheless, during meiotic entry (SPO 4h), Cyc8 binding was completely lost while it was still being expressed in the cell, suggesting that other mechanisms are involved in keeping Cyc8 from binding the *IME1* promoter. In conclusion, changes in Cyc8 protein abundance may in part explain the changes in Cyc8 occupancy at the *IME1* promoter. Tup1 protein levels do not change in different nutrient conditions, and thus protein abundance cannot explain changes in Tup1 occupancy at the *IME1* promoter.

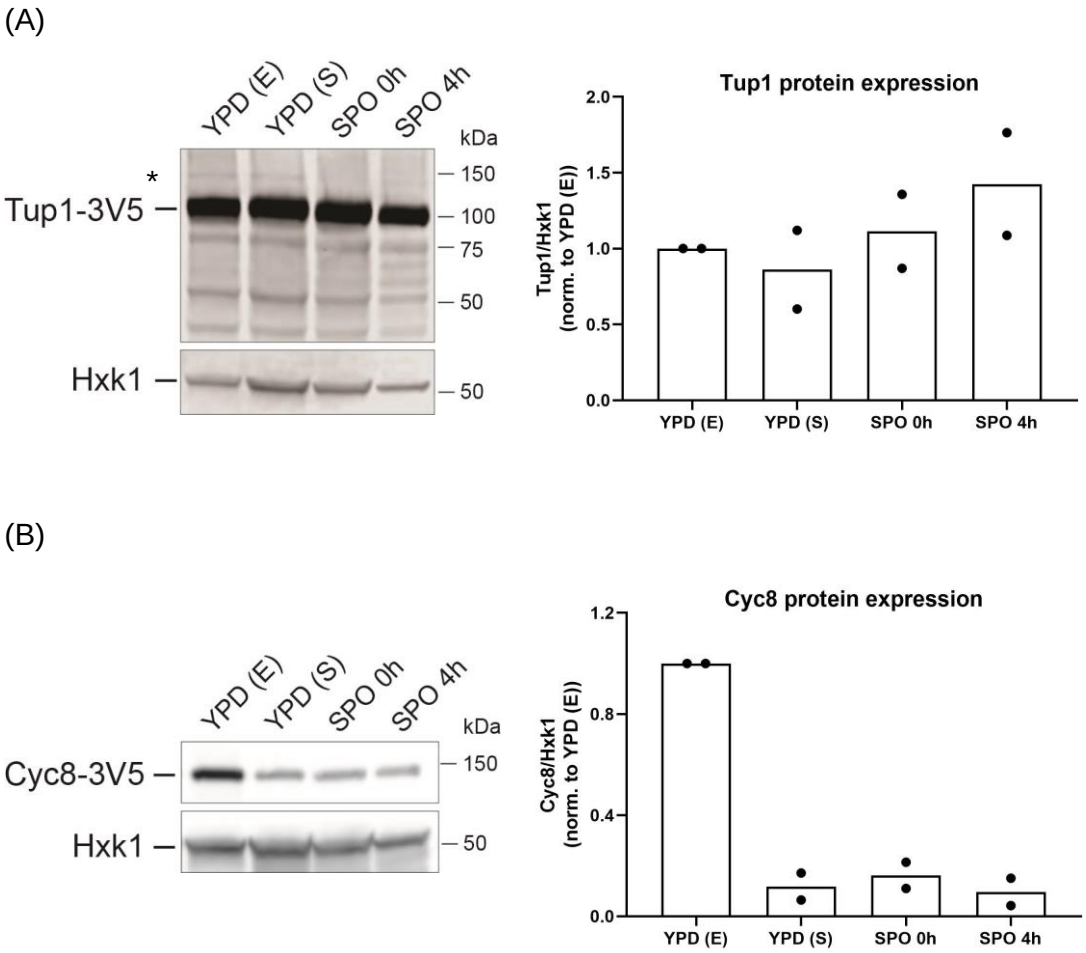

Figure 15. Tup1 protein remains strongly expressed when nutrients are depleted, while Cyc8 expression decreases when cells are grown to saturation.
Representative western blots and quantification data of (A) Tup1-V5 (FW3456), and (B) Cyc8-V5 (FW6381) from cells in exponential growth phase (YPD (E)), grown to saturation (YPD (S)), prior to (SPO 0h) and during (SPO 4h) entry into meiosis. Protein levels were normalised over Hxk1 levels, and the normalised levels are presented relative to YPD (E). Uncropped western blots can be found in Supplementary figure 2 and Supplementary figure 3. Bars represent mean normalised signals relative to YPD (E) and dots indicate individual biological replicates. Asterisk in (A) indicates the appearance of a heavier band that might suggest post-translational modifications.

Given that the changes in Tup1 and Cyc8 levels did not fully explain their eviction from the *IME1* promoter upon sporulation induction, I asked whether these proteins would re-localise to the cytoplasm in response to nutrient deprivation in the environment. To study this question, I labelled Tup1 and Cyc8 with the green-yellow fluorescent protein mNeonGreen (Tup1-mNeonGreen and Cyc8-mNeonGreen) by

endogenously fusing the DNA sequence encoding mNeonGreen to the 3' ends of *TUP1* and *CYC8* respectively (Argüello-Miranda et al., 2018). I studied the localisation patterns of Tup1-mNeonGreen and Cyc8-mNeonGreen in cells prior to (SPO 0h) and during (SPO 4h) meiotic entry by widefield fluorescence microscopy (Figure 16). I also quantified the signal intensities of the mNeonGreen-tagged proteins in the whole cell, nucleus, and cytosol (whole cell – nucleus). To assess whether there was a change in the sub-cellular distribution of Tup1 and Cyc8, I calculated the total mNeonGreen signals detected in the nuclei before and during entry into meiosis (Figure 16B). In addition, I calculated a ratio of nuclear mNeonGreen signal vs cytosolic mNeonGreen signal for each cell (Figure 16C).

My imaging data indicate that Tup1 and Cyc8 are located exclusively in the cell nucleus prior to entry into meiosis, consistent with their roles in regulating gene transcription (Figure 16A). Upon induction to enter meiosis, Tup1 and Cyc8 remained strongly expressed in the nucleus. Notably, the signal intensities of Tup1-mNeonGreen and Cyc8-mNeonGreen in the nucleus were similar before and during meiotic entry, suggesting that a major nuclear export event did not take place (Figure 16B). Furthermore, Tup1 and Cyc8 did not re-localise to the cytoplasm during meiotic entry since the nuclear to cytoplasmic signal ratios were unaffected (Figure 16C). These observations match the western blot data (Figure 15) that Tup1 and Cyc8 protein levels are unchanged during entry into meiosis (SPO 0h vs SPO 4h). Taken together, Tup1 and Cyc8 are expressed within the nucleus prior to and during entry into meiosis, therefore Tup1 and Cyc8 do not dissociate from the *IME1* promoter via cellular re-localisation.

(A)

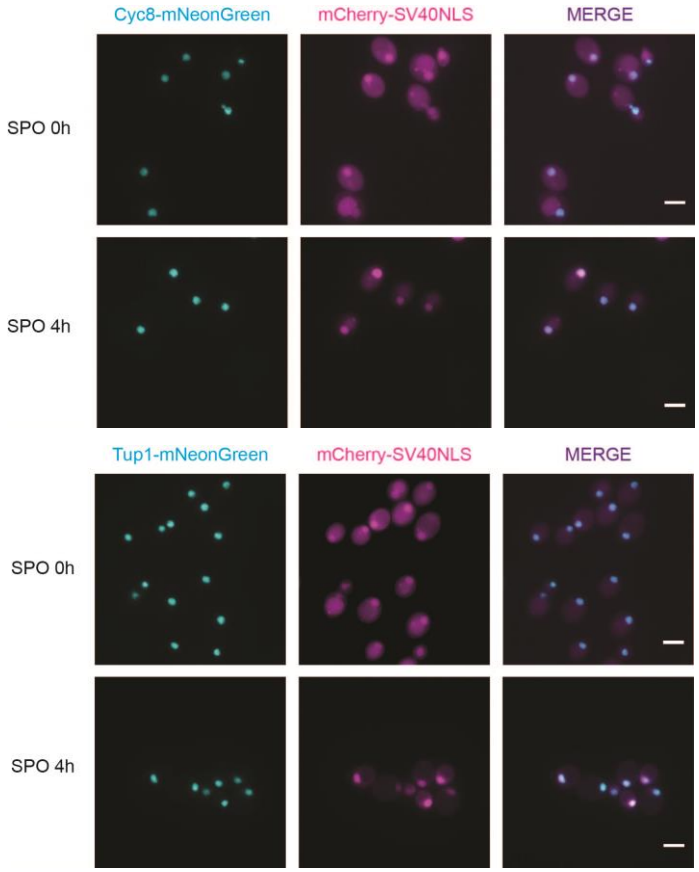
Cyc8-mNeonGreen
mCherry-SV40NLS
MERGE
SPO 0h
SPO 4h
Tup1-mNeonGreen
mCherry-SV40NLS
MERGE
SPO 0h
SPO 4h

(B)

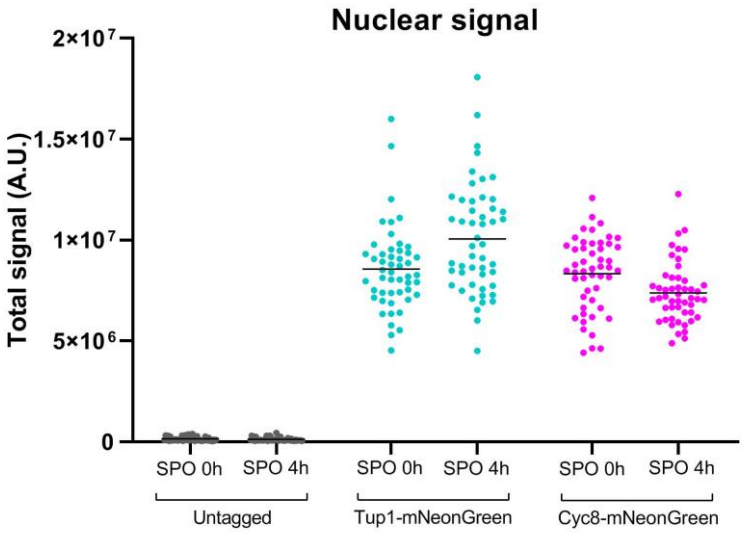
Nuclear signal
Total signal (A.U.)
2×10⁷
1.5×10⁷
1×10⁷
5×10⁶
0
SPO 0h
SPO 4h
SPO 0h
SPO 4h
SPO 0h
SPO 4h
Untagged
Tup1-mNeonGreen
Cyc8-mNeonGreen

(C)

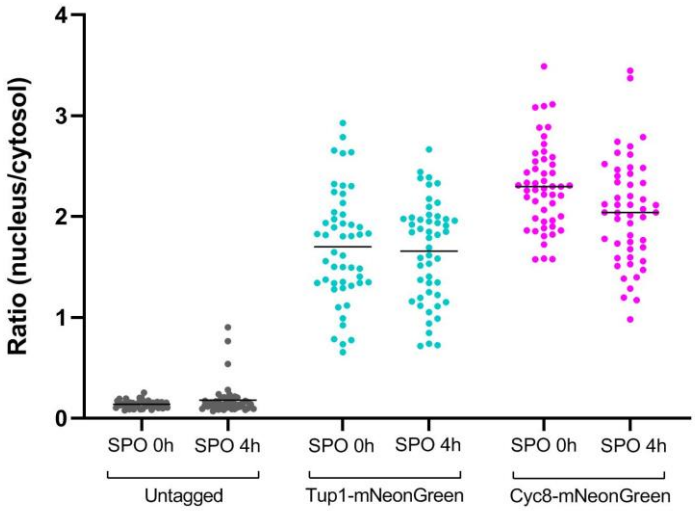

Figure 16. Tup1 and Cyc8 are expressed in the nucleus before and during entry into meiosis.

(A) Representative widefield microscopy images of Tup1-mNeonGreen (FW7644) and Cyc8-mNeonGreen (FW7642) before (SPO 0h) and during (SPO 4h) entry into meiosis. Separate and merged channel images for mNeonGreen fusion proteins and mCherry-SV40NLS are presented. Scale bars indicate 5µm.

(B) Scatter dot plot representing the mNeonGreen signal detected in the nucleus of each cell. Measurements of nuclear mNeonGreen signals were directed by the nuclear marker (mCherry-SV40NLS). Quantification data for 50 cells that were untagged (FW5199), or expressing Tup1-mNeonGreen (FW7644) or Cyc8-mNeonGreen (FW7642) are presented. The black line denotes the mean nuclear signal intensity of the cell population.

(C) Scatter dot plot representing the nuclear/cytosolic mNeonGreen ratios determined in the same cells analysed in (B). The cytosolic mNeonGreen signal was derived from (whole cell signal – nuclear signal). The black line denotes the mean nuclear/cytosolic mNeonGreen ratio of the cell population.

3.2 Both Tup1 and Cyc8 mediate the repression of *IME1* when rich nutrients are present

In the Tup1-Cyc8 complex, Tup1 and Cyc8 play distinct roles where Cyc8 recruits the complex to the promoter and Tup1 represses transcriptional activity. Thus, deleting either subunit should result in full de-repression of the gene target (Fleming et al., 2014). Given that Tup1 and Cyc8 co-localise at the *IME1* promoter in nutrient-rich condition (Figure 13 and Figure 14) (Weidberg et al., 2016), I asked whether both Tup1 and Cyc8 mediate *IME1* repression.

To study this question, I employed the auxin-based degron system (Nishimura et al., 2009) to deplete Tup1 and Cyc8 respectively. Briefly, Tup1 and Cyc8 proteins were tagged with an auxin-induced degron (AID) by endogenously fusing the *AID* sequence to the 3' ends of *TUP1* and *CYC8*. Additionally, TIR1 ligase was expressed from a plasmid, which interacts with the SCF E3 ubiquitin ligase complex. Upon addition of auxin indole-3-acetic acid (3-IAA), the AID-fused proteins interact with the SCF-TIR1 complex and are ubituitylated by the E2 ubiquitin conjugating enzyme. As a consequence, the ubiquitylated proteins are targeted for proteasomal degradation, allowing depletion of specific AID-tagged proteins. In this experiment, I treated cells expressing Tup1-AID and Cyc8-AID with 3-IAA and control DMSO respectively in nutrient-rich medium. Cells were sampled at different time points, and the expression levels of Tup1-AID and Cyc8-AID were detected by western blotting (Figure 17A). Addition of 3-IAA efficiently depleted Tup1 and Cyc8 fused with the AID degron in cells, since both proteins were undetectable 30 minutes after treatment. When identifying Tup1-AID on the blot, a second band of approximately 100 kDa was also detected (Figure 17A). Although this band matched the size of Tup1-V5 on western blot, Tup1 was not bound to the *IME1* promoter when Tup1-AID was depleted (Chapter 4: Figure 24). Thus, the AID tags induced rapid and efficient depletion of Tup1 and Cyc8 in the presence of 3-IAA.

Next, I measured the level of *IME1* de-repression in cells with Tup1 or Cyc8 depleted. These measurements were made by extracting total RNA followed by reverse transcription, and *IME1* transcripts were detected by quantitative PCR (RT-qPCR). Depletion of Tup1 at 30 minutes after 3-IAA addition led to rapid increase in

IME1 transcript level (Figure 17B). Notably, *IME1* expression at 30 minutes was comparable to that detected during entry into meiosis (SPO 4h), suggesting that Tup1 is responsible for repressing *IME1* transcription in nutrient-rich condition. In addition, *IME1* was already fully de-repressed at 30 minutes after 3-IAA treatment, indicating that the activation process following Tup1 depletion was very efficient. Similarly, depletion of Cyc8 resulted in significant de-repression of *IME1* at 30 minutes after 3-IAA treatment and the *IME1* transcript level detected was even higher than that during entry into meiosis (Figure 17B). Thus, Cyc8 is also responsible for repressing *IME1* transcription in nutrient-rich condition. Notably, my data suggest that Cyc8 depletion resulted in higher *IME1* transcript levels compared to Tup1 depletion in nutrient-rich condition. In the Tup1-Cyc8 complex, it is generally thought that Cyc8 associates the complex to the recruiting transcription factors while Tup1 represses transcription of the target gene (section 1.12). Yet, past studies have demonstrated that Cyc8 may possess some ability to repress gene transcription. For example, Cyc8 can interact with histone deacetylases (HDACs) such as Rpd3 and Hos2 in the absence of Tup1 (Davie et al., 2003). Furthermore, Cyc8 has been shown to partially repress transcription at the *FLO1* locus independent of Tup1 (Fleming et al., 2014). Hence, it is possible that Cyc8 occupancy confers partial transcriptional repression at the *IME1* promoter. In addition, the level of *IME1* transcripts detected upon Cyc8 depletion in nutrient-rich condition was higher than that during entry into meiosis (Figure 17B). One plausible explanation is that more *IME1* activators are readily available to bind the promoter in nutrient-rich condition than in sporulation condition.

To summarise, *IME1* transcription is significantly de-repressed in nutrient-rich condition when Tup1 or Cyc8 is depleted. These observations support that the Tup1-Cyc8 complex is responsible for maintaining transcriptional repression of *IME1* in nutrient-rich condition. Importantly, *IME1* de-repression occurs with no detectable delay after Tup1 or Cyc8 depletion, suggesting that the *IME1* promoter may be poised for activation under nutrient-rich condition.

(A)

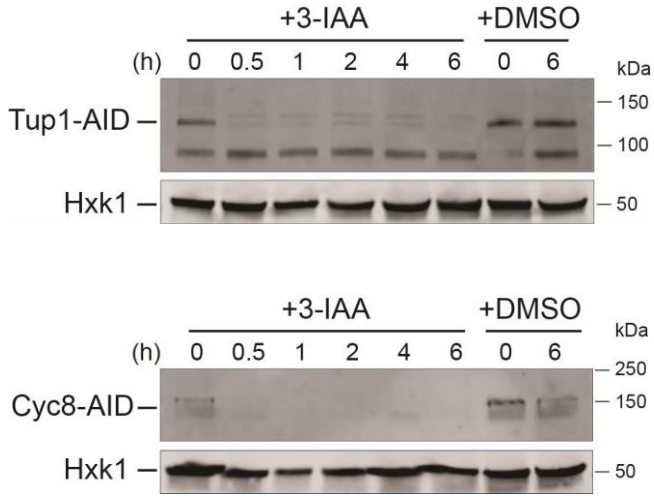

(B)

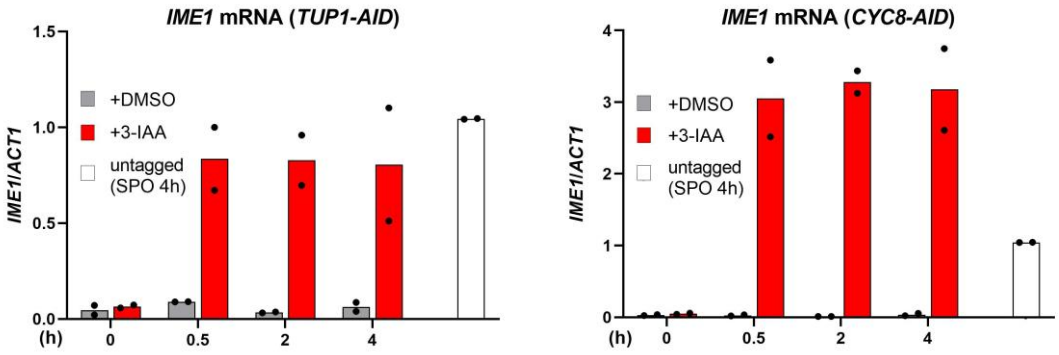

Figure 17. Depletion of Tup1 or Cyc8 de-represses *IME1* transcription in nutrient-rich condition.

(A) Representative western blot showing the responses of Tup1-AID (FW5057) and Cyc8-AID (FW6371) to addition of 3-IAA and DMSO respectively in nutrient-rich YPD medium. Cells were harvested at indicated time points, and total proteins were extracted and separated by SDS-PAGE. Proteins fused with AID tag were detected using an anti-V5 antibody. Uncropped western blots can be found in Supplementary figure 4 and Supplementary figure 5.

(B) *IME1* transcript levels detected by RT-qPCR in *TUP1-AID* (FW5057) and *CYC8-AID* (FW6371) cells treated with 3-IAA and DMSO respectively in nutrient-rich YPD medium. *IME1* transcript levels were determined in cells at 0, 0.5, 2, and 4 hours after treatment. Primers flanking approximately +850 bp of the *IME1* ORF were used for qPCR, and signals were normalised over actin *ACT1*. As control,

the *IME1* level detected in wild-type cells (FW1511) at 4 hours after sporulation induction (SPO 4h) is also presented. Bars represent mean normalised *IME1* levels and dots indicate individual biological replicates.

3.3 *IME1* promoter is poised for activation when repressed by Tup1-Cyc8

IME1 transcripts are detected in nutrient-rich medium quickly after Tup1 or Cyc8 is depleted (Figure 17). Based on previous reports, Tup1 can repress its target promoters by impeding the recruitment or compromising the activation properties of transcriptional activators (see Introduction: section 1.12 – Mechanisms of transcriptional repression mediated by Tup1-Cyc8). I hypothesised that the *IME1* promoter is poised for transcriptional activation when Tup1-Cyc8 is bound in nutrient-rich condition. If this hypothesis was true, *IME1* transcripts should be detected immediately after Tup1 depletion as transcriptional activators are already bound or readily available to bind. To closely examine the kinetics of *IME1* activation after Tup1 depletion, I measured *IME1* expression in additional time points after inducing Tup1 depletion with the auxin-based degron system. I sampled cells minutes after the addition of 3-IAA, and quantified *IME1* transcript levels to determine when transcription became activated. To improve sensitivity, I measured the absolute levels of *IME1* transcripts in single cells using single molecule RNA fluorescence *in situ* hybridisation (smFISH). smFISH allows every single copy of *IME1* to be visualised, thus improves the sensitivity and accuracy of the assay. Furthermore, smFISH provides single molecule resolution that would indicate whether the gene is heterogeneously expressed in the entire cell population. In this experiment, I employed smFISH probes that hybridise to *IME1* (AF594) and *ACT1* (Cy5) transcripts. *ACT1* signals serve as a control to ensure that the probes successfully entered the cells and hybridised to RNA. The same set up was also used for *IME1* transcript measurements later in this thesis (Chapter 5 and Chapter 6) when higher sensitivity was required.

Tup1-AID was rapidly depleted by the addition of 3-IAA (Figure 18A). The level of Tup1-AID began to decline at 10 minutes, and was greatly diminished at 15 minutes after 3-IAA treatment. At 30 minutes, Tup1 was completely depleted in cells (Figure 18A). I monitored *IME1* transcript levels in cells treated with 3-IAA and DMSO by smFISH (Figure 18B-D). As control, the expression and distribution of *ACT1* were similar across all conditions (Figure 18D). In nutrient-rich condition (0 min), *IME1* expression was largely repressed since around 72% of cells displayed less than four copies of *IME1* (Figure 18C). After adding 3-IAA for 2 to 5 minutes, there was no

significant difference in *IME1* expression between 3-IAA and DMSO treated cells (Figure 18B). Notably, number of *IME1* transcripts gently increased in the population at 10 minutes after 3-IAA addition. At this time point, the mean number of *IME1* transcripts in 3-IAA treated cells was slightly higher than DMSO treated cells (2.281 vs 0.761 *IME1* transcripts per cell) (Figure 18B). As Tup1-AID levels dropped at 15 minutes after 3-IAA addition, a substantial increase in the number of *IME1* transcripts was simultaneously detected in cells (Figure 18B). With most of Tup1-AID depleted at 15 minutes, 12% of the population displayed more than 10 *IME1* transcripts, while this was detected in only around 2% of control cells (Figure 18C). Finally, when Tup-AID was completely lost at 30 minutes, a sharp increase in *IME1* transcripts was detected in the population (Figure 18B). There was also a significant shift in the distribution of *IME1* transcripts in single cells, in which 56% of the population exhibited more than 10 *IME1* transcripts (Figure 18C).

It is worth mentioning that small sub-populations of cells expressed more than 10 copies of *IME1* transcripts without 3-IAA addition (0 min and DMSO-treated cells) (Figure 18B and Figure 18C). Thus, the auxin-based degron system may induce leaky degradation of Tup1-AID. To further examine this, I also measured *IME1* transcript levels in cells expressing TIR ligase by smFISH (Figure 18E). I found that cells expressing only TIR1 ligase did not produce more than four *IME1* transcripts in a single cell before and after 3-IAA treatment. Furthermore, the distribution of *IME1* transcripts became very similar to that detected in exponentially growing wild-type cells. Thus, the leaky *IME1* expression observed in uninduced *TUP1-AID* cells was likely due to leaky degradation of Tup1, or interference with Tup1 function by the AID tag.

In conclusion, I found that depletion of Tup1 or Cyc8 is sufficient to induce full *IME1* transcription in the presence of rich nutrients. In addition, *IME1* is transcribed rapidly when Tup1 of Cyc8 is depleted from cells in nutrient-rich condition. By monitoring *IME1* transcription closely when Tup1 is depleted, I found that there is no detectable delay between depletion of Tup1 and *IME1* transcription. These data suggest that *IME1* transcription commences as soon as Tup1 is depleted. I hypothesised that transcriptional activators are bound or readily available to bind the *IME1* promoter. In nutrient-rich condition, Tup1-Cyc8 is recruited to the *IME1*

promoter to mute transcriptional activity and thereby represses *IME1* transcription. Hence, I propose that the default state of the *IME1* promoter is active, and *IME1* transcription is primarily regulated by Tup1-Cyc8 repression. To investigate this hypothesis, I examined the binding patterns of known and putative *IME1* activators at the *IME1* promoter under different nutrient conditions and the results are presented in the next section (Figure 19).

(A)

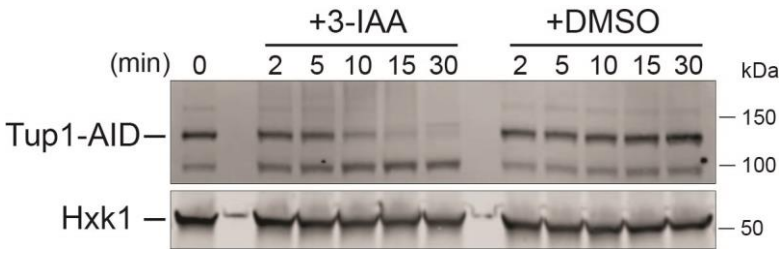
+3-IAA
+DMSO
(min) 0 2 5 10 15 30 2 5 10 15 30
kDa
Tup1-AID
Hxk1
150
100
50

(B)

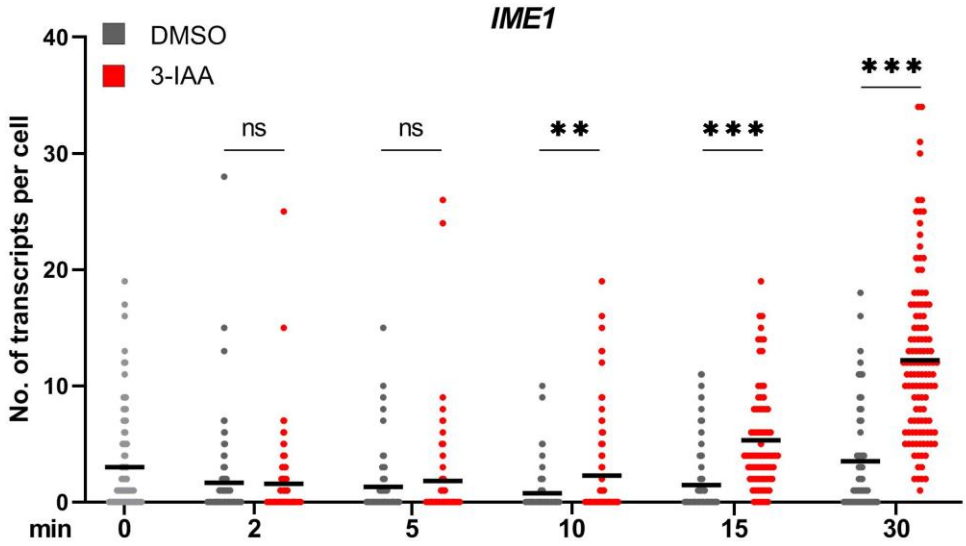
IME1
DMSO
3-IAA
No. of transcripts per cell
ns
ns
**
***
***
min 0 2 5 10 15 30

(C)

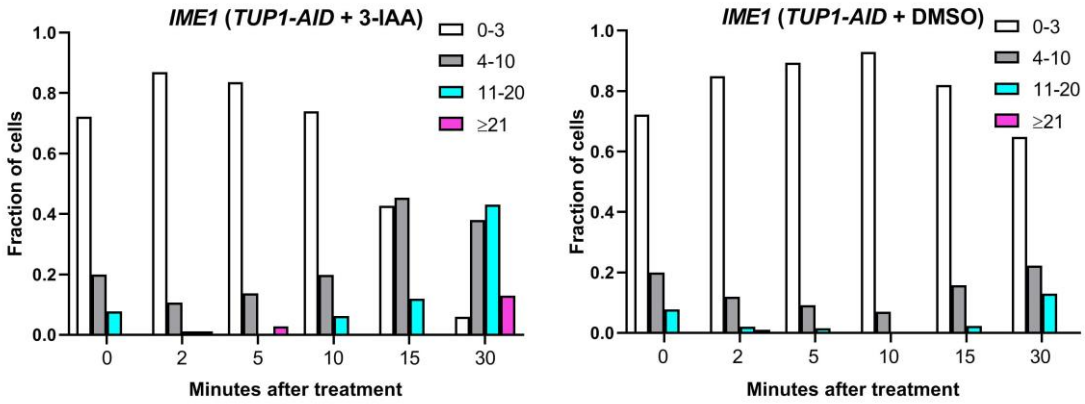
IME1 (TUP1-AID + 3-IAA)
IME1 (TUP1-AID + DMSO)
0-3
4-10
11-20
≥21
Fraction of cells
Minutes after treatment

(D)

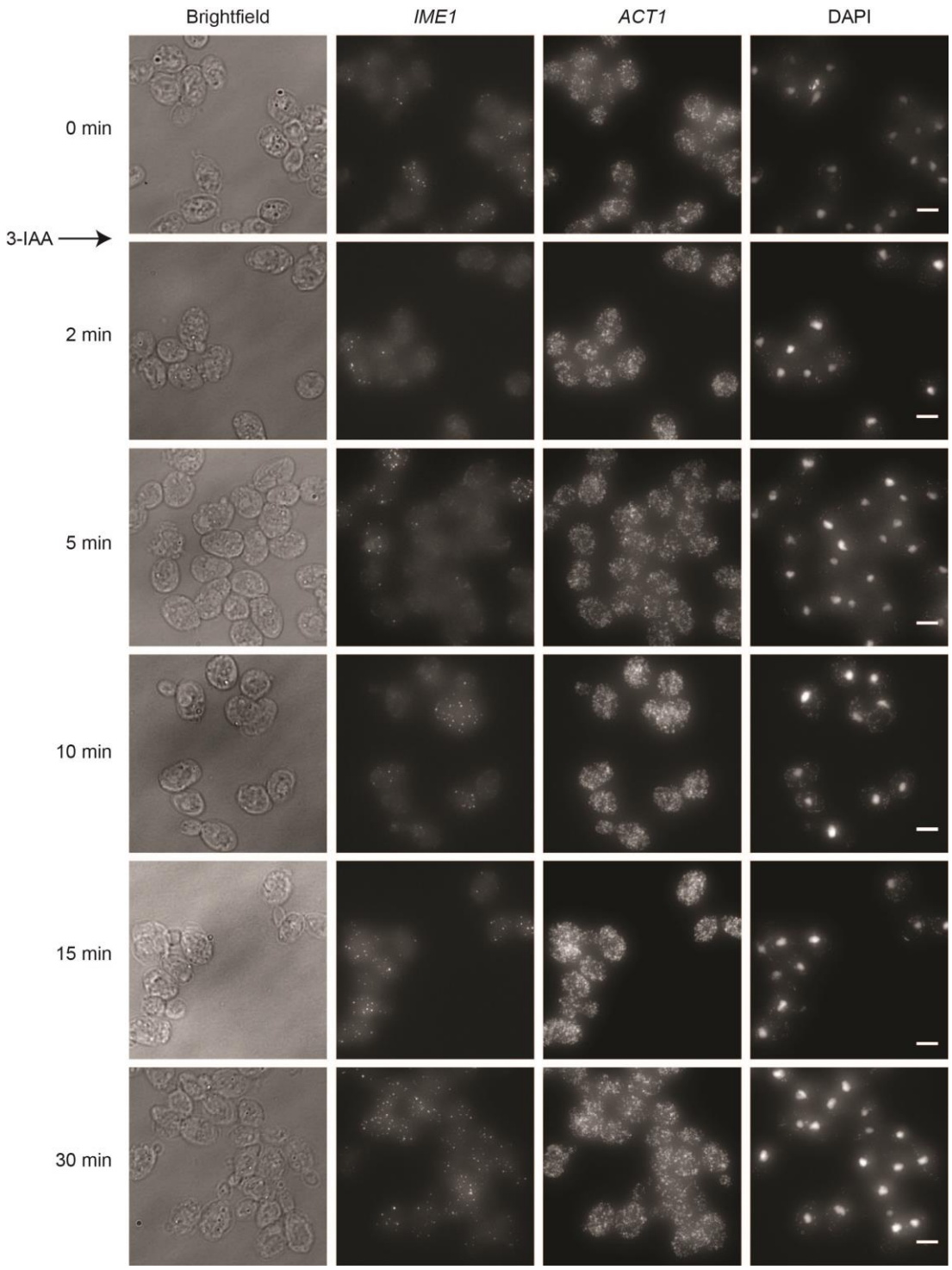
Brightfield
IME1
ACT1
DAPI
0 min
3-IAA
2 min
5 min
10 min
15 min
30 min

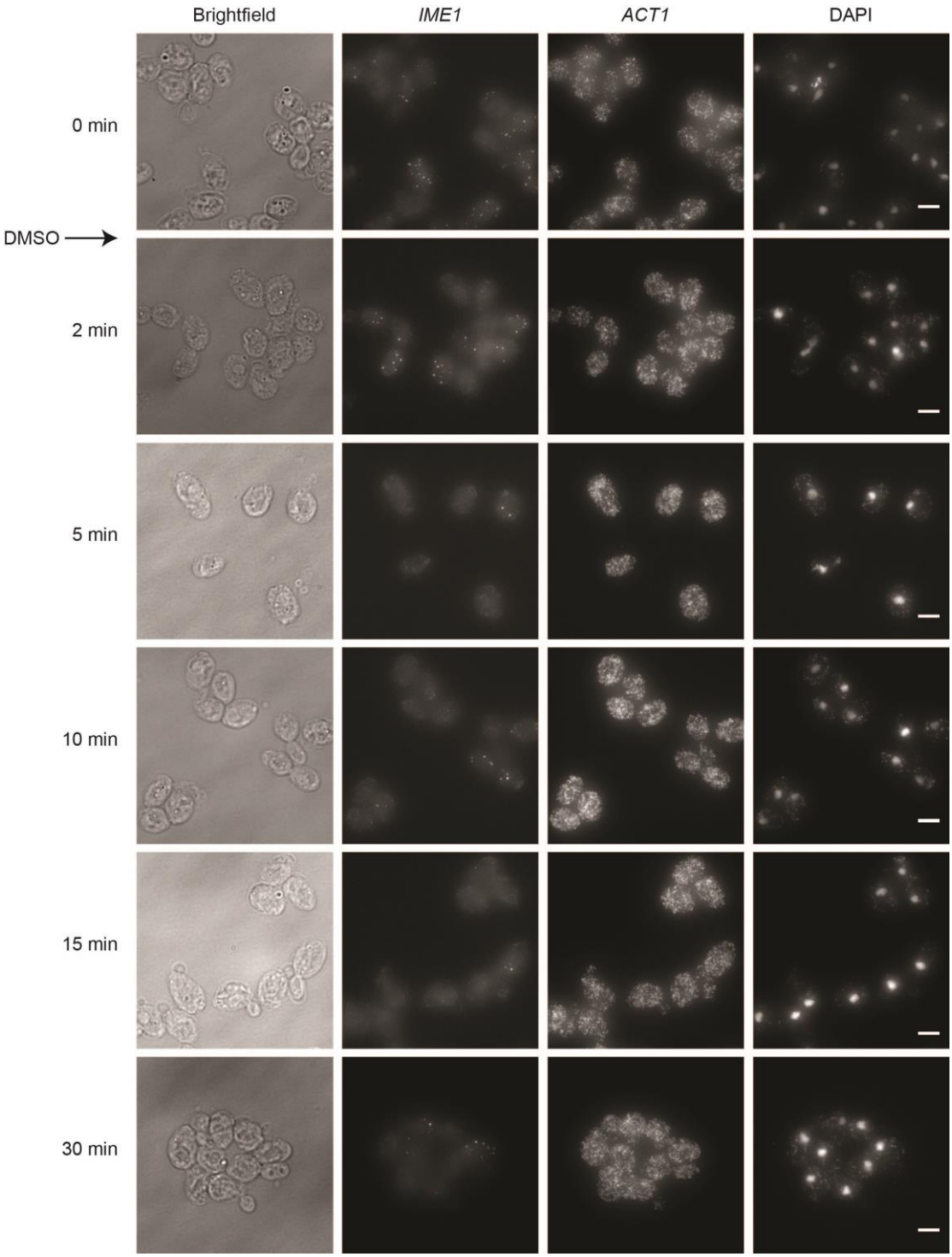
Brightfield
IME1
ACT1
DAPI
0 min
DMSO
2 min
5 min
10 min
15 min
30 min

(E)

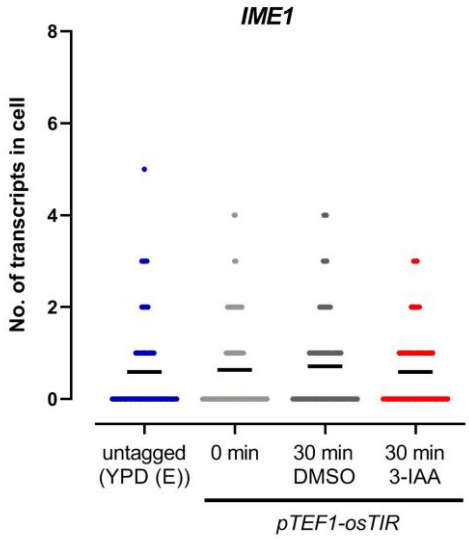

Figure 18. *IME1* transcript level increases instantly as Tup1 level declines.

(A) Representative western blot showing the response of Tup1-AID (FW5057) to the addition of 3-IAA and DMSO respectively in nutrient-rich YPD medium. Cells were harvested just before treatment (0 min), and at 2, 5, 10, 15, and 30 minutes post treatment. Tup1-AID was detected using an anti-V5 antibody. Uncropped western blot can be found in Supplementary figure 6.

(B) Scatter dot plot representing number of *IME1* transcripts detected per cell in Tup1-AID (FW5057) cells treated with 3-IAA and DMSO respectively in nutrient-rich YPD medium. Cells were fixed at the indicated time points in (A), and hybridised with probes detecting *IME1* (AF594) and *ACT1* (Cy5). Only cells that were positive for *ACT1* were included in the analysis. Approximately 50-120 cells were analysed for each cell population. The black line denotes the mean number of *IME1* transcripts per cell in the population. Unpaired parametric two-tailed Welch's t-test was carried out between 3-IAA and DMSO treated samples at each time point with 95% confidence. P-values are indicated in the graph, where ns stands for non-significant, * = ≤ 0.05, ** = ≤ 0.01, *** = ≤ 0.001.

(C) Histogram showing data in (B) that were binned into intervals by the number of *IME1* transcripts in cells. Data were binned into four intervals corresponding to 0-3, 4-10, 11-20, and 21 or more *IME1* transcripts per cell. Each bar represents the fraction of the cell population falling into that division.

(D) Representative smFISH images of Tup1-AID cells (FW5057) treated with 3-IAA and DMSO respectively in nutrient-rich YPD medium. *IME1* and *ACT1* transcripts were detected by AF594 and Cy5 probes respectively. Cell nuclei were visualised by DAPI staining. Scale bar indicates 5µm.

(E) Scatter dot plot representing number of *IME1* transcripts detected per cell in wild-type cells (FW1511) and cells expressing only TIR1 ligase (FW1908) in nutrient-rich YPD medium. Wild-type cells were harvested during exponential growth (YPD (E)). Cells expressing TIR1 ligase were treated with 3-IAA and DMSO, and cells were collected before treatment (0 min) and 30 minutes post treatment. Around 100 cells that were positive for *ACT1* were analysed for each cell population. The black line denotes the mean number of *IME1* transcripts in the population.

Since removing Tup1 repression by depletion was sufficient to induce *IME1* expression, I speculated that the *IME1* promoter is occupied with transcriptional activators that are inhibited by Tup1-Cyc8 under nutrient-rich conditions. For this reason, I decided to inspect the binding pattern of Pog1, a known *IME1* activator. Pog1 is a transcriptional activator discovered in 1999 that is involved in cell cycle regulation (Leza and Elion, 1999, Oshiro and Takagi, 2014). Pog1 has also been characterised as an activator of *IME1* (van Werven et al., 2012). In this study, Pog1 was reported to bind at the *IME1* promoter around 1000 bp upstream of the start codon prior to entry into meiosis and three hours after sporulation induction. Furthermore, the *pog1*Δ mutant displays a delay in *IME1* expression and meiotic divisions (van Werven et al., 2012). However, whether Pog1 occupies the *IME1* promoter in nutrient-rich conditions was unknown. To determine whether Pog1 is bound to the *IME1* promoter under repressive conditions, I examined its binding by ChIP-qPCR in exponentially growing cells (YPD (E)), cells grown to saturation (YPD (S)), before (SPO 0h) and during (SPO 4h) entry into meiosis (Figure 19A). I found that Pog1 was already associating with the *IME1* promoter during the exponential phase when nutrients are rich. Prior to entry into meiosis, Pog1 displayed increased binding to the *IME1* promoter which is likely to prepare the *IME1* promoter for activation (Figure 19A). As expected, Pog1 remained bound in sporulation conditions and this is in line with previous observations (van Werven et al., 2012). These results support the hypothesis that transcriptional activators occupy the *IME1* promoter in repressive conditions.

Next, I set out to identify transcription factors that are potentially *IME1* activators. Using the results from an *IME1-lacZ* reporter screen (unpublished data), I found three candidate transcription factors, Fkh1, Fkh2, and Com2 that are possibly involved in regulating *IME1* transcription. The consensus binding sites of these three transcription factors were predicted in the *IME1* promoter, at approximately 1000 bp upstream of the start codon (Figure 19B). Fkh1 and Fkh2 are paralogous forkhead family transcriptional activators that activate *CLB2* during G2-M phase in the cell cycle (Kumar et al., 2000). They have been described to have opposite roles in cell cycle progression and *HMR*a cassette silencing (Hollenhorst et al., 2000). In addition, Com2 shares the same DNA-binding residues with the stress-induced activator Msn2 (Siggers et al., 2014). Com2 binds to the *IME1* promoter near 1200 bp upstream of

the start codon in the presence of nutrients (Kahana-Edwin et al., 2013). To determine whether Fkh1, Fkh2, and Com2 bind the *IME1* promoter, I attached three copies of V5 epitope to each transcription factor and performed ChIP to detect their binding (Figure 19C). In nutrient-rich condition, I found that Fkh1 and Fkh2 were bound at the *IME1* promoter at 1000 bp upstream of the start codon. Conversely, Com2 did not bind to the *IME1* promoter in my experimental set up (Figure 19C). Taken together, putative regulators of the *IME1* promoter, Fkh1 and Fkh2 occupy the *IME1* promoter in repressive conditions. However, further experiments are required to dissect how Fkh1 and Fkh2 regulate the *IME1* promoter. To follow up on whether Fkh1 and Fkh2 contribute to *IME1* activation, the binding of these two transcription factors at the *IME1* promoter should also be examined under nutrient-poor conditions including before (SPO 0h) and during (SPO 4h) entry into meiosis. In addition, *IME1* expression should be examined when Tup1 is depleted in *fkh1*Δ, *fkh2*Δ, and *fkh1*Δ*fkh2*Δ cells to determine whether less *IME1* transcripts are generated. It would also be interesting to investigate whether Fkh1 and Fkh2 have any roles in Tup1 recruitment by examining Tup1 binding levels in *fkh1*Δ, *fkh2*Δ, and *fkh1*Δ*fkh2*Δ cells.

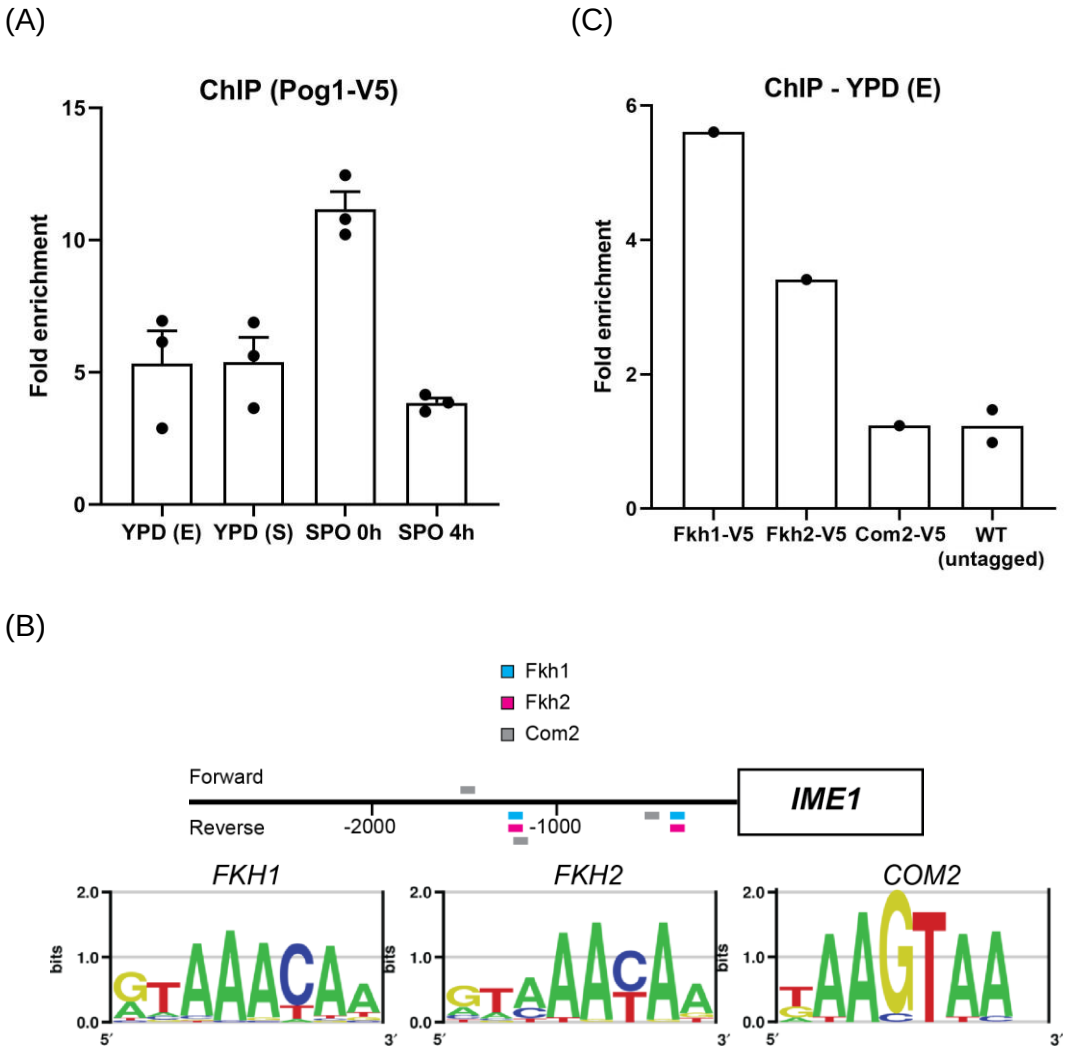

Figure 19. Known and putative transcriptional activators of *IME1* occupy the *IME1* promoter in nutrient-rich condition.

(A) ChIP-qPCR of Pog1-V5 (FW968) from cells in exponential growth phase (YPD (E)), grown to saturation (YPD (S)), before (SPO 0h) and during (SPO 4h) entry into meiosis. For qPCR, a primer pair flanking the region 1000 bp upstream of the *IME1* start codon was used. ChIP signals were normalised over the silent mating type cassette *HMR*. Bars represent mean (SEM) and dots indicate individual biological replicates.

(B) Schematic diagram depicting the Fkh1, Fkh2, and Com2 consensus binding motifs in the *IME1* promoter. The consensus binding motifs were acquired from the Yeast Transcription Factor Specificity Compendium (YeTFaSCo) database (de Boer and Hughes, 2012).

(C) ChIP-qPCR of Fkh1-V5 (FW8432), Fkh2-V5 (FW969), and Com2-V5 (FW8473) from cells in exponential growth phase (YPD (E)). Primers used and

normalisation method were the same as (A). As negative control, ChIP signals from wild-type untagged cells were also included in the graph. Bars represent mean normalised ChIP signals and dots indicate individual biological replicates.

3.4 Histone deacetylases Rpd3 and Hda1 only partially contribute to *IME1* repression

One of the prevalent mechanisms by which the Tup1-Cyc8 complex mediates repression of its target genes is by establishing repressive chromatin state in the gene promoter. The Tup1 repressor is able to interact with H3 and H4 histone tails with its repression domain, and recruit histone deacetylases (HDACs) to deacetylate the H3 and H4 histones (Edmondson et al., 1996). To determine whether HDACs are also involved in repressing *IME1*, I deleted the genes encoding different HDACs and measured *IME1* expression in the exponential growth phase. Budding yeast contains five related HDACs, including Rpd3, Hda1, Hos1, Hos2, and Hos3 to regulate gene transcription (Kurdistani and Grunstein, 2003). These HDACs have been categorised into different classes based on their sequences and properties. Class I HDACs are classified as HDACs with homology to Rpd3 and members of this class include Rpd3, Hos1, and Hos2 (Watson et al., 2000). Furthermore, HDACs with homology to Hda1 are known as Class II HDACs (Dokmanovic et al., 2007). The human homologues of the two classes of HDACs have revealed both similarities and differences between them (reviewed in Dokmanovic et al., 2007). Structurally, both Class I and Class II HDACs possess zinc-containing catalytic sites and can be chemically inhibited by trichostatin A and vorinostat. However, the two classes of HDACs exhibit different cellular localisation patterns: Class I HDACs are found in the nucleus while class II HDACs move between the nucleus and cytoplasm. In addition, Class I and Class II HDACs have different cellular functions in humans. Class I HDACs are involved in regulating cell proliferation and maintaining survival, as knocking out HDACs of this class result in cardiac defect and elevated expression of cell cycle genes (Dokmanovic et al., 2007). In comparison, Class II HDACs are more likely to have tissue-specific functions and may play roles in maintaining various tissues such as cartilage, blood vessel, and the heart. Finally, yeast also contains a sixth unrelated HDAC, Sir2 which belongs to the Sirtuin family and establishes the third class of HDACs (Class III) (Baidyaroy et al., 2001). In contrast to Class I and Class II HDACs, Sir2 is a NAD^+-dependent enzyme that does not contain zinc in its catalytic site and is not chemically inhibited by trichostatin A and vorinostat (Dokmanovic et al., 2007). In yeast, Sir2 is involved in transcriptional silencing at

silent mating type loci and telomeres by inducing H3K9, H3K14, and H4K16 deacetylation (Imai et al., 2000).

In this experiment, I examined the contribution of four HDACs including three Class I HDACs: Rpd3, Hos1, Hos2, and Class II HDAC: Hda1. These four HDACs were included in this analysis since they were previously demonstrated to repress or associate with histone proteins at various targets of the Tup1-Cyc8 complex (Watson et al., 2000, Wu et al., 2001, Fleming et al., 2014). Furthermore, Hos1 and Hos2 were shown to physically interact with Tup1-Cyc8 *in vivo* (Davie et al., 2003). Hence, I deleted Rpd3, Hos1, Hos2, or Hda1 in cells to determine whether these HDACs contribute to Tup1-Cyc8 mediated repression. To increase sensitivity, I assessed the *IME1* transcript level by smFISH (Figure 20). My smFISH data indicate that *IME1* transcription is repressed in the nutrient-rich exponential growth phase. In wild-type cells, 99.3% of cells displayed less than four *IME1* transcripts (Figure 20B). No significant de-repression of *IME1* was observed in the *rpd3*Δ, *hda1*Δ, *hos1*Δ, *hos2*Δ single mutants (Figure 20A). Notably, *rpd3*Δ cells displayed even less *IME1* transcripts than wild-type cells, suggesting that Rpd3 might play an activating role. I conclude that single deletions of Rpd3, Hos1, Hos2, or Hda1 cannot de-repress *IME1* transcription in exponentially growing cells.

Next, I constructed double deletion mutants to examine whether deleting two HDACs was sufficient to relieve *IME1* from Tup1-Cyc8 mediated repression. Analyses of individual Tup1-Cyc8 regulated genes have revealed that Rpd3 is often involved in maintaining transcriptional repression of the target genes. For example, the flocculation-specific *FLO1* gene is de-repressed in the absence of Rpd3 and Hda1 (Fleming et al., 2014). In addition, the mating type-specific *MFA2* gene and the glucose-repressible *SUC2* gene are both de-repressed when Rpd3, Hos1, and Hos2 are lost (Watson et al., 2000). Therefore, I generated *rpd3*Δ*hos1*Δ, *rpd3*Δ*hos2*Δ, and *rpd3*Δ*hda1*Δ strains and examined *IME1* expression in the double deletion mutants. I observed an increase in the number of *IME1* transcripts in *rpd3*Δ*hda1*Δ cells, in which 9.15% of cells carried at least four copies of *IME1* (Figure 20B). *IME1* expression in *rpd3*Δ*hos1*Δ and *rpd3*Δ*hos2*Δ cells was not de-repressed (Figure 20A). These data suggest that Rpd3 and Hda1 contribute to *IME1* repression. However, *IME1* expression in *rpd3*Δ*hda1*Δ cells was de-repressed to a much lesser extent than

Tup1 or Cyc8 depletion (Figure 17 and Figure 18). I conclude that Rpd3 and Hda1 only have a marginal contribution to *IME1* repression mediated by Tup1-Cyc8.

Further investigation should be carried out to follow up on the results in this experiment and to determine the roles that the HDACs play in regulating *IME1* transcription. Firstly, more HDAC combinations should be tested to confirm whether *IME1* transcription can be further de-repressed. It would be interesting to examine *IME1* transcript levels in triple deletion mutants such as *rpd3*Δ*hos1*Δ*hos2*Δ, *rpd3*Δ*hos1*Δ*hda1*Δ, and *rpd3*Δ*hos2*Δ*hda1*Δ cells (Watson et al., 2000). In addition, Hos3 and Sir2 should be included in future analyses. In order to fully understand how Tup1-Cyc8 mediates *IME1* repression, future studies should determine whether histone deacetylation at the *IME1* promoter is correlated with repression of *IME1* transcription. This can be achieved by measuring changes in the levels of histone acetylation at the *IME1* promoter when Tup1-Cyc8 or various HDACs are removed. To quantify histone acetylation level, ChIP analyses of the *IME1* promoter can be performed using antibodies that are specific to acetylated lysines on H3 or H4 histone proteins. For example, histone acetylation can be measured at H4K12 at *rpd3*Δ cells and H3K18 in *hda1*Δ cells since hyperacetylation of these lysines are well correlated with increased expression in *tup1*Δ cells (Robyr et al., 2002). Finally, I observed a marginal drop in *IME1* transcript level in *rpd3*Δ, *rpd3*Δ*hos1*Δ, and *rpd3*Δ*hos2*Δ cells (Figure 20) suggesting that these HDACs may also play activator roles in *IME1* transcription. Previous study reported that Rpd3 associates with osmotic stress-responsive genes to activate gene expression upon osmotic stress (De Nadal et al., 2004). Loss of Rpd3, Hos1, and Hos2 were also found to reduce or delay transcriptional activation of multiple genes including *PHO5*, *GAL1*, and *MFA2* (Rundlett et al., 1996, Wang et al., 2002, Watson et al., 2000). Future experiments can further address whether HDACs are required for *IME1* activation under sporulating conditions.

(A)

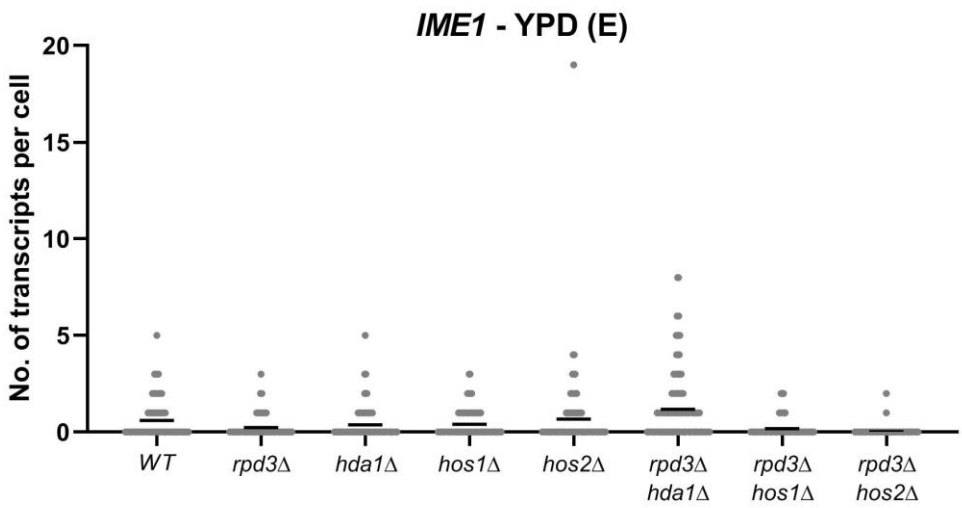

(B)

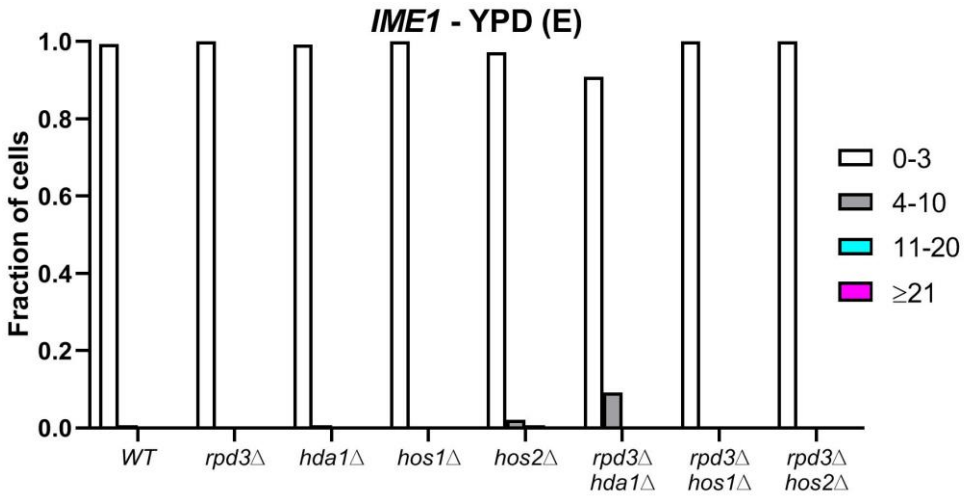

Figure 20. Rpd3 and Hda1 partially contribute to *IME1* repression in nutrient-rich condition.

(A) Scatter dot plot representing number of *IME1* transcripts detected per cell during exponential growth phase in nutrient-rich YPD medium (YPD (E)). Wild-type cells (FW3456) and cells bearing different HDAC deletions were examined. The tested HDAC deletions include: *rpd3*Δ (FW8102), *hda1*Δ (FW8426), *hos1*Δ (FW8430), *hos2*Δ (FW8103), *rpd3*Δ*hda1*Δ (FW8457), *rpd3*Δ*hos1*Δ (FW8428), and *rpd3*Δ*hos2*Δ (FW8171). At least 100 cells that were positive for *ACT1* were assessed in each population. The black line denotes the mean number of *IME1* transcripts per cell in the population.

(B) Histogram representing the data in (A) that were binned into intervals by the number of *IME1* transcripts in cells. Data were binned into four intervals corresponding to 0-3, 4-10, 11-20, and 21 or more *IME1* transcripts per cell. Each bar represents the fraction of the cell population falling into that division.

3.5 Chapter summary

In this chapter, I explored how the Tup1-Cyc8 repressor complex regulates *IME1* repression in nutrient-rich condition. Firstly, I showed that Tup1 and Cyc8 co-localise at the *IME1* promoter, likely as a complex to repress *IME1* promoter activity in the presence of rich nutrients (YPD). Cyc8 binds to the *IME1* promoter at approximately 1000 bp upstream of the start codon, where Tup1 also binds. Depletion of either Tup1 or Cyc8 significantly de-represses *IME1* transcription, suggesting that Tup1 and Cyc8 are both sufficient to silent *IME1* expression in nutrient-rich condition. Furthermore, recruitment of Tup1 and Cyc8 to the *IME1* promoter is nutrient-sensitive. Tup1 and Cyc8 bind to the promoter when nutrients are present, and dissociate during starvation (Figure 21). Notably, my data indicate that the occupancies of Tup1 and Cyc8 at the *IME1* promoter are differentially regulated by nutrients. My ChIP data indicate that Tup1 is strongly bound at the promoter during exponential and saturated growth phases and prior to entry into meiosis. In contrast, Cyc8 is strongly bound in exponentially growing cells and its binding reduces during the transition from exponential to saturated growth phase (Figure 21). I further found that Tup1 expression is not affected by nutrient starvation, while Cyc8 expression decreases which may partially disrupt its interaction with the *IME1* promoter. Nevertheless, Tup1 and Cyc8 are both expressed in the nucleus during meiotic entry, thus protein degradation or cellular re-localisation are not the primary mechanisms that prevent Tup1-Cyc8 from binding the *IME1* promoter during starvation. It is possible that nutrient starvation induces conformational changes in the local chromatin architecture at the *IME1* promoter and thereby prevents the Tup1-Cyc8 complex from binding. Alternatively, Tup1 and/or Cyc8 proteins may undergo post-translational modifications that render the proteins unable to interact with the *IME1* promoter under sporulation-inducing conditions.

How does Tup1-Cyc8 repress *IME1* expression when it is bound to the promoter in the presence of rich nutrients? I found that Tup1 depletion leads to rapid induction of *IME1*, suggesting that the *IME1* promoter is poised for activation. In support of this theory, I found that the *IME1* activator Pog1 already associates with the *IME1* promoter even under nutrient-rich condition. In addition, two putative *IME1* activators, Fkh1 and Fkh2 also bind to the *IME1* promoter during exponential growth

but whether they play regulatory roles in *IME1* transcription remains to be determined. Finally, I tested whether Tup1-Cyc8 represses the *IME1* promoter via HDACs. I found that HDACs Rpd3 and Hda1 play a very minor role in repressing the *IME1* promoter. Taken together, Tup1-Cyc8 is the key repressor of *IME1* transcription in nutrient-rich condition (Figure 21).

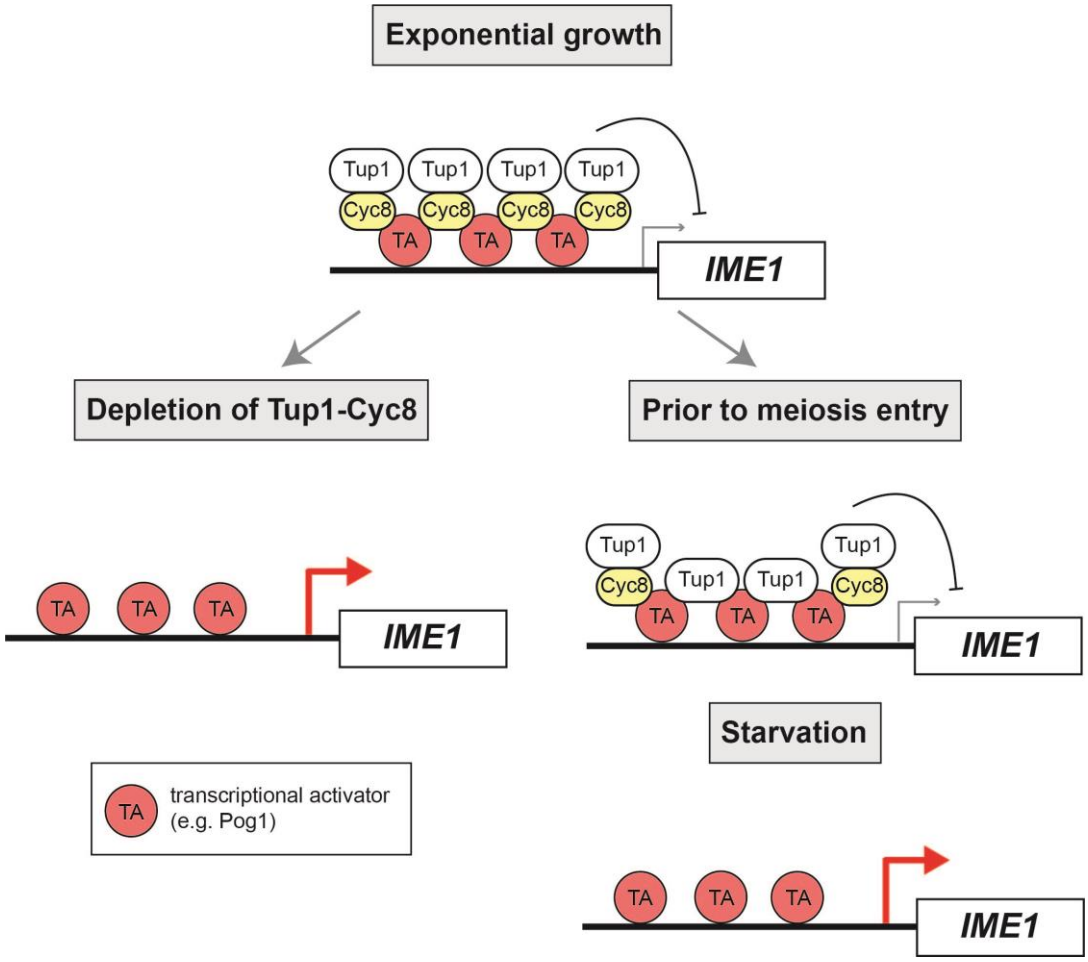

Figure 21. Tup1-Cyc8 inhibits *IME1* activation in the presence of rich nutrients. Schematic diagram depicting how Tup1-Cyc8 represses *IME1* in the presence of rich nutrients. Transcriptional activators are bound to the *IME1* promoter in nutrient-rich condition, suggesting that the promoter is poised for activation when it is repressed. Tup1-Cyc8 binds to the *IME1* promoter and inhibits the transcriptional activators, and thereby represses *IME1*. Depletion of Tup1 removes inhibition of the transcriptional activators, thus *IME1* is transcribed immediately when Tup1 is depleted (left). As cells enter saturated growth phase, the protein abundance of Cyc8 decreases. Cyc8 binding at the *IME1* promoter also reduces, while Tup1 remains strongly bound until prior to entry into meiosis (right, top panel). When the growth medium is deprived of nutrients, both Tup1 and Cyc8 are lost at the *IME1* promoter. Promoter-bound transcriptional activators are no longer inhibited, and thus can activate *IME1* transcription and induce entry into meiosis (right, bottom panel). Please note that the *IME1* promoter depicted in the diagram is not drawn to scale and only represents the region where Tup1-Cyc8 interacts, i.e. 750 to 1400 bp upstream of the start codon.

Chapter 4. A diverse group of nutrient-sensitive transcription factors co-localise with Tup1-Cyc8 at the *IME1* promoter

In the previous chapter, I demonstrated that the Tup1-Cyc8 complex is recruited to the *IME1* promoter in the presence of nutrients, which is crucial for repressing *IME1* expression. When nutrients become depleted, Tup1-Cyc8 leaves the *IME1* promoter and *IME1* level rapidly increases to induce entry into meiosis. Importantly, Tup1-Cyc8 relies on sequence-specific DNA-binding transcription factors to interact with its target promoters (see Introduction: section 1.12 – Tup1-Cyc8 associates with promoter-bound transcription factors). The particular transcription factors that recruit Tup1-Cyc8 to its different targets are specific to the pathways that regulate the targets (reviewed in Smith and Johnson, 2000). For example, glucose-repressible genes are repressed by Tup1-Cyc8 via interactions with the Cys2His2 zinc finger transcription factor Mig1. Conversely, Tup1-Cyc8 repression of **a**-specific genes in cells with *MATα* mating type is facilitated by homeodomain and MADS-box proteins α2 and Mcm1. How Tup1-Cyc8 is recruited to the *IME1* promoter is unknown. Identifying the transcription factors that mediate Tup1-Cyc8 association may reveal the mechanism that underpins how nutrient signals are integrated at the *IME1* promoter. For this reason, I set out to find the transcription factors which bind to the *IME1* promoter and have the potential to interact with Tup1-Cyc8.

The *IME1* promoter is decorated with many transcription factor binding sites (Kahana et al., 2010). As shown by ChIP data, Tup1-Cyc8 binding is centred at around 1000 bp upstream of the *IME1* start codon (Chapter 3: Figure 13) (Weidberg et al., 2016). In order to identify the transcription factors that potentially interact with Tup1-Cyc8 at the *IME1* promoter, I searched for transcription factors that were described to interact with Tup1 or Cyc8 in the literature. Furthermore, I asked whether their consensus binding sites were predicted near the Tup1-Cyc8 binding site in the *IME1* promoter. Using the curated transcription factor binding motifs in the Yeast Transcription Factor Specificity Compendium (YeTFaSCo) database (de Boer and Hughes, 2012), I scrutinised the *IME1* promoter from 700 to 1100 bp upstream of the start codon for binding motifs of the Tup1 or Cyc8 interacting transcription

factors. By doing so, I shortlisted 16 candidate transcription factors that were shown or implicated to interact with Tup1-Cyc8, and have consensus binding motifs between 700 and 1100 bp upstream of the *IME1* start codon where Tup1-Cyc8 binds. I have summarised the functions of these transcription factors, their primary DNA-binding motifs, putative binding sites in the *IME1* promoter, and whether these transcription factors interact with Tup1 or Cyc8 in Table 2. The binding sites of these transcription factors were mainly predicted using the scanning algorithm provided by the YeTFaSCo database, with at least 70% of the maximum possible score (de Boer and Hughes, 2012). Representation of the predicted transcription factor binding motifs in the *IME1* promoter can be found in Supplementary figure 13. The shortlisted transcription factors play roles in various pathways in yeast, and most of them are regulators of stress-responsive genes and glucose-repressible genes.

Among the 16 candidate transcription factors, Sok2 was considered a strong candidate as it was shown to negatively regulate a portion of the *IME1* upstream region (Shenhar and Kassir, 2001). Moreover, the expression of Sok2 is downregulated prior to entry into meiosis (Shenhar and Kassir, 2001). Yet, a link between Sok2 and Tup1-Cyc8 in regulating the *IME1* promoter had not be drawn. Thus, I aimed to determine whether Sok2 exerts its repressor function via Tup1-Cyc8. It is also worth noting that Sok2 plays an activating role in regulating *Ashbya gossypii* sporulation (a fungal species related to budding yeast) (Wasserstrom et al., 2017), suggesting that Sok2 is an important regulator of yeast sporulation that has diversified its function throughout evolution. In my list, I also included three transcription factors that were not described to interact with Tup1 or Cyc8, or do not have clear binding sites predicted in the *IME1* promoter. The first one is Nrg2, a transcriptional repressor that is involved in glucose repression (Berkey et al., 2004). Nrg2 is a paralogue of Nrg1, which physically interacts with Tup1-Cyc8 and also mediates glucose repression. Furthermore, the binding sites of Nrg1 and Nrg2 indicate that they target opposite strands of the same sites (Table 2). Therefore, although Nrg2 has not been demonstrated to directly interact with Tup1 or Cyc8, it is generally accepted that Nrg1 and Nrg2 function closely with each other and interact with the Tup1-Cyc8 complex. The second one is Smp1, a MADS-box transcription factor that was reported to interact with the *IME1* promoter close to where Tup1-Cyc8 binds in a recent study (Zhao et al., 2018). The authors demonstrated that Smp1

binds to the *IME1* promoter during vegetative growth and dissociates from the promoter when meiosis is induced (Zhao et al., 2018). In respiration-deficient cells that do not contain Rim101 or Ndi1, Smp1 was found to bind the *IME1* promoter and repress *IME1* expression (Zhao et al., 2018) (see Introduction: section 1.10). Notably, deletion of Tup1 partially relieves *IME1* from repression in *ndi1*Δ cells, suggesting that Smp1 and Tup1 might function to repress *IME1* in the same pathway (Zhao et al., 2018). To examine this possibility, I included Smp1 in my analysis despite no clear consensus binding motif and no interaction with Tup1 or Cyc8 previously described. Gts1, a transcription factor that recognises AT hook motifs and physically interacts with Cyc8, was reported to delay entry into meiosis in budding yeast when overexpressed (Yaguchi et al., 1996). Thus, I also considered Gts1 as a potential interactor of Tup1-Cyc8 at the *IME1* promoter even though its binding site was not predicted between 700 and 1100 bp upstream of the *IME1* start codon.

TF	Primary function	Consensus motif(s)	Position (bp upstream)	Interaction (P: Physical G: Genetic)	Reference(s)
Cin5 (Yap6)	Regulates pleiotropic drug resistance and salt tolerance	**bZIP** TTAC(A/G)TAA	837-844	Tup1 (P) Cyc8 (P)	(Hanlon et al., 2011)
Cup9	Represses peptide transport	**Homeodomain** ATGTGTCA	882-889, 1006-1013	Cyc8 (P)	(Xia et al., 2008)
Gts1	Regulates processes including heat tolerance, endocytosis, apoptosis, and flocculation	**AT hook** TACCAA	None	Cyc8 (P)	(Sanada et al., 2011)
Mig1	Main repressor of glucose-repressible genes	**C2H2 ZF** CCCC(G/A)C	701-710, 728-734	Tup1 (G) Cyc8 (P, G)	(Shankar et al., 1996) (Treitel and Carlson, 1995) (Papamichos-Chronakis et al., 2004) (Lin et al., 2014)
Mot3	Regulates osmotic stress-inducible genes, repressor of hypoxic genes	**C2H2 ZF** AGG(A/C)A	719-724, 766-771, 771-776, 888-893, 920-925, 965-970, 969-975, 1005-1010, 1028-1033, 1067-1072 AGAAA(A/C): 709-715, 948-954, 1016-1022 TATGTAAT: 838-845	Cyc8 (G)	(Mennella et al., 2003)
Nrg1 (Nrg2)	Repressor of glucose-repressible genes	**C2H2 ZF** GGACCCT TGTGCCT	865-868, 1006-1012, 1042-1048 CCCTC: 772-777	Tup1 (P) Cyc8 (P)	(Hanlon et al., 2011) (Park et al., 1999)
Nrg2 (Nrg1)	Repressor of glucose-repressible genes	**C2H2 ZF** AGGGTCC	773-776, 865-868, 1044-1048	Nrg1 (G)	(Kuchin et al., 2002) (Snoek et al., 2010) (Serra-Cardona et al., 2014)
Phd1 (Sok2)	Activator of pseudohyphal growth	**Helix-loop-helix** (A/C)TGCA AGGCAC	875-884, 922-931, 997-1002, 1006-1011 GCNGCNGG: 793-800	Tup1 (P) Cyc8 (P)	(Hanlon et al., 2011)
Rgt1	Regulates glucose transporter genes	**Zinc cluster** CGGAAAAA	666-672 GGAGGG: 1103-1108	Cyc8 (P)	(Tomás-Cobos and Sanz, 2002) (Polish et al., 2005) (Roy et al., 2013)
Sfl1	Represses flocculation genes and activates stress-induced genes	**HSF** GAAGCTTC	CAATCTTG: 743-750 GAAGTGTC: 883-890	Cyc8 (P)	(Conlan and Tzamarias, 2001)

TF	Primary function	Consensus motif(s)	Position (bp upstream)	Interaction (P: Physical G: Genetic)	Reference(s)
Skn7	Regulates oxidative stress-inducible genes and required for osmoregulation	**HSF** GGC(C/T)GGC	792-797	Tup1 (P) Cyc8 (P)	(Hanlon et al., 2011)
Sko1	Regulates osmotic and oxidative stress-inducible genes	**bZIP (ATF/CREB)** ATGACGTA	ATGACG: 1060-1065	Tup1 (P) Cyc8 (P)	(Pascual-Ahuir et al., 2001) (Proft et al., 2001) (Hanlon et al., 2011)
Smp1	Regulates osmotic stress response	**MADS-box** no clear consensus	ACCCCCAGCC: 702-711	Tup1 (G)	(Zhao et al., 2018)
Sok2 (Phd1)	Repressor of pseudohyphal differentiation	**Helix-loop-helix** CCTGCA AGGCA(C/A)	795-802, 870-877, 875-885, 925-932, 970-977, 1003-1014, 1029-1036	Tup1 (G) Cyc8 (G)	(Boorsma et al., 2008)
Sut1	Activates sterol uptake genes in anaerobic conditions and regulates hypoxic genes	**Zn(II)2Cys6** CGC(G/C)GGG	730-736	Cyc8 (P)	(Régnacq et al., 2001) (Hanlon et al., 2011)
Yap6 (Cin5)	Regulates salt tolerance and carbohydrate metabolism	**bZIP** TTA(T/C)GTAA	837-844 TGTGCCT: 1006-1012	Tup1 (P) Cyc8 (P)	(Hanlon et al., 2011)

Table 2. Candidate transcription factors that interact with Tup1-Cyc8 and their DNA binding motifs between 700 and 1100 bp upstream of the *IME1* start codon.
Candidate transcription factors shortlisted as putative Tup1-Cyc8 interactors. Paralogues of the transcription factors that were also included as candidates are noted in parentheses. The primary cellular functions of the transcription factors were summarised from the *Saccharomyces* Genome Database (Cherry et al., 2012). The main consensus binding motifs of the transcription factors were acquired from the YeTFaSCo database (de Boer and Hughes, 2012). The predicted consensus binding motifs in the *IME1* upstream region between 700 and 1100 bp upstream of the start codon are presented. Other matched sites that are different from the consensus binding motif are also indicated. The transcription factor binding sites were predicted using the scanning function in the YeTFaSCo database (de Boer and Hughes, 2012) (black), reported in previous *IME1* promoter study (Kahana et al., 2010) (blue), or labelled manually by scrutinising the *IME1* upstream region of interest (magenta). Binding sites predicted by

YeTFaSCo have at least 70% of the maximum possible score. Two Rgt1 sites were predicted immediately next to the region of interest and these are indicated in the table. Most of the shortlisted transcription factors interact with Tup1/Cyc8 as indicated in the *Saccharomyces* Genome Database (Cherry et al., 2012), except for Nrg2, paralogue of Nrg1. The genetic interactions of Mot3, Smp1, and Sok2 with Tup1/Cyc8 have been implicated in the literature (Mennella et al., 2003, Zhao et al., 2018, Boorsma et al., 2008). TF = transcription factor.

4.1 Nine candidate transcription factors co-localise with Tup1-Cyc8 at the *IME1* promoter

The binding sites predicted in the *IME1* promoter for the candidate transcription factors were based on matching promoter sequences to known binding motifs. To test whether the candidate transcription factors physically interact with the *IME1* promoter, I tagged each transcription factor with three copies of the V5 epitope by endogenously fusing the DNA sequence encoding the V5 epitopes to the 3' ends of the genes encoding the transcription factors. I performed ChIP-qPCR to determine whether each transcription factor is associated with the *IME1* promoter in nutrient-rich condition. Previous work and my work have demonstrated that Tup1 and Cyc8 bind to the *IME1* promoter in the region between 750 and 1400 bp upstream of the start codon. The strongest enrichment was detected at approximately 1000 bp upstream of the *IME1* start codon (Chapter 3: Figure 13) (Weidberg et al., 2016). I hypothesised that the transcription factors contributing to Tup1-Cyc8 recruitment should also be detected at the *IME1* promoter where Tup1-Cyc8 binds, i.e. around 1000 bp upstream of the start codon. Therefore, in this experiment, I examined whether the transcription factors associate with the region that is 1000 bp upstream of the *IME1* start codon to determine whether they may contribute to Tup1-Cyc8 recruitment. Since Tup1 and Cyc8 display strong interactions with the *IME1* promoter during exponential growth (YPD (E)) when nutrients are rich (Figure 14), I studied whether the shortlisted transcription factors interact with the *IME1* promoter in exponentially growing cells (Figure 22).

Among the 16 shortlisted transcription factors described in Table 2, I discovered that nine transcription factors displayed enrichment above background (untagged wild-type cells) at the *IME1* promoter. Furthermore, five candidates with clear binding motifs displayed no enrichment. I found that some of the bound transcription factors exhibited higher fold enrichment at the *IME1* promoter than the others in exponentially growing cells, which could be due to higher binding affinity or presence of more copies of the transcription factor. Cup9, a transcription factor involved in repressing peptide transport, showed almost 25 times over background enrichment at the *IME1* promoter, which was the highest among all the tested candidates (Figure 22). Three transcription factors Yap6, Sok2, and Phd1 were

enriched with at least 10 fold. Interestingly, Cin5, the Yap6 paralogue was not enriched despite that the two proteins share many common targets (Ni et al., 2009). Sut1, Mot3, Sko1, Nrg1, and Nrg2 displayed three to six fold enrichment (Figure 22). Although Nrg2 showed only three fold enrichment, I still considered Nrg2 as a candidate of interest because of its role in repressing glucose-repressible genes together with its paralogue, Nrg1. Finally, Gts1, Smp1, Skn7, Cin5, Sfl1, Mig1, and Rgt1 displayed less than three fold enrichment at the *IME1* promoter and their ChIP signals were close to background levels detected in untagged cells (1.23 fold). Thus, I regarded these seven transcription factors as not binding to the *IME1* promoter, and they were excluded from further analyses. It should also be noted that ChIP is a technique that consists a series of experimental procedure. ChIP sensitivity highly relies on the efficiencies of a number of steps, including formaldehyde crosslinking of protein-DNA complexes, cell lysis, chromatin shearing, immunoprecipitation, sample washes, and reverse crosslinking. Thus, weak transcription factor binding may have been reported as false negatives in this experiment (Figure 22). Taken together, Tup1-Cyc8 co-localises with at least nine transcription factors that were shown or implicated to interact with the complex at the *IME1* promoter in nutrient-rich condition.

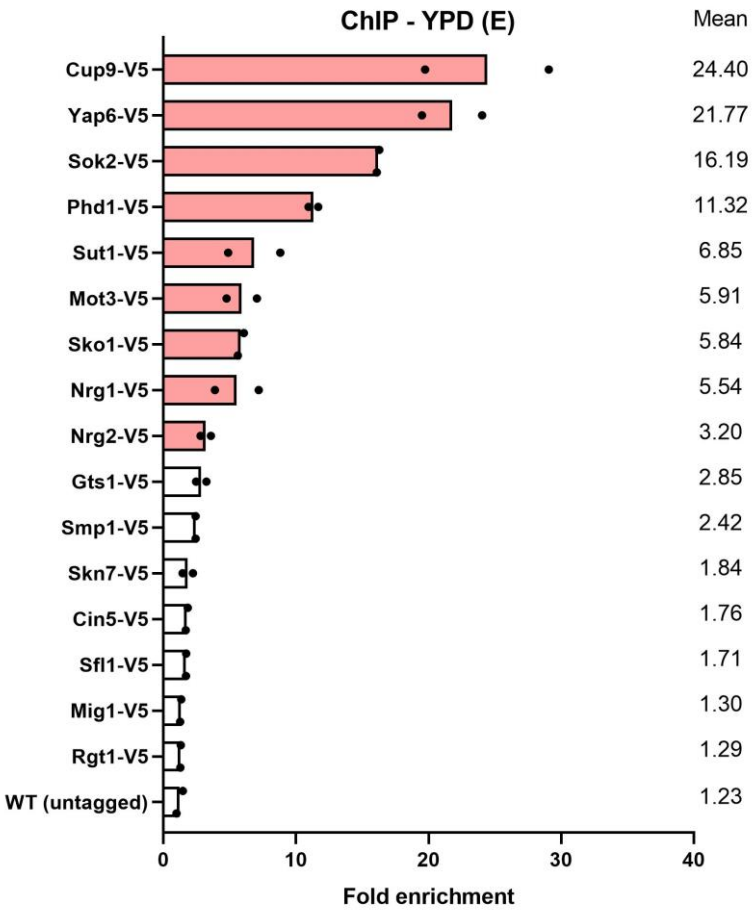

Figure 22. Nine candidate transcription factors interact with the *IME1* promoter where Tup1 and Cyc8 preferentially bind during nutrient-rich exponential phase. ChIP-qPCR of candidate transcription factors bearing three copies of V5 epitope in exponential growth phase (YPD (E)). The assessed transcription factors include Cup9-V5 (FW6976), Yap6-V5 (FW3833), Sok2-V5 (FW5638), Phd1-V5 (FW4466), Sut1-V5 (FW6974), Mot3-V5 (FW4383), Sko1-V5 (FW4389), Nrg1-V5 (FW4393), Nrg2-V5 (FW4396), Gts1-V5 (FW6377), Smp1-V5 (FW7068), Skn7-V5 (FW4399), Cin5-V5 (FW7072), Sfl1-V5 (FW7070), Mig1-V5 (FW4665), Rgt1-V5 (FW4386), and the untagged wild-type strain (FW1511) as negative control. ChIP signals were normalised over the silent mating type cassette *HMR*. Bars represent mean normalised ChIP signals (also indicated for each transcription factor in the figure) and dots represent individual biological replicates. The transcription factors are ordered by the strongest to weakest association with the *IME1* promoter. Bars shaded in light red indicate the nine binders of the *IME1* promoter (cutoff = three fold enrichment over *HMR*) that were taken on for further analyses in this thesis.

In addition, I asked the question whether the transcription factors that displayed binding at the *IME1* promoter would primarily interact with 1000 bp upstream of the start codon similar to Tup1/Cyc8, or if they are also enriched in another region. If binding of the transcription factor peaks near -1000 bp rather than throughout the entire *IME1* promoter, the transcription factor is more likely to associate with the *IME1* promoter to recruit the Tup1-Cyc8 complex. To study this question, I performed ChIP on a subset of transcription factors and measured their binding to various parts of the *IME1* promoter using different primer pairs in qPCR (described in Chapter 3: Figure 13). Binding of the examined transcription factors throughout the *IME1* upstream region in exponentially growing cells is presented in Figure 23. The stronger binders Yap6, Sok2, and Phd1 showed interaction with the *IME1* promoter from 750 to 1700 bp upstream of the start codon, and their binding was the highest at 1000 bp upstream (Figure 23A). Among the three transcription factors, Yap6 associates with the broadest region as it was also detected at 400 bp upstream and possibly closer to the *IME1* start codon. Binding of the weaker binders Sut1, Mot3, Sko1, Nrg1, and Nrg2 spanned from 750 to 1700 bp upstream of the *IME1* start codon, where highest binding was detected at 750 and 1000 bp upstream of *IME1* (Figure 23B). In conclusion, the interactions of the examined candidate transcription factors with the *IME1* promoter are highly localised to the region between 750 and 1000 bp upstream of the start codon. Thus, these candidate transcription factors may be involved in recruiting Tup1-Cyc8 to the *IME1* promoter.

(A)

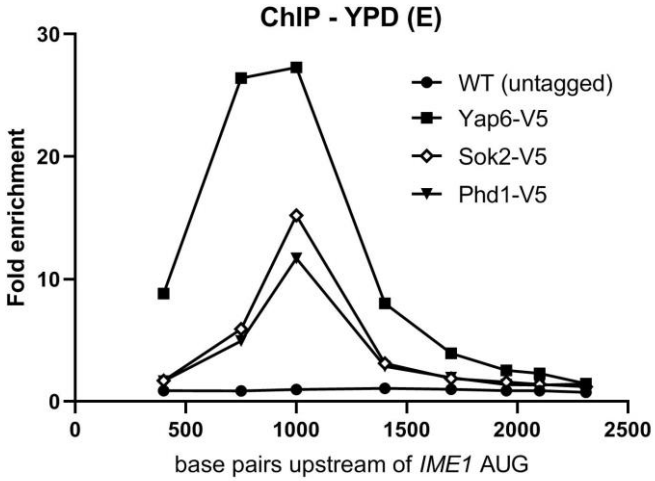

(B)

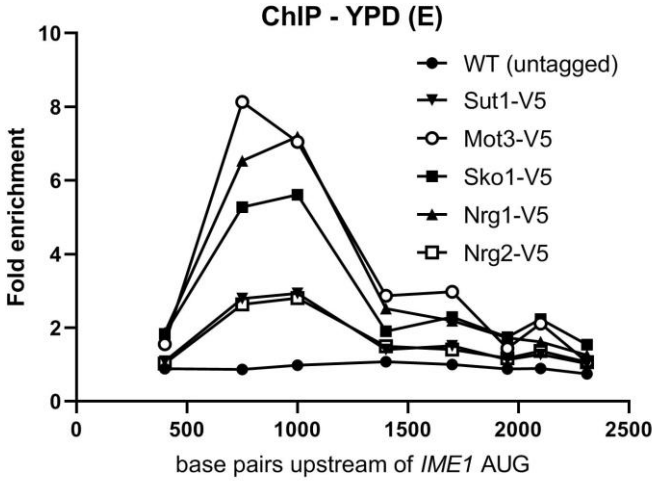

Figure 23. Candidate transcription factors display binding patterns similar to that of Tup1 and Cyc8 at the *IME1* promoter.

ChIP-qPCR of V5 epitope-tagged candidate transcription factors to scan for binding across the *IME1* promoter. Binding was detected in cells grown to exponential growth phase (YPD (E)). The subset of transcription factors examined in this experiment include (A) the strong binders Yap6-V5 (FW3833), Sok2-V5 (FW5638), and Phd1-V5 (FW4466); and (B) the weak binders Sut1-V5 (FW6974), Mot3-V5 (FW4383), Sko1-V5 (FW4389), Nrg1-V5 (FW4393), and Nrg2-V5 (FW4396). The untagged wild-type strain (FW1511) was included as negative binding control. Primer pairs that amplify 400, 750, 1000, 1400, 1700, 1950, 2100, and 2310 bp upstream of the *IME1* start codon were used for qPCR. ChIP signals were normalised over the silent mating type cassette *HMR*.

So far, my ChIP data demonstrate that Tup1-Cyc8 co-localises with the transcription factors at the *IME1* promoter. In the ChIP procedure, formaldehyde crosslinking mainly captures protein-chromatin complexes, but proteins indirectly bound to the *IME1* promoter via protein-protein interactions may also be detected. Given that the candidate transcription factors that showed enrichment were shortlisted due to their interactions with Tup1-Cyc8 (Table 2), I speculated that some transcription factors may be interacting with the Tup1-Cyc8 complex that is bound to the *IME1* promoter (Figure 24A, bottom) rather than associating with the *IME1* promoter themselves (Figure 24A, top). I hypothesised that most transcription factors are directly bound to the *IME1* promoter rather than associating with Tup1-Cyc8 since the candidate transcription factors have clear binding sites predicted in the *IME1* promoter (Table 2). To distinguish between the two possibilities, I set out to determine whether the binding of the transcription factors relies on the presence of Tup1 at the *IME1* promoter.

Using the auxin-based degron system, I depleted Tup1 fused with the auxin-induced degron (AID) in nutrient-rich condition and measured the binding of V5 epitope-tagged transcription factors to the *IME1* promoter. I first examined the protein levels of Tup1-AID and V5 epitope-tagged transcription factors by western blotting. Given that the AID tag also contained the V5 epitope, all proteins were detected using an antibody targeting V5. Tup1-AID protein was completely depleted four hours after the addition of auxin 3-IAA, but not in control cells treated with DMSO. (Figure 24B). It is worth noting that a second protein band of approximately 100 kilodaltons (kDa) was also detected in the *TUP1-AID* cells which was not degraded when auxin was added (Figure 24B, Chapter 3: Figure 17A). This band might represent a truncated Tup1 protein. Importantly, when 3-IAA was added, Tup1 binding was not detected at the *IME1* promoter, illustrating that the truncated Tup1 protein had no ability to bind to the *IME1* promoter (Figure 24C). Therefore, the lower size band detected in *TUP1-AID* cells was non-specific. The western blot data also indicate that Yap6, Sok2, Phd1, Mot3, Nrg1, Nrg2, and Sko1 are expressed with or without auxin treatment, suggesting that auxin does not have an apparent effect on the protein expression of these transcription factors (Figure 24B). Next, I inspected the binding of Tup1-AID and the V5 epitope-tagged transcription factors to the *IME1* promoter. Due to the overlapped use of V5 epitope tags on Tup1-AID and the transcription

factors, it was not possible to distinguish between the binding of Tup1 and the transcription factors to the *IME1* upstream region by ChIP-qPCR. Therefore, I determined the level of Tup1 binding in cells containing only the Tup1-AID fusion protein (*TUP1-AID* in Figure 24C), and used this as a proxy for Tup1 binding in all the other strains. My ChIP results indicate that Yap6, Sok2, and Phd1 remained strongly associated with the *IME1* promoter when Tup1 was depleted, and the levels were comparable to cells that were treated with DMSO (Figure 24C). Although experimental variation was observed between biological replicates, the same results were obtained in each individual experiment. Therefore, I conclude that Yap6, Sok2, and Phd1 can stably bind to the *IME1* promoter without Tup1 and are likely to be associating with DNA directly. Similarly, the binding levels of the weaker binders Mot3, Nrg1, and Nrg2 were unaffected by the degradation of Tup1 (Figure 24C). Strikingly, the binding of Sko1 was no longer detected at the *IME1* promoter when Tup1 was depleted, suggesting that the binding of Sko1 to the *IME1* promoter depends on the presence of Tup1 (Figure 24C). Thus, Sko1 binding at the *IME1* promoter may not be sequence-specific and thus may not contribute to Tup1-Cyc8 recruitment. To summarise, all candidate transcription factors, except Sko1, associate with the *IME1* promoter independent of Tup1 binding.

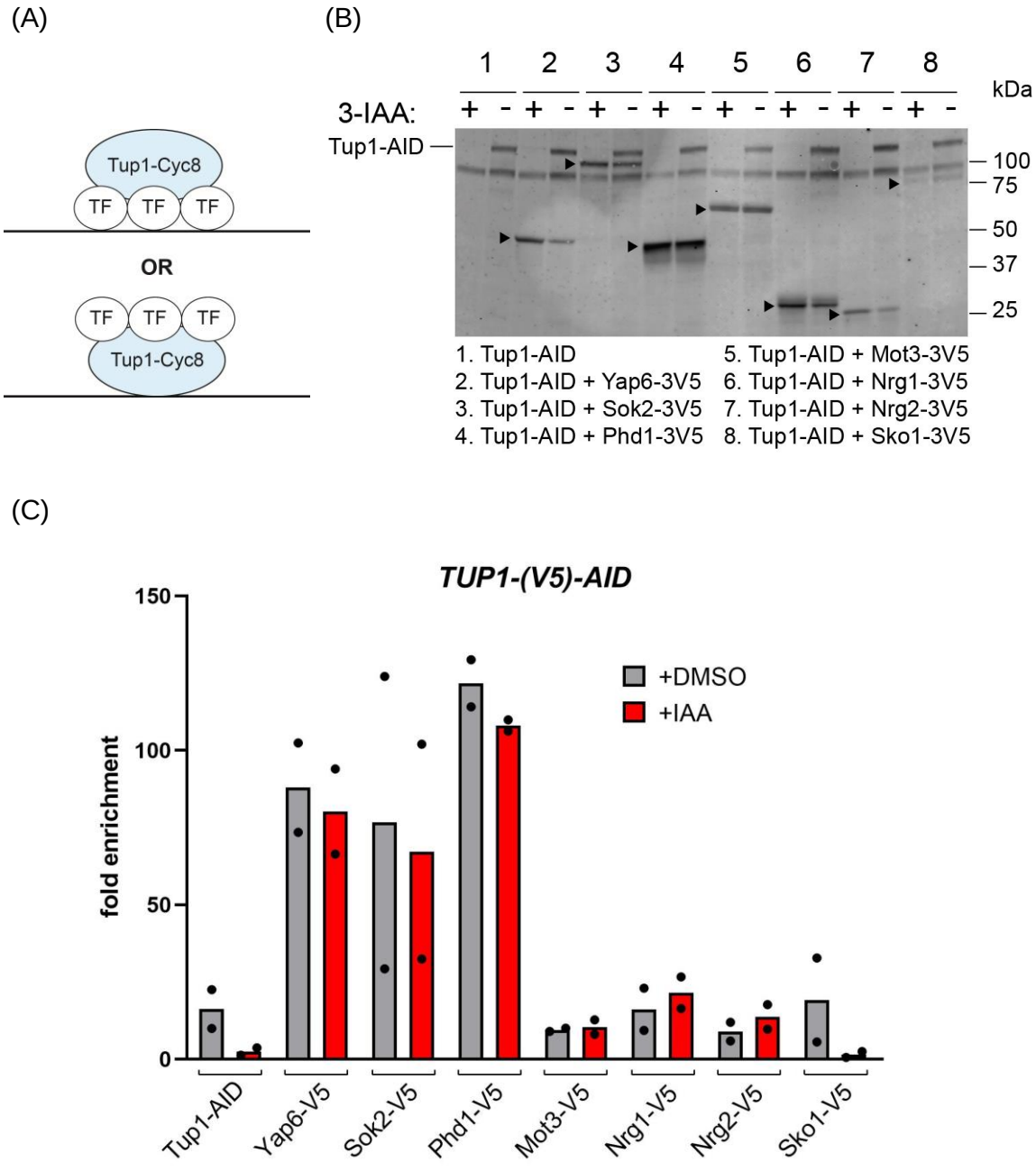

Figure 24. Sko1 requires the presence of Tup1 to bind to the *IME1* promoter.

(A) Schematic diagram depicting different models of interaction between Tup1-Cyc8 and candidate transcription factors near 1000 bp upstream of *IME1*. Candidate transcription factors may bind to DNA directly and associate with Tup1-Cyc8 (top), or interact with Tup1-Cyc8 attached at the promoter without interacting with DNA (bottom). TF = transcription factor.

(B) Representative western blot showing the response of Tup1-AID (FW5057) and Tup1-AID in cells carrying V5 epitope-tagged Yap6 (FW4214), Sok2 (FW4218), Phd1 (FW5056), Mot3 (FW4229), Nrg1 (FW4230), Nrg2 (FW5055), and Sko1

(FW4224) to 3-IAA and DMSO in nutrient-rich YPD medium. The band representing Tup1-AID is labelled in the figure and the black arrows indicate the V5 epitope-tagged transcription factors detected. The proteins detected in each strain are listed below the figure. Uncropped western blot can be found in Supplementary figure 7.

(C) ChIP-qPCR of Tup1-AID and the V5 epitope-tagged transcription factors in the presence of Tup1-AID using a primer pair that flanks 1000 bp upstream of the *IME1* codon. Cells were grown to exponential stage in nutrient-rich YPD medium and treated with 3-IAA and DMSO respectively. ChIP signals were normalised over the silent mating type cassette *HMR*. Since Tup1-AID and the transcription factors were tagged with V5 epitope, the Tup1-AID fold enrichment was subtracted in strains carrying both Tup1-AID and V5 epitope-tagged transcription factor to determine the enrichment of the transcription factor at the *IME1* promoter. Bars represent mean normalised ChIP signals of Tup1-AID or the transcription factors and dots indicate individual biological replicates.

4.2 Binding of the transcription factors to the *IME1* promoter is sensitive to nutrients in the growth medium

In Chapter 3: Figure 14, I demonstrated that the binding of Tup1 and Cyc8 to the upstream region of *IME1* responds to nutrient availability in the growth medium. My data suggest that Tup1-Cyc8 associates with the *IME1* promoter in the nutrient-rich exponential growth phase, and leaves the promoter in nutrient-poor sporulation medium. Since Tup1-Cyc8 does not re-localise to other cell compartments under sporulation conditions (Chapter 3: Figure 16), I reasoned that the eviction of Tup1-Cyc8 may be caused by local changes at the *IME1* promoter such as disassembly of the transcription factors which recruit Tup1-Cyc8. To test this hypothesis, I examined the interactions between the candidate transcription factors and the *IME1* promoter in exponential growth phase, before and during entry into meiosis. If my hypothesis was true, the candidate transcription factors should co-localise with Tup1-Cyc8 in exponentially growing cells, and detach from the *IME1* promoter during entry into meiosis.

Cells are exposed to different nutrient environments during exponential growth phase (YPD (E)), prior to (SPO 0h) and during (SPO 4h) entry into meiosis. During exponential growth, rich nutrients including glucose and nitrogen compounds are supplied to cells in the YPD medium. Cells are grown to saturation and transferred to a pre-sporulation medium (BYTA), which provides acetate as a carbon source to promote respiration. When growth in pre-sporulation medium reaches saturation, cells are transferred to the nutrient-depleted sporulation medium (SPO). SPO induces meiotic entry, which typically occurs at around four hours in SPO. The ChIP results indicate that all nine candidate transcription factors displayed binding to the *IME1* upstream region in exponentially growing cells (YPD (E)) and prior to entry into meiosis (SPO 0h) (Figure 25). I noticed that five transcription factors, Yap6, Sok2, Sut1, Mot3, and Sko1 showed stronger interactions with the *IME1* promoter during exponential growth when glucose is present. In contrast, two transcription factors, Phd1 and Nrg1, displayed stronger binding prior to entry into meiosis when glucose is absent from the growth medium. Furthermore, the binding levels of Cup9 and Nrg2 at the *IME1* promoter during exponential growth and before meiotic entry were similar (Figure 25). These observations imply that the transcription factors may respond

differently to nutrients and perhaps contribute to Tup1-Cyc8 recruitment at the *IME1* promoter under different nutrient conditions (further investigated in Figure 26, Chapter 5: Figure 31, Figure 33, Figure 34, and Figure 36). Remarkably, all nine candidate transcription factors rapidly dissociated from the *IME1* promoter upon induction of meiotic entry (SPO 4h). The sharp decrease in transcription factor binding may be linked to the depletion of nutrients, which further implies that the transcription factors are sensitive to nutrient signals. The binding patterns of the candidate transcription factors resemble that of Tup1 and Cyc8 (Chapter 3: Figure 14), and may explain how Tup1-Cyc8 dissociates from the *IME1* promoter to allow *IME1* expression during meiotic entry. Interestingly, using the same cutoff as in Figure 22, I noticed that Yap6, Phd1, and Nrg1 displayed over three fold enrichment and therefore considered marginally enriched during meiotic entry (Yap6: 3.52 fold, Phd1: 3.53 fold, Nrg1: 3.72 fold) (Figure 25). It is possible that Yap6, Phd1, and Nrg1 have other roles during *IME1* activation.

In summary, nine transcription factors Cup9, Yap6, Sok2, Phd1, Sut1, Mot3, Sko1, Nrg1, and Nrg2 display different levels of binding in different nutrient conditions. The transcription factors associate with the *IME1* promoter strongly in exponentially growing cells and prior to meiotic entry, but dissociate when entry into meiosis is induced. Since the transcription factors were shown or implicated to interact with Tup1-Cyc8, loss of binding may be a means to evict Tup1-Cyc8 during entry into meiosis in SPO. Importantly, the behaviour of these Tup1-Cyc8 interacting transcription factors at the *IME1* promoter is in contrast with that of the *IME1* activator Pog1, which remains to bind the *IME1* promoter during entry into meiosis (Chapter 3: Figure 19A). Taken together, my ChIP data propose a model in which nutrient starvation causes loss of Tup1-Cyc8 recruiting transcription factors at the *IME1* promoter, which leads to the eviction of Tup1-Cyc8 and *IME1* activators remain to induce *IME1* transcription (Figure 29).

Transcription factors that bind more strongly during exponential growth (YPD (E)):

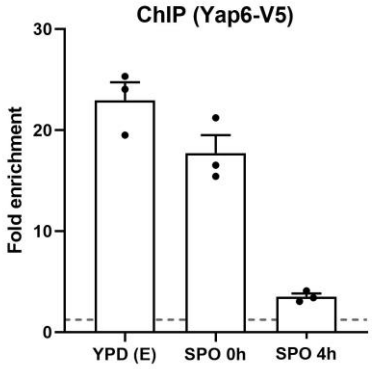

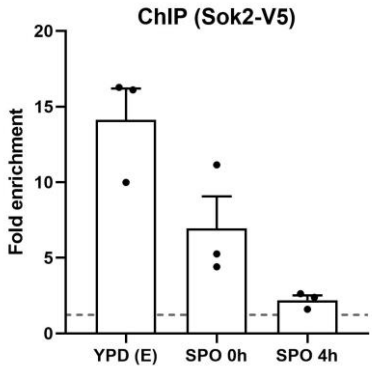

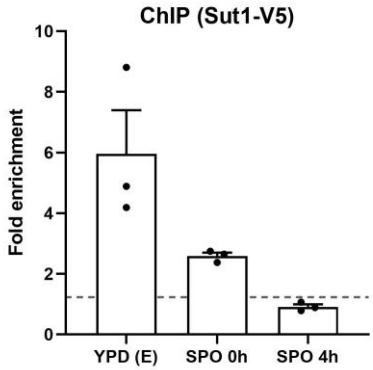

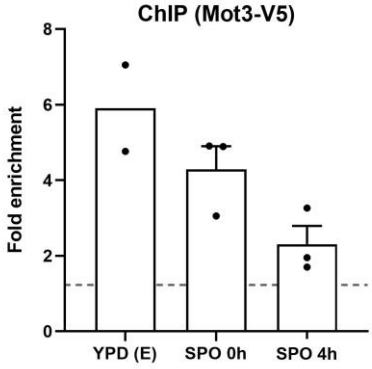

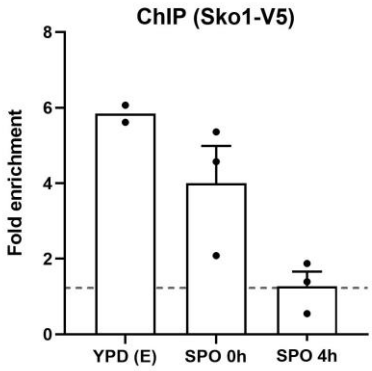

Transcription factors that bind more strongly prior to entry into meiosis (SPO 0h):

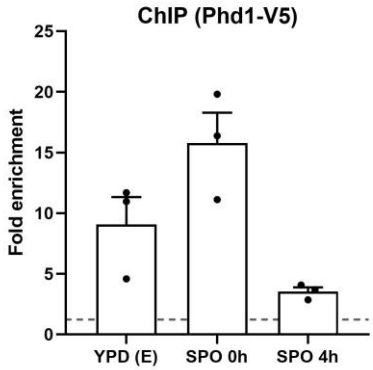

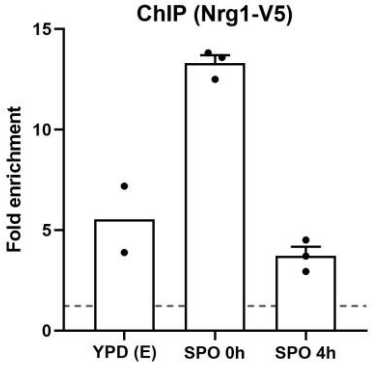

Transcription factors that display similar levels of binding during exponential growth (YPD (E)) and prior to entry into meiosis (SPO 0h):

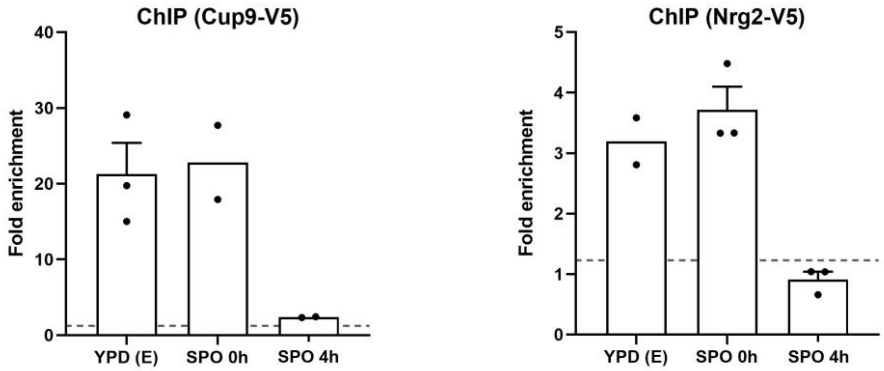

Figure 25. Candidate transcription factors dissociate from the *IME1* promoter during meiotic entry.

ChIP-qPCR of Cup9-V5 (FW6976), Yap6-V5 (FW3833), Sok2-V5 (FW5638), Phd1-V5 (FW4466), Sut1-V5 (FW6974), Mot3-V5 (FW4383), Sko1-V5 (FW4389), Nrg1-V5 (FW4393), and Nrg2-V5 (FW4396) using a primer pair that amplifies the region 1000 bp upstream of the *IME1* start codon. Binding of the transcription factors was measured during exponential growth (YPD (E)), and at 0h (SPO 0h) and 4h (SPO 4h) after sporulation induction. ChIP signals were normalised over the silent mating type cassette *HMR*. Bars represent mean normalised ChIP signals, error bars represent SEM, and dots indicate individual biological replicates. The grey dashed lines denote the fold enrichment detected in the untagged wild-type strain (FW1511) during exponential growth as negative control. The transcription factors are classified into three groups based on their binding patterns at the *IME1* promoter in the exponential growth phase and at 0h after sporulation induction.

Based on the data in Figure 25, the transcription factors interact with the *IME1* promoter in a nutrient-dependent manner. Notably, I noticed that even though all transcription factors displayed binding to the *IME1* promoter during exponential growth (YPD (E)) and prior to meiotic entry (SPO 0h), their binding were regulated differently in the two distinct growth stages. For example, Mot3 bound more strongly in the exponential growth phase than prior to meiotic entry, suggesting that its binding depends on the presence of glucose provided only during exponential growth. Conversely, Nrg1 bound more strongly to the *IME1* promoter prior to meiotic entry, implying that glucose plays less of a role in regulating its interaction with the *IME1* promoter. Therefore, I speculated that the nine transcription factors are differentially regulated by glucose and nitrogen compounds in nutrient-rich medium. To explore this possibility, I designed an experiment to systematically study the response of the transcription factors to distinct nutrient conditions. In the laboratory, yeast cells are typically grown in the nutrient-rich YPD medium supplemented with tryptophan, uracil, and adenine. The standard YPD medium I used for my experiments contained 1% yeast extract, 2% peptone, and 2% glucose, in which the yeast extract and peptone (YP) provided nutrients including the nitrogen source for yeast cells to grow. In contrast, the sporulation (SPO) medium that was used to induce yeast sporulation contained no nitrogen or glucose, thus yeast cells shifted to SPO medium would starve and enter meiosis. To study how transcription factor binding to the *IME1* promoter responds to different nutrients, I set up four defined medium conditions that provided different kinds of nutrients to cells. Firstly, I included the SPO medium that represents the nutrient-poor condition. Additionally, the standard YPD medium containing 2% glucose (Glc) represents the nutrient environment with both YP rich nutrients and glucose provided. To assess the effect of YP rich nutrients and glucose separately, I set up a glucose-only medium by adding 2% glucose to SPO medium (SPO + 2% Glc), and a YP medium that contained only 0.05% glucose (YP + 0.05% Glc).

Tup1 was previously demonstrated to associate with the *IME1* promoter when PKA and TORC1 pathways are active (Weidberg et al., 2016). I examined Tup1 binding in the four conditions outlined above. Yeast cells carrying V5 epitope-tagged Tup1 were grown to saturation in YPD and subsequently in pre-sporulation conditions before shifting to the four different media. Binding of Tup1 to the *IME1*

promoter was inspected when cells were shifted (SPO 0h) and after four hours in SPO, SPO + 2% Glc, YP + 0.05% Glc, and YPD (YP + 2% Glc) (Figure 26A). Tup1 rapidly dissociated from the *IME1* promoter in the absence of glucose and YP rich nutrients (SPO) (Figure 26B). By transferring cells to the glucose-only condition (SPO + 2% Glc), I discovered that glucose only partially contributed to the binding of Tup1 to the *IME1* promoter. The majority of Tup1 binding was mediated by the nutrients provided in YP, as indicated in the YP + 0.05% Glc and YP + 2% Glc conditions (Figure 26B). These results show that Tup1 binding to the *IME1* promoter is controlled by both glucose and nutrients provided in yeast extract and peptone.

Next, I inspected the candidate transcription factors that were shown or implicated to interact with Tup1-Cyc8 using the same experimental workflow. I measured the binding of Cup9, Yap6, Sok2, Phd1, Sut1, Mot3, Sko1, Nrg1, and Nrg2 in SPO, SPO + 2% Glc, YP + 0.05% Glc, and YP + 2% Glc by ChIP (Figure 26C). All nine transcription factors dissociated from the *IME1* promoter in the absence of glucose and YP rich nutrients (SPO). The nine transcription factors can be divided into three groups based on their responses to the availability of glucose and YP rich nutrients in the medium. The first group of transcription factors, including Yap6, Sok2, Phd1, Nrg1, and Sko1, interacted with the *IME1* promoter in response to nutrients provided in YP but not glucose (Figure 26C). Conversely, the second group of transcription factors, including Mot3 and Nrg2, exhibited the opposite binding pattern. The binding of Mot3 and Nrg2 was entirely glucose-dependent and did not require the presence of YP (Figure 26C). Thus, the two groups of transcription factors behaved very differently from each other in the four conditions, suggesting that the transcription factors respond to distinct nutrients in the growth medium. Finally, a third group of transcription factors, including Cup9 and Sut1, required both glucose and nutrients from YP to interact with the *IME1* promoter (Figure 26C). In particular, Cup9 was found to partially bind in both glucose-only and YP-only conditions, while Sut1 was only detected at the *IME1* promoter in YPD (YP + 2% Glc). Finally, I also assessed the binding of Pog1, a known transcriptional activator of *IME1* in the four nutrient conditions (Figure 26D). In short, Pog1 was associated with the *IME1* promoter in all four nutrient conditions, with higher occupancy in the presence of YP (YP + 0.05% Glc and YP + 2% Glc). Glucose seems to be less important in regulating Pog1 binding, since Pog1 binding in SPO and SPO with glucose (SPO + 2% Glc)

was comparable (Figure 26D). Remarkably, Pog1 was the only transcription factor that clearly remained to be bound in SPO medium. It is worth noting that the binding of Pog1 at the *IME1* promoter is higher in YP-containing medium than that in SPO medium. Why does the *IME1* activator Pog1 interact with the *IME1* promoter more strongly in repressive conditions than in activating conditions? I speculate that the interaction of Pog1 with the *IME1* promoter is stabilised by other transcription factors that bind to the promoter in response to nutrients present in YP, including Tup1, Yap6, Sok2, Phd1, Sko1, and Nrg1 (Figure 26B and Figure 26C). Furthermore, previous studies have provided evidence that turnover of transcriptional activators is coupled to their potential in stimulating gene transcription (Iñigo et al., 2012, Spoel et al., 2009, Salghetti et al., 2000). Hence, Pog1 may exhibit higher turnover rate and thus shorter residence time at the *IME1* promoter upon induction of sporulation. The protein half-life of Pog1 should be examined in future experiments to test this hypothesis. The ChIP data in Figure 26 demonstrate that the transcription factors occupying the *IME1* promoter are controlled differently by nutrients. My data further suggest that Tup1-Cyc8 recruitment may be regulated by different transcription factors under different nutrient conditions.

Taken together, my data reveal that at least 10 transcription factors bind to the *IME1* upstream region in a nutrient-sensitive manner, illustrating the complexity of nutrient regulation of the *IME1* promoter. In addition, I found that Tup1 binding is mainly mediated by YP nutrients and partially contributed by glucose. The large number of transcription factors mediating nutrient signals could be a mechanism to secure recruitment of Tup1-Cyc8 in nutrient-rich conditions. As cells are induced to enter meiosis when nutrients are depleted, the dissociation of these nutrient-sensitive transcription factors also ensure that Tup1-Cyc8 is evicted and *IME1* transcription is de-repressed.

(A)

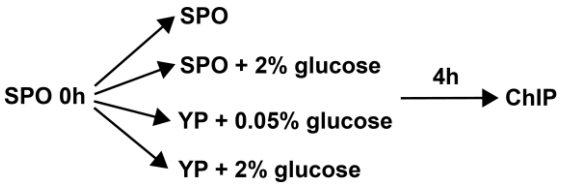

(B)

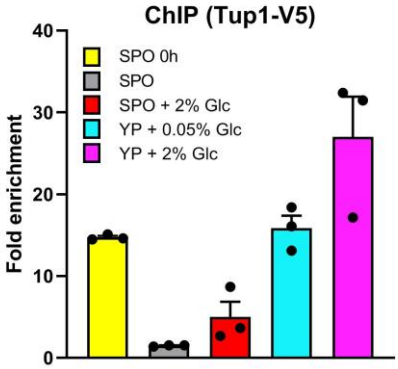

(C)

Transcription factor binding primarily responds to nutrients in YP:

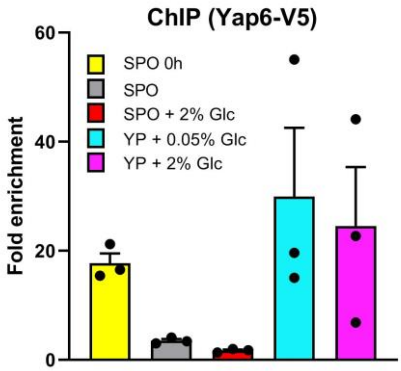

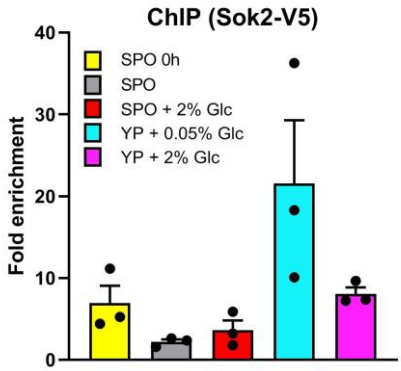

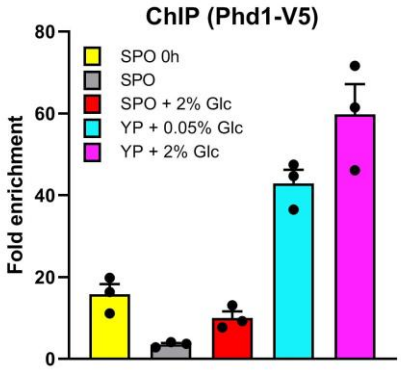

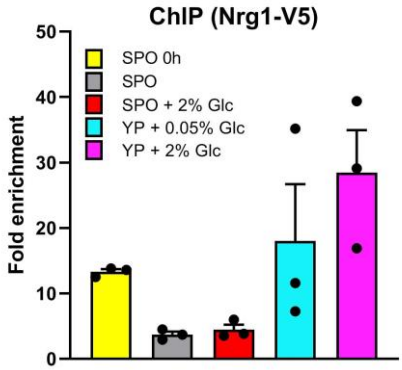

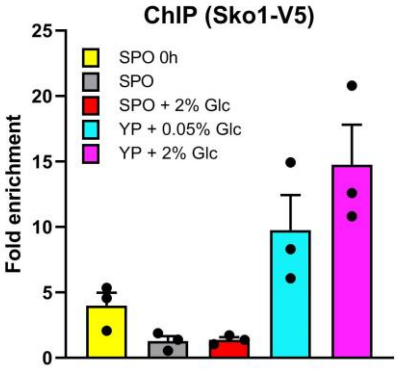

Transcription factor binding primarily responds to glucose:

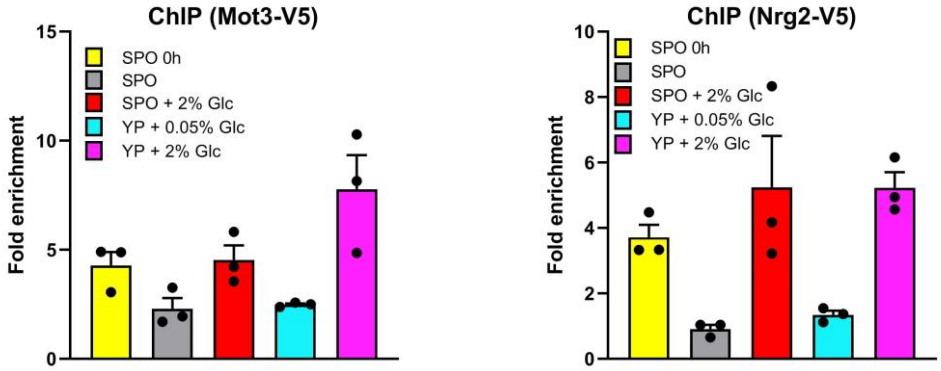

Transcription factor binding responds to both glucose and nutrients in YP:

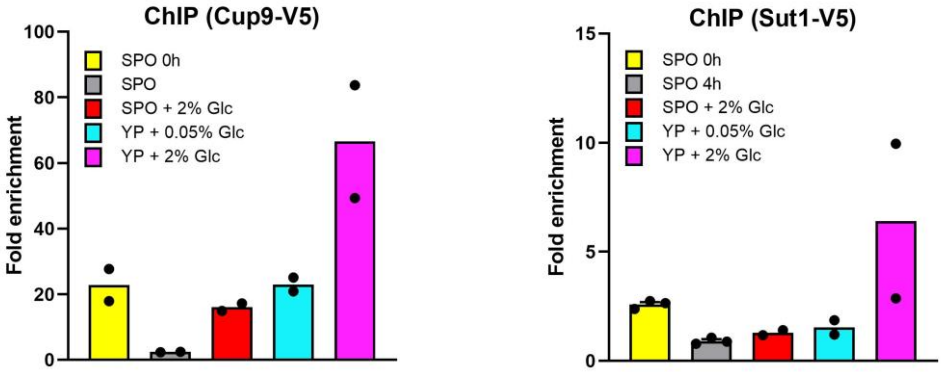

(D)

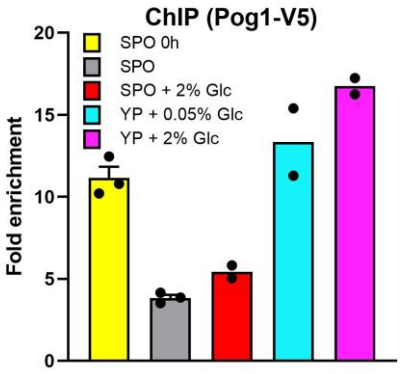

Figure 26. Distinct nutrients in rich medium mediate the binding of Tup1-Cyc8 interacting transcription factors to the *IME1* promoter.

(A) Schematic diagram depicting the experimental workflow. Cells were grown to saturation in YPD medium and shifted to pre-sporulation medium BYTA. Subsequently, cells grown to saturation in BYTA were transferred to four media

with distinct nutrient contents including sporulation medium (SPO), glucose-only medium (SPO + 2% Glc), YP medium without glucose (YP + 0.05% Glc), and nutrient-rich YPD medium (YP + 2% Glc). Samples were taken at 0 hour in SPO and after 4 hours in different nutrient conditions.

(B) ChIP-qPCR of Tup1-V5 (FW3456) prior to meiotic entry (SPO 0h) and at 4 hours in SPO, SPO + 2% Glc, YP + 0.05% Glc, and YP + 2% Glc. For qPCR, a primer pair flanking the region 1000 bp upstream of the *IME1* start codon was used. ChIP signals were normalised over the silent mating type cassette *HMR*. Bars represent mean (SEM) and dots represent individual biological replicates.

(C) Same as (B) except that V5 epitope-tagged transcription factors were examined. These transcription factors include Cup9-V5 (FW6976), Yap6-V5 (FW3833), Sok2-V5 (FW5638), Phd1-V5 (FW4466), Sut1-V5 (FW6974), Mot3-V5 (FW4383), Sko1-V5 (FW4389), Nrg1-V5 (FW4393), and Nrg2-V5 (FW4396). ChIP signals were normalised over the silent mating type cassette *HMR*. Bars represent mean normalised ChIP signals, error bars represent SEM, and dots represent individual biological replicates. The transcription factors are classified into three groups based on their responses to glucose and nutrients in YP.

(D) Same as (B) except that V5 epitope-tagged Pog1 (FW968) was examined. ChIP signals were normalised over the silent mating type cassette *HMR*. Bars represent mean normalised ChIP signals, error bars represent SEM, and dots represent individual biological replicates.

4.3 Dissociation of strongly bound transcription factors Cup9, Yap6, Sok2, and Phd1 is not primarily due to cellular changes in localisation and protein abundance

In the previous section of this chapter (4.2), I presented experimental evidence that the nine putative recruiters of Tup1-Cyc8 bind to the *IME1* upstream region in the presence of nutrients, and dissociate when nutrients are deprived presumably as a means to evict Tup1-Cyc8. How do nutrient signals regulate binding of the transcription factors? In yeast, changes in the nutrient signalling pathways can alter protein expression by modulating protein expression levels and regulating protein re-localisation. For example, when galactose replaces glucose as a carbon source in yeast, Mig1 and Mig2 repressors are phosphorylated and thus evicted from the nucleus by nuclear export and proteasomal degradation (Conrad et al., 2014). Another example is Yak1, a serine/threonine kinase that is re-localised to the cytoplasm upon Ras/PKA activation (Broach, 2012). Therefore, I set out to investigate whether dissociation of the transcription factors at the *IME1* promoter during meiotic entry is regulated by protein degradation and nuclear export. Cup9, Yap6, Sok2, and Phd1 displayed the strongest binding (more than 10 fold enrichment over background) during the exponential growth phase, and showed significant dissociation from the *IME1* promoter during entry into meiosis (Figure 25). I considered these four transcription factors as prime candidates for recruiting Tup1-Cyc8 to the *IME1* promoter. Hence, I focussed on Cup9, Yap6, Sok2, and Phd1, and determined their protein levels and sub-cellular localisation before and during entry into meiosis when *IME1* is transcribed.

Firstly, I asked whether the protein expression of Cup9, Yap6, Sok2, and Phd1 is affected during entry into meiosis when *IME1* transcription is activated. I prepared cells undergoing exponential growth (YPD (E)), grown to saturation (YPD (S)), before (SPO 0h) and during (SPO 4h) entry into meiosis. The V5-tagged transcription factors were detected by western blotting, and their expression levels were normalised over the endogenous control Hxk1 (Figure 27). In exponentially growing cells, Cup9 was strongly expressed and its level decreased in cells grown to saturation (Figure 27A). Cup9 expression was slightly increased at SPO 0h, and declined at SPO 4h (Figure 27A). Although the levels of Cup9 decrease before and

during meiotic entry, my ChIP data demonstrate that Cup9 is strongly bound at the *IME1* promoter prior to, but not during meiotic entry (Figure 25). These observations suggest that Cup9 binding at the *IME1* promoter is not mainly regulated by protein abundance. Next, Yap6 was generally weakly expressed in all conditions tested (Figure 27B). The expression of Yap6 declined when cells were grown to saturation and prior to meiotic entry, followed by a mild increase when sporulation was induced (Figure 27B). In addition, Sok2 and Phd1, which are paralogous transcription factors, exhibited similar protein expression patterns in the conditions tested (Figure 27C and Figure 27D). The protein levels of both transcription factors diminished in cells grown to saturation, and stayed almost constant prior to and during entry into meiosis (Figure 27C and Figure 27D).

Taken together, the protein expression of Cup9, Yap6, Sok2, and Phd1 in sporulation conditions is generally lower than that during exponential growth (Figure 27). Yet, in contrast to the sharp decrease of transcription factor binding at the *IME1* promoter from before to during entry into meiosis (Figure 25), Cup9, Yap6, Sok2, and Phd1 did not show a comparable decrease in expression levels. These results indicate that cellular changes in protein expression is not the main mechanism that induces loss of Cup9, Yap6, Sok2, and Phd1 binding at the *IME1* promoter from before to during meiotic entry.

(A)

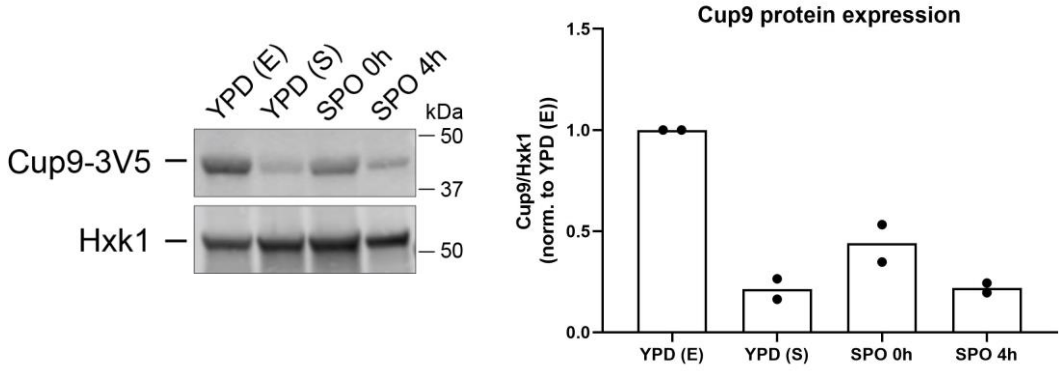
YPD (E)
YPD (S)
SPO 0h
SPO 4h
kDa
Cup9-3V5
Hxk1
50
37
50
Cup9 protein expression
Cup9/Hxk1 (norm. to YPD (E))
1.5
1.0
0.5
0.0
YPD (E)
YPD (S)
SPO 0h
SPO 4h

(B)

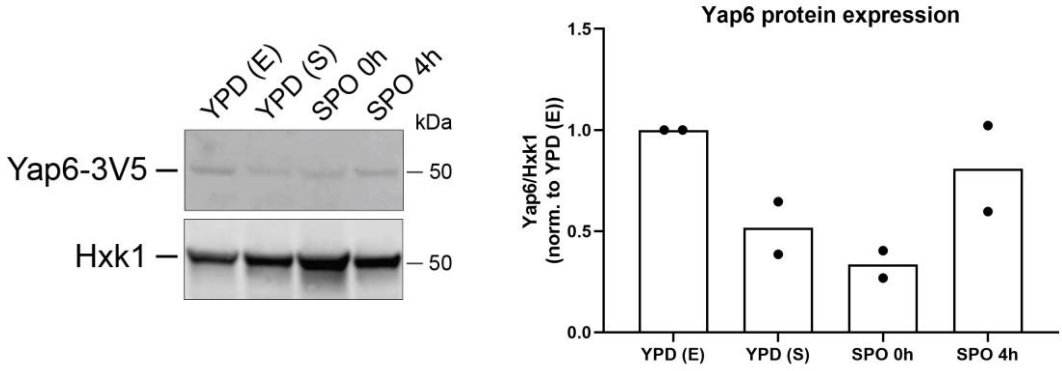
YPD (E)
YPD (S)
SPO 0h
SPO 4h
kDa
Yap6-3V5
Hxk1
50
50
Yap6 protein expression
Yap6/Hxk1 (norm. to YPD (E))
1.5
1.0
0.5
0.0
YPD (E)
YPD (S)
SPO 0h
SPO 4h

(C)

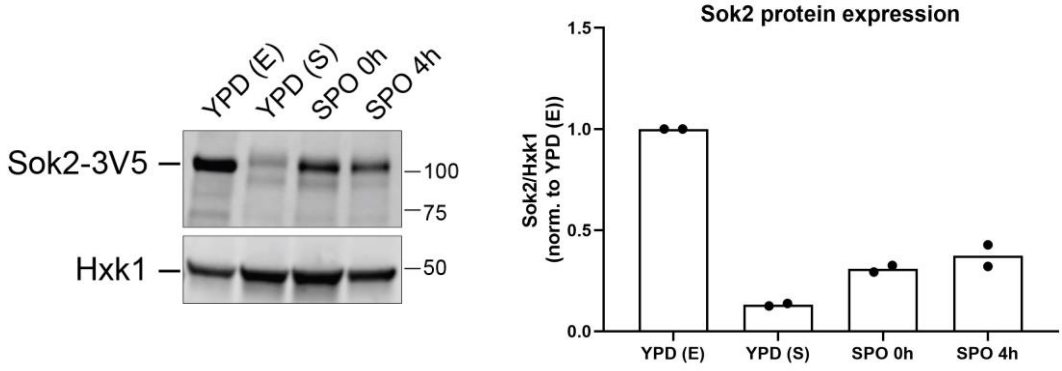
YPD (E)
YPD (S)
SPO 0h
SPO 4h
Sok2-3V5
Hxk1
100
75
50
Sok2 protein expression
Sok2/Hxk1 (norm. to YPD (E))
1.5
1.0
0.5
0.0
YPD (E)
YPD (S)
SPO 0h
SPO 4h

(D)

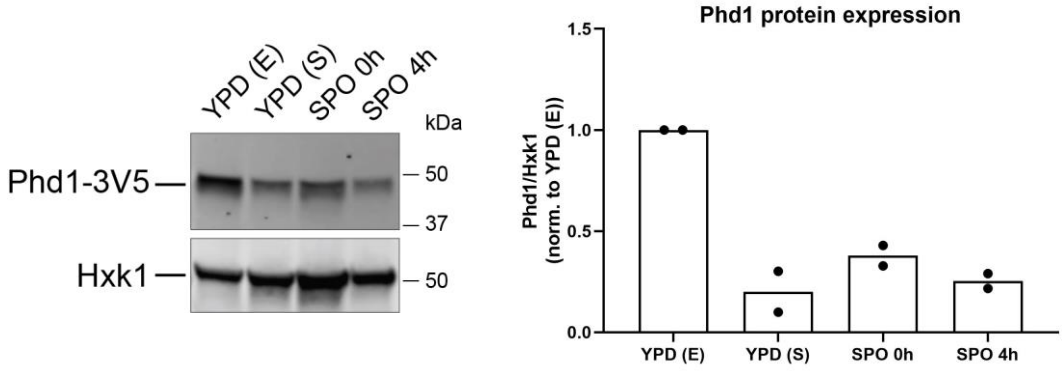

Figure 27. Protein expression of Cup9, Yap6, Sok2, and Phd1 in different growth stages.

Representative western blots and quantification data of (A) Cup9-V5 (FW6976), (B) Yap6-V5 (FW3833), (C) Sok2-V5 (FW5638), and (D) Phd1-V5 (FW4466) from cells in exponential growth phase (YPD (E)), grown to saturation (YPD (S)), before (SPO 0h) and during (SPO 4h) entry into meiosis. Protein levels were normalised over Hxk1 levels, and the normalised protein levels are presented relative to YPD (E). Uncropped western blots can be found in Supplementary figure 8, Supplementary figure 9, Supplementary figure 10, and Supplementary figure 11. Bars represent mean normalised signals relative to YPD (E) and dots indicate individual biological replicates.

Given that dissociation of Cup9, Yap6, Sok2, and Phd1 from the *IME1* promoter is not a direct result of altered protein expression, I speculated whether changes in cellular localisation could explain how the transcription factors dissociate from the *IME1* promoter. To test this hypothesis, I examined the sub-cellular localisation of Cup9, Yap6, Sok2, and Phd1. Firstly, I generated yeast strains with each transcription factor labelled with the mNeonGreen fluorescent protein at the C-terminus by endogenously fusing the *mNeonGreen* sequence to the 3' ends of the genes encoding the transcription factors. Secondly, I determined the localisation of each transcription factor before (SPO 0h) and during (SPO 4h) meiotic entry by widefield fluorescence microscopy (Figure 28). Thirdly, I quantified the signal intensities of the mNeonGreen-tagged proteins in the whole cell, nucleus, and cytosol (whole cell - nucleus). To inspect whether there was a change in the sub-cellular transcription factor distribution, I determined the total mNeonGreen signals detected in the nuclei (Figure 28B). Furthermore, I also calculated the ratio of nuclear mNeonGreen signal vs cytosolic mNeonGreen signal for each cell (Figure 28C).

In agreement with the roles of Cup9, Yap6, Sok2, and Phd1 as transcription factors, the four transcription factors were localised to the nucleus before entry into meiosis (Figure 28A). Notably, all four transcription factors were observed in the nucleus during entry into meiosis, suggesting that the transcription factors are still readily available to interact with chromatin during meiotic entry. Interestingly, my data suggest that the abundance of Cup9 increases in the nucleus during meiotic entry (SPO 4h) (Figure 28B). To find out whether Cup9 expression was altered in the cytosol, I determined the nucleus/cytosol ratio of Cup9-mNeonGreen before and during meiotic entry. I found that the Cup9-mNeonGreen nucleus/cytosol ratios increased similar to the mCup9-mNeonGreen nuclear signals, indicating that there was a specific increase in Cup9 abundance in the nucleus during entry into meiosis (Figure 28C). The differences observed between the western blot data in Figure 27A and the imaging data for Cup9 could be due to the V5 and mNeonGreen tags slightly altering protein properties when fused to Cup9 or due to experimental variations.

Yap6 is known to be constitutively expressed in the nucleus (Rodrigues-Pousada et al., 2019). In agreement with the literature, Yap6 expression was nuclear before and during entry into meiosis and the nuclear intensity was unaffected (Figure

28B). No changes in the whole cell or cytosolic expression of Yap6 were observed as the mean nucleus/cytosol ratio of Yap6-mNeonGreen was unaltered (Figure 28C). Finally, Sok2 is a dynamic transcriptional repressor that normally resides in the nucleus and re-localises to the cytosol under hypoxic conditions (Dastidar et al., 2012), while Phd1 is expressed in the nucleus under nutrient-rich conditions in immunofluorescence experiments (Gimeno and Fink, 1994). In my experiments, I found that the nuclear signal intensities and the nucleus/cysotol ratios of Sok2 and Phd1 were unaltered before and during meiotic entry (Figure 28B and Figure 28C). Thus, Yap6, Sok2, and Phd1 sub-cellular distributions are unaffected by induction of sporulation.

Taken together, I determined the protein expression and cellular distribution of Cup9, Yap6, Sok2, and Phd1 to explore how transcription factors bound to the *IME1* promoter dissociate during entry into meiosis. I found that changes in protein expression and cellular localisation of the four transcription factors cannot explain their loss of binding at the *IME1* promoter during meiotic entry. These observations point to the involvement of other mechanisms such as post-translational modifications of the transcription factors and local signal effect to the *IME1* promoter during entry into meiosis.

(A)

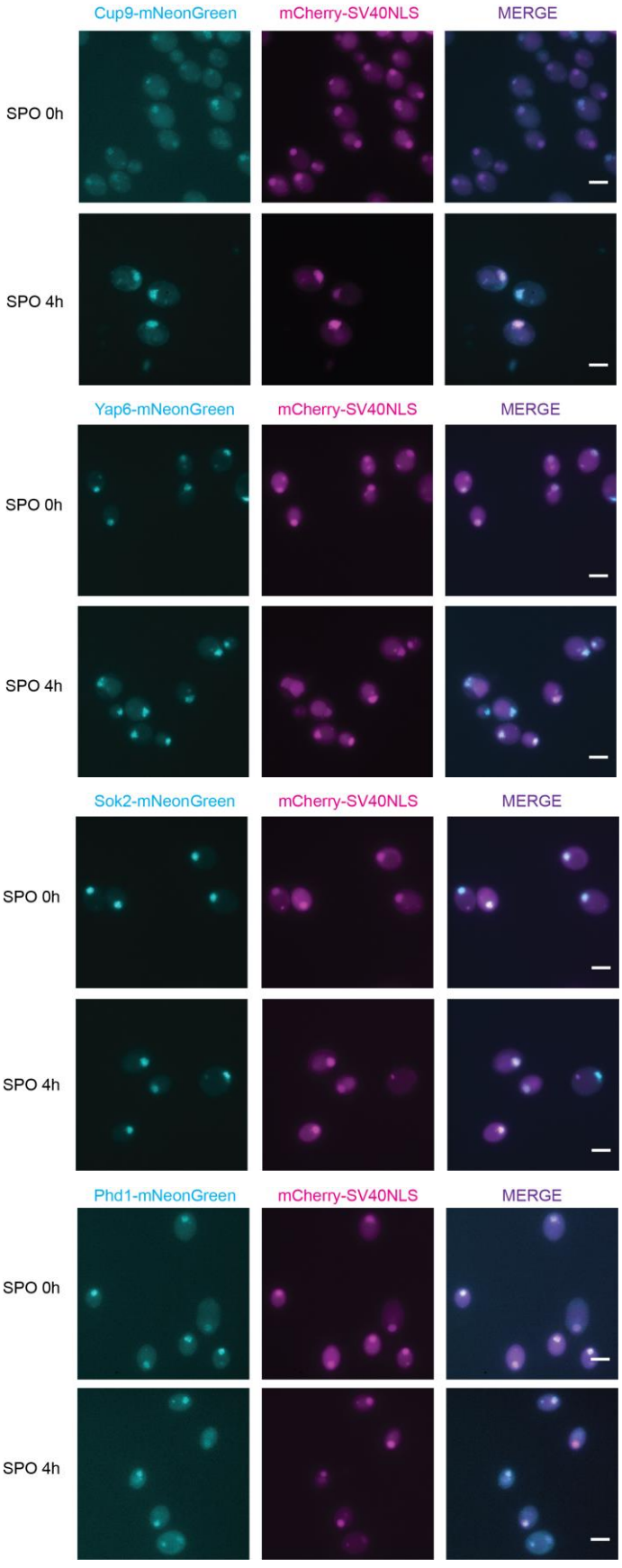
Cup9-mNeonGreen
mCherry-SV40NLS
MERGE
SPO 0h
SPO 4h
Yap6-mNeonGreen
mCherry-SV40NLS
MERGE
SPO 0h
SPO 4h
Sok2-mNeonGreen
mCherry-SV40NLS
MERGE
SPO 0h
SPO 4h
Phd1-mNeonGreen
mCherry-SV40NLS
MERGE
SPO 0h
SPO 4h

(B)

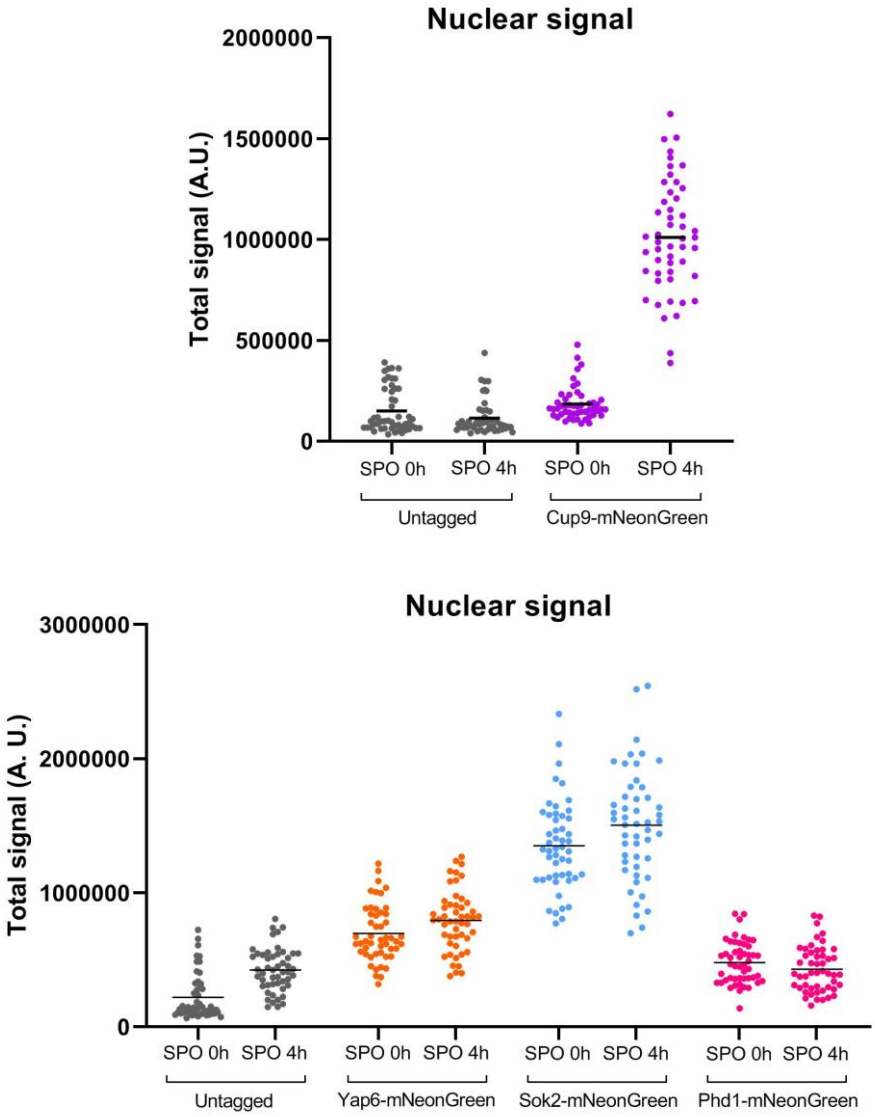
Nuclear signal
Total signal (A.U.)
2000000
1500000
1000000
500000
0
SPO 0h
SPO 4h
SPO 0h
SPO 4h
Untagged
Cup9-mNeonGreen
Nuclear signal
Total signal (A. U.)
3000000
2000000
1000000
0
SPO 0h
SPO 4h
SPO 0h
SPO 4h
SPO 0h
SPO 4h
SPO 0h
SPO 4h
Untagged
Yap6-mNeonGreen
Sok2-mNeonGreen
Phd1-mNeonGreen

(C)

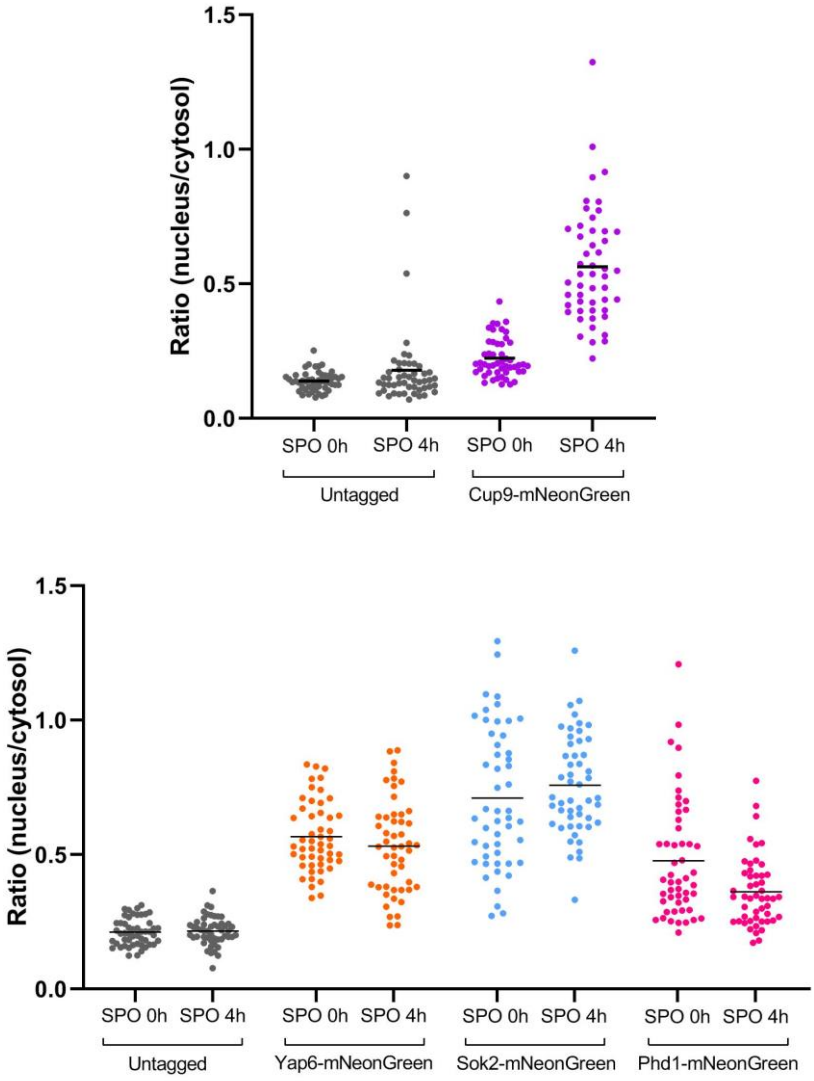

Figure 28. Cup9, Yap6, Sok2, and Phd1 are expressed in the nucleus before and during entry into meiosis.

(A) Representative widefield microscopy images of Cup9-mNeonGreen (FW7646), Yap6-mNeonGreen (FW7473), Sok2-mNeonGreen (FW7475), and Phd1-mNeonGreen (FW7477) before (SPO 0h) and during entry into meiosis (SPO 4h). Separate and merged channel images are presented for the mNeonGreen fusion proteins and mCherry-SV40NLS. Scale bars indicate 5µm.

(B) Scatter dot plot representing the mNeonGreen signals detected in the nucleus of each cell. Measurements of nuclear mNeonGreen signals were directed by the nuclear marker (mCherry-SV40NLS). Quantification data for 50 cells are presented for wild-type untagged cells (FW5199) and for each strain described

in (A). The black line denotes the mean nuclear signal intensity of the cell population.

(C) Scatter dot plot representing the nuclear/cytosolic mNeonGreen ratios determined in the same cells analysed in (B). The cytosolic mNeonGreen signal was derived from (whole cell signal – nuclear signal). The black line denotes the mean nuclear/cytosolic mNeonGreen ratio of the cell population.

4.4 Chapter summary

In this chapter, I investigated how Tup1-Cyc8 is recruited to the *IME1* upstream region in nutrient-rich conditions by identifying the transcription factors that associate Tup1-Cyc8 to the *IME1* promoter. I shortlisted 16 candidate transcription factors which were shown or implicated to interact with Tup1-Cyc8, and have consensus binding motifs predicted in the region where Tup1-Cyc8 binds. Among the 16 shortlisted transcription factors, I discovered that Cup9, Yap6, Sok2, and Phd1 bind strongly to the *IME1* promoter, whereas Sut1, Mot3, Sko1, Nrg1, and Nrg2 are weaker binders. Furthermore, Yap6, Sok2, Phd1, Sut1, Mot3, Nrg1, and Nrg2 can interact with the *IME1* promoter independent of Tup1, suggesting that the binding of these transcription factors is sequence-specific. The *IME1* promoter sequences that are bound by these transcription factors will be further discussed in Chapter 6. In contrast, Sko1 does not bind the *IME1* promoter in the absence of Tup1, therefore the occupancy of Sko1 at the promoter is dependent on Tup1.

Importantly, all of the Tup1-Cyc8 interacting transcription factors dissociate from the *IME1* promoter in response to nutrient starvation, demonstrating that their binding is regulated by nutrient signals. I further dissected how Tup1, the Tup1-Cyc8 interacting transcription factors, and Pog1 respond to different nutrients by shifting cells to media providing distinct nutrients. I found that the interaction of Tup1 with the *IME1* promoter is partially mediated by glucose, and mostly contributed by rich nutrients including nitrogen compounds from yeast extract and peptone (YP). Furthermore, the Tup1-Cyc8 interacting transcription factors are differentially regulated by glucose and YP, suggesting that they mediate different nutrient signals to modulate binding of Tup1-Cyc8 (Figure 29). Notably, the transcriptional activator Pog1 binds to the *IME1* promoter in both nutrient-rich and nutrient-depleted conditions, indicating that nutrients play little role in controlling recruitment of transcriptional activators.

Finally, I examined the protein expression and sub-cellular localisation of the most strongly bound candidate transcription factors, Cup9, Yap6, Sok2, and Phd1, to understand how they dissociate from the *IME1* promoter when nutrients are depleted. I found that Cup9, Yap6, Sok2, and Phd1 are clearly expressed in the

nucleus under nutrient deprivation, suggesting that the transcription factors may be unable to bind the *IME1* promoter due to local changes at the *IME1* promoter, or by post-translational modifications of the transcription factors or Tup1-Cyc8 itself. Taken together, my data propose a model in which multiple transcription factors mediate distinct nutrient signals to control Tup1-Cyc8 binding in nutrient-rich conditions. Upon nutrient starvation, the Tup1-Cyc8 recruiting transcription factors dissociate from the *IME1* promoter and thus Tup1-Cyc8 leaves the *IME1* promoter (Figure 29).

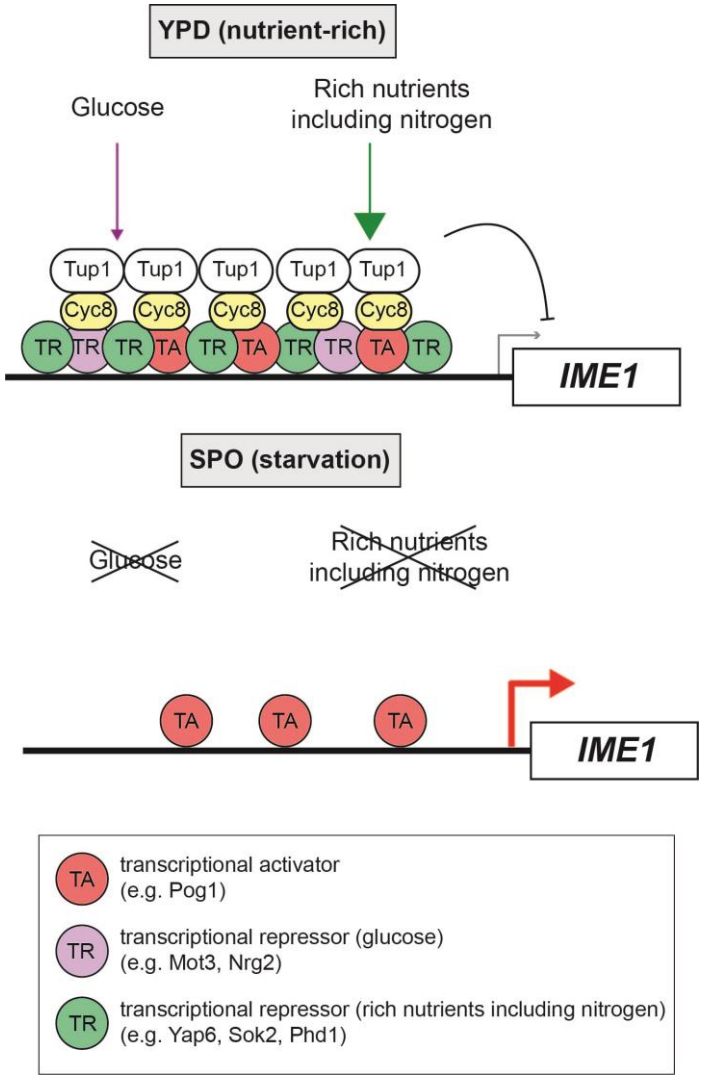

Figure 29. An array of Tup1-Cyc8 interacting transcription factors binds to the *IME1* promoter in nutrient-rich YPD medium.

Schematic diagram representing the large complex of transcription factors that binds to the *IME1* promoter in YPD medium, near 1000 bp upstream of the start codon. At least nine Tup1-Cyc8 interacting transcription factors are bound, and their binding is differentially regulated by nutrients in the YPD medium. A subset of transcription factors responds to glucose, while the other transcription factors respond to rich nutrients including nitrogen compounds. Together, these transcription factors regulate binding of Tup1-Cyc8 at the *IME1* promoter. Upon sporulation inducing conditions, all Tup1-Cyc8 interacting transcription factors dissociate from the *IME1* promoter, thus Tup1-Cyc8 is evicted. Transcriptional activators such as Pog1 remain bound to the *IME1* promoter and induce transcription. Please note that the *IME1* promoter depicted in the diagram is not

drawn to scale and only represents the region where Tup1-Cyc8 interacts, i.e. 750 to 1400 bp upstream of the start codon.

Chapter 5. Yap6, Sok2, and Phd1 mediate Tup1-Cyc8 binding and repression of the *IME1* promoter

Tup1-Cyc8 is recruited to the *IME1* promoter in nutrient-rich condition by interacting with specific transcription factors bound to the promoter. I discovered that the region where Tup1-Cyc8 binds in the *IME1* promoter is also associated with multiple transcription factors. Tup1-Cyc8 binds between 750 and 1400 bp upstream of the *IME1* start codon (Chapter 3: Figure 13) (Weidberg et al., 2016). Using the YeTFaSCo database, I found that the Tup1-Cyc8 binding region is overlaid with the consensus binding sites of at least 18 transcription factors (Chapter 3: Figure 19B, Chapter 4: Table 2). My ChIP data also demonstrate that at least nine transcription factors that were shown or implicated to interact with Tup1-Cyc8 co-localise with Tup1-Cyc8 at the *IME1* promoter (Chapter 4: Figure 22). These transcription factors are Cup9, Yap6, Sok2, Phd1, Sut1, Mot3, Sko1, Nrg1, and Nrg2. Notably, apart from Sko1, all transcription factors bind to the *IME1* promoter independent of Tup1, suggesting that the binding may be sequence-specific.

Are these transcription factors functionally related to Tup1-Cyc8 binding at the *IME1* promoter in nutrient-rich medium? This question encompasses two specific questions. First, I examined whether the transcription factors are responsible for Tup1 binding at the *IME1* promoter. Among the prime candidates that mediate Tup1-Cyc8 binding, Sok2, a repressor of pseudohyphal growth was previously shown to downregulate a part of the *IME1* promoter (Shenhar and Kassir, 2001). However, whether Sok2 regulates *IME1* promoter activity by mediating Tup1-Cyc8 binding was not established. Second, do the transcription factors mediate Tup1-Cyc8 binding under specific nutrient conditions? To explore this question, I examined Tup1 binding in different transcription factor mutants under multiple nutrient conditions. Furthermore, I also inspected whether the Tup1-Cyc8 recruiting transcription factors are under the control of PKA (protein kinase A) and TORC1 (target of rapamycin complex 1) signalling pathways.

In addition, I investigated how Tup1-Cyc8 recruiting transcription factors regulate *IME1* transcription and entry into meiosis. *IME1* encodes the transcription factor that

is crucial to initiate entry into meiosis in yeast. In the presence of nutrients, Tup1-Cyc8 binds to the *IME1* promoter to repress *IME1* transcription, and thereby inhibits meiosis initiation. I examined whether loss of Tup1-Cyc8 recruiting transcription factors alleviates repression of *IME1* transcription in nutrient-rich condition and prior to entry into meiosis. Since *IME1* expression is directly linked to onset of meiosis, I inspected whether the timing of meiotic entry is affected when Tup1-Cyc8 recruiting transcription factors are lost. Taken together, I aimed to dissect how rich nutrient signals repress *IME1* transcription and meiotic entry by controlling transcription factors that mediate Tup1-Cyc8 binding to the *IME1* promoter.

5.1 Tup1-Cyc8 binding to the *IME1* promoter depends on more than one transcription factor

In the previous chapter, I described four transcription factors, Cup9, Yap6, Sok2, and Phd1 that are strongly bound at the *IME1* promoter in nutrient-rich condition (Chapter 4: Figure 22). Since these four transcription factors displayed markedly higher binding at the *IME1* promoter, I considered Cup9, Yap6, Sok2, and Phd1 as prime candidates for mediating Tup1-Cyc8 recruitment at the *IME1* promoter. To investigate whether Tup1-Cyc8 is brought to the *IME1* promoter by interacting with one of these four transcription factors, I deleted each of the four transcription factors and measured the binding of Tup1 tagged with V5 epitope by ChIP-qPCR. I determined the level of Tup1 binding during exponential growth (YPD (E)) and prior to entry into meiosis (SPO 0h) when Tup1 stably binds to the *IME1* upstream region (Chapter 3: Figure 14).

Deletions of Cup9, Yap6, Sok2, and Phd1 had various effects on Tup1 association with the *IME1* promoter (Figure 30). Deletions of Yap6 (*yap6*Δ) and Sok2 (*sok2*Δ) mildly reduced Tup1 binding in the exponentially growth phase. Tup1 was approximately 11 fold enriched over *HMR* in the wild-type strain and its binding was reduced to 8.3 fold and 9.8 fold enriched in the *yap6*Δ and *sok2*Δ strains respectively (Figure 30). These results imply that Yap6 and Sok2 mildly contribute to Tup1 recruitment during exponential growth. In addition, Tup1 recruitment was also affected prior to entry into meiosis when Yap6 or Sok2 was deleted. Tup1 recruitment was moderately reduced to 63% of the wild-type level in the *yap6*Δ mutant. Remarkably, Tup1 recruitment was strongly diminished to less than 25% of the wild-type level in the *sok2*Δ mutant, highlighting its importance in mediating Tup1 to the *IME1* promoter before meiotic entry. It is worth mentioning that Tup1 was still detected at the *IME1* promoter in both *yap6*Δ and *sok2*Δ mutants, suggesting that more than one transcription factor mediate the interaction of Tup1-Cyc8 with the *IME1* promoter.

Deletion of Phd1 (*phd1*Δ), which is paralogous to Sok2, did not reduce Tup1 binding compared to the wild-type cells (Figure 30). Interestingly, Tup1 ChIP signals increased in exponentially growing cells with *phd1*Δ, suggesting that more Tup1 is

recruited to the *IME1* promoter when Phd1 is absent. Given that Sok2 and Phd1 are paralogues and share highly similar binding motifs (Sok2: CCTGCA and AGGCA(C/A), Phd1: (A/C)TGCA and AGGCAC), it is possible that more Sok2 proteins are able to bind to the *IME1* promoter and recruit Tup1 in the absence of Phd1. I hypothesised that the two transcription factors may occupy the same sites in the *IME1* upstream region and interchange with each other to interact with Tup1-Cyc8. Perhaps the effect of *phd1*Δ was masked by the presence of Sok2. Given the potential redundancy of Sok2 and Phd1, I examined Tup1 binding at the *IME1* promoter in *sok2*Δ*phd1*Δ cells in the next section (Figure 31). Finally, deleting Cup9 (*cup9*Δ) also resulted in an increase in Tup1 ChIP signals during exponential growth phase and prior to entry into meiosis (Figure 30). However, biological replicates are required to confirm the reproducibility of this data before any conclusions can be drawn. Taken together, I found that Yap6 and Sok2 contribute to Tup1-Cyc8 binding at the *IME1* promoter during exponential growth phase and prior to entry into meiosis. Furthermore, more than one transcription factor are involved in recruiting Tup1-Cyc8 to the *IME1* promoter.

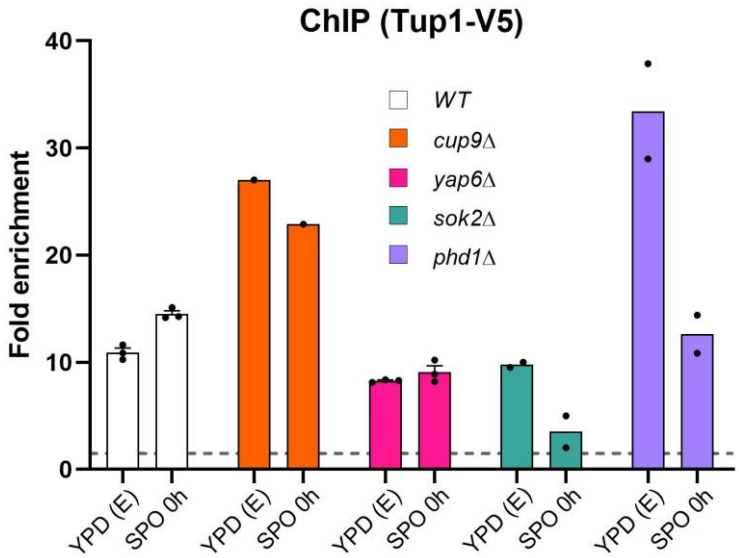

Figure 30. Deleting Cup9, Yap6, Sok2, or Phd1 has various effects on Tup1 binding at the *IME1* upstream region.

ChIP-qPCR of V5 epitope-tagged Tup1 in *WT* (FW3456), *cup9*Δ (FW6379), *yap6*Δ (FW3603), *sok2*Δ (FW3979), and *phd1*Δ (FW3991) cells. For qPCR, a primer pair flanking the region 1000 bp upstream of the *IME1* start codon was used, and the signals

were normalised over the silent mating type cassette *HMR*. Tup1 binding was determined in exponential growth phase (YPD (E)) and prior to entry into meiosis (SPO 0h). Bars represent mean normalised ChIP signals, error bars represent SEM, and dots indicate individual biological replicates. The grey dashed line denotes the level of Tup1 binding (1.48 fold) in wild-type cells during entry into meiosis (SPO 4h) (Chapter 3: Figure 14).

5.2 Yap6, Sok2, and Phd1 mediate Tup1-Cyc8 recruitment at the *IME1* promoter

My data indicate that more than one transcription factor recruit Tup1-Cyc8 to the *IME1* promoter (Figure 30). In particular, I speculated that the paralogous transcription factors Sok2 and Phd1 have redundant roles in recruiting Tup1-Cyc8 to the *IME1* promoter, and that the contribution of Phd1 in mediating Tup1-Cyc8 binding may be masked when Sok2 is present. To examine whether multiple transcription factors are important for Tup1-Cyc8 recruitment, I constructed *yap6*Δ*sok2*Δ, *sok2*Δ*phd1*Δ, and *yap6*Δ*phd1*Δ double deletion strains that expressed V5 epitope-tagged Tup1. To characterise how Tup1 recruitment is affected in different nutrient environments, I measured Tup1 binding at the *IME1* promoter in exponentially growing cells (YPD (E)) and prior to entry into meiosis (SPO 0h) by ChIP-qPCR. My data demonstrate that Tup1 occupancy at the *IME1* promoter prior to entry into meiosis was drastically reduced in *yap6*Δ*sok2*Δ and *sok2*Δ*phd1*Δ cells (Figure 31). These observations complement the conclusion from earlier data that Sok2 plays an important role in recruiting Tup1 before meiotic entry (Figure 30). Notably, Tup1 binding detected in *yap6*Δ*sok2*Δ cells was slightly lower than that determined in *sok2*Δ cells (*yap6*Δ*sok2*Δ: 1.73 fold vs *sok2*Δ: 3.52 fold) (Figure 30 and Figure 31), which may suggest that Yap6 also mildly contributes to Tup1 recruitment prior to entry into meiosis.

Despite the mild individual contributions of Yap6 and Sok2 to Tup1 recruitment during the exponential growth phase (Figure 30), little effect was observed in *yap6*Δ*sok2*Δ cells suggesting the involvement of other transcription factors (Figure 31). Deleting the paralogous transcription factors Sok2 and Phd1 reduced Tup1 recruitment in exponentially growing cells compared to *phd1*Δ cells in two out of three biological replicates (Figure 30 and Figure 31), but the double deletions were insufficient to remove all Tup1 at the *IME1* promoter. Finally, the *yap6*Δ*phd1*Δ cells exhibited less Tup1 binding compared to the wild-type strain in the exponential growth phase, and the effects were more pronounced than *yap6*Δ cells (*yap6*Δ*phd1*Δ: 6.99 fold enrichment vs *yap6*Δ: 8.27 fold enrichment) (Figure 30 and Figure 31). These results indicate that Phd1 contributes to Tup1 recruitment during exponential growth, and that Yap6 may be one of the contributors to the increased

Tup1 ChIP signals detected in *phd1*Δ cells. I conclude that Yap6, Sok2, and Phd1 are involved in recruiting Tup1-Cyc8 to the *IME1* promoter in the exponential growth phase and prior to entry into meiosis.

So far, my data imply that Yap6, Sok2, and Phd1 participate in recruiting Tup1 to the *IME1* promoter under different nutrient conditions. Yet, Tup1 was still readily detected in the double deletion strains tested (Figure 31), indicating that a complex composed of at least three transcription factors keeps Tup1-Cyc8 in place at the *IME1* upstream region. To test this hypothesis, I constructed a strain bearing triple deletions for Yap6, Sok2, and Phd1 (*yap6*Δ*sok2*Δ*phd1*Δ), and measured Tup1 binding at the *IME1* promoter in exponential growth phase (YPD (E)) and prior to entry into meiosis (SPO 0h). I found that *yap6*Δ*sok2*Δ*phd1*Δ cells displayed similar Tup1 binding level as *sok2*Δ*phd1*Δ cells during exponential growth and resembled that of *yap6*Δ*sok2*Δ cells prior to entry into meiosis (Figure 31). Prior to entry into meiosis, Tup1 recruitment was severely reduced in *yap6*Δ*sok2*Δ*phd1*Δ cells (2.61 fold) compared to wild-type cells (14.5 fold) (Figure 31). In exponentially growing cells, Tup1 binding was readily detected at the *IME1* promoter in *yap6*Δ*sok2*Δ*phd1*Δ cells (*yap6*Δ*sok2*Δ*phd1*Δ: 27.0 fold vs wild type: 10.9 fold) suggesting that other transcription factors recruit Tup1 during this stage. Nevertheless, functional assays of Yap6, Sok2, and Phd1 and their binding sites at the *IME1* promoter (presented in later sections) indicate that these three transcription factors contribute to Tup1-Cyc8 recruitment during exponential growth (Chapter 5: Figure 33, Chapter 6: Figure 43A-C and Figure 44). Hence, the interactions between Tup1-Cyc8 and the *IME1* promoter may be de-stabilised during exponential growth in the absence of Yap6, Sok2, and Phd1. Taken together, my data suggest that Yap6, Sok2, and Phd1 are responsible for recruiting Tup1-Cyc8 to the *IME1* promoter. I propose that Sok2 is the major contributor to Tup1-Cyc8 recruitment prior to entry into meiosis. In exponentially growing cells, more transcription factors are involved in recruiting Tup1-Cyc8 to the *IME1* promoter.

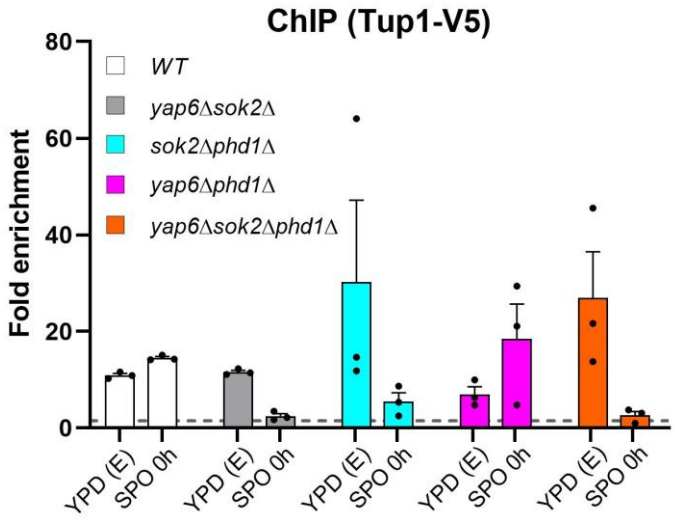

Figure 31. Tup1 binding at the *IME1* promoter is strongly diminished before entry into meiosis when Yap6 and Sok2 are lost in cells.

ChIP-qPCR of V5 epitope-tagged Tup1 in *WT* (FW3456), *yap6*Δ*sok2*Δ (FW4239), *sok2*Δ*phd1*Δ (FW4710), *yap6*Δ*phd1*Δ (FW4406), and *yap6*Δ*sok2*Δ*phd1*Δ (FW4010) cells. For qPCR, a primer pair flanking the region 1000 bp upstream of the *IME1* start codon was used, and the signals were normalised over the silent mating type cassette *HMR*. Tup1 binding was determined in exponentially growing cells (YPD (E)) and prior to entry into meiosis (SPO 0h). Bars represent mean (SEM) and dots indicate individual biological replicates. The grey dashed line denotes the level of Tup1 binding (1.48 fold) in wild-type cells during entry into meiosis (SPO 4h) (Chapter 3: Figure 14).

Since Cup9 binds strongly to the *IME1* promoter and is known to physically interact with Cyc8, I also generated a quadruple mutant strain (*yap6*Δ*sok2*Δ*phd1*Δ*cup9*Δ) with V5 epitope-tagged Tup1. Additional deletion of Cup9 had no effect on Tup1 binding to *yap6*Δ*sok2*Δ*phd1*Δ cells in exponential growth phase (YPD (E)) (Figure 32). Surprisingly, in cells prior to meiotic entry, a slight increase was detected in *yap6*Δ*sok2*Δ*phd1*Δ*cup9*Δ cells compared to *yap6*Δ*sok2*Δ*phd1*Δ cells. In the previous chapter, I demonstrated that at least nine transcription factors co-bind to the *IME1* promoter region where Tup1-Cyc8 binds, and their binding sites overlap with each other in this region (Chapter 4: Figure 22 and Table 2, Supplementary figure 13). When Cup9, Yap6, Sok2, and Phd1 are lost, the sites that mediate Tup1-Cyc8 recruitment in the *IME1* promoter may become exposed to other transcription factors. Transcription factors may bind to the *IME1*

promoter and mediate low level of Tup1 binding. Another possibility is that deletions of multiple transcription factors induced pleiotropic effects that indirectly affected Tup1-Cyc8 binding at the *IME1* promoter via other pathways. Next, to understand whether the weaker interactors Sko1, Nrg1 and its paralogue Nrg2 contribute to Tup1-Cyc8 recruitment, I constructed mutant strains bearing *yap6*Δ*sok2*Δ*phd1*Δ*sko1*Δ, *yap6*Δ*sok2*Δ*phd1*Δ*nrg1*Δ, and *yap6*Δ*sok2*Δ*phd1*Δ*nrg1*Δ*nrg2*Δ with V5 epitope-tagged Tup1. My ChIP data indicate that Tup1 binding in the exponential phase was unaltered when Sko1, Nrg1, and Nrg2 were also deleted, compared to *yap6*Δ*sok2*Δ*phd1*Δ cells (Figure 32). I noticed a minor increase in Tup1 binding prior to entry into meiosis in *yap6*Δ*sok2*Δ*phd1*Δ*nrg1*Δ and *yap6*Δ*sok2*Δ*phd1*Δ*nrg1*Δ*nrg2*Δ cells, similar to *yap6*Δ*sok2*Δ*phd1*Δ*cup9*Δ cells. These data indicate that deleting Cup9, Sko1, Nrg1, and Nrg2 is not sufficient to disrupt binding of Tup1-Cyc8 during exponential growth phase. I propose that at least five transcription factors mediate Tup1-Cyc8 binding in exponentially growing cells. Further examination of additional transcription factors would be challenging, since deleting additional transcription factors is extremely laborious. Furthermore, pleiotropic effects may arise from multiple mutations and complicate the interpretation of the results. For example, it is hard to determine whether the increased Tup1 binding in *yap6*Δ*sok2*Δ*phd1*Δ*nrg1*Δ*nrg2*Δ cells prior to meiotic entry indicates binding of other transcription factors, or is due to secondary effect (Figure 32).

In conclusion, Tup1-Cyc8 associates with the *IME1* promoter via interacting with a complex of sequence-specific transcription factors that bind to the *IME1* promoter. By studying the candidate transcription factors identified in the previous chapter, I discovered that three transcription factors, Yap6, Sok2, and Phd1 contribute to Tup1 recruitment at the *IME1* promoter. Deletions of Yap6, Sok2, and Phd1 lead to nearly complete loss of Tup1 binding at the *IME1* promoter prior to entry into meiosis. I propose that Tup1 binding in exponentially growing cells is mediated by additional transcription factor(s) that remain to be identified. The redundant roles of these transcription factors in recruiting Tup1-Cyc8 to the *IME1* promoter may be a way to safeguard Tup1-Cyc8 binding when nutrients are present.

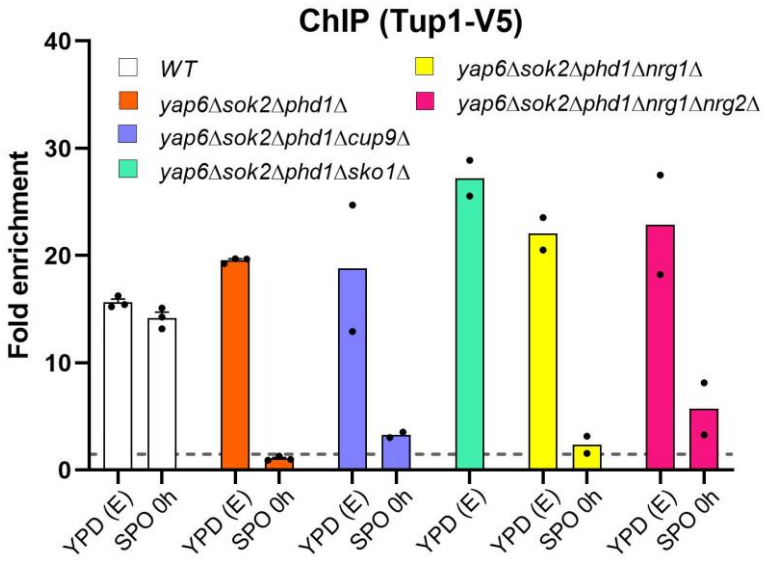

Figure 32. Additional deletions of Cup9, Sko1, Nrg1, and Nrg2 do not further reduce Tup1 binding at the *IME1* promoter.

ChIP-qPCR of V5 epitope-tagged Tup1 in *WT* (FW3456), *yap6Δsok2Δphd1Δ* (FW4010), *yap6Δsok2Δphd1Δcup9Δ* (FW7544), *yap6Δsok2Δphd1Δsko1Δ* (FW7430), *yap6Δsok2Δphd1Δnrg1Δ* (FW5657), and *yap6Δsok2Δphd1Δnrg1Δnrg2Δ* (FW5890) cells. For qPCR, a primer pair flanking the region 1000 bp upstream of the *IME1* start codon was used, and the signals were normalised over the silent mating type cassette *HMR*. Tup1 binding was determined in exponential growth phase (YPD (E)) and prior to entry into meiosis (SPO 0h). Bars represent mean normalised ChIP signals, error bars represent SEM, and dots indicate individual biological replicates. The grey dashed line denotes the level of Tup1 binding (1.48 fold) in wild-type cells during entry into meiosis (SPO 4h) (Chapter 3: Figure 14).

5.3 *IME1* transcription is moderately de-repressed in exponentially growing cells when Yap6, Sok2, and Phd1 are lost

In yeast, entry into meiosis is triggered by nutrient deprivation in the surrounding environment. When glucose and nitrogen compounds are depleted, the Ras/PKA and TORC1 signalling pathways become inactive. Consequently, Tup1-Cyc8 leaves the *IME1* promoter and permits *IME1* transcription, and thereby induces entry into meiosis. In Chapter 3: Figure 17, I demonstrated that depleting Tup1-Cyc8 in exponentially growing cells induces transcription of *IME1*. Next, I examined how Yap6, Sok2, and Phd1 contribute to *IME1* repression in nutrient-rich condition. I hypothesised that deleting multiple transcription factors mediating Tup1-Cyc8 recruitment should lead to de-repression of *IME1* transcription in the presence of rich nutrients.

First, I examined the effects of single transcription factor deletions on *IME1* transcription in exponentially growing cells (YPD (E)). To identify subtle differences between the mutants, I employed smFISH to detect *IME1* transcripts in cells. I examined whether single mutations, *yap6*Δ, *sok2*Δ, or *phd1*Δ affects *IME1* repression (Figure 33). The *sok2*Δ cells showed a very slight increase in *IME1* transcription, as about 3.5% of *sok2*Δ cells displayed at least four *IME1* transcripts while this was found in only 0.5% of the wild-type population (Figure 33B). In the *yap6*Δ and *phd1*Δ mutant cells, *IME1* stayed fully repressed and the distributions were indistinguishable from that of wild-type cells (Figure 33A and Figure 33B). I conclude that single deletions of Yap6, Sok2, or Phd1 have no or negligible effects on *IME1* repression in nutrient-rich condition.

Next, I detected *IME1* in the *yap6*Δ*sok2*Δ, *sok2*Δ*phd1*Δ, and *yap6*Δ*phd1*Δ double deletion strains with smFISH. Strikingly, cells without Sok2 and Phd1 demonstrated further de-repression of *IME1* (Figure 33A). The distribution of *IME1* per cell was markedly shifted, in which 13.9% of the population showed four to 10 copies of *IME1* transcripts and 3.2% displayed 11 to 20 copies (Figure 33B). In contrast, *IME1* signals detected in *yap6*Δ*sok2*Δ and *yap6*Δ*phd1*Δ cells resembled the levels in the single mutant cells (Figure 33A). The data imply that Sok2 and Phd1 are highly redundant during exponential growth, and removing either transcription factor

has little consequence on *IME1* repression. Finally, I inspected *IME1* smFISH signals in *yap6*Δ*sok2*Δ*phd1*Δ cells. *IME1* expression in *yap6*Δ*sok2*Δ*phd1*Δ cells was gently higher than that in *sok2*Δ*phd1*Δ cells, with 16% of cells having four to 10 copies of *IME1* transcripts and 7.2% with 11 to 20 copies (Figure 33B). Although *yap6*Δ*sok2*Δ*phd1*Δ led to considerable *IME1* transcription compared to wild-type cells, the level of de-repression was much weaker compared to that detected when Tup1 was depleted in nutrient-rich medium (Chapter 3: Figure 18B and Figure 18C). This indicates that removing the three transcription factors is insufficient to completely de-repress *IME1* transcription. These data agree with the observation that Tup1 was still binding to the *IME1* promoter in exponentially growing *yap6*Δ*sok2*Δ*phd1*Δ cells (Figure 31). I propose that loss of Yap6, Sok2, and Phd1 does not affect Tup1-Cyc8 recruitment in the exponential growth phase, due to the presence of other Tup1-Cyc8 interacting transcription factors.

(A)

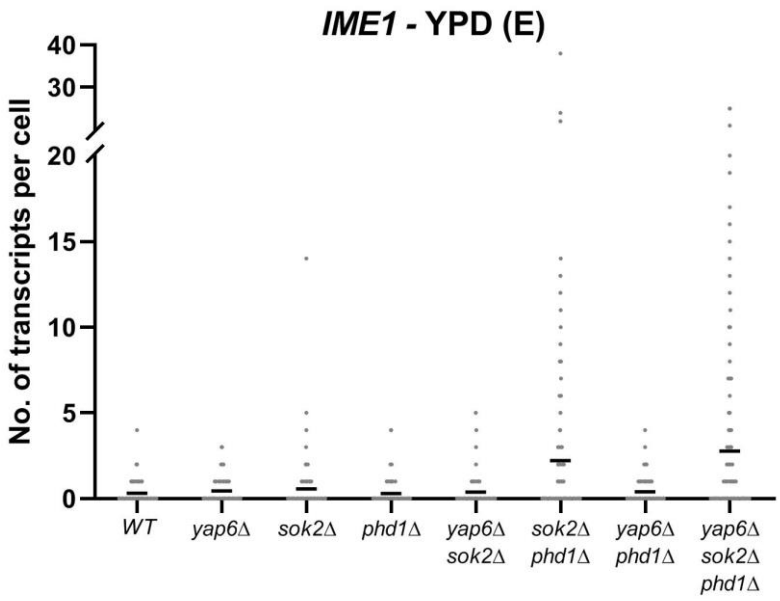

(B)

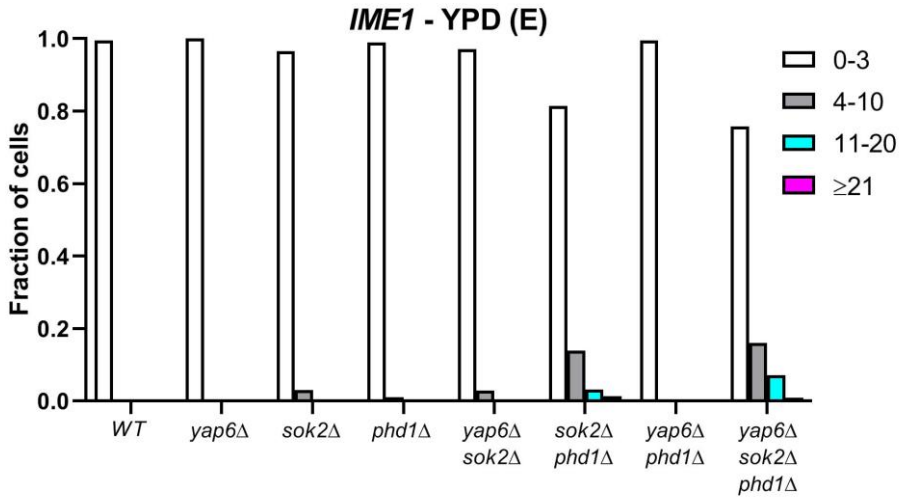

Figure 33. *IME1* transcripts are detected in a sub-population of exponentially growing cells when Yap6, Sok2, and Phd1 are lost.

(A) Scatter dot plot representing number of *IME1* transcripts detected per cell in the *WT* (FW3456), *yap6*Δ (FW3603), *sok2*Δ (FW3979), *phd1*Δ (FW3991), *yap6*Δ*sok2*Δ (FW4239), *sok2*Δ*phd1*Δ (FW4710), *yap6*Δ*phd1*Δ (FW4406), and *yap6*Δ*sok2*Δ*phd1*Δ (FW4010) cell populations. Around 200 cells that were positive for *ACT1* were analysed for each population. Each black line denotes the mean number of *IME1* transcripts per cell in the population.

(B) Histogram illustrating the same data shown in (A) binned into intervals by the number of *IME1* transcripts in cells. The data were binned into four intervals corresponding to 0-3, 4-10, 11-20, and 21 or more *IME1* transcripts per cell. Each bar represents the fraction of the cell population falling into that division.

The ChIP data presented in Figure 31 indicate that combining *yap6*Δ, *sok2*Δ, and *phd1*Δ reduces Tup1 binding at the *IME1* promoter prior to entry into meiosis. Since Tup1 binding and *IME1* transcription are anti-correlated (Chapter 3: Figure 18), I asked whether the effects of *yap6*Δ*sok2*Δ*phd1*Δ on Tup1 recruitment would affect *IME1* transcription. To monitor *IME1* transcription in different nutrient environments, I isolated total RNA from cells in exponential growth phase (YPD (E)) and prior to entry into meiosis (SPO 0h). Subsequently, I performed reverse transcription coupled to quantitative PCR (RT-qPCR) to measure the abundance of *IME1* in cells, and the signals were normalised over actin *ACT1* (Figure 34). I found that in exponentially growing cells, little differences in *IME1* transcription were detected which may be attributed to the lower sensitivity of RT-qPCR compared to smFISH. In cells prior to entry into meiosis, I observed that *IME1* transcription was affected in different mutants. In wild-type cells, *IME1* was about 1.5 fold enriched relative to *ACT1* expression prior to meiotic entry (Figure 34). *IME1* transcription in *yap6*Δ*sok2*Δ cells was elevated to more than seven fold enriched prior to entry into meiosis (Figure 34), which is consistent with reduced Tup1 binding in this nutrient condition (Figure 31). *IME1* was significantly de-repressed in *sok2*Δ*phd1*Δ cells to more than 10 fold enriched prior to meiotic entry (Figure 34). Conversely, *IME1* expression was not affected in *yap6*Δ*phd1*Δ cells (Figure 34). These results demonstrate that Sok2 significantly contributes to *IME1* repression before meiotic entry in line with earlier Tup1 ChIP data (Figure 30 and Figure 31). When Yap6 and Phd1 were also deleted, the *yap6*Δ*sok2*Δ*phd1*Δ triple deletion mutant exhibited the strongest *IME1* de-repression prior to entry into meiosis, producing nearly 14 fold of *IME1* relative to *ACT1* (Figure 34). The levels of *IME1* transcripts detected in *yap6*Δ*sok2*Δ, *sok2*Δ*phd1*Δ, and *yap6*Δ*sok2*Δ*phd1*Δ cells were much higher compared to that in wild-type cells during entry into meiosis (SPO 4h) (Chapter 3: Figure 17). These results indicate that *IME1* is fully relieved from transcriptional repression before meiotic entry in the absence of these transcription factors.

In summary, Tup1 binding at the *IME1* promoter is well correlated with repression of *IME1* transcription at SPO 0h. Prior to entry into meiosis, Sok2 plays a pivotal role in mediating Tup1 binding and *IME1* repression in cells while Yap6 and Phd1 play supplementary functions. Yap6, Sok2, and Phd1 also contribute to *IME1* repression in exponentially growing cells along with other transcription factors.

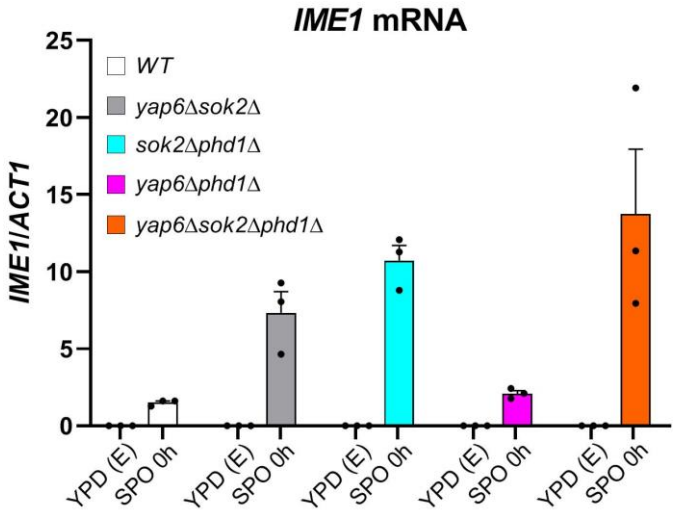

Figure 34. *IME1* transcripts accumulate to high levels in the absence of Sok2 compared to wild-type cells prior to entry into meiosis.

IME1 transcript levels detected by RT-qPCR in *WT* (FW3456), *yap6Δsok2Δ* (FW4239), *sok2Δphd1Δ* (FW4710), *yap6Δphd1Δ* (FW4406), and *yap6Δsok2Δphd1Δ* (FW4010) cells. Primers flanking approximately +850 bp of the *IME1* ORF were used for qPCR, and signals were normalised over actin *ACT1*. *IME1* levels were quantified in exponentially growing cells (YPD (E)) and prior to entry into meiosis (SPO 0h). Bars represent mean (SEM) and dots denote individual biological replicates.

5.4 Yeast cells exhibit early entry into meiosis when Sok2 is absent

IME1 is the transcription factor that dictates entry into meiosis in yeast. Thus, the expression of *IME1* directly regulates cell's decision to enter meiosis. Since deletions of Yap6, Sok2, and Phd1 affect *IME1* transcription (Figure 34), I hypothesised that the timing of meiotic entry should be altered in the mutant cells. Therefore, I examined how different transcription factor mutations affect initiation of meiosis. To study the kinetics of meiotic divisions in cells, I induced yeast cells to sporulate using the standard protocol and fixed cells at multiple time points after sporulation induction. I visualised the cell nuclei by DAPI staining, and scored the number of cells with one or more than one DAPI mass. Cells containing more than one DAPI mass would indicate that cells underwent nuclear divisions. In wild-type cells, nuclear divisions were observed from five to six hours after sporulation induction, and close to 90% of cells completed meiosis after 24 hours (Figure 35). The *sok2*Δ cells entered meiotic divisions much earlier, in which nuclear divisions were observed one hour after sporulation induction, while *yap6*Δ and *phd1*Δ cells displayed kinetics comparable to wild-type cells (Figure 35A). This is consistent with earlier data in this chapter that *sok2*Δ reduced Tup1 binding and de-repressed *IME1* prior to entry into meiosis (Figure 30, Figure 31, and Figure 34). I conclude that de-repression of *IME1* transcription prior to entry into meiosis in *sok2*Δ cells leads to early onset of meiosis.

Next, I examined cells bearing double and triple deletions of Yap6, Sok2, and Phd1. As expected, *yap6*Δ*sok2*Δ and *sok2*Δ*phd1*Δ cells displayed early entry into meiosis due to high levels of *IME1* transcripts prior to entry into meiosis (Figure 34 and Figure 35B). At two hours after sporulation induction, 56% of *yap6*Δ*sok2*Δ cells and 18% of *sok2*Δ*phd1*Δ cells underwent nuclear divisions. After 10 hours, almost all cells with *sok2*Δ*phd1*Δ or *yap6*Δ*sok2*Δ genotype were able to undergo meiotic divisions (97% for *sok2*Δ*phd1*Δ and 90.5% for *yap6*Δ*sok2*Δ). Prior to entry into meiosis, *yap6*Δ*phd1*Δ cells displayed *IME1* levels similar to wild-type and thus exhibited wild-type kinetics of meiotic divisions (Figure 34 and Figure 35B). Finally, *yap6*Δ*sok2*Δ*phd1*Δ cells underwent the fastest meiotic divisions, in which more than 80% of cells displayed nuclear divisions three hours after sporulation induction (Figure 35B). In comparison, 69.5% of *yap6*Δ*sok2*Δ and 62.4% of *sok2*Δ*phd1*Δ cells

underwent meiosis at the same time point. After five hours, over 90% of *yap6*Δ*sok2*Δ*phd1*Δ cells underwent meiotic divisions (Figure 35B). These observations are in agreement with earlier Tup1 ChIP and *IME1* expression data that Sok2 is the major contributor to Tup1-Cyc8 mediated *IME1* repression prior to entry into meiosis, while Yap6 and Phd1 play minor functions (Figure 30, Figure 31, and Figure 34). The differences in the onset of meiosis were marginal among *yap6*Δ*sok2*Δ, *sok2*Δ*phd1*Δ, and *yap6*Δ*sok2*Δ*phd1*Δ cells, likely because *IME1* was accumulated to high levels prior to meiotic entry in all three strains (Figure 34). Hence, these cells were committed to meiotic divisions as soon as nutrients were removed. Taken together, I conclude that *IME1* transcription is strongly de-repressed prior to entry into meiosis when Yap6, Sok2, and Phd1 are lost in cells. *IME1* accumulation in *yap6*Δ*sok2*Δ*phd1*Δ cells causes cells to enter and complete meiosis much faster than wild-type cells.

(A)

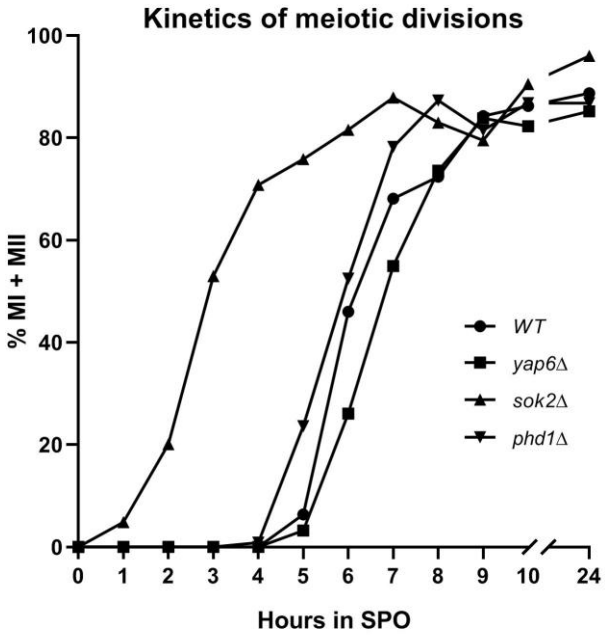

(B)

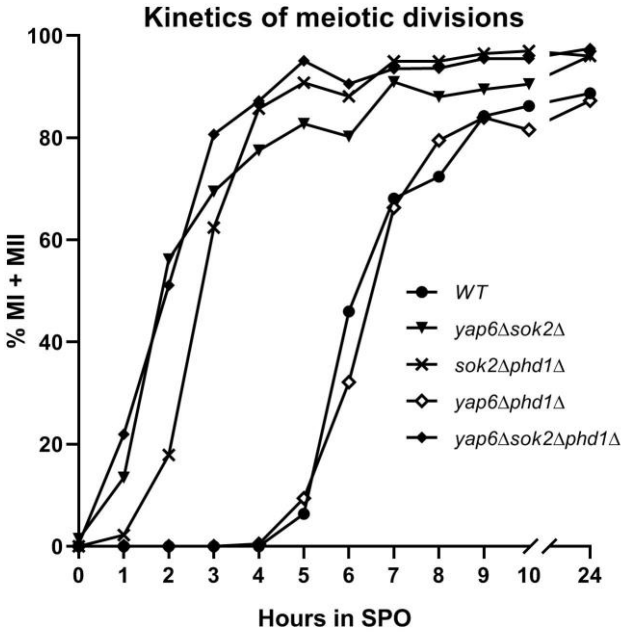

Figure 35. Onset of meiosis occurs much earlier in the absence of Sok2.

(A) Meiotic divisions determined in *WT* (FW3456), *yap6*Δ (FW3603), *sok2*Δ (FW3979), and *phd1*Δ (FW3991) cells. Cells in sporulation medium (SPO) were sampled at indicated time points, fixed, and stained with DAPI. Cells with two to four DAPI masses were considered as cells that underwent meiotic divisions (MI

+ MII). The percentage of cells that underwent meiotic divisions is presented for each time point. At least 200 cells were scored for each time point.

(B) Meiotic divisions determined in *WT* (FW3456), *yap6*Δ*sok2*Δ (FW4239), *sok2*Δ*phd1*Δ (FW4710), *yap6*Δ*phd1*Δ (FW4406), and *yap6*Δ*sok2*Δ*phd1*Δ (FW4010) cells by DAPI counting. The percentage of cells that underwent meiotic divisions (MI + MII) is presented for each time point. At least 200 cells were scored for each time point.

5.5 Yap6, Sok2, and Phd1 integrate nutrient signals to recruit Tup1 and thereby repress *IME1*

Tup1-Cyc8 acts as a signal integrator at the *IME1* promoter to ensure that *IME1* is only expressed when nutrients become deficient in the environment. As demonstrated by ChIP data in Chapter 3: Figure 14, Tup1-Cyc8 interacts with the *IME1* promoter in response to rich nutrients and leaves under starvation conditions. Furthermore, I showed that the binding of Tup1 at the *IME1* promoter is mediated by different nutrients present in the growth medium (Chapter 4: Figure 26B). Tup1 binding was the strongest in rich medium (YPD), lowest in sporulation medium, and intermediate in the presence of either glucose or rich nutrients including nitrogen compounds (YP). How Tup1-Cyc8 integrates different nutrient cues in the growth medium and interacts with the *IME1* upstream region was not understood.

So far, my data suggest that Yap6, Sok2, and Phd1 mediate Tup1-Cyc8 binding at the *IME1* promoter under certain, but not all nutrient conditions. Firstly, Yap6, Sok2, and Phd1 associate with the *IME1* promoter in nutrient-rich growth conditions and dissociate during nutrient starvation (Chapter 4: Figure 25). In this chapter, I also found that deletions of Yap6, Sok2, and Phd1 significantly reduce Tup1 binding and de-repress *IME1* expression prior to entry into meiosis, but not during exponential growth (Figure 31 and Figure 34). Furthermore, all three transcription factors display strong interaction with the *IME1* promoter in YP medium without glucose (YP + 0.05% Glc), thus they primarily respond to rich nutrients including nitrogen compounds (Chapter 4: Figure 26C). However, functional data of how different nutrients control Tup1-Cyc8 binding that is mediated by Yap6, Sok2, and Phd1 at the *IME1* promoter were lacking. Therefore, I examined how different nutrients control Tup1-Cyc8 binding by regulating Yap6, Sok2, and Phd1 recruitment. Specifically, I grew *yap6*Δ*sok2*Δ*phd1*Δ cells harbouring V5 epitope-tagged Tup1 in pre-sporulation medium (BYTA), and transferred cells to different nutrient conditions using the approach described in Chapter 4: Figure 26A. Tup1 binding was measured by ChIP-qPCR at the point of shift (SPO 0h), and in cells shifted to sporulation medium (SPO), glucose-only medium (SPO + 2% Glc), YP medium without glucose (YP + 0.05% Glc), and YPD medium (YP + 2% Glc) respectively. Remarkably, Tup1 binding in YP medium without glucose was completely lost in *yap6*Δ*sok2*Δ*phd1*Δ

cells, but was unaffected in glucose-only condition (Figure 36). Given that glucose is most abundant during the exponential growth phase, the data complement the finding that Tup1 binding is maintained in exponentially growing *yap6*Δ*sok2*Δ*phd1*Δ cells by other transcription factors (Figure 31). In contrast, glucose is not present prior to entry into meiosis, thus the data explain why Tup1 binding is lost in the absence of Yap6, Sok2, and Phd1 prior to meiotic entry. In conclusion, in nutrient-rich YPD medium, rich nutrients including nitrogen (YP) induce Tup1-Cyc8 recruitment by mediating binding of Yap6, Sok2, and Phd1 at the *IME1* promoter. Tup1-Cyc8 binding is also regulated by glucose through transcription factors that remain to be identified.

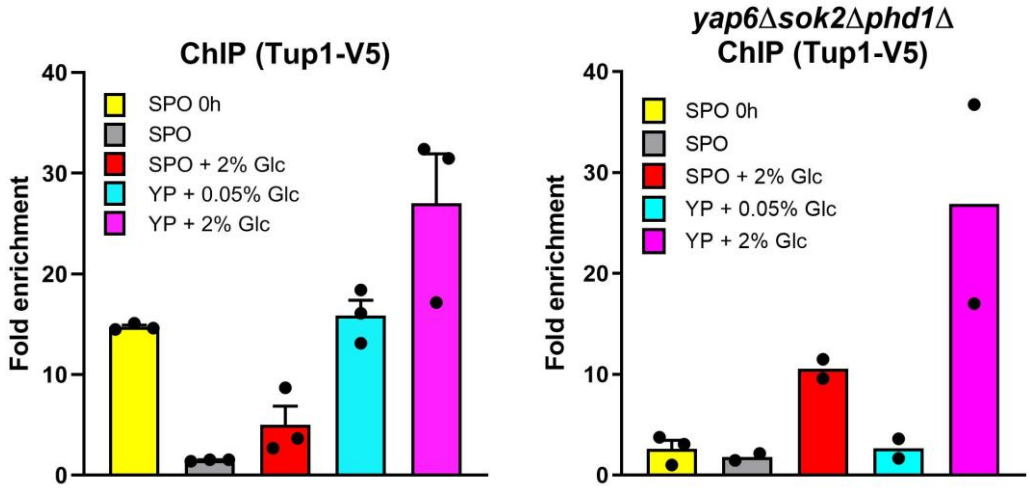

Figure 36. Rich nutrients including nitrogen, but not glucose regulate Yap6, Sok2, and Phd1 binding to modulate recruitment of Tup1 to the *IME1* promoter.

ChIP-qPCR of V5 epitope-tagged Tup1 in *WT* (FW3456) and *yap6*Δ*sok2*Δ*phd1*Δ (FW4010) cells prior to entry into meiosis (SPO 0h), and at 4 hours in sporulation medium (SPO), glucose-only medium (SPO + 2% Glc), YP medium without glucose (YP + 0.05% Glc), and YPD medium (YP + 2% Glc). For qPCR, a primer pair flanking 1000 bp upstream of the *IME1* start codon was used, and signals were normalised over the silent mating type cassette *HMR*. Bars represent mean, error bars represent SEM, and dots indicate individual biological replicates.

Previous study reported that the recruitment of Tup1 to the *IME1* upstream region depends on signals from the Ras/PKA and TORC1 pathways (Weidberg et al., 2016). How PKA and TORC1 mediate Tup1 binding to the *IME1* promoter was unknown. Given that Yap6, Sok2, and Phd1 integrate nutrient signals at the *IME1* promoter, I asked whether these three transcription factors are sensitive to PKA and TORC1 signals in nutrient-rich conditions. To study this question, I inhibited the PKA and TORC1 pathways and examined effects on the levels of the transcription factors. The catalytic subunits of the cAMP-dependent PKA in budding yeast are encoded by *TPK1*, *TPK2*, and *TPK3* which are functionally redundant (Toda et al., 1987). In this experiment, yeast cells possessed an analogue-sensitive *TPK1* (*tpk1-as*) allele whereas *TPK2* and *TPK3* were deleted from the genome. The compound 1NM-PP1 was added to inhibit the PKA pathway by blocking the modified Tpk1 active site. In addition, rapamycin was added to inhibit the TORC1 pathway. Cells expressing V5 epitope-tagged Yap6, Sok2, and Phd1 were treated with either or both inhibitors for six hours, and the transcription factors were detected and quantified by western blotting (Figure 37). In line with the western blot results presented in Chapter 4: Figure 27, Yap6 was weakly detected in untreated cells whereas Sok2 and Phd1 displayed strong protein expression (Figure 37). Yap6 expression drastically declined when either or both PKA and TORC1 pathways were inhibited (Figure 37A). For Sok2 and Phd1, inhibition of PKA signals led to substantial reduction in protein expression (Figure 37B and Figure 37C). This is not surprising given that Sok2 and Phd1 were both implicated as regulators in the PKA pathway (Ward et al., 1995, Malcher et al., 2011). Additionally, Phd1 responded to TORC1 inhibition as its level decreased by 40% when treated with rapamycin only (Figure 37C). Taken together, PKA and TORC1 signalling pathways regulate the cellular levels of Yap6, Sok2, and Phd1. Sok2 and Phd1 are mainly regulated by PKA, whereas Yap6 is regulated by both PKA and TORC1.

I found that the levels of Yap6, Sok2, and Phd1 detected during entry into meiosis (SPO 4h) were considerably higher than that detected when PKA and TORC1 were inhibited (Chapter 4: Figure 27 and Figure 37). One possibility is that Yap6, Sok2, and Phd1 respond to the partially active TORC1 pathway (Weidberg et al., 2016) and possibly residual PKA activity during induction of sporulation. Another possibility is that Yap6, Sok2, and Phd1 are regulated by PKA locally at the *IME1*

promoter. ChIP-chip studies have reported that the PKA catalytic subunits Tpk1 and Tpk2 interact with the chromatin in budding yeast (Pokholok et al., 2006), suggesting that PKA signals can act locally at the chromatin. Tpk1 was found to preferentially occupy genes that are glucose-sensitive, and shifting to a non-fermentable carbon source abolished the binding of Tpk1 (Pokholok et al., 2006). Given that *IME1* matches the profile of Tpk1 targets, Yap6, Sok2, and Phd1 might respond to local PKA signalling mediated by Tpk1 in nutrient-rich conditions. As cells enter nutrient starvation, loss of Tpk1 binding might trigger local loss of Yap6, Sok2, and Phd1 as indicated by the *tpk1-as* cells (Figure 37) but not in the whole cell. The binding of Sko1, a known physical interactor of Tpk1 (Ptacek et al., 2005) to the *IME1* promoter supports this hypothesis (Chapter 4: Figure 22). Further work is required to elucidate the mechanism of how PKA and TORC1 regulate the interaction of Yap6, Sok2, and Phd1 with the *IME1* promoter.

(A)

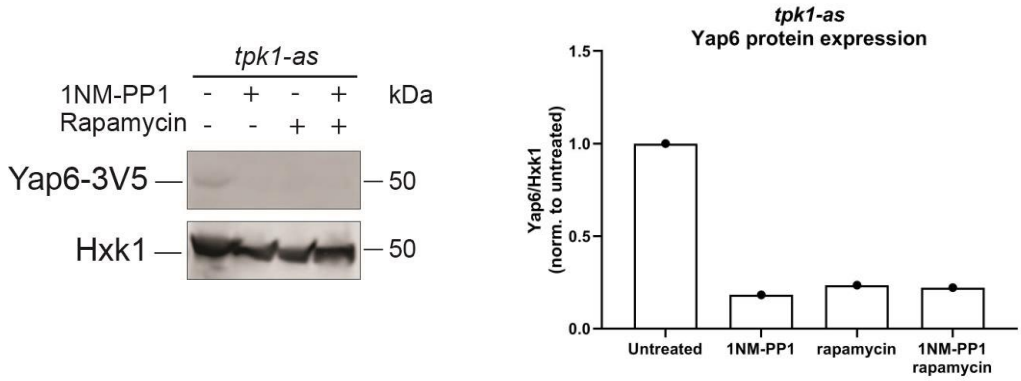

(B)

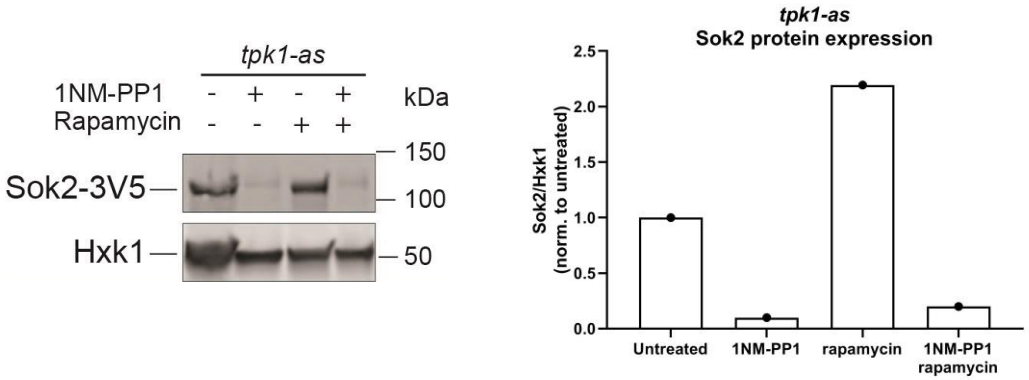

(C)

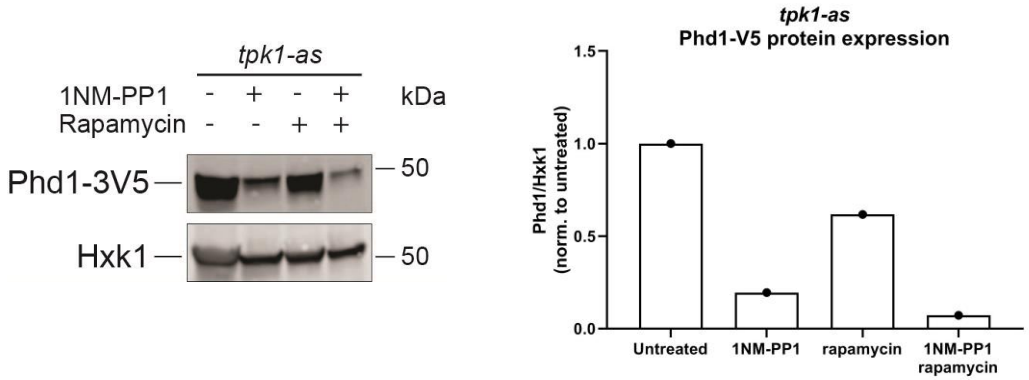

Figure 37. Protein expression of Yap6, Sok2, and Phd1 reduce upon inhibition of PKA and TORC1 signalling pathways.

Representative western blots and quantification data of (A) Yap6-V5 (FW5453), (B) Sok2-V5 (FW5454), and (C) Phd1-V5 (FW5528) in cells bearing the *tpk1-as* allele. Cells were treated with 1NM-PP1, rapamycin, or both. Protein levels were normalised over Hxk1 levels, and are presented as fold changes over untreated cells in the bar charts. Uncropped western blots can be found in Supplementary figure 12.

5.6 Chapter summary

In this chapter, I demonstrated that Tup1-Cyc8 associates with the *IME1* promoter by interacting with multiple redundant transcription factors that respond to distinct nutrient cues present in the environment. Three transcription factors, Yap6, Sok2, and Phd1 were found to bind strongly at the *IME1* promoter and recruit Tup1-Cyc8 to mediate *IME1* repression. When the three transcription factors are lost prior to entry into meiosis, Tup1-Cyc8 does not bind the *IME1* promoter, leading to accumulation of *IME1* and early entry into meiosis. In particular, Sok2 contributes most significantly to Tup1-Cyc8 mediated repression at the *IME1* promoter. Single deletion of Sok2 strongly reduces Tup1 binding at the *IME1* promoter before entry into meiosis. When *sok2*Δ is combined with *yap6*Δ or *phd1*Δ, Tup1 binding is further decreased at the *IME1* promoter, resulting in de-repression of *IME1* transcription prior to entry into meiosis. In comparison, Yap6 and Phd1 have mild effects on Tup1 recruitment when deleted alone or with each other. Notably, Sok2 deletion only moderately affects Tup1 recruitment and has a minimal impact on *IME1* repression in exponentially growing cells. *IME1* de-repression is more notable in *sok2*Δ*phd1*Δ and *yap6*Δ*sok2*Δ*phd1*Δ cells during exponential growth phase, highlighting the importance of transcription factors other than Sok2 in maintaining repression of *IME1* transcription. Yet, *IME1* transcription is only partially relieved in *yap6*Δ*sok2*Δ*phd1*Δ cells during exponential growth, implying that other transcription factors also contribute to Tup1-Cyc8 mediated repression.

In addition, I investigated whether Yap6, Sok2, and Phd1 mediate Tup1-Cyc8 recruitment in response to distinct nutrients in the growth medium. I found that Yap6, Sok2, and Phd1 associate with the *IME1* promoter in response to rich nutrients including nitrogen compounds (YP) in the growth medium, which in turn recruit Tup1-Cyc8. In glucose-deficient conditions like prior to entry into meiosis, nutrient sensitivity of Tup1 is completely dependent on Yap6, Sok2, and Phd1. In glucose-rich conditions such as the exponential growth phase, Tup1-Cyc8 recruitment is mediated by additional transcription factors that respond to glucose signals (Figure 38). Therefore, in exponentially growing cells, *yap6*Δ*sok2*Δ*phd1*Δ has little effect on Tup1-Cyc8 residency on the *IME1* promoter and only partially relieves *IME1* repression. Finally, Yap6, Sok2, and Phd1 may be implicated in PKA and TORC1

signal integration to modulate *IME1* repression, but the mechanism remains to be elucidated. In conclusion, Tup1-Cyc8 is recruited to the *IME1* promoter by multiple transcription factors. I propose that multiple redundant transcription factors mediating Tup1-Cyc8 binding is likely a mechanism to ensure that *IME1* is only expressed in an environment that is deprived of glucose and other rich nutrients including nitrogen compounds (Figure 38).

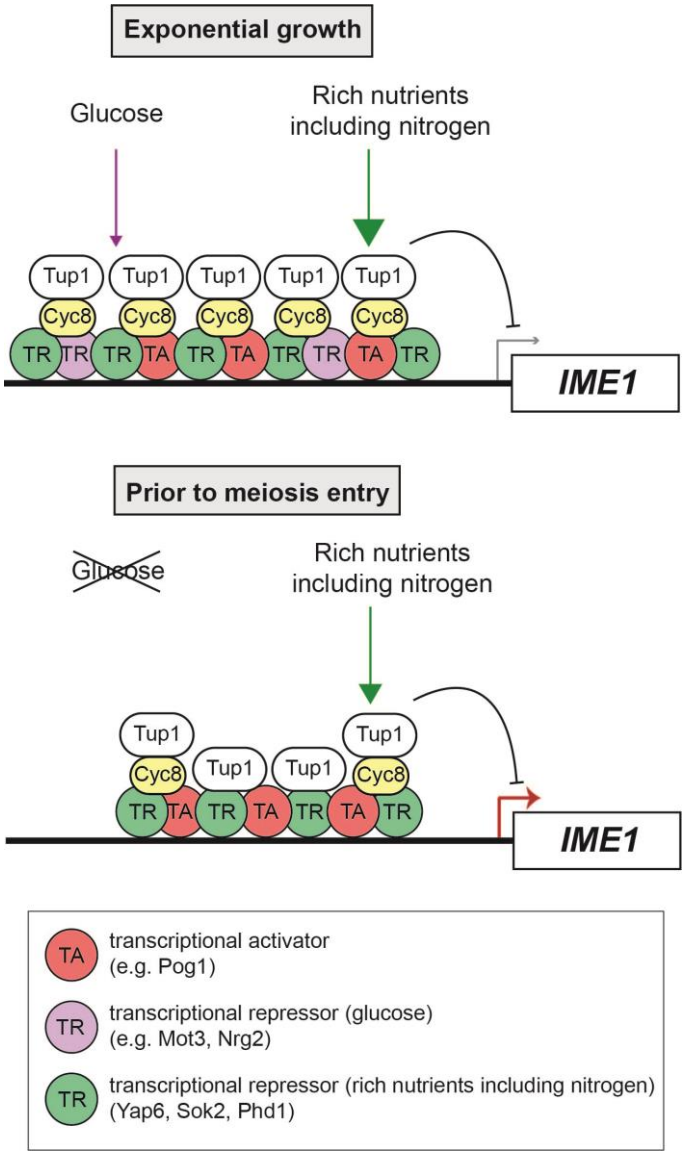

Figure 38. Yap6, Sok2, and Phd1 are recruited to the *IME1* promoter by rich nutrients including nitrogen compounds to mediate Tup1-Cyc8 binding.

Schematic diagram summarising the findings in this chapter. Tup1-Cyc8 is recruited to the *IME1* promoter by multiple redundant transcription factors that respond to glucose or rich nutrients including nitrogen compounds in nutrient-rich YPD medium. During exponential growth, Yap6, Sok2, and Phd1 are recruited to the *IME1* promoter by signals arising from rich nutrients including nitrogen, which in turn associate Tup1-Cyc8 to the *IME1* promoter. Other transcription factors that respond to glucose signals also contribute to Tup1-Cyc8 recruitment. Prior to entry into meiosis, glucose is absent in the medium and low levels of *IME1* transcripts can be detected. Rich nutrients including nitrogen compounds continue to mediate Tup1-Cyc8 recruitment

through Yap6, Sok2, and Phd1. Please note that the *IME1* promoter depicted in the diagram is not drawn to scale and only represents the region where Tup1-Cyc8 interacts, i.e. 750 to 1400 bp upstream of the start codon.

Chapter 6. Functional analyses of the sequence motifs important for Tup1-Cyc8 recruitment in the *IME1* promoter

Tup1-Cyc8 plays a crucial role in inhibiting entry into meiosis when nutrients are ample in the surrounding environment. In nutrient-rich condition, I propose that Tup1-Cyc8 inhibits the transcriptional activators bound at the *IME1* promoter, which remains poised for activation under the repressive condition (Chapter 3: Figure 17, Figure 18, and Figure 19). Nutrients stimulate the Ras/PKA and TORC1 signalling pathways that induce Tup1-Cyc8 to bind to the *IME1* promoter (Weidberg et al., 2016). Tup1-Cyc8 co-localises with transcriptional activator such as Pog1 at the *IME1* promoter (Weidberg et al., 2016) (Chapter 3: Figure 13 and Figure 19), and may act to repress *IME1* transcription by masking the activation domains of Pog1 (Wong and Struhl, 2011). Tup1-Cyc8 itself has no DNA-binding ability. In order to bind to the target promoter, the complex must interact with transcription factors that recognise DNA sequences in the promoter. In Chapter 4, I shortlisted 16 candidate transcription factors that interact with Tup1-Cyc8 and have binding sites predicted in the *IME1* promoter. Among the candidate transcription factors, I found nine transcription factors to bind the *IME1* promoter. Notably, binding of these transcription factors is regulated by different nutrients in the medium (Chapter 4: Figure 26C). This suggests that different transcription factors mediate Tup1-Cyc8 binding in different nutrient conditions. In addition, I discovered three transcription factors, Yap6, Sok2, and Phd1, to be important in repressing *IME1* when nutrients are present. Yap6, Sok2, and Phd1 respond to rich nutrients including nitrogen (YP) and recruit Tup1-Cyc8 to the *IME1* promoter. Sok2 has a major contribution in Tup1-Cyc8 recruitment prior to entry into meiosis, while Yap6 and Phd1 play supplementary functions (Chapter 5: Figure 30 and Figure 31). Strikingly, loss of Yap6, Sok2, and Phd1 altogether results in reduced Tup1 binding, *IME1* accumulation, and early entry into meiosis (Chapter 5: Figure 31, Figure 34, and Figure 35). Importantly, Tup1-Cyc8 recruitment at the *IME1* promoter requires additional transcription factors during exponential growth or in other glucose-containing conditions (Chapter 5: Figure 31 and Figure 36).

IME1 has one of the longest promoters in budding yeast (~2.3 kb), which is known to contain complex regulatory elements (Kahana et al., 2010). While previous studies have sought to decipher the DNA sequences in the *IME1* promoter (reviewed in Kassir et al., 2003), little is known about which DNA motifs are regulated by nutrients. In this chapter, I set out to investigate which DNA sequences in the *IME1* promoter are bound by Tup1-Cyc8. I examined the binding sites of the transcription factors that interact with Tup1-Cyc8 and bind to the *IME1* promoter. Since Yap6, Sok2, and Phd1 play important roles in recruiting Tup1-Cyc8, I propose that the Yap6, Sok2, and Phd1 binding sites mediate Tup1-Cyc8 recruitment at the *IME1* promoter. Furthermore, Tup1-Cyc8 co-localises with transcriptional activators and inhibits transcriptional activation of *IME1* in nutrient-rich condition (Chapter 3: Figure 18 and Figure 19). I hypothesised that Tup1-Cyc8 and transcriptional activators bind to the same DNA sequences in the *IME1* promoter. To explore this further, I carried out functional analyses of the DNA motifs in the *IME1* promoter to determine whether DNA sequences that are important for *IME1* repression are also needed for activation. I also tested whether transcription factors that interact with Tup1-Cyc8 can act as transcriptional activators. The goals of these analyses were to pinpoint the DNA sequences that recruit transcription factors which in turn mediate Tup1-Cyc8 binding, and dissect whether the same sequences are also important for *IME1* activation when Tup1-Cyc8 is removed.

6.1 Tup1-Cyc8 and *IME1* activators bind to the same part of the *IME1* upstream regulatory region

Tup1-Cyc8 binds to the *IME1* promoter in a region between 750 and 1400 base pairs (bp) upstream of the *IME1* start codon (Chapter 3: Figure 13) (Weidberg et al., 2016). In exponentially growing cells, at least one transcriptional activator of *IME1*, i.e. Pog1 binds to the *IME1* promoter where Tup1 binding is also detected (Chapter 3: Figure 19A). Since *IME1* is efficiently transcribed when Tup1 is removed (Chapter 3: Figure 18), I hypothesised that Tup1 inhibits the transcriptional activators bound to the same sites in exponentially growing cells. To test this hypothesis, I generated mutant strains with truncations in the *IME1* upstream region and examined the onset of meiotic divisions by DAPI counting. I assessed six heterozygous mutant strains that harboured one *ime1*Δ allele and a truncated *IME1* promoter in the other allele. The truncations of the *IME1* promoter start from 2315 bp upstream of the *IME1* start codon, and end at different points of the *IME1* promoter. The largest *IME1* promoter truncation spanned from 600 to 2315 bp upstream of the *IME1* start codon, while the smallest truncation spanned from 1600 to 2315 bp upstream. The intermediate *IME1* promoter truncations allow 200 bp intervals between 600 and 1600 bp upstream of the start codon to be examined (Figure 39A). The *pIME1*(*-600-2315*Δ) and *pIME1*(*-800-2315*Δ) mutants did not undergo meiotic divisions (Figure 39B). These data suggest that the region that is 800 bp upstream of the *IME1* start codon is insufficient for *IME1* activation. In contrast, the *pIME1*(*-1600-2315*Δ) and *pIME1*(*-1400-2315*Δ) cells underwent meiosis with comparable kinetics to the wild-type control strain (Figure 39B). These observations suggest that the promoter region between 800 and 1400 bp upstream of the *IME1* start codon contains important regulatory elements for *IME1* activation. In addition, about 20% of *pIME1*(*-1000-2315*Δ) cells displayed meiotic divisions (Figure 39B). The results of the *pIME1*(*-800-2315*Δ) and *pIME1*(*-1000-2315*Δ) cells indicate that essential regulatory elements are present in the *IME1* promoter between 800 and 1000 bp upstream of the *IME1* start codon. Furthermore, the *pIME1*(*-1200-2315*Δ) mutant displayed increased meiosis compared to *pIME1*(*-1000-2315*Δ) cells (Figure 39B). These results suggest that additional regulatory elements are present between 1000 and 1200 bp upstream of the *IME1* start codon (Figure 39B). Yet, *pIME1*(*-1200-2315*Δ) cells showed reduced meiosis compared to wild-type control cells (38.69% vs 60.5% at 24 hours) (Figure 39B). I conclude that

full *IME1* expression also requires the promoter region between 1200 and 1400 bp upstream of the *IME1* start codon.

Next, I further dissected the region between 800 and 1000 bp, and between 1200 and 1400 upstream of the *IME1* start codon. I generated additional mutants with smaller *IME1* promoter truncations within these regions. First, I examined the region between 800 and 1000 bp upstream of the *IME1* start codon at 50 bp intervals with the *pIME1*(*-850-2315*Δ), *pIME1*(*-900-2315*Δ), and *pIME1*(*-950-2315*Δ) truncations (Figure 39C). I found that the *pIME1*(*-850-2315*Δ), *pIME1*(*-900-2315*Δ), and *pIME1*(*-950-2315*Δ) cells underwent meiosis with comparable kinetics and efficiency. Thus, the region between 800 and 850 bp upstream of the *IME1* start codon contains important regulatory elements for *IME1* activation. Additionally, cells bearing smaller truncations between 1200 and 1400 bp upstream of the *IME1* start codon (*pIME1*(*-1250-2315*Δ) and *pIME1*(*-1350-2315*Δ)) underwent slower meiosis in comparison with the wild-type control (Figure 39C). Therefore, full *IME1* activation also requires sequences up to 1400 bp upstream of the *IME1* start codon.

Taken together, full *IME1* activation requires the 600 bp interval between 800 and 1400 bp upstream of the *IME1* start codon. The response elements critical for *IME1* activation overlap with sequences that bind Tup1-Cyc8, implying that this part of the *IME1* promoter is essential for regulating *IME1* transcription.

(A)

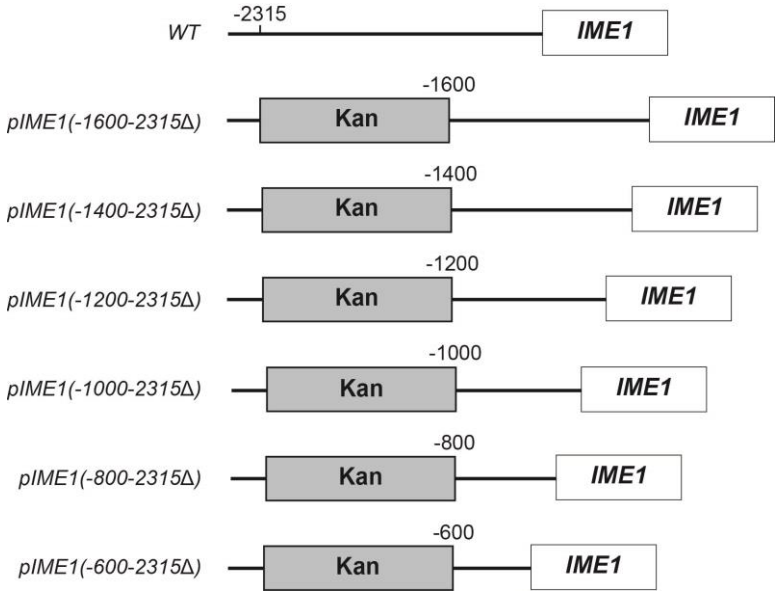
WT
-2315
IME1
pIME1(-1600-2315Δ)
-1600
Kan
IME1
pIME1(-1400-2315Δ)
-1400
Kan
IME1
pIME1(-1200-2315Δ)
-1200
Kan
IME1
pIME1(-1000-2315Δ)
-1000
Kan
IME1
pIME1(-800-2315Δ)
-800
Kan
IME1
pIME1(-600-2315Δ)
-600
Kan
IME1

(B)

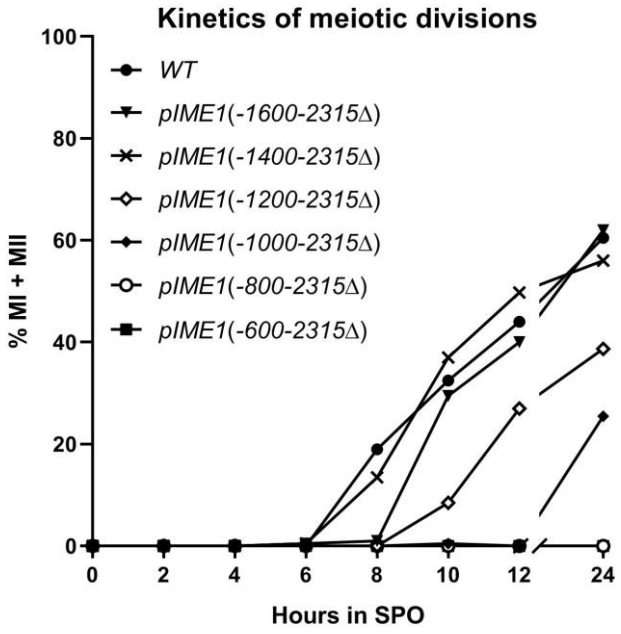
Kinetics of meiotic divisions
WT
pIME1(-1600-2315Δ)
pIME1(-1400-2315Δ)
pIME1(-1200-2315Δ)
pIME1(-1000-2315Δ)
pIME1(-800-2315Δ)
pIME1(-600-2315Δ)
% MI + MII
100
80
60
40
20
0
0
2
4
6
8
10
12
24
Hours in SPO

(C)

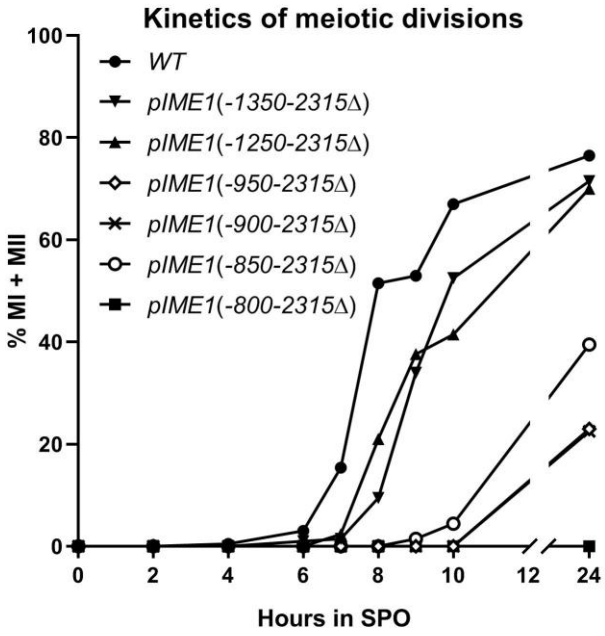

Figure 39. *IME1* promoter regions bound by the Tup1-Cyc8 repressor complex are also important for transcriptional activation of *IME1*.

(A) Schematic diagram depicting the structures of the *IME1* promoters in the truncation mutants. The coordinates of the starting and ending points of the truncations are indicated in the figure. Kan = kanamycin resistance cassette.

(B) Meiotic divisions determined in cells harbouring one *ime1*Δ allele and a truncated *IME1* promoter in the other allele. The promoter truncations assessed include *pIME1*(*-1600-2315*Δ) (FW3946), *pIME1*(*-1400-2315*Δ) (FW3947), *pIME1*(*-1200-2315*Δ) (FW3948), *pIME1*(*-1000-2315*Δ) (FW3949), *pIME1*(*-800-2315*Δ) (FW3950), and *pIME1*(*-600-2315*Δ) (FW3951). Control wild-type strain contained only one intact *IME1* allele (FW4128). Cells in sporulation medium (SPO) were sampled at indicated time points, fixed, and stained with DAPI. Cells with two to four DAPI masses were considered as cells that underwent meiotic divisions (MI + MII). The percentage of cells that underwent meiotic divisions (MI + MII) is presented for each time point. At least 200 cells were assessed for each time point.

(C) Same as (B) but promoter truncations assessed were *pIME1*(*-1350-2315*Δ) (FW4781), *pIME1*(*-1250-2315*Δ) (FW4780), *pIME1*(*-950-2315*Δ) (FW4779), *pIME1*(*-900-2315*Δ) (FW4778), *pIME1*(*-850-2315*Δ) (FW4777), and *pIME1*(*-800-2315*Δ) (FW3944). Control wild-type strain contained one intact *IME1* allele (FW4128). The percentage of cells that underwent meiotic divisions (MI + MII) is

presented for each time point. At least 200 cells were assessed for each time point.

6.2 Binding motifs of transcription factors that interact with Tup1-Cyc8 contain activating elements of *IME1* transcription

In Chapter 4: Figure 22, I identified nine sequence-specific transcription factors that co-localise with Tup1-Cyc8 at the *IME1* promoter. These nine transcription factors are Cup9, Yap6, Sok2, Phd1, Sut1, Mot3, Sko1, Nrg1, and Nrg2. In addition, these nine transcription factors were known or implicated to interact with the Tup1-Cyc8 complex. To test whether the transcription factors recruit Tup1 by binding to specific sequence motifs in the *IME1* promoter, I set out to investigate the contribution of the transcription factor binding sites to Tup1 binding. I employed a strategy that involved the use of single-copy integration plasmids. Single-copy integration plasmid ensures that the linearised plasmid can only incorporate into the genome once during transformation. This is important for the study of *IME1* expression and entry into meiosis, as *IME1* functions in a dosage-dependent manner. In my experiments, I used a single-copy integration plasmid that contained the upstream and downstream untranslated regions (UTRs) of *TRP1* (Figure 40A). In between the *TRP1* UTRs, I cloned the full-length *IME1* promoter and *IME1* gene tagged with *sfGFP* into the plasmid. Once expressed, sfGFP-Ime1 can be visualised and quantified easily to monitor Ime1 expression. The plasmid was then linearised to release the fragment containing *pIME1-sfGFP-IME1*, and integrated into the *TRP1* locus of a strain that lacked the endogenous *IME1* gene and promoter. Since there is only one *TRP1* locus in the yeast genome, only one copy of *pIME1-sfGFP-IME1* should be integrated into the genome during transformation. The strain also expressed Tup1 tagged with three copies of the V5 epitope to measure Tup1 binding at the *IME1* promoter.

It was essential to confirm that the *IME1* promoter integrated at the *TRP1* locus reflected the regulation at the endogenous *IME1* locus. I characterised Tup1 recruitment and meiosis kinetics in cells with wild-type *IME1* promoter and *IME1* gene integrated at the *TRP1* locus (*pIME1-WT*) (Figure 40C and Figure 40D). The levels of Tup1 binding detected in wild-type cells (*WT*) and *pIME1-WT* cells using the same primer pair were comparable. The onset of meiosis, rate of meiotic divisions and percentage of cells that underwent meiosis were also comparable in *WT* and

pIME1-WT cells. Hence, the integrated *IME1* promoter exhibited characteristics of the endogenous *IME1* promoter.

Next, I used the same strategy to study individual transcription factor binding motifs in the *IME1* promoter by introducing binding site mutations. I examined the region between 700 and 1100 bp upstream of the *IME1* start codon, since this region is strongly bound by Tup1-Cyc8 and contains most predicted transcription factor binding sites (Supplementary figure 13). To incorporate binding site mutations into this region, a short oligo (500 bp) corresponding to 701 to 1100 bp upstream of *IME1* with mutated sequences was commercially synthesised, and incorporated into the *IME1* promoter on the single-copy integration plasmid. This approach allowed easy and fast generation of *IME1* promoters with multiple mutated binding sites. I examined whether the predicted binding motifs of the Tup1-Cyc8 interacting transcription factors that bind to the *IME1* promoter contribute to Tup1 binding. Using the information curated in Chapter 4: Table 2, I mutated key nucleotides in the predicted transcription factor binding sites in the *IME1* promoter. By doing so, I modified 103 nucleotides between 700 and 1100 bp upstream of the *IME1* start codon (Supplementary figure 15). Yeast cells carrying the *IME1* promoter with transcription factor binding sites mutations (*pIME1-bs*∆) were inspected. I found that binding of Tup1 to the *IME1* promoter was lost in *pIME1-bs*∆ cells during exponential growth (Figure 40C). These data suggest that the putative binding sites of the identified transcription factors are required for recruiting Tup1. I then measured *IME1* expression in *pIME1-WT* and *pIME1-bs*∆ cells. I used smFISH to detect *IME1* transcripts, as it is a more sensitive method than RT-qPCR. The smFISH data indicate that there was little difference in *IME1* transcription between the *pIME1-WT* and *pIME1-bs*∆ promoters in nutrient-rich condition (Figure 40E and Figure 40F). In earlier chapter (Chapter 3), I demonstrated that depletion of Tup1 in nutrient-rich condition leads to substantial de-repression of *IME1* transcription (Chapter 3: Figure 18). Although Tup1 binding was not detected at the *pIME1-bs*∆ promoter in nutrient-rich condition, much less *IME1* transcripts were detected compared to Tup1 depletion. These observations suggest that the binding site mutations in the *pIME1-bs*∆ cells also affected transcriptional activation. Furthermore, I inspected *IME1* transcription in *pIME1-WT* and *pIME1-bs*∆ cells in sporulation inducing conditions (SPO) (Figure 40G). For sporulation conditions, I measured *IME1* transcription by RT-qPCR since *IME1* is expressed at much higher levels. I found that *IME1*

activation was also delayed in *pIME1-bs*Δ cells during sporulation induction. Consistent with the RT-qPCR results, sfGFP-Ime1 signals were lower in *pIME1-bs*Δ cells during sporulation induction (Figure 40H). As a result, meiosis was affected in *pIME1-bs*Δ cells (Figure 40D).

I conclude that Tup1-Cyc8 binding to the *IME1* promoter depends on DNA sequence motifs of transcription factors that interact with Tup1-Cyc8. My data further suggest that the transcription factors directly bind to the *IME1* promoter and mediate the recruitment of Tup1-Cyc8. In addition, the binding motifs of these transcription factors are also required for full activation of *IME1*, suggesting that the promoter response elements possess both repressing and activating potential.

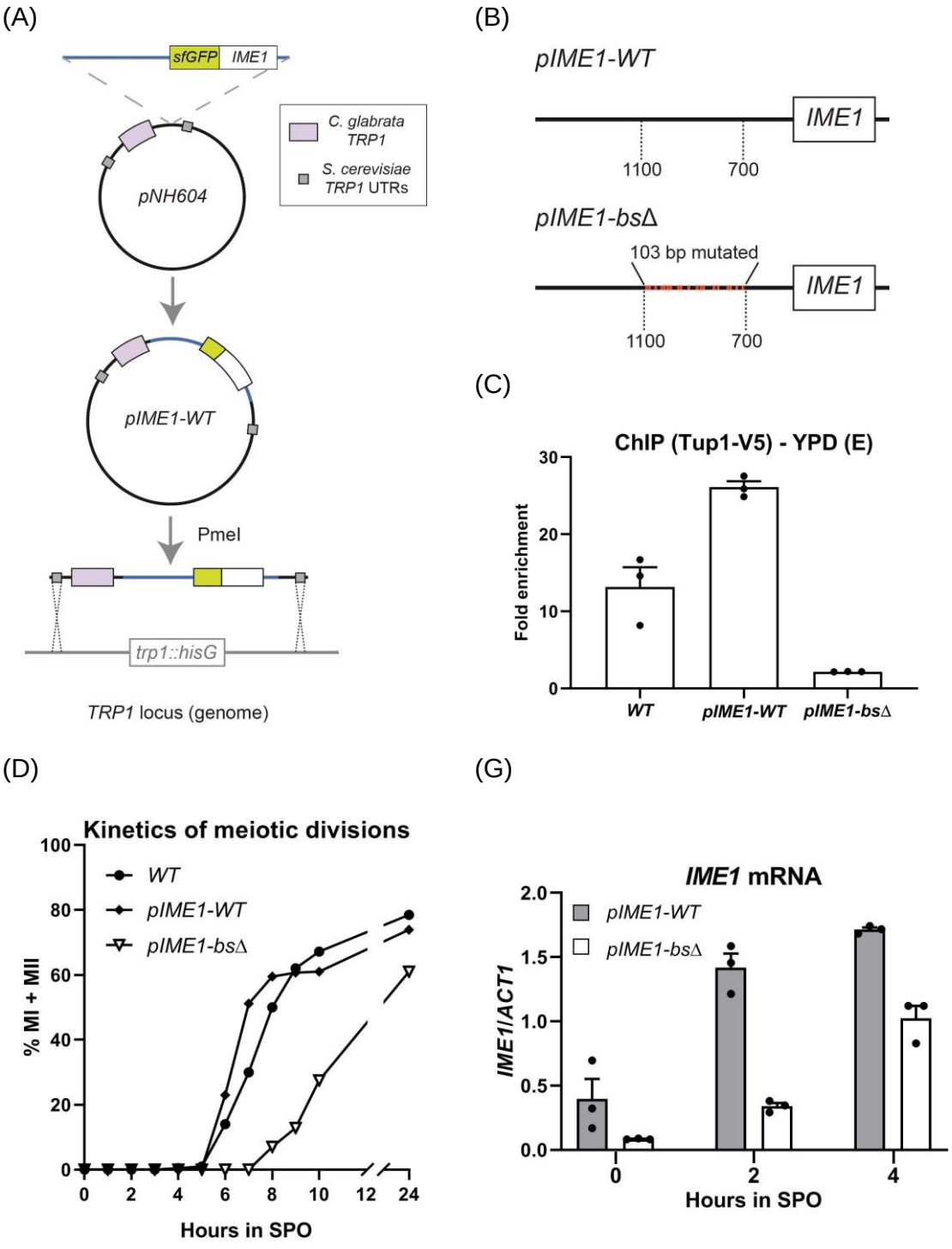
(A)
sfGFP
IME1
C. glabrata TRP1
S. cerevisiae TRP1 UTRs
pNH604
pIME1-WT
PmeI
trp1::hisG
TRP1 locus (genome)
(B)
pIME1-WT
IME1
1100
700
pIME1-bsΔ
103 bp mutated
IME1
1100
700
(C)
ChIP (Tup1-V5) - YPD (E)
Fold enrichment
30
20
10
0
WT
pIME1-WT
pIME1-bsΔ
(D)
Kinetics of meiotic divisions
% MI + MII
100
80
60
40
20
0
WT
pIME1-WT
pIME1-bsΔ
0
2
4
6
8
10
12
24
Hours in SPO
(G)
IME1 mRNA
IME1/ACT1
2.0
1.5
1.0
0.5
0.0
pIME1-WT
pIME1-bsΔ
0
2
4
Hours in SPO

(E)

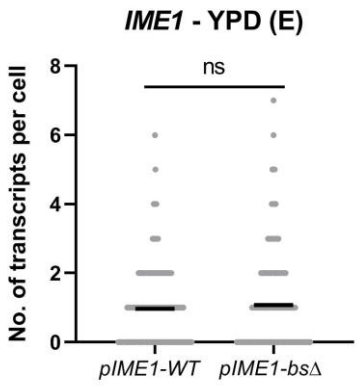
IME1 - YPD (E)
ns
No. of transcripts per cell
8
6
4
2
0
pIME1-WT
pIME1-bsΔ

(F)

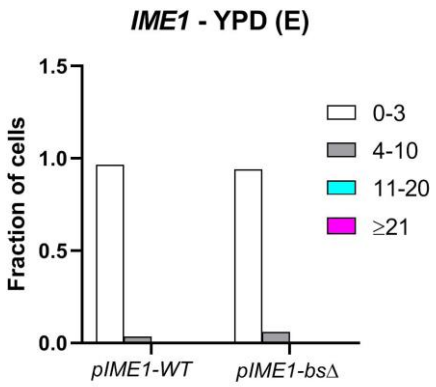
IME1 - YPD (E)
Fraction of cells
1.5
1.0
0.5
0.0
0-3
4-10
11-20
≥21
pIME1-WT
pIME1-bsΔ

(H)

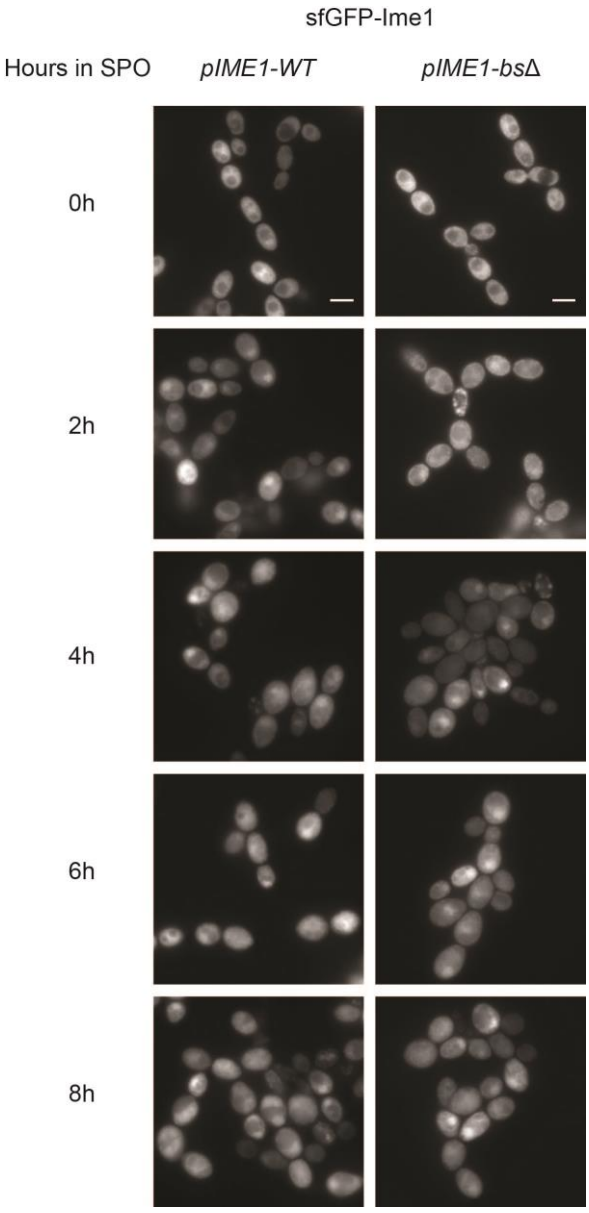
sfGFP-Ime1
Hours in SPO
pIME1-WT
pIME1-bsΔ
0h
2h
4h
6h
8h

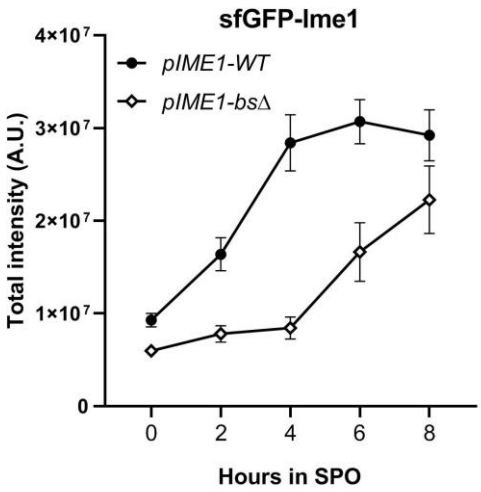
sfGFP-Ime1
pIME1-WT
pIME1-bsΔ
Total intensity (A.U.)
4×10⁷
3×10⁷
2×10⁷
1×10⁷
0
0
2
4
6
8
Hours in SPO

Figure 40. Mutating binding motifs of Yap6, Sok2, Phd1, Mot3, Sko1, Nrg1, and Nrg2 reduces Tup1 binding and delays *IME1* activation.

(A) Schematic diagram depicting the experimental workflow of the single-copy integration plasmid cloning strategy. Fragment containing full-length *IME1* promoter, *sfGFP*, and *IME1* was incorporated into the single-copy integration plasmid *pNH604*. The resulting *pIME1-WT* plasmid (*pFW506*) was linearised with PmeI and was integrated into the *TRP1* locus of the yeast genome.

(B) Schematic diagram representing the *IME1* promoter in the *pIME1-bs*Δ mutant. Number of mutated nucleotides is stated. Red = mutated nucleotides.

(C) ChIP-qPCR of V5 epitope-tagged Tup1 in *WT* (FW3456), *pIME1-WT* (FW5370), and *pIME1-bs*Δ (FW5372) cells. Tup1 binding was determined in exponentially growing cells (YPD (E)). A primer pair that amplifies 1000 bp upstream of the *IME1* start codon was used for qPCR. ChIP signals were normalised over the silent mating type cassette *HMR*. Bars represent mean (SEM) and dots denote individual biological replicates.

(D) Meiotic divisions determined in *WT* (FW3456), *pIME1-WT* (FW5370), and *pIME1-bs*Δ (FW5372) cells in sporulation medium (SPO) by DAPI counting. The percentage of cells that underwent meiotic divisions (MI + MII) is presented for each time point. At least 200 cells were scored for each time point.

(E) Scatter dot plot representing number of *IME1* transcripts detected per cell in *pIME1-WT* (FW5370) and *pIME1-bs*Δ (FW5372) cell populations by smFISH during exponential growth (YPD (E)). At least 50 cells that were positive for *ACT1* were analysed for each population. The black line represents the mean number of *IME1* transcripts per cell in the population. Unpaired parametric two-tailed Welch's t-test was performed between *pIME1-WT* and *pIME1-bs*Δ cells with 95% confidence. P-values are indicated in the graph, where ns stands for non-significant, * = ≤ 0.05, ** = ≤ 0.01, *** = ≤ 0.001.

(F) Histogram representing the same data shown in (E) binned into intervals by the number of *IME1* transcripts in cells. The data were binned into four intervals corresponding to 0-3, 4-10, 11-20, and 21 or more *IME1* transcripts per cell. Each bar represents the fraction of the cell population falling into that division.

(G) *IME1* transcript levels detected by RT-qPCR in *pIME1-WT* (FW5370) and *pIME1-bs*Δ (FW5372) cells in SPO at 0, 2, and 4 hours. Primers amplifying +850 bp of the *IME1* ORF were used for qPCR, and signals were normalised over actin

ACT1. Bars represent mean (SEM) and dots indicate individual biological replicates.

(H) Representative widefield microscopy images and quantification of sfGFP-Ime1 expression in *pIME1-WT* (FW5370) and *pIME1-bs*Δ (FW5372) cells in SPO. Cells in SPO were sampled at indicated time points, fixed with formaldehyde, and imaged. Scale bars indicate 5μm. The mean ± 95% CI of total sfGFP signals detected in 50 cells is presented for each time point.

6.3 Yap6, Sok2, and Phd1 binding motifs mediate Tup1 binding and transcriptional activation of *IME1*

In the last section (Figure 40), I showed that the putative binding sites of the transcription factors that interact with Tup1-Cyc8 are responsible for recruiting Tup1 to the *IME1* promoter. Next, I examined the contribution of the binding sites of different transcription factors to Tup1-Cyc8 recruitment and *IME1* expression. I aimed to pinpoint the DNA sequences in the *IME1* promoter that mediate Tup1-Cyc8 binding, and deduce which motifs are also required for *IME1* activation. I restored different transcription factor binding sites in the *pIME1-bs*Δ promoter and measured whether there was a gain in Tup1 binding by ChIP-qPCR. First, I replaced the mutated sites of Yap6, Sok2, Phd1, Nrg1, or Sko1 in the *pIME1-bs*Δ promoter with the wild-type DNA motif sequences. Thus, the remaining DNA motifs remained mutated in the promoters. Overall, I generated five *IME1* promoter constructs: *pIME1-bsΔyap6*, *pIME1-bsΔsok2*, *pIME1-bsΔphd1*, *pIME1-bsΔnrg1*, and *pIME1-bsΔsko1* in Figure 41. The sequences of these constructs can be found in Supplementary figure 16 to Supplementary figure 20. My ChIP data reveal that restoration of the consensus Yap6, Sok2, and Phd1 binding sites markedly rescued Tup1 recruitment at the *IME1* promoter (Figure 41A). In contrast, constructs that harboured the Nrg1 and Sko1 consensus binding sites showed a very minor increase in Tup1 binding (Figure 41A). Nrg2 binds to the reverse complementary sequence of the Nrg1 consensus binding motif (Nrg1: GGACCCT, Nrg2: AGGGTCC), thus the result of *pIME1-bsΔnrg1* is representative of having Nrg1 and Nrg2 sites reinstated in the *pIME1-bs*Δ promoter. These data suggest that the Yap6, Sok2, and Phd1 binding sites in the *IME1* promoter are sufficient for recruiting Tup1-Cyc8.

In light of the minor Tup1 recruitment at the *pIME1-bsΔnrg1* and *pIME1-bsΔsko1* promoters, more biological replicates are required to determine whether the binding is reproducible. Further work is also required to understand whether the restored sites in these promoters contribute to Tup1-Cyc8 binding. One possibility is that the restored sites did not successfully rescue binding of Nrg1, Nrg2, and Sko1. In my experiments, I did not measure the binding of Nrg1, Nrg2, and Sko1 on the promoter constructs. It is possible that the promoter constructs only rescued low levels of transcription factor binding, thus their contribution to Tup1-Cyc8 binding was

not fully represented. Another possibility is that the Nrg1, Nrg2, and Sko1 binding sites mediate Tup1-Cyc8 binding in conjunction with other binding sites. Previous study demonstrated that transcription factor binding sites with weaker affinity for Tup1-Cyc8 play auxiliary roles to binding sites that bind Tup1-Cyc8 strongly (Mathias et al., 2004). Whether the Nrg1, Nrg2, and Sko1 binding sites play auxiliary roles to strong Tup1-Cyc8 binding sites in the *IME1* promoter, such as the Yap6, Sok2, and Phd1 motifs, remains to be investigated.

Next, I measured meiosis in cells with *pIME1-bsΔyap6*, *pIME1-bsΔsok2*, *pIME1-bsΔphd1*, *pIME1-bsΔnrg1*, and *pIME1-bsΔsko1* constructs. I determined meiosis by DAPI counting (Figure 41B and Figure 41C). Cells harbouring Yap6, Sok2, and Phd1 putative binding sites showed improved ability to undergo meiosis (Figure 41B). Conversely, the kinetics of meiosis in cells with *pIME1-bsΔnrg1* and *pIME1-bsΔsko1* constructs were similar to that with *pIME1-bsΔ* (Figure 41C). These data implicate how the Yap6, Sok2, Phd1, Sko1, Nrg1, and Nrg2 sites may regulate Tup1-Cyc8 binding and *IME1* activation. The improved meiosis observed in cells with *pIME1-bsΔyap6*, *pIME1-bsΔsok2*, *pIME1-bsΔphd1* indicate that the Yap6, Sok2, and Phd1 putative binding sites have activation potential. Interestingly, I noted that restoring the consensus binding motifs of the paralogous Sok2 or Phd1 at the mutated *IME1* promoter (*pIME1-bsΔsok2* and *pIME1-bsΔphd1*) largely improved onset of meiosis to near wild-type kinetics (Figure 41B). Yet, Tup1 recruitment was almost fully restored in *pIME1-bsΔsok2* cells but was only partially restored in *pIME1-bsΔphd1* cells (Figure 41A). As paralogues, Sok2 and Phd1 share similar consensus binding motifs (Table 2). However, some sequences in the *IME1* promoter were predicted to match the consensus motif of one transcription factor but not the other. For example, Sok2, but not Phd1, has a predicted binding site at 1030 to 1035 bp upstream of the start codon (Supplementary figure 16 and Supplementary figure 17). Overall, three of the restored sites in the *pIME1-bsΔsok2* promoter construct are also found in the *pIME1-bsΔphd1* construct. I propose that these overlapped sites are important for *IME1* activation and likely some level of Tup1 recruitment, while the other sites present in the *pIME1-bsΔsok2* but not the *pIME1-bsΔphd1* construct also contribute to Tup1 binding.

Assume that Yap6, Sok2, and Phd1 do bind to their putative binding sites, I propose two models that explain how these sites contribute to transcriptional activation, based on previously reported Tup1-Cyc8 models (Mathias et al., 2004, Wong and Struhl, 2011). In the first model, transcriptional repressors and activators of *IME1* are two separate groups of transcription factors. In nutrient-rich condition, Yap6, Sok2, and Phd1 bind to the *IME1* promoter and mediate Tup1-Cyc8 binding to repress *IME1*. When sporulation is induced, Yap6, Sok2, and Phd1 dissociate from the *IME1* promoter, allowing the promoter-bound transcriptional activators such as Pog1 to induce *IME1* transcription and entry into meiosis. In the second model, transcriptional repressors and activators of *IME1* are the same proteins. This model postulates that Yap6, Sok2, and Phd1 act as repressors by mediating Tup1-Cyc8 in nutrient-rich condition, and transform into activators when nutrients are depleted. I speculated that the former model is more likely to be true, since the binding of Yap6, Sok2, and Phd1 is lost during entry into meiosis (Chapter 4: Figure 25). To determine which model is true, I examined whether Yap6, Sok2, and Phd1 have the ability to activate *IME1* transcription and the results are presented in the next section (Figure 44). Whether the putative Sko1, Nrg1, and Nrg2 binding sites mediate Tup1-Cyc8 binding and *IME1* activation in co-operation with other DNA sequences in the *IME1* promoter remains elusive.

(A)

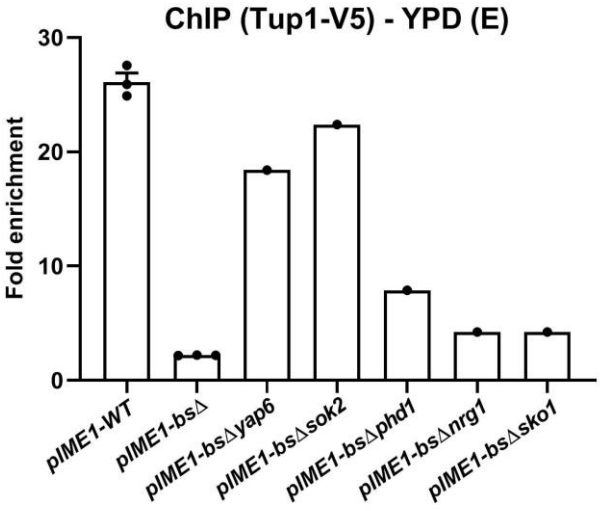

(B)

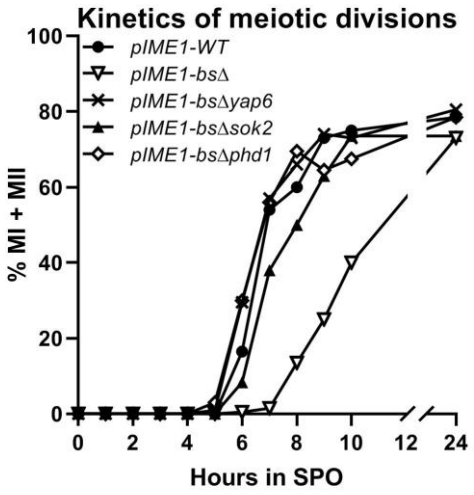

(C)

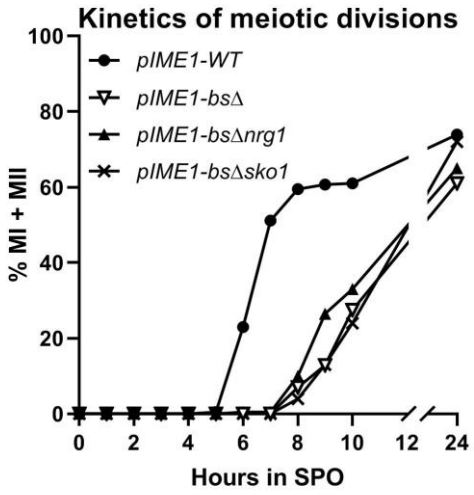

Figure 41. Yap6, Sok2, and Phd1 consensus motifs mediate both repression and activation of *IME1*.

(A) ChIP-qPCR of V5 epitope-tagged Tup1 in cells harbouring *IME1* promoter constructs that were partially rescued from *pIME1-bs*Δ. Cells were harvested during exponential growth (YPD (E)). The promoter constructs carried restored consensus motifs of Yap6 (*pIME1-bs*Δ*yap6*) (FW5694), Sok2 (*pIME1-bs*Δ*sok2*) (FW5800), Phd1 (*pIME1-bs*Δ*phd1*) (FW5696), Nrg1 (*pIME1-bs*Δ*nrg1*) (FW7092), and Sko1 (*pIME1-bs*Δ*sko1*) (FW7074) as indicated in Supplementary figure 13. Sequences of the promoter constructs can be found in Supplementary figure 16 to Supplementary figure 20. Tup1-V5 binding was also detected in *pIME1-WT*

(FW5370) and *pIME1-bs*Δ (FW5372) cells. A primer pair flanking 1000 bp upstream of the *IME1* start codon was used for qPCR. ChIP signals were normalised over the silent mating type cassette *HMR*. Bars represent mean (SEM) and dots denote individual biological replicates.

(B) Meiotic divisions determined in *pIME1-WT* (FW5370), *pIME1-bs*Δ (FW5372), *pIME1-bs*Δ*yap6* (FW5694), *pIME1-bs*Δ*sok2* (FW5800), and *pIME1-bs*Δ*phd1* (FW5696) cells by DAPI counting. The percentage of cells that underwent meiotic divisions (MI + MII) is presented for each time point. At least 200 cells were scored per time point.

(C) Meiotic divisions determined in *pIME1-WT* (FW5370), *pIME1-bs*Δ (FW5372), *pIME1-bs*Δ*nrg1* (FW7092), and *pIME1-bs*Δ*sko1* (FW7074) cells by DAPI counting. The percentage of cells that underwent meiotic divisions (MI + MII) is presented for each time point. At least 200 cells were scored per time point.

In Chapter 5, I reported that Yap6, Sok2, and Phd1 contribute significantly to Tup1-Cyc8 mediated repression of *IME1*. I showed that in *yap6*Δ*sok2*Δ*phd1*Δ cells, Tup1 binding was markedly reduced in acetate-containing medium (Chapter 5: Figure 31). Consequently, *IME1* transcripts accumulated, and cells entered meiosis earlier than wild-type cells (Chapter 5: Figure 34 and Figure 35). Furthermore, the consensus binding sites of Yap6, Sok2, and Phd1 are also important for both Tup1-Cyc8 recruitment and *IME1* activation (Figure 41A and Figure 41B). Yap6, Sok2, and Phd1 bind to more than one type of sequence motif in the *IME1* promoter, as predicted by the YeTFaSCo database (de Boer and Hughes, 2012). Yap6 is one of the Yeast Activator (AP1-like) Proteins (Yap) that is known to predominantly bind to Yap response element adjacent (YRE-A) (Kuo et al., 2010), TTACGTAA from structural evidence and various ChIP-chip analyses (Fujii et al., 2000, MacIsaac et al., 2006, Chen et al., 2008, Tan et al., 2008). In the region between 700 to 1100 bp upstream of *IME1*, there is one TTATGTAA site (-837-844) that matches the YRE-A motif. Another Yap6 site was predicted at a TGTGCCT motif (-1006-1012), which was computationally predicted from ChIP-chip data (Reddy et al., 2007). Sok2 and Phd1 are paralogous transcription factors sharing 82% homology in their binding domains (Ward et al., 1995). Sok2 and Phd1 recognise consensus helix-loop-helix motifs (Pan and Heitman, 2000). As expected, the DNA-binding motifs curated for Sok2 and Phd1 are highly similar. Both transcription factors interact with MTGCA and AGGCAM motifs, in which M represents A or C (Harbison et al., 2004, MacIsaac et al., 2006, Zhao et al., 2009, Badis et al., 2008). Based on the prediction of Sok2 sites, five sequences with close match to MTGCA and two sequences with close match to AGGCAM exist between 700 and 1100 bp upstream of the *IME1* start codon. To further dissect whether Tup1-Cyc8 binding depends on all four types of binding motifs, I decided to study the contribution from each sequence motif separately. I studied the functions of these binding motifs by replacing the mutated sequences in the *pIME1-bs*Δ construct with the wild-type sequences. I generated four new *IME1* promoter constructs (*pIME1-bs*Δ*1*, *pIME1-bs*Δ*2*, *pIME1-bs*Δ*3*, and *pIME1-bs*Δ*4*) and the restored sites are described in Figure 42A. Only *pIME1-bs*Δ*1* and *pIME1-bs*Δ*3* displayed Tup1 binding at the *IME1* promoter (Figure 42B). This suggests that TTATGTAA (-837-844) and the sequences matching MTGCA directly bind Tup1-Cyc8 recruiting transcription factors. Furthermore, TGTGCCT (-1006-1012) and motifs matching AGGCAM by themselves are insufficient to mediate Tup1 binding.

Nevertheless, I found that the levels of Tup1 binding detected at the *pIME1-bsΔ1* and *pIME1-bsΔ3* promoter constructs were around half of that detected in *pIME1-bsΔyap6* and *pIME1-bsΔsok2* cells respectively (Figure 41A and Figure 42B). Thus, even though TTATGTAA (-837-844) and MTGCA-like sites are sufficient to mediate Tup1-Cyc8 binding, the TGTGCCT (-1006-1012) and AGGCAM-like sites may provide auxiliary functions in recruiting Tup1-Cyc8 to the *IME1* promoter. Taken together, Tup1-Cyc8 binds to the *IME1* promoter by interacting with specific transcription factor binding sites, but full Tup1-Cyc8 recruitment also requires other transcription factor binding sites that may play auxiliary roles.

(A)

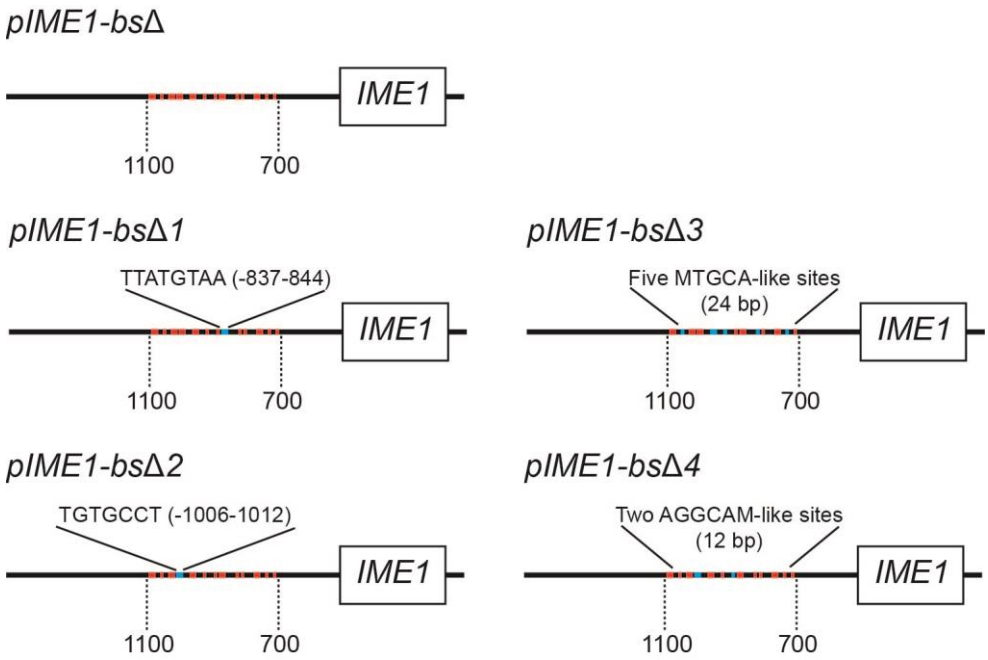

(B)

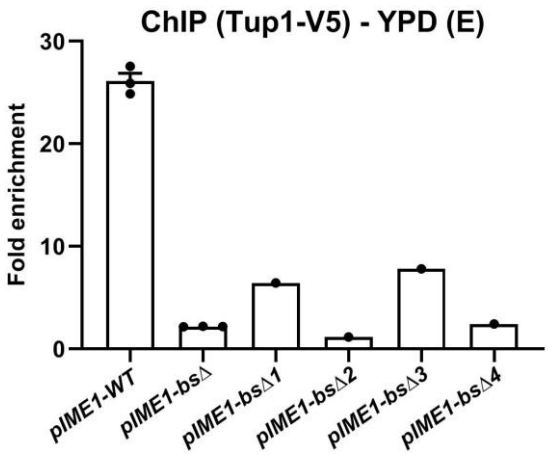

Figure 42. The TTATGTAA motif and MTGCA-like motifs are sufficient to recruit Tup1.

(A) Schematic diagram representing the *IME1* promoter constructs *pIME1-bsΔ1* to *pIME1-bsΔ4*. The constructs contained mutated sequences in *pIME1-bsΔ* with particular motifs reinstated, as indicated in the diagram. Sequences of the promoter constructs can be found in Supplementary figure 21 to Supplementary figure 24. The coordinates and number of restored nucleotides are indicated. Red = mutated nucleotides; blue = restored nucleotides.

(B) ChIP-qPCR of V5 epitope-tagged Tup1 in cells with *pIME1-bsΔ1* (FW7084), *pIME1-bsΔ2* (FW7094), *pIME1-bsΔ3* (FW7086), and *pIME1-bsΔ4* (FW7096)

promoter constructs. Cells were harvested during exponential growth (YPD (E)). A primer pair flanking 1000 bp upstream of the *IME1* start codon was used for qPCR. ChIP signals were normalised over the silent mating type cassette *HMR*. Bars represent mean (SEM) and dots indicate individual biological replicates.

To investigate the importance of Yap6, Sok2, and Phd1 binding sites in recruiting Tup1-Cyc8 and regulating *IME1* transcription, I further constructed two versions of *IME1* promoter constructs. I aimed to inspect how much Tup1-Cyc8 recruitment depends on the transcription factor binding sites that are sufficient to mediate Tup1 binding (Figure 42). Therefore, I decided to focus on the Yap6 and Sok2/Phd1 sites that were present in the *pIME1-bsΔ1* and *pIME1-bsΔ3* constructs (Figure 42A). In the two new promoter constructs, I analysed TTATGTAA (-837-844) and six MTGCA sites together, which were predicted to bind Yap6 and Sok2/Phd1 respectively. Since the sequence motifs were predicted for Sok2, Phd1, and Yap6, I named the two new promoter constructs *pIME1-bsΔ-spy* and *pIME1-spyΔ*. The *pIME1-bsΔ-spy* promoter construct was rescued from the *pIME1-bsΔ* promoter, in which the seven Yap6/Sok2/Phd1 binding motifs were reinstated while other binding sites remained mutated. The *pIME1-spyΔ* promoter construct was designed based on the same principle, only that the seven binding sites were mutated from the wild-type promoter while all other sequences remained intact (Figure 43A). To confirm that the seven *spy* sites are directly bound by Yap6, Sok2, and Phd1, I tagged each transcription factor with three copies of the V5 epitope and measured their binding at the *IME1* promoter by ChIP-qPCR. At the wild-type *IME1* promoter integrated at the *TRP1* locus (*pIME1-WT*), Yap6, Sok2, and Phd1 displayed strong binding similar to the endogenous locus in exponentially growing cells (YPD (E)) (Figure 43B). These observations indicate that the binding of Yap6, Sok2, and Phd1 at the *IME1* promoter is sequence-dependent. Yap6, Sok2, and Phd1 were completely unable to bind the *IME1* promoter in *pIME1-bsΔ* cells (Figure 43B). This suggests that the transcription factor binding sites mutated (103 bp) include the binding sites of the three transcription factors. Furthermore, in *pIME1-bsΔ-spy* cells, Yap6, Sok2, and Phd1 were enriched at the *IME1* promoter (Figure 43B). However, their binding was not complete compared to the wild-type promoter (*pIME1-WT*). The binding sites present in the *pIME1-bsΔ2* and *pIME1-bsΔ4* constructs (Figure 42), which were insufficient to mediate Tup1 binding by themselves and thus excluded in *pIME1-bsΔ-*

spy, may co-operate with the binding sites restored in *pIME1-bs*Δ*-spy* to mediate Yap6, Sok2, and Phd1 binding. I conclude that Yap6, Sok2, and Phd1 bind to the predicted sequence motifs in the *IME1* promoter.

Next, I measured Yap6, Sok2, and Phd1 binding at the *IME1* promoter in *pIME1-spy*Δ cells. The *pIME1-spy*Δ promoter construct contained wild-type promoter sequence, with the seven Yap6, Sok2, and Phd1 binding sites mutated. Since the binding sites were sufficient to mediate Yap6, Sok2, and Phd1 binding at the *pIME1-bs*Δ*-spy* promoter construct, I expected Yap6, Sok2, and Phd1 binding to be at least partially lost in the *pIME1-spy*Δ promoter construct. Indeed, I found that the binding of the three transcription factors was reduced in *pIME1-spy*Δ cells (Figure 43B). In *pIME1-spy*Δ cells, I found that Yap6 and Phd1 binding was reduced to levels similar to *pIME1-bs*Δ cells. However, Sok2 was still enriched at the *pIME1-spy*Δ promoter, suggesting that the Sok2 binding sites were not completely mutated in the construct (Figure 43B). Therefore, it is important to note that the *pIME1-spy*Δ construct could only represent partial, but not full loss of Sok2 binding near the Tup1-Cyc8 binding site. Nevertheless, the *pIME1-bs*Δ*-spy* and *pIME1-spy*Δ results confirm that Yap6, Sok2, and Phd1 bind to their putative binding sites at the *IME1* promoter, and their binding is sequence-dependent. Furthermore, the *pIME1-bs*Δ*-spy* and *pIME1-spy*Δ constructs could be used to explore how gain or loss of Yap6, Sok2, and Phd1 binding affects Tup1-Cyc8 binding at the *IME1* promoter.

Using the *pIME1-bs*Δ*-spy* and *pIME1-spy*Δ promoters, I investigated whether the seven Yap6, Sok2, and Phd1 binding sites are important for Tup1-Cyc8 recruitment at the *IME1* promoter. First, I inspected Tup1 binding in *pIME1-bs*Δ*-spy* cells. Tup1 was enriched at the *pIME1-bs*Δ*-spy* promoter construct (Figure 43C). Intriguingly, although the binding of Yap6, Sok2, and Phd1 was partially restored at the *pIME1-bs*Δ*-spy* promoter construct, Tup1 recruitment detected at this construct was close to wild-type levels (Figure 43B and Figure 43C). These results indicate that the three transcription factors play redundant roles in associating Tup1 to the *IME1* promoter. In addition, in *pIME1-spy*Δ cells, Tup1 binding was reduced compared to *pIME1-WT* and *pIME1-bs*Δ*-spy* cells. I noted that Tup1 was still detected at the *pIME1-spy*Δ promoter (Figure 43C). This suggests that other binding sites that recruit Tup1-Cyc8 were still present in the *pIME1-spy*Δ promoter construct. Since Sok2 was enriched

at the *pIME1-spy*Δ promoter construct (Figure 43B), I speculate that the remaining Sok2 binding sites contributed to Tup1 binding in *pIME1-spy*Δ cells. Taken together, I discovered seven DNA motifs in the *IME1* promoter that are important for recruiting Yap6, Sok2, and Phd1 to the *IME1* promoter. Furthermore, these DNA motifs also contribute to Tup1-Cyc8 binding at the *IME1* promoter.

My ChIP data suggest that the seven Yap6, Sok2, and Phd1 binding sites are important for Tup1-Cyc8 binding to the *IME1* promoter. I asked whether the same sites also contribute to *IME1* activation when sporulation is induced. To study this question, I induced *pIME1-WT*, *pIME1-bs*Δ, *pIME1-bs*Δ*-spy*, and *pIME1-spy*Δ cells to sporulate, and monitored *IME1* transcript levels by RT-qPCR in the first four hours. The delay in *IME1* activation in *pIME1-bs*Δ cells was rescued by reinstating the seven *spy* sites in *pIME1-bs*Δ*-spy* cells (Figure 43D). This indicates that the Yap6, Sok2, and Phd1 DNA motifs are important for *IME1* transcription. Mutating the seven motifs in the wild-type promoter (*pIME1-spy*Δ) had little impact on *IME1* activation (Figure 43D). This suggests that the presence of other transcription factor binding motifs compensated for the lost activating elements. I also examined whether the Yap6, Sok2, and Phd1 binding sites are important for entry into meiosis by tracking meiotic divisions in cells (Figure 43E). The meiosis kinetics displayed by *pIME1-bs*Δ*-spy* and *pIME1-spy*Δ cells were in line with the *IME1* levels detected in cells in Figure 43D. I found that restoring the seven Yap6, Sok2, and Phd1 binding sites (*pIME1-bs*Δ*-spy*) markedly improved the onset and rate of meiotic divisions, compared to *pIME1-bs*Δ cells (Figure 43E). Meanwhile, the *pIME1-spy*Δ cells showed meiosis kinetics similar to *pIME1-WT* (Figure 43E). These *IME1* expression and functional data demonstrate that the activating elements in the *IME1* promoter also have redundant functions, given that the activating elements present within or outside the *spy* sites are sufficient to induce *IME1* transcription and meiotic onset at wild-type kinetics (Figure 43D and Figure 43E).

In conclusion, I identified seven short sequences in the *IME1* promoter, each 4-8 bp long, to facilitate Yap6, Sok2, and Phd1 binding. Yap6, Sok2, and Phd1 in turn recruit Tup1-Cyc8 to repress the *IME1* promoter. Since nutrients induce the binding of Yap6, Sok2, and Phd1 to the *IME1* promoter (Chapter 4: Figure 25 and Figure 26C), these seven DNA motifs act as nutrient response elements in the *IME1*

upstream region. Importantly, upon induction of meiotic entry, the Yap6, Sok2, and Phd1 binding motifs also contribute significantly to *IME1* activation. I conclude that *IME1* repression and activation depend on the same DNA sequences in the *IME1* promoter.

(A)

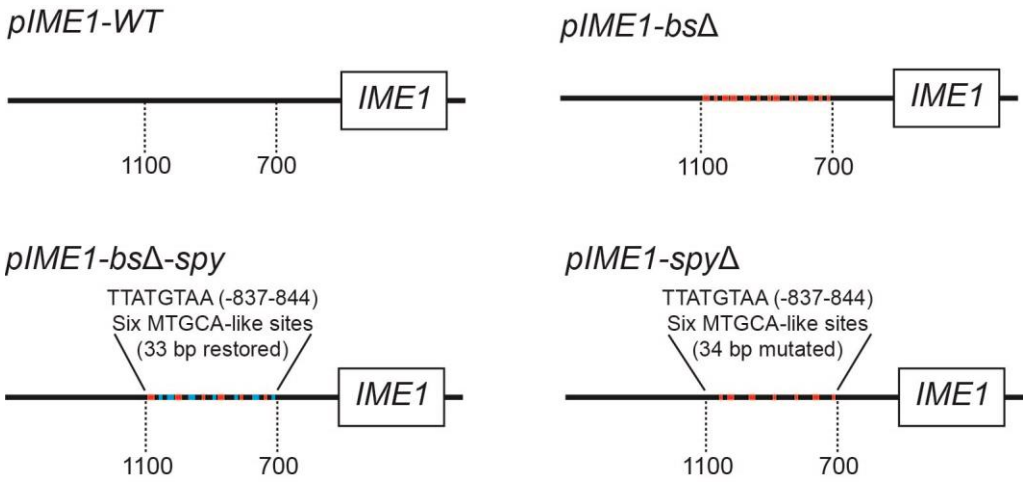

(B)

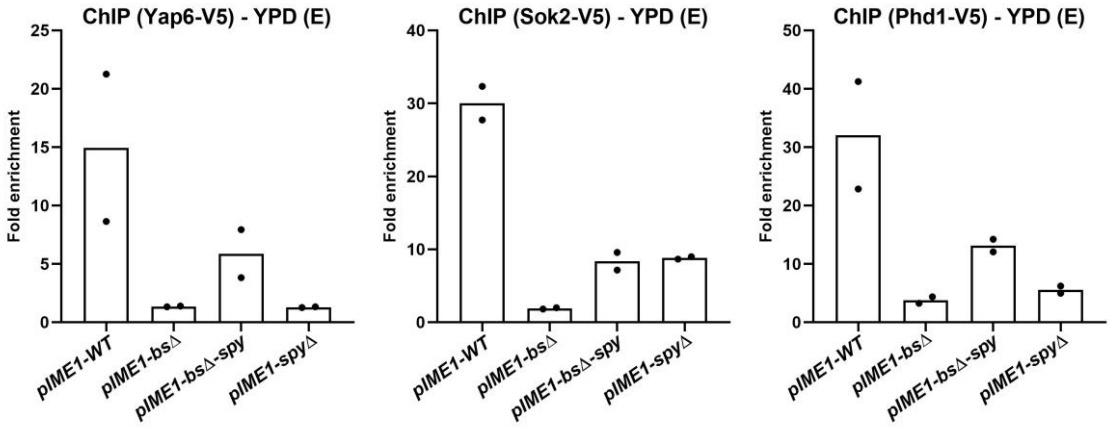

(C)

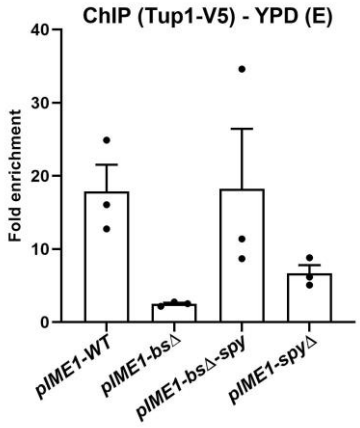

(D)

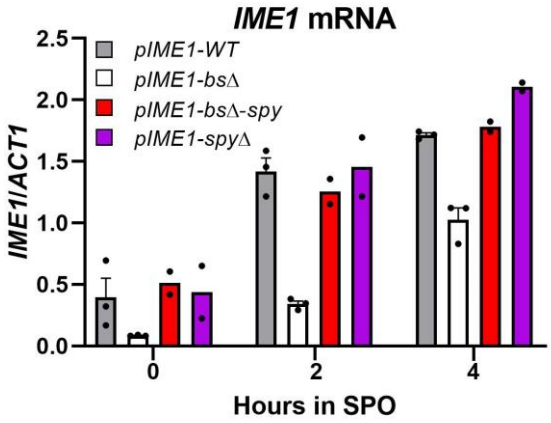

(E)

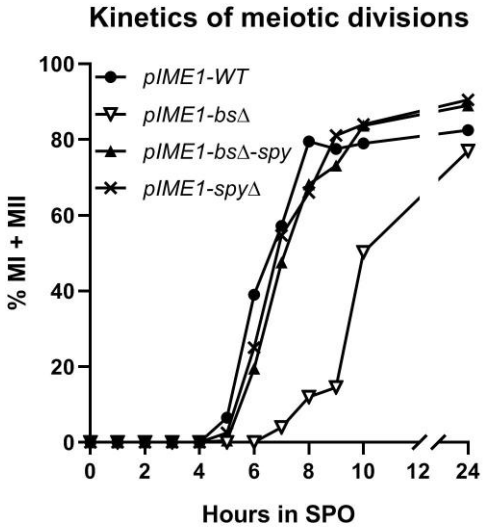

Figure 43. Seven DNA motifs in the *IME1* promoter are important for both repression and activation of *IME1*.

(A) Schematic diagram representing the *pIME1-bsΔ-spy* and *pIME1-spyΔ* promoter constructs. The *pIME1-bsΔ-spy* construct contained mutated sequences in *pIME1-bsΔ* with seven consensus motifs of Yap6, Sok2, and Phd1 reinstated. The same motifs were mutated in the *pIME1-spyΔ* construct, while all other sequences remained wild-type. The number of nucleotides restored/mutated in the constructs is indicated in the diagram. Sequences of the *pIME1-bsΔ-spy* and *pIME1-spyΔ* constructs can be found in Supplementary figure 25 and Supplementary figure 26. Red = mutated nucleotides; blue = restored nucleotides.

(B) ChIP-qPCR of V5 epitope-tagged Yap6, Sok2, and Phd1 in cells bearing *pIME1-WT* (FW8079, FW8081, FW8083), *pIME1-bs*Δ (FW8085, FW8087, FW8089), *pIME1-bs*Δ*-spy* (FW8091, FW8093, FW8095), and *pIME1-spy*Δ (FW8097, FW8098, FW8100) promoter constructs. Transcription factor binding was detected during exponential growth (YPD (E)). For qPCR, a primer pair amplifying 1000 bp upstream of the *IME1* start codon was used. ChIP signals were normalised over silent mating type cassette *HMR*. Bars represent mean normalised ChIP signals and dots indicate individual biological replicates.

(C) Same as (B) but V5 epitope-tagged Tup1 was detected in cells bearing *pIME1-WT* (FW5370), *pIME1-bs*Δ (FW5372), *pIME1-bs*Δ*-spy* (FW7733), and *pIME1-spy*Δ (FW7731) promoter constructs. Bars represent mean (SEM) and dots indicate individual biological replicates.

(D) *IME1* transcript levels detected by RT-qPCR in cells described in (C) at 0, 2, and 4 hours in sporulation medium (SPO). For qPCR, a primer pair flanking approximately +850 bp of *IME1* ORF was used, and signals were normalised over actin *ACT1*. Bars represent mean normalised *IME1* levels, error bars represent SEM, and dots denote individual biological replicates.

(E) Meiotic divisions determined in cells described in (C) at indicated time points in SPO by DAPI counting. The percentage of cells that underwent meiotic divisions (MI + MII) is presented. At least 200 cells were scored for each time point.

6.4 Yap6, Sok2, and Phd1 act as repressors, but not activators of *IME1*

My data thus far demonstrate that *IME1* promoter sequences that facilitate Tup1-Cyc8 binding are also important for *IME1* activation. In particular, DNA sequences that recruit Yap6, Sok2, and Phd1 in nutrient-rich condition turn into activating sequences upon sporulation induction (Figure 43). How do these DNA sequences play different functions depending on the nutrient availability in the surrounding environment? I propose two different models. In the first model, Yap6, Sok2, and Phd1 are transcriptional repressors. Yap6, Sok2, and Phd1 mediate Tup1-Cyc8 binding to repress the *IME1* promoter in nutrient-rich condition. Upon nutrient depletion, Yap6, Sok2, and Phd1 leave the *IME1* promoter. Transcriptional activators that are bound at the *IME1* promoter (e.g. Pog1) induce *IME1* transcription. In the second model, Yap6, Sok2, and Phd1 have dual roles as transcriptional repressors and activators. As proposed by previous study, Tup1-Cyc8 can interact with transcription factors with activation potential, and inhibit their functions by masking their activation domains (Wong and Struhl, 2011). According to this model, Yap6, Sok2, and Phd1 themselves are transcriptional activators, which mediate Tup1-Cyc8 binding to repress *IME1* in nutrient-rich condition. A few observations support the second model. First, all three transcription factors are present in the nucleus prior to and during meiotic entry (Chapter 4: Figure 28). Second, Yap6 and Phd1 have been traditionally characterised as transcriptional activators (Hanlon et al., 2011). Third, during entry into meiosis, Yap6 and Phd1 may weakly associate with the *IME1* promoter thus may contribute to *IME1* activation (Chapter 4: Figure 25).

To determine whether Yap6, Sok2, and Phd1 have activating functions at the *IME1* promoter, I constructed strains with *yap6*Δ*sok2*Δ*phd1*Δ mutations that harboured the *pIME1-WT*, *pIME1-bs*Δ, and *pIME1-bs*Δ*-spy* promoter constructs. In *pIME1-bs*Δ*-spy* cells, *IME1* activation and entry into meiosis were rescued by restoring the DNA sequences that recruit Yap6, Sok2, and Phd1 (Figure 43D and Figure 43E). Therefore, the logic to delete Yap6, Sok2, and Phd1 in these cells was to deduce whether Yap6, Sok2, and Phd1 contributed to the improved *IME1* activation. Since Yap6, Sok2, and Phd1 are strongly bound to the *IME1* promoter during the exponential growth phase (YPD (E)) (Chapter 4: Figure 22), I inspected exponentially growing cells and examined whether the three transcription factors

have activating functions. To detect *IME1* transcripts with high sensitivity, I examined the cells by smFISH. In the presence of Yap6, Sok2, and Phd1, *IME1* transcription from *pIME1-WT*, *pIME1-bs*Δ, and *pIME1-bs*Δ*-spy* promoter constructs was comparable (Figure 44). In *pIME1-bs*Δ*-spy* cells, Yap6, Sok2, and Phd1 bind to the restored DNA sequences and mediate Tup1-Cyc8 binding (Figure 43B and Figure 43C). Tup1-Cyc8 represses *IME1* transcription, thus significant *IME1* de-repression was not observed in *pIME1-bs*Δ*-spy* cells. Yet, there was a subtle increase in the number of *IME1* transcripts detected in *pIME1-bs*Δ*-spy* cells, compared to *pIME1-WT* cells (1.364 vs 0.9710 *IME1* transcripts per cell on average) (Figure 44A). These data suggest that *IME1* repression was mildly alleviated with the *pIME1-bs*Δ*-spy* promoter construct. Given that Yap6, Sok2, and Phd1 binding was partial at the *pIME1-bs*Δ*-spy* promoter (Figure 43B), Tup1-Cyc8 binding may be reduced or less stable and thus *IME1* was partially de-repressed. Next, I examined *IME1* transcript levels in *yap6*Δ*sok2*Δ*phd1*Δ cells bearing *pIME1-WT*, *pIME1-bs*Δ, and *pIME1-bs*Δ*-spy* promoter constructs. As expected, in cells harbouring the wild-type *IME1* promoter (*pIME1-WT*), *yap6*Δ*sok2*Δ*phd1*Δ deletions increased *IME1* levels (*WT*: 0.9710 vs *yap6*Δ*sok2*Δ*phd1*Δ: 1.623 *IME1* transcripts per cell on average) (Figure 44A). The effects of *yap6*Δ*sok2*Δ*phd1*Δ were similar on the endogenous *IME1* promoter (Chapter 5: Figure 33). Therefore, loss of Yap6, Sok2, and Phd1 likely de-stabilises Tup1-Cyc8 binding at the *IME1* promoter during exponential growth. Deleting Yap6, Sok2, and Phd1 also had a minor effect on *IME1* transcription in *pIME1-bs*Δ cells. In the presence of Yap6, Sok2, and Phd1, 5.9% of *pIME1-bs*Δ cells expressed four or more *IME1* transcripts, while this was found in 13% of cells when Yap6, Sok2, and Phd1 were lost (Figure 44B). It is worth noting that in the *pIME1-bs*Δ construct, I only mutated transcription factor binding sites between 700 and 1100 bp upstream of the *IME1* start codon. As a result, Tup1 binding was diminished at its primary binding site, around 1000 bp upstream of the *IME1* start codon (Figure 40C). However, Tup1-Cyc8 also interacts with regions outside of 700 to 1100 bp upstream of the *IME1* start codon (Chapter 3: Figure 13) (Weidberg et al., 2016), and possibly mediated by Yap6, Sok2, and Phd1. This suggests that *yap6*Δ*sok2*Δ*phd1*Δ may disrupt Tup1-Cyc8 binding at other parts of the promoter, and thereby de-represses *IME1* transcription. Finally, I compared *IME1* levels in *pIME1-bs*Δ*-spy* cells with or without Yap6, Sok2, and Phd1. Strikingly, *yap6*Δ*sok2*Δ*phd1*Δ further increased *IME1* transcript levels in *pIME1-bs*Δ*-spy* cells (Figure 44A). Approximately 16.8% of cells

expressed over 10 *IME1* transcripts in *pIME1-bs∆-spy* cells with *yap6∆sok2∆phd1∆*, in contrast to 0.4% when Yap6, Sok2, and Phd1 were present (Figure 44B). Importantly, *IME1* transcription in *yap6∆sok2∆phd1∆* cells bearing the *pIME1-bs∆-spy* construct was markedly higher than that detected in cells with *pIME1-WT* and *pIME1-bs∆* constructs during exponential growth (Figure 44). In the previous chapter (Chapter 5), I demonstrated that Tup1-Cyc8 is enriched at the *IME1* promoter in *yap6∆sok2∆phd1∆* cells during the exponential growth phase (Chapter 5: Figure 31). This suggests that Yap6, Sok2, Phd1, and other transcription factors have redundant roles in mediating Tup1-Cyc8 recruitment during the exponential growth phase. In the *pIME1-bs∆-spy* promoter construct, all DNA sequences that bind Tup1-Cyc8 were mutated except for the Yap6, Sok2, and Phd1 binding motifs. Therefore, when Yap6, Sok2, and Phd1 were lost, *IME1* transcription was substantially de-repressed in *pIME1-bs∆-spy* cells, presumably because all transcription factors that mediate Tup1-Cyc8 binding were not bound. Furthermore, when Yap6, Sok2, and Phd1 were lost, *IME1* transcription was much higher in *pIME1-bs∆-spy* cells compared to *pIME1-bs∆* cells. These data suggest that the DNA sequences bound by Yap6, Sok2, and Phd1 are involved in *IME1* activation, but *IME1* activation does not require the presence of Yap6, Sok2 and Phd1. Taken together, I conclude that Yap6, Sok2, and Phd1 mediate repression of *IME1* transcription, but not activation.

(A)

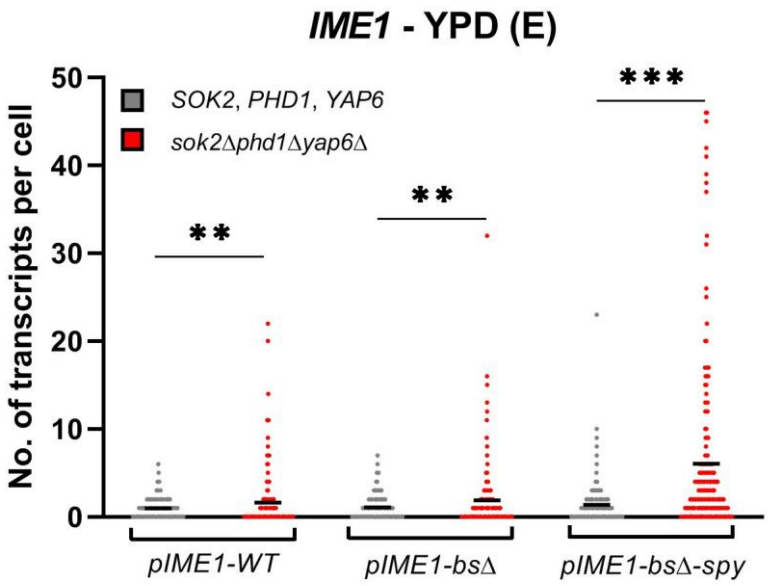

(B)

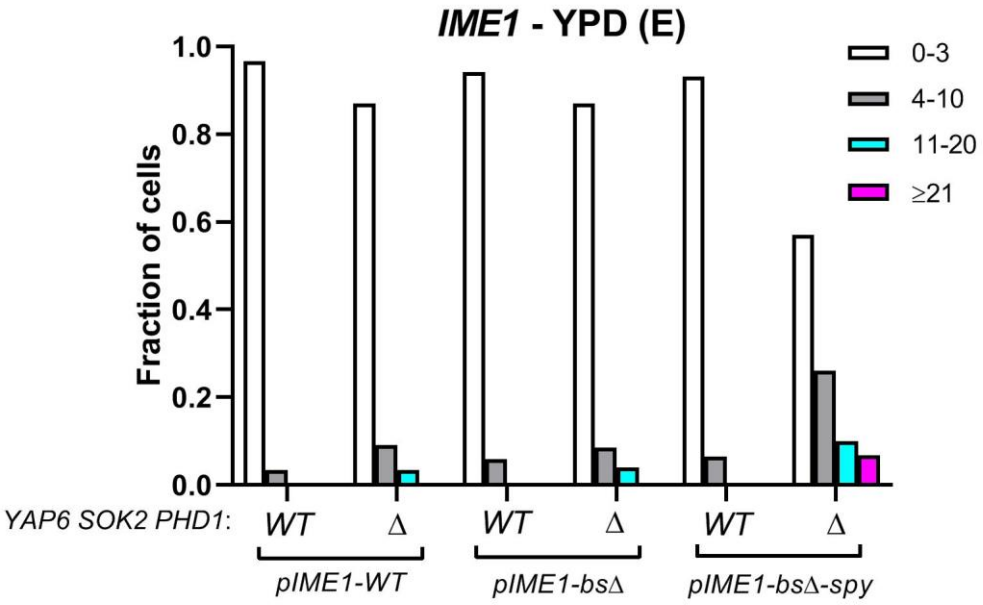

Figure 44. Yap6, Sok2, and Phd1 do not play activating roles in *IME1* transcription.

(A) Scatter dot plot representing number of *IME1* transcripts detected per cell in wild-type and *yap6Δsok2Δphd1Δ* cells harbouring *pIME1-WT* (FW5370, FW7650), *pIME1-bsΔ* (FW5372, FW8420), and *pIME1-bsΔ-spy* (FW7733, FW8177) promoter constructs. Approximately 200 cells that were positive for *ACT1* were analysed for each cell population. The black line denotes the mean number of *IME1* transcripts per cell in the population. Unpaired parametric two-tailed

Welch's t-test was performed between *WT* and *yap6*Δ*sok2*Δ*phd1*Δ cells carrying the same *IME1* promoter construct with 95% confidence. P-values are indicated in the graph, where ns stands for non-significant, * = ≤ 0.05, ** = ≤ 0.01, *** = ≤ 0.001.

(B) Histogram showing data in (A) that were binned into intervals by the number of *IME1* transcripts in cells. Data were binned into four intervals corresponding to 0-3, 4-10, 11-20, and 21 or more *IME1* transcripts per cell. Each bar represents the fraction of the cell population falling into that division.

6.5 Chapter summary

In this chapter, I investigated the DNA sequences in the *IME1* promoter where Tup1-Cyc8 and the candidate transcription factors that interact with Tup1-Cyc8 bind. I performed a systematic analysis of the *IME1* promoter by deleting different regions of the *IME1* promoter. By using this approach, I revealed that the 600 bp region between 800 and 1400 bp upstream of the *IME1* start codon is crucial for *IME1* activation. Remarkably, Tup1-Cyc8 associates with the *IME1* promoter from 750 to 1400 bp upstream of the start codon, suggesting that transcriptional repressors and activators regulate the same part of the *IME1* promoter. Further supporting this hypothesis, I mutated key nucleotides (103 bp) in the predicted binding sites of the Tup1-Cyc8 interacting transcription factors in this promoter region (*pIME1-bs*Δ) and Tup1 binding was strongly diminished. Importantly, disruption of the Tup1-Cyc8 recruiting sites also delayed *IME1* activation. Hence, *IME1* repression and activation rely on the same DNA sequences in the *IME1* promoter.

Next, I further examined the transcription factor DNA motifs by examining their contribution to Tup1-Cyc8 recruitment separately. By restoring the putative binding sites for each transcription factor, I found that the DNA sequences predicted to bind Yap6, Sok2, and Phd1 are sufficient to rescue Tup1 recruitment at the *IME1* promoter. These observations are in agreement with my data presented in the previous chapter that these three transcription factors mediate Tup1-Cyc8 repression of the *IME1* promoter (Chapter 5: Figure 30, Figure 31, Figure 33, Figure 34, Figure 35 and Figure 36). Further dissections of the Yap6, Sok2, and Phd1 DNA motifs revealed seven short sequences, each 4-8 bp long, to be important for Tup1-Cyc8 recruitment in nutrient-rich condition. My data demonstrate that these seven DNA motifs partially rescue Yap6, Sok2, and Phd1 binding and almost fully restores Tup1 recruitment at the *IME1* promoter. Hence, the three transcription factors have redundant functions in recruiting Tup1. Furthermore, I found that the seven DNA motifs switch into activating elements to promote *IME1* transcription when Tup1-Cyc8 is not bound (Figure 45). Although these sequences are bound by Yap6, Sok2, and Phd1, the three transcription factors are not involved in *IME1* activation. These results suggest a model that transcription factors with designated repressor or activator functions contact the same DNA sequences in the *IME1* promoter. I

propose that transcription factors including Yap6, Sok2, and Phd1 function as repressors (by recruiting Tup1-Cyc8), and co-localise with activators such as Pog1 at the *IME1* promoter. When sporulation is induced, Yap6, Sok2, and Phd1 leave the *IME1* promoter and evict Tup1-Cyc8, while Pog1 and other activators activate *IME1* transcription. I also propose that the seven DNA motifs act as nutrient-sensing elements in the *IME1* promoter by binding Yap6, Sok2, and Phd1, which in turn recruit Tup1-Cyc8 in nutrient-rich condition (Figure 45).

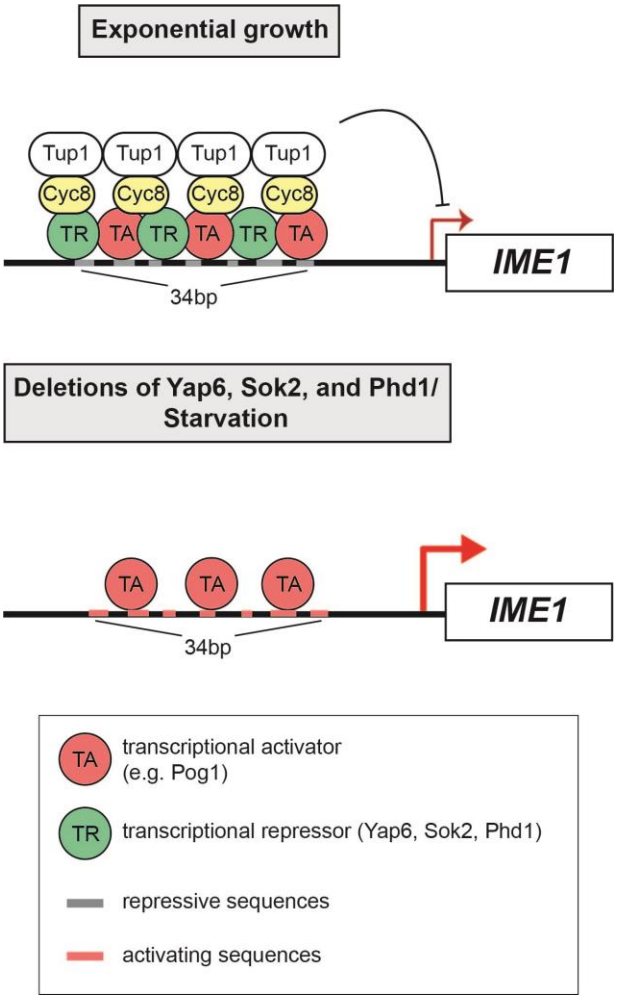

Figure 45. Yap6, Sok2, and Phd1 recruit Tup1-Cyc8 to *IME1* promoter sequences with activation potential to inhibit *IME1* transcription in nutrient-rich condition.
Schematic diagram summarising the results in this chapter. I discovered seven short sequence motifs in the *IME1* promoter that are sufficient to partially recruit Yap6, Sok2, and Phd1 and mediate Tup1-Cyc8 binding in nutrient-rich YPD medium. When nutrients are ample, these sequence motifs act as repressive elements in the *IME1* promoter by recruiting Tup1-Cyc8 to repress *IME1* transcription. Conversely, upon nutrient starvation or in the absence of Yap6, Sok2, and Phd1, the *IME1* promoter is relieved from repression and the promoter bound activators are no longer inhibited. The activators induce *IME1* transcription and promote entry into meiosis. Hence, the sequence motifs that were previously occupied by Tup1-Cyc8 switch into activating sequences in starvation conditions. Please note that the *IME1* promoter depicted in the diagram is not drawn to scale and only represents the region where Tup1-Cyc8 interacts, i.e. 750 to 1400 bp upstream of the start codon.

Chapter 7. Discussion

7.1 Overview

The decision to enter meiosis and form gametes is regulated by nutrient availability in the surrounding environment. In nutrient-depleted environment, diploid yeast cells activate transcription of *IME1*, the crucial regulator of entry into meiosis. *IME1* encodes for a transcriptional activator that induces expression of early meiotic genes in yeast. Importantly, cells must inhibit initiation of meiosis in nutrient-rich conditions. Therefore, *IME1* must be tightly repressed when nutrients are present. Previous study suggested that the transcriptional repressor complex, Tup1-Cyc8, is important for repressing *IME1* transcription in nutrient-rich condition (Weidberg et al., 2016). Nutrients activate Ras/PKA and TORC1 signalling pathways, and induce binding of the Tup1-Cyc8 complex to the *IME1* promoter. However, how Tup1-Cyc8 regulates repression of *IME1* transcription was poorly understood. Decades of work has established that Tup1-Cyc8 can mediate repression of its targets via different mechanisms. Examples of these mechanisms include stabilising and re-positioning nucleosomes, mediating histone deacetylation, interfering with transcriptional machinery, and blocking recruitment or activity of transcriptional activators. Genome-wide dataset analysis suggested that binding of Tup1-Cyc8 correlates with the presence of nucleosomes in the *IME1* promoter at around 250 bp upstream of the start codon (Weidberg et al., 2016, Rizzo et al., 2011). Yet, the importance of Tup1-Cyc8 in repressing *IME1* transcription was not understood. Given that Tup1-Cyc8 dissociates during induction of sporulation, I speculated that Tup1-Cyc8 integrates nutrient signals to bind to the *IME1* promoter. In order to bind to the *IME1* promoter, Tup1-Cyc8 needs to interact with transcription factors that bind to DNA sequences in the *IME1* promoter. Although some transcription factors were implied to bind to the *IME1* promoter and negatively regulate *IME1* (Shenhar and Kassir, 2001, Zhao et al., 2018), a link between their roles and Tup1-Cyc8 had not been described. Thus, I set out to identify the transcription factors that mediate Tup1-Cyc8 binding at the *IME1* promoter. I also investigated how nutrient signals regulate binding of these transcription factors to dissect how signal integration is achieved by Tup1-Cyc8. In addition, functional analyses of the DNA sequence motifs mediating nutrient regulation of the *IME1* promoter were lacking. Previous *IME1* promoter analyses

have established a region from 1122 to 1153 bp upstream of the *IME1* start codon (IREu) as a region that is regulated by nutrients (Sagee et al., 1998, Shenhar and Kassir, 2001, Kahana et al., 2010). In this thesis, I investigated which DNA sequence motifs are responsible for Tup1-Cyc8 recruitment and therefore mediate nutrient regulation of *IME1* transcription.

Based on the findings described in this thesis, I propose that the *IME1* promoter is poised for transcriptional activation given that multiple known and putative *IME1* activators are stably bound to the *IME1* promoter when Tup1-Cyc8 is also recruited during exponential growth phase (Figure 46). In nutrient-rich condition, Tup1-Cyc8 is recruited to the *IME1* promoter to repress transcriptional activation. I propose that Tup1-Cyc8 represses *IME1* transcription primarily by inhibiting activation, but the exact mechanism remains elusive. I found that Tup1-Cyc8 binding at the *IME1* promoter is mediated by at least five transcription factors (Chapter 5: Figure 32). In this thesis, I examined 16 transcription factors that have the potential to interact with the Tup1-Cyc8 complex (Chapter 4: Figure 22). Among the candidate transcription factors, I identified three transcription factors, Yap6, Sok2, and Phd1 to contribute to Tup1-Cyc8 mediated repression of *IME1*. The DNA sequences that are predicted to interact with Yap6, Sok2, and Phd1 respectively are sufficient to recruit Tup1 to the *IME1* promoter (Chapter 6: Figure 41A and Figure 42). Remarkably, Tup1 recruitment was almost fully restored at a mutated *IME1* promoter (*pIME1-bs*Δ) by partially rescuing the binding of Yap6, Sok2, and Phd1 (*pIME1-bs*Δ*-spy*) (Chapter 6: Figure 43A-C), indicating that the three transcription factors have redundant functions in Tup1 recruitment at the *IME1* promoter. Functional analyses demonstrate that Yap6, Sok2, and Phd1 facilitate *IME1* repression through mediating Tup1-Cyc8 recruitment. When Yap6, Sok2, and Phd1 are lost in cells, Tup1 recruitment is strongly diminished before entry into meiosis (Chapter 5: Figure 31). As a result, *IME1* transcription is de-repressed and high levels of *IME1* transcripts induce cells to undergo early entry into meiosis (Chapter 5: Figure 34 and Figure 35). I noted that Sok2 has a major contribution in associating Tup1 to the *IME1* promoter prior to entry into meiosis, while Yap6 and Phd1 play supplementary roles in Tup1 recruitment (Chapter 5: Figure 30, Figure 31, Figure 34 and Figure 35). When Sok2 is expressed, the effect of *yap6*Δ*phd1*Δ on Tup1 recruitment and *IME1* repression is minimal. During exponential growth phase when glucose is present, single and

combined deletions of Yap6, Sok2, and Phd1 had very little effect on Tup1 recruitment or resulted in higher ChIP signals of Tup1 (Chapter 5: Figure 30 and Figure 31). Functional analyses revealed that single deletion of Sok2 had negligible effects on *IME1* repression in exponential growth phase (Chapter 5: Figure 33), suggesting that Sok2 might play a lesser role in Tup1-Cyc8 recruitment in the exponential growth phase. Although the combined deletions of Yap6, Sok2, and Phd1 resulted in higher levels of *IME1* transcripts in cells, the level of *IME1* de-repression was much lower compared to Tup1 depletion (Chapter 3: Figure 18, Chapter 5: Figure 33). Taken together, my data indicate that Tup1-Cyc8 is recruited to the *IME1* promoter by additional transcription factors that likely repond to glucose signals during exponential growth (Chapter 4: Figure 26, Chapter 5: Figure 36).

How is nutrient integration achieved at the *IME1* promoter? I propose that nutrients regulate the binding of Tup1-Cyc8 through modulating the binding of the recruiting transcription factors (Chapter 4: Figure 25 and Figure 26C). Upon nutrient starvation, I found that the Tup1-Cyc8 interacting transcription factors dissociate from the *IME1* promoter which is likely how Tup1-Cyc8 is evicted (Chapter 3: Figure 14, Chapter 4: Figure 25). Furthermore, Tup1-Cyc8 and the interacting transcription factors are still present within the nucleus at this stage suggesting that other mechanisms such as post-translational modifications or local signalling events may prevent the proteins from interacting with the *IME1* promoter (Chapter 3: Figure 16, Chapter 4: Figure 28). Interestingly, the occupancies of Tup1 and Cyc8 may be differentially regulated at the *IME1* promoter (Figure 46). My data demonstrate that both protein level and *IME1* promoter occupany of Cyc8 reduces as cells shift from exponential to saturated growth phase. In contrast, Tup1 remains strongly expressed and bound at the *IME1* promoter prior to entry into meiosis (Chapter 3: Figure 14 and Figure 15). Importantly, the Tup1-Cyc8 recruiting transcription factors mediate signals from distinct nutrients to recruit Tup1-Cyc8 to the *IME1* promoter (Chapter 4: Figure 25 and Figure 26C). In agreement with the results from the functional analyses (Chapter 5: Figure 31 and Figure 34), Yap6, Sok2, and Phd1 mediate signals from rich nutrients including nitrogen compounds while other transcription factors respond to glucose signals to recruit Tup1-Cyc8 (Chapter 5: Figure 36). Notably, the Tup1-Cyc8 recruiting transcription factors are highly redundant as deletions of multiple transcription factors did not completely remove Tup1-Cyc8

binding (Chapter 5: Figure 31 and Figure 32). I propose that having multiple redundant transcription factors recruit Tup1-Cyc8 is a mechanism to ensure that Tup1-Cyc8 is bound to repress *IME1* when some nutrients are present.

Finally, I examined the DNA sequences in the *IME1* promoter that are important for recruiting Tup1-Cyc8 and carried out functional analyses on these sites. My data indicate that the *IME1* promoter regions bound by Tup1-Cyc8 also contain sequences that are required for full activation of *IME1* (Chapter 6: Figure 39). In particular, I discovered seven 4-8 bp motifs that are sufficient to partially interact with Yap6, Sok2, and Phd1 and mediate Tup1-Cyc8 recruitment at the *IME1* promoter when nutrients are present (Chapter 6: Figure 43). Upon nutrient starvation, Tup1-Cyc8 and the recruiting transcription factors leave their binding sites at the *IME1* promoter. Importantly, the same DNA sequence motifs that were previously occupied by Tup1-Cyc8 and the recruiting transcription factors switch into activating elements of *IME1* transcription as transcriptional activators are de-repressed (Chapter 6: Figure 43). Consequently, *IME1* is transcribed, and cells are induced to enter meiosis. In conclusion, I propose that the *IME1* promoter is poised for activation in nutrient-rich condition. Changes in nutrient availability control *IME1* transcription and entry into meiosis by regulating Tup1-Cyc8 mediated repression, rather than activation of the *IME1* promoter (Figure 46).

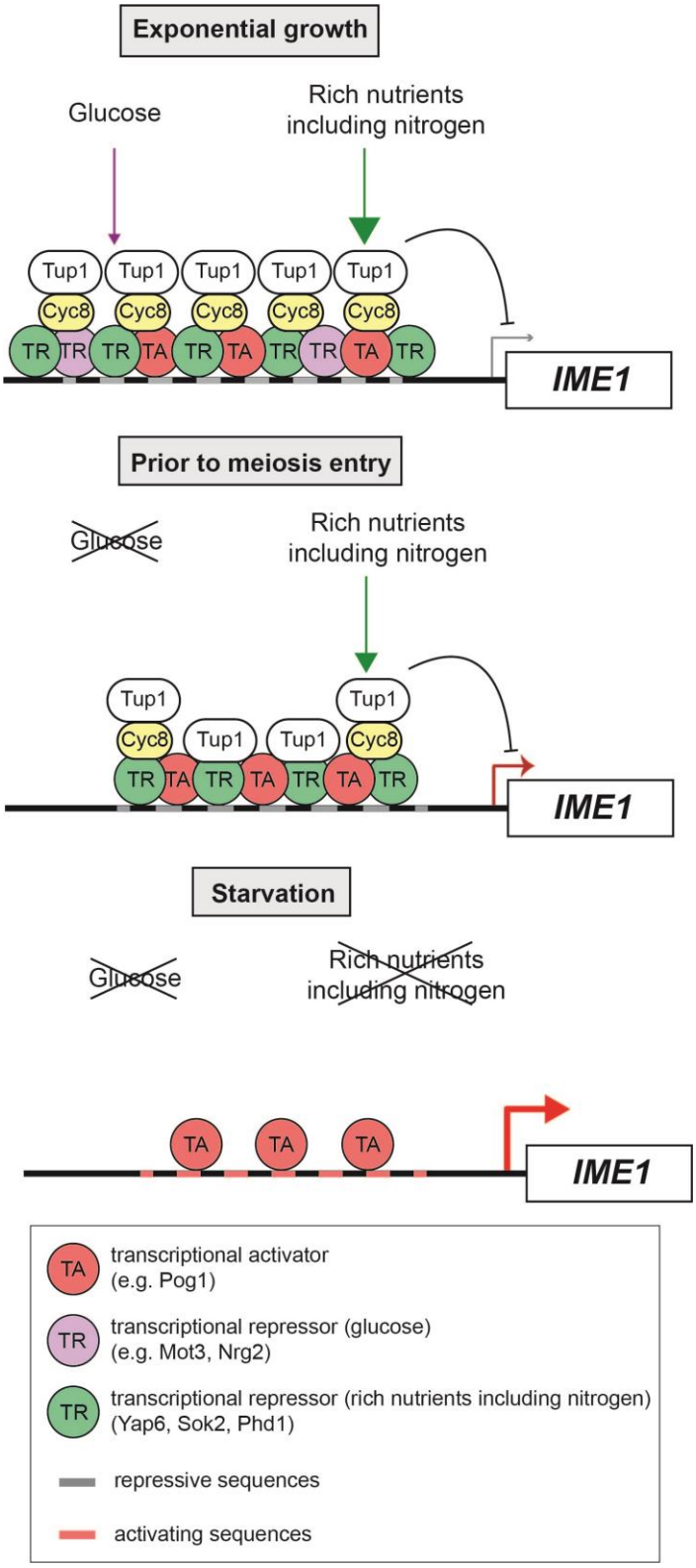

Figure 46. *IME1* transcription is regulated by Tup1-Cyc8 mediated repression.

Model of Tup1-Cyc8 mediated regulation of *IME1* transcription proposed in this thesis. Transcriptional activators of *IME1* are bound to the *IME1* promoter when nutrients are

present and during starvation. Hence, the *IME1* promoter is poised for transcriptional activation and repression of *IME1* is achieved by inhibition of transcriptional activation. During exponential growth phase, rich nutrients mediate binding of multiple transcription factors to the *IME1* promoter, which in turn recruit the Tup1-Cyc8 repressor complexes. Three transcription factors, Yap6, Sok2, and Phd1, mediate signals from rich nutrients including nitrogen compounds, while other transcription factors mediate glucose signals. Tup1-Cyc8 binding inhibits transcriptional activators and thereby represses *IME1* transcription. Prior to entry into meiosis, Cyc8 expression is downregulated and less Cyc8 is detected at the *IME1* promoter. Since glucose is absent in the growth medium, transcription factors that are sensitive to glucose dissociate from the *IME1* promoter. At this stage, Tup1-Cyc8 binding is mediated by Yap6, Sok2, and Phd1. Upon starvation, rich nutrients including nitrogen compounds are also absent in the medium. Yap6, Sok2, and Phd1 dissociate from the *IME1* promoter and Tup1-Cyc8 is evicted. Transcriptional activators are no longer inhibited and can activate *IME1* transcription. Sequence motifs that are co-bound by Tup1-Cyc8 recruiting transcription factors and transcriptional activators act as repressive elements in the presence of nutrients, and switch into activating elements upon starvation. Please note that the *IME1* promoter depicted in the diagram is not drawn to scale and only represents the region where Tup1-Cyc8 interacts, i.e. 750 to 1400 bp upstream of the start codon.

7.2 Model of Tup1-Cyc8 repression at the *IME1* promoter

Tup1-Cyc8 is the major repressor of *IME1* transcription that is regulated by nutrient signals. In rich medium (YPD), Tup1 and Cyc8 co-localise to the *IME1* promoter near 1000 bp upstream of the open reading frame (Chapter 3: Figure 13) (Weidberg et al., 2016). *IME1* is normally repressed in rich medium, and the depletion of either Tup1 or Cyc8 is able to fully de-repress *IME1* transcription (Chapter 3: Figure 17). Importantly, nutrient signals regulate *IME1* transcription by modulating Tup1-Cyc8 mediated repression, rather than transcriptional activation. The *IME1* promoter is poised for activation regardless of the nutrient availability in the surrounding environment. Several observations in my data support that the *IME1* promoter is poised for transcriptional activation under nutrient-rich condition when *IME1* is repressed. The first evidence is binding of Pog1, a transcriptional activator that is known to contribute to *IME1* activation upon induction of sporulation (van Werven et al., 2012). My ChIP data show that Pog1 occupies the *IME1* promoter in the exponential growth phase, during which glucose and nitrogen compounds are ample (Chapter 3: Figure 19A). Furthermore, I identified two transcription factors, Fkh1 and Fkh2 that are potentially *IME1* activators from an *IME1-lacZ* reporter screen (unpublished data). During exponential growth, Fkh1 and Fkh2 are also bound to the *IME1* promoter (Chapter 3: Figure 19C). These results indicate that transcriptional activators interact with the *IME1* promoter under repressive conditions. Next, nutrients play little role in regulating *IME1* activation. Pog1 is enriched at the *IME1* promoter in both nutrient-depleted condition and nutrient-rich conditions (YP and YPD) (Chapter 4: Figure 26D). Thus, binding of transcriptional activators is not facilitated by nutrient depletion upon induction of sporulation. In addition, *IME1* transcription is activated immediately when Tup1-Cyc8 is removed in nutrient-rich condition. Kinetics analyses of *IME1* transcription indicate that *IME1* transcription occurs concurrently with Tup1 depletion (Chapter 3: Figure 18). Given that there is almost no delay between loss of Tup1 and *IME1* transcription, I conclude that transcriptional activators must already be bound or readily available to bind the *IME1* promoter in nutrient-rich condition.

In previous study, analysis of genome-wide MNase-seq data indicated that the absence of Tup1 is correlated with depletion of nucleosomes in the *IME1* promoter

(Weidberg et al., 2016, Rizzo et al., 2011). This suggests that Tup1-Cyc8 might establish a repressive chromatin state at the *IME1* promoter. The ATP-dependent chromatin remodelling enzyme, Isw2, mediates chromatin remodelling induced by Tup1-Cyc8 binding (Rizzo et al., 2011, Zhang and Reese, 2004b). However, *IME1* expression is upregulated in the *tup1*Δ and *cyc8*Δ mutants, but not in the *isw2*Δ mutant from the same dataset (Kemmeren et al., 2014). Therefore, Tup1-Cyc8 is unlikely to repress *IME1* by establishing repressive promoter structure via Isw2-mediated chromatin remodelling. Other studies also support that nucleosome occupancy and positioning is not a pre-requisite for Tup1-Cyc8 repression (Redd et al., 1996, Wong and Struhl, 2011).

I propose that the primary mechanism by which Tup1-Cyc8 represses *IME1* transcription is inhibition of transcriptional activation. My data suggest that Tup1-Cyc8 counteracts the transcriptional activators bound or readily available to bind the *IME1* promoter in nutrient-rich condition. Firstly, Tup1-Cyc8 binds to the regions that are important for *IME1* activation in nutrient-rich condition. Tup1-Cyc8 binding spans from 750 to 1400 bp upstream of the *IME1* start codon, where the strongest binding occurs at 1000 bp upstream of *IME1* (Chapter 3: Figure 13) (Weidberg et al., 2016). Meanwhile, *IME1* regulatory elements required for full *IME1* activation are found between 800 and 1400 bp upstream of the *IME1* start codon (Chapter 6: Figure 39B). Moreover, I characterised seven Yap6, Sok2, and Phd1 binding motifs spanning from 796 to 1035 bp upstream of the *IME1* start codon, which are sufficient to mediate Tup1-Cyc8 binding at the *IME1* promoter (Chapter 6: Figure 43C). The same sequence motifs also contribute significantly to transcriptional activation (Chapter 6: Figure 43D, Figure 43E, and Figure 44). In addition, Tup1-Cyc8 co-localises with transcriptional activators at the *IME1* promoter in nutrient-rich condition. Pog1, a known *IME1* activator, and two putative *IME1* activators Fkh1 and Fkh2, bind to the region approximately 1000 bp upstream of the *IME1* start codon in nutrient-rich condition where Tup1-Cyc8 also binds (Chapter 3: Figure 19). Taken together, these data suggest that binding of Tup1-Cyc8 in nutrient-rich condition compromises the functions of the transcriptional activators bound at the *IME1* promoter. My data is consistent with previous observations that transcriptional activators can co-bind with Tup1-Cyc8 at gene promoters. For example, transcriptional activator Gal4 is recruited to promoter constructs that are repressed by the α2 repressor, which

mediates Tup1-Cyc8 binding (Redd et al., 1996). Furthermore, Wong and Struhl showed that transcriptional activator Gcn4 and Tup1-Cyc8 can co-bind to artificial promoter constructs in close proximity (Wong and Struhl, 2011). The exact mechanism of how Tup1-Cyc8 inhibits transcriptional activation of *IME1* remains unclear. Previous study proposed that Tup1-Cyc8 binding masks the activation domains of the transcriptional activators bound to the promoter (Wong and Struhl, 2011). In this study, Tup1-Cyc8 was found to physically interact with transcriptional activators (Wong and Struhl, 2011). Furthermore, Tup1-Cyc8 binding impairs activation potential of the transcriptional activators by preventing recruitment of co-activator complexes such as Swi/Snf and the Mediator (Wong and Struhl, 2011). Further work can be carried out to dissect whether Tup1-Cyc8 physically interacts with *IME1* activators such as Pog1, and obstruct transcriptional co-activators from binding to the *IME1* promoter. In addition, I cannot exclude the possibility that Tup1-Cyc8 also blocks recruitment of transcriptional activators by masking their DNA-binding motifs. Some transcriptional activators of *IME1* may compete for binding sequences with Tup1-Cyc8, thus they can only bind to the *IME1* promoter when Tup1-Cyc8 dissociates. More transcriptional activators of *IME1* need to be identified in order to determine whether all *IME1* activators co-bind with Tup1-Cyc8 in nutrient-rich conditions. Candidate transcription factors that are potentially *IME1* activators will be discussed in section 7.4.

One mechanism that Tup1-Cyc8 represses its targets is by recruiting histone deacetylases (HDACs) to the H3 and H4 histones at the promoter. For example, deletions of Rpd3 and Hda1 result in significant de-repression at the *FLO1* promoter (Fleming et al., 2014). I found that HDACs play a very minor role in regulating the *IME1* promoter. Among all the HDACs I tested, I found that deleting Rpd3 and Hda1 causes slight de-repression of *IME1* in nutrient-rich condition (Chapter 3: Figure 20). However, de-repression of *IME1* induced by Rpd3 and Hda1 deletions is much milder compared to Tup1 depletion (Chapter 3: Figure 18B and Figure 18C). These data indicate that Rpd3 and Hda1 contribute to repression of *IME1*, but only to a very low extent. Further work can be carried out to dissect how Rpd3 and Hda1 contribute to Tup1-Cyc8 mediated repression of *IME1*. For example, ChIP experiments can be performed to address whether Tup1-Cyc8 depletion and HDAC deletions affect H3

and H4 acetylation (e.g. H3K9Ac, H3K18Ac, H4Ac) at the *IME1* promoter (Fleming et al., 2014, Watson et al., 2000).

Finally, Tup1-Cyc8 represses transcription by directly interfering with the transcriptional machinery. Multiple studies have demonstrated that Tup1-Cyc8 interacts with subunits of the RNA polymerase II holoenzyme (Papamichos-Chronakis et al., 2000, Zaman et al., 2001). Furthermore, Tup1-Cyc8 binding can prevent transcription by blocking TATA-binding protein and RNA polymerase II from binding to the promoter (Kuras and Struhl, 1999, Mennella et al., 2003, Zaman et al., 2001). Inhibiting transcriptional activators and interfering with basal transcriptional machinery are not mutually exclusive mechanisms. Notably, in the model that Tup1-Cyc8 interferes with the transcriptional machinery, the transcriptional machinery is in close proximity with the promoter suggesting that the promoter may be poised for transcriptional activation. In this thesis, I did not examine recruitment of the components of the transcriptional machinery to the *IME1* promoter in the presence and absence of Tup1-Cyc8, hence I cannot speculate whether Tup1-Cyc8 directly interferes with *IME1* transcription. Future studies can address this question by investigating whether Tup1-Cyc8 interacts with subunits of the RNA polymerase II holoenzyme, such as Srb10 and Srb11 (Zaman et al., 2001) at the *IME1* promoter.

7.3 Comparisons with other proposed Tup1-Cyc8 models

Transcriptional repressors in eukaryotes are known to mediate repression of gene transcription through a variety of mechanisms (reviewed in Gaston and Jayaraman, 2003). Typically, transcriptional repressors can silence gene transcription by targeting the general transcriptional machinery such as modification of the RNA polymerase II, blocking recruitment of TATA-binding proteins, and preventing interactions between general transcription factors. Transcriptional repressors can also induce formation of repressive chromatin environment around the promoters to limit their accessibility to transcription factors and the transcriptional machinery. This is usually achieved by recruiting chromatin remodelling factors, such as histone modifying enzymes and the Swi/Snf ATP-dependent remodelling complex. Furthermore, transcriptional repressors can also counteract the functions of transcriptional activators by, for example, inhibiting their interactions with promoters and altering their cellular localisation. During development, transcriptional repressors play a fundamental role in regulating transcriptional responses. Specifically, repressors bind to transcriptionally active sites in the promoters. While repressed, gene promoters remain primed for transcriptional activation to enhance responsiveness to changes in developmental and environmental signalling (Reynolds et al., 2013). In addition, some studies observed that transcriptional repressors themselves can also contribute to the process of transcriptional activation. Examples include HDAC subunits Sin3 and Rpd3 in budding yeast, and the NuRD (nucleosome remodelling deacetylase) complex in mice (De Nadal et al., 2004, Miccio et al., 2010). The Tup1-Cyc8 repressor complex in yeast was traditionally thought to silence gene transcription by establishing repressive promoter structure and inhibiting initiation of transcription. More recently, multiple models have emerged proposing that Tup1-Cyc8 also plays a role in modulating transcriptional activation. These models postulate that Tup1-Cyc8 counteracts the functions of promoter-bound transcriptional activators or inhibits binding of transcriptional activators (Wong and Struhl, 2011, Mathias et al., 2004). Moreover, Tup1-Cyc8 has been suggested to promote transcription under activating conditions (Proft and Struhl, 2002). Hence, Tup1-Cyc8 may repress its targets by inducing loss of transcriptional activation, rather than gain of transcriptional repression.

I propose that Tup1-Cyc8 primarily represses *IME1* transcription by inhibiting promoter-bound transcriptional activators. First, Tup1-Cyc8 and transcriptional activators, such as Pog1, co-occupy the *IME1* promoter under repressive conditions (Chapter 3: Figure 19). When Tup1 is depleted, *IME1* is rapidly transcribed in nutrient-rich condition (Chapter 3: Figure 18). Second, upon nutrient depletion, Tup1-Cyc8 and its recruiting transcription factors dissociate from the *IME1* promoter (Chapter 3: Figure 14, Chapter 4: Figure 25, Figure 26B, and Figure 26C). Transcriptional activators remain bound to the *IME1* promoter and activate *IME1* transcription (Chapter 3: Figure 19A, Chapter 4: Figure 26D). Third, transcription factors that recruit Tup1-Cyc8, such as Yap6, Sok2, and Phd1, do not activate *IME1* transcription when bound to the *IME1* promoter (Chapter 6: Figure 44). Tup1-Cyc8 commonly represses its targets by recruiting HDACs to establish repressive chromatin structure (Fleming et al., 2014, Watson et al., 2000). My data disfavour the model that Tup1-Cyc8 primarily represses *IME1* by altering chromatin structure based on three observations. Firstly, my data demonstrate that deletions of Rpd3 and Hda1 de-repress *IME1* transcription to a very low extent (Chapter 3: Figure 20). Next, I showed that more than 10 transcription factors, including the *IME1* activator Pog1, are able to bind the *IME1* promoter under repressive conditions (Chapter 3: Figure 19, Chapter 4: Figure 22). Thus, the *IME1* promoter is accessible when Tup1-Cyc8 is bound. Furthermore, if Tup1-Cyc8 primarily represses the *IME1* promoter by forming repressive chromatin, a delay should be detected between Tup1 depletion and *IME1* transcription due to assembly of transcriptional activators, co-activators, and the pre-initiation complex. My data demonstrate that *IME1* transcription is activated instantly upon Tup1 depletion, therefore the *IME1* promoter is likely to be primed for transcriptional activation.

My data strongly suggest that Tup1-Cyc8 mutes *IME1* activation in nutrient-rich conditions. The Tup1-Cyc8 repression model that I propose in this thesis is largely consistent with the model described in (Wong and Struhl, 2011). Wong and Struhl suggested that the transcription factors mediating Tup1-Cyc8 binding are repressor-activator proteins with dual functions. As Tup1-Cyc8 interacts with these transcription factors, Tup1-Cyc8 masks their activation domains. The activation potential of these transcription factors is lost, and thus these transcription factors act as repressors by mediating Tup1-Cyc8 binding. When Tup1-Cyc8 dissociates from the transcription

factors, the transcription factors re-gain their activating functions and promote the recruitment of co-activators. The Wong and Struhl model and my model of Tup1-Cyc8 repression both postulate that transcriptional activators are bound at the promoters under repressive conditions. In both models, Tup1-Cyc8 interferes with the activity of the transcriptional activators bound at the target promoters, and dissociation of Tup1-Cyc8 allows transcriptional activators to initiate transcription. Moreover, both models predict the repressed target to express concurrently with loss of Tup1-Cyc8 binding, as transcriptional activators are already bound at the promoter. However, while the Wong and Struhl model proposed that Tup1-Cyc8 binds to repressor-activator proteins (Wong and Struhl, 2011), my model indicates that the transcription factors recruiting Tup1-Cyc8 to the *IME1* promoter are separate from the transcriptional activators that promote *IME1* transcription. On this aspect, my model is in line with other Tup1-Cyc8 models that suggest the Tup1-Cyc8 recruiting transcription factors are distinct from transcriptional activators. One example is the *HO* promoter, at which Tup1-Cyc8 is recruited by the **a**1-α2 heterodimer to prevent recruitment of transcriptional activator Swi5 to the promoter (Mathias et al., 2004). Hence, the Tup1-Cyc8 repression model at the *IME1* promoter merges features from previously proposed Tup1-Cyc8 models, given that Tup1-Cyc8 interacts with a specific set of transcription factors and inhibits transcriptional activators bound at the *IME1* promoter.

Tup1-Cyc8 has also been proposed to switch from transcriptional repressor to activator under activating conditions (Proft and Struhl, 2002). This model was proposed based on study of Sko1, the transcription factor that recruits Tup1-Cyc8 to osmotic stress-inducible genes. In this model, Sko1 and Tup1-Cyc8 remain bound to the promoter under activating conditions. The Hog1 kinase translocates into the nucleus to phosphorylate Sko1, and thereby recruits SAGA and Swi/Snf chromatin remodelling complexes to promote transcription initiation. This model is unlikely to explain how Tup1-Cyc8 regulates the *IME1* promoter due to a number of reasons. First, Tup1-Cyc8 and its interacting transcription factors dissociate from the *IME1* promoter under nutrient-depleted condition (Chapter 3: Figure 14, Chapter 4: Figure 25). Second, Yap6, Sok2, and Phd1 do not play roles in *IME1* activation (Chapter 6: Figure 44). Third, *IME1* is transcribed instantly when Tup1-Cyc8 dissociates

(Chapter 3: Figure 18), whereas the Proft and Struhl model predicts slower activation of gene transcription (a few minutes).

7.4 Candidate transcriptional activators of *IME1*

The *pog1*Δ mutant displays mild delay in meiotic entry (van Werven et al., 2012), suggesting that multiple transcriptional activators are involved in initiating *IME1* transcription. Identifying *IME1* activators and characterising their binding under different nutrient conditions will improve my current model of Tup1-Cyc8 repression at the *IME1* promoter. For example, future work can be done to examine whether all transcriptional activators are bound at the *IME1* promoter in nutrient-rich condition. Alternatively, some transcriptional activators may be recruited only when Tup1-Cyc8 has dissociated from the *IME1* promoter.

Candidate transcription factors with regulatory roles on *IME1* remain to be tested in further studies. The forkhead transcription factors, Fkh1 and Fkh2 are prime candidates as *IME1* regulators. Fkh1 and Fkh2 are paralogous transcription factors that have opposite regulatory roles in cell cycle and mating type cassette silencing (Hollenhorst et al., 2000). Data from *IME1-lacZ* reporter screen (unpublished) indicated that Fkh1 and Fkh2 play repressive and activating roles respectively in *IME1* transcription. My data show that both transcription factors are bound at the *IME1* promoter in exponential growth phase (Chapter 3: Figure 19C), where Tup1-Cyc8 also binds. Furthermore, Fkh2 regulates meiosis in fission yeast. In fission yeast, Fkh2 represses middle meiotic genes by binding to their promoters and blocking the recruitment of transcription factor Mei4. During meiosis, Fkh2 is phosphorylated and leaves the promoters, allowing Mei4 to bind and induce transcription of middle meiotic genes (Alves-Rodrigues et al., 2016). Whether Fkh1 and Fkh2 also regulate meiotic entry in budding yeast remains to be illuminated.

Other transcription factors that may play regulatory roles at the *IME1* promoter are Msn2 and Msn4. Msn2 and Msn4 are well-characterised transcriptional activators that are induced by stress in budding yeast. Notably, Msn2 and Msn4 are under the control of PKA and TORC1 signalling pathways. The PKA and TORC1 signalling pathways prevent Msn2 and Msn4 nuclear localisation, and thereby inhibit their functions (Rajvanshi et al., 2017). In addition, Msn2 and Msn4 were shown to bind the IREu sequence (1122 to 1153 bp upstream of the start codon) in the *IME1* promoter and contribute to activation in acetate-containing medium (Sagee et al.,

1998). Yet, the contribution of Msn2 and Msn4 to full *IME1* activation is unknown. How Msn2 and Msn4 bind the *IME1* promoter under different nutrient conditions also remains to be investigated.

Finally, my data demonstrate that the 50 bp region between 800 and 850 bp upstream of the *IME1* start codon contains *IME1* activating elements (Chapter 6: Figure 39C). I identified two transcriptional activators that have predicted binding sites within this region using the YeTFaSCo database (de Boer and Hughes, 2012). The first transcription factor is Yap3, which also belongs to the Yeast Activator (AP1-like) Proteins family with Yap6. Yap3 is a transcription factor that responds to multiple stresses such as hydroquinone and ER stresses (Rodrigues-Pousada et al., 2019). Yap3 shares the same binding motif (TTACGTAA) with Yap6, and has been shown to be a transcriptional activator (Rodrigues-Pousada et al., 2019, Fernandes et al., 1997). The second transcription factor is Gln3, a GATA-type transcription activator that is sensitive to both glucose and nitrogen (Bertram et al., 2002). The cellular localisation of Gln3 is regulated by the TORC1 pathway. In nitrogen rich conditions, Gln3 is sequestered in the cytoplasm (Beck and Hall, 1999). When nitrogen source is limiting in the medium, Gln3 is imported into the nucleus to activate genes that are normally repressed by nitrogen (Tate et al., 2018). Gln3 binds to the conserved GATAA motif (ter Schure et al., 2000), which has two matches in the *IME1* promoter according to the YeTFaSCo database (de Boer and Hughes, 2012). Further work is required to dissect whether Yap3 and Gln3 bind to the *IME1* promoter and play regulatory roles in *IME1* transcription.

Based on my observations in this thesis, I speculate that Fkh1 and Fkh2 are more likely to be transcriptional activators of *IME1* transcription. Tup1-Cyc8 depletion is sufficient to induce full *IME1* activation in nutrient-rich condition, suggesting that transcriptional activators must be bound or readily available to bind the *IME1* promoter in nutrient-rich condition. In this thesis, I showed that Fkh1 and Fkh2 bind to the *IME1* promoter when nutrients are present. Conversely, Msn2, Msn4, Yap3, and Gln3 are known to be active in response to stress conditions, thus they may not be expressed in the nucleus in nutrient-rich condition. Nevertheless, these four transcription factors are still worth examining given that they have clear binding sites in regions of the *IME1* promoter that have been shown to contain activating elements.

Furthermore, these transcription factors may contribute to *IME1* activation in other conditions.

7.5 Nutrients regulate binding of multiple transcription factors to control *IME1* repression

One of the goals of this thesis was to understand how nutrient signals converge onto Tup1-Cyc8, which in turn regulates *IME1* transcription. In this thesis, I found that nutrients regulate Tup1-Cyc8 binding by controlling binding of the Tup1-Cyc8 interacting transcription factors at the *IME1* promoter. I identified nine candidate transcription factors that were previously shown or implicated to interact with Tup1-Cyc8 to co-localise with Tup1-Cyc8 at the *IME1* promoter. These transcription factors include Cup9, Yap6, Sok2, Phd1, Sut1, Mot3, Sko1, Nrg1, and Nrg2 (Chapter 4: Figure 22). Remarkably, binding of all nine transcription factors at the *IME1* promoter is induced by nutrients (Chapter 4: Figure 25). Furthermore, distinct nutrients in the growth medium differentially regulate binding of these transcription factors. My experimental data demonstrate that the transcription factors are regulated in three different ways by glucose and rich nutrients including nitrogen compounds from YP (yeast extract and peptone) in the growth medium (Chapter 4: Figure 26C). First, Mot3 and Nrg2 primarily respond to glucose. Second, Yap6, Sok2, Phd1, Nrg1, and Sko1 primarily respond to rich nutrients including nitrogen compounds. Third, Cup9 and Sut1 respond to both glucose and rich nutrients including nitrogen compounds in the growth medium. Under nutrient starvation, all nine transcription factors leave the *IME1* promoter. Consequently, Tup1-Cyc8 can no longer interact with the *IME1* promoter, and thereby allows de-repression of *IME1* transcription.

Transcription factors that mediate Tup1-Cyc8 binding at the *IME1* promoter are highly redundant. Among the nine transcription factors, I showed that Yap6, Sok2, and Phd1 contribute significantly to Tup1-Cyc8 recruitment at the *IME1* promoter. Yap6, Sok2, and Phd1 bind to the *IME1* promoter primarily in response to rich nutrients including nitrogen compounds in YP, but not glucose. Deleting Yap6, Sok2, and Phd1 (*yap6*Δ*sok2*Δ*phd1*Δ) substantially reduces Tup1-Cyc8 binding in growth medium containing only YP (YP + 0.05% Glc) (Chapter 5: Figure 36). Furthermore, *yap6*Δ*sok2*Δ*phd1*Δ also substantially reduces Tup1 binding prior to meiotic entry, during which glucose is not present (Chapter 5: Figure 31). However, in glucose-rich conditions such as exponential growth phase and growth medium containing only glucose (SPO + 2% Glc), Tup1-Cyc8 binding is unaffected in *yap6*Δ*sok2*Δ*phd1*Δ

cells (Chapter 5: Figure 31 and Figure 36). Further deleting Cup9, Sko1, or Nrg1/Nrg2 in *yap6*Δ*sok2*Δ*phd1*Δ cells does not reduce Tup1-Cyc8 binding in exponentially growing cells (Chapter 5: Figure 32). Thus, at least five transcription factors mediate Tup1-Cyc8 binding, among which Yap6, Sok2, and Phd1 mediate nutrient signals from rich nutrients including nitrogen compounds, and other transcription factors mediate glucose signals. It was technically challenging to study Tup1-Cyc8 binding in yeast strains bearing more than five transcription factor deletions. Construction of yeast strains with many transcription factor deletions is laborious, and the results may be inconclusive due to secondary effects. To circumvent these issues, binding sites of multiple transcription factors can be mutated on the *IME1* promoter using the single-copy integration plasmid strategy described in this thesis (Chapter 6: Figure 40A and Figure 40B).

Tup1-Cyc8 is strongly bound to 1000 bp upstream of the *IME1* start codon in nutrient-rich condition. DNA motif analyses of the *IME1* promoter sequence between 600 and 1200 bp upstream of the *IME1* start codon revealed that this region is packed with binding sites of the nine Tup1-Cyc8 interacting transcription factors. Nearly 50 transcription factor binding sites were predicted to bind Tup1-Cyc8 within this 600 bp region (Supplementary figure 13). Furthermore, most transcription factors were predicted to have more than one binding site within this region. The transcription factor binding motifs suggest that multiple sites mediate the binding of Tup1-Cyc8 in nutrient-rich conditions. I propose that having redundant transcription factors and multiple DNA-binding sequence motifs to mediate Tup1-Cyc8 binding at the *IME1* promoter is a mechanism to govern *IME1* transcription. The transcription factor system ensures that *IME1* is only expressed when both glucose and nitrogen compounds are depleted in the environment. First, having redundant transcription factors recruit Tup1-Cyc8 assures that Tup1-Cyc8 is still stably recruited when one or more transcription factors are lost or misfolded. Second, in conditions where either glucose or nitrogen is present, Tup1-Cyc8 binding is maintained by a distinct set of transcription factors and *IME1* is still tightly repressed. Third, Tup1-Cyc8 can only dissociate from the *IME1* promoter only when all nine (or more) transcription factors dissociate under nutrient starvation. Thus, each Tup1-Cyc8 interacting transcription factor acts as an individual nutrient sensor to regulate Tup1-Cyc8 binding and thereby control *IME1* expression. In budding yeast, it is not unprecedented that cell

fate gene promoters are regulated by multiple redundant transcription factor binding sites. One example is the *HO* gene promoter, which controls conversion of mating type in haploid cells. In diploid cells, Tup1-Cyc8 represses the *HO* promoter by interacting with the **a**1-α2 heterodimer. The *HO* promoter consists of an array of 10 **a**1-α2 binding sites, at which the **a**1-α2 heterodimer binds with different affinities (Mathias et al., 2004). Notably, in both *IME1* and *HO* promoters, some DNA motifs are sufficient for Tup1-Cyc8 binding while other motifs play auxiliary functions in stabilising or promoting Tup1-Cyc8 binding at the main sites (Chapter 6: Figure 41A and Figure 42B) (Mathias et al., 2004). Hence, having redundant transcription factor binding sites with varying functions in mediating Tup1-Cyc8 binding may be a conserved feature to govern fate promoters in budding yeast.

7.6 De-repression of *IME1* is induced by local changes or post-translational modifications

IME1 transcription is controlled by multiple redundant transcription factors that mediate Tup1-Cyc8 binding at the *IME1* promoter. When nutrients including glucose and nitrogen are depleted in the medium, all transcription factors must dissociate from the *IME1* promoter to evict the Tup1-Cyc8 repressor complex and allow de-repression of *IME1* transcription. How do the Tup1-Cyc8 recruiting transcription factors dissociate from the *IME1* promoter in a swift and concerted manner upon induction of sporulation? Previous study reported PKA and TORC1 inhibition was sufficient to dissociate Tup1 from the *IME1* promoter in nutrient-rich condition (Weidberg et al., 2016). Thus, changes in the PKA and TORC1 signalling pathways are likely responsible for dissociating the Tup1-Cyc8 recruiting transcription factors all at once when nutrients are depleted in the environment. In this thesis, I gained insights into how PKA and TORC1 signalling may regulate binding of the Tup1-Cyc8 recruiting transcription factors at the *IME1* promoter. Firstly, I investigated whether nutrient depletion may trigger sequestration of Tup1-Cyc8 and its recruiting transcription factors into the cytoplasm. I examined the cellular localisation of Tup1-Cyc8 and four strongly bound transcription factors, Cup9, Yap6, Sok2, and Phd1 before and during entry into meiosis (Chapter 3: Figure 16, Chapter 4: Figure 28). My data indicate that Tup-Cyc8 and the four transcription factors do not evacuate from the nucleus upon induction of sporulation. Tup1-Cyc8 and its recruiting transcription factors are clearly expressed in the nucleus during meiotic entry, suggesting that the proteins are still readily available to bind the *IME1* promoter. Furthermore, I inspected whether nutrient depletion may affect the protein abundance of Tup1-Cyc8 and its recruiting transcription factors (Chapter 3: Figure 15, Chapter 4: Figure 27). I found that reduced protein expression levels may partially contribute to the loss of binding of Cyc8 and Cup9 upon induction of sporulation, but not Tup1, Yap6, Sok2, and Phd1. Taken together, my data suggest that nutrient depletion may induce changes to the Tup1-Cyc8 complex and the transcription factors, such as post-translational modifications, or to the local architecture of the *IME1* promoter. In budding yeast, Tup1-Cyc8 is involved in repressing more than 150 gene targets (Smith and Johnson, 2000). Cup9, Yap6, Sok2, and Phd1 also perform other functions in regulating peptide transport, salt tolerance, and pseudohyphal

differentiation respectively in yeast (Xia et al., 2008, Rodrigues-Pousada et al., 2019, Pan and Heitman, 2000, Gimeno and Fink, 1994). I propose that binding of Tup1-Cyc8 and the four transcription factors may be regulated locally at the *IME1* promoter so that regulation of the other targeted gene loci are not affected upon induction of sporulation.

How is the binding of the transcription factors regulated locally at the *IME1* promoter? In my experiments, I inhibited PKA and TORC1 pathways with chemical compounds, and examined the protein expression of Yap6, Sok2, and Phd1 (Chapter 5: Figure 37). The changes in Yap6, Sok2, and Phd1 protein levels induced by PKA and TORC1 inhibition were markedly more dramatic compared to nutrient depletion. These data suggest that PKA and TORC1 are not completely inactive under sporulation conditions, which agrees with previous report that partial TORC1 activity is required for yeast meiosis (Weidberg et al., 2016). Strikingly, all three transcription factors were diminished upon PKA inhibition. Hence, I speculate that PKA signalling plays a more important role in regulating Yap6, Sok2, and Phd1. One possibility is that PKA signals locally to the *IME1* promoter to control Yap6, Sok2, and Phd1 binding. I propose that the *IME1* promoter may be regulated locally by the PKA catalytic subunit Tpk1 based on a number of observations. First, Tpk1 can interact with chromatin in budding yeast (Pokholok et al., 2006). Second, Tpk1 preferentially regulates glucose-sensitive genes. Tpk1 occupancy is induced by glucose, and is abolished in acetate-containing medium (Pokholok et al., 2006). Third, blocking Tpk1 activity in my experiments strongly reduced Yap6, Sok2, and Phd1 expression. Fourth, Sko1, a known physical interactor of Tpk1, is detected at the *IME1* promoter in nutrient-rich condition (Chapter 4: Figure 22). It would be interesting to determine whether Tpk1 or other PKA catalytic subunits interact with the *IME1* promoter by ChIP.

Changes in nutrient signalling can modulate protein structure and binding properties by post-translational modifications. Tup1-Cyc8 and its recruiting transcription factors may be modified upon induction of sporulation and thus dissociate from the *IME1* promoter. In support of this theory, post-translational modifications of Tup1, Cyc8, Yap6, Sok2, and Phd1 have been reported in the literature. Sok2 and Phd1 are both phosphorylated proteins regulated by the PKA

pathway (Raithatha et al., 2012, Shenhar and Kassir, 2001, Malcher et al., 2011). Yap6 contains two phosphorylation sites (Swaney et al., 2013), which could be dependent on PKA similar to its paralogue, Cin5 (Pereira et al., 2009). In addition, Tup1 and Cyc8 proteins are also modified. Both Tup1 and Cyc8 are phosphorylated proteins (Soulard et al., 2010, Redd et al., 1997). Notably, the Groucho and TLE1 proteins are also phosphorylated proteins, and their phosphorylated forms were demonstrated to be important for their nuclear functions (Husain et al., 1996). Hence, Tup1 phosphorylation may be conserved among Groucho/TLE1-like repressor proteins, and may play crucial role in regulating its ability to interact with chromatin. Furthermore, Tup1 and Cyc8 are both subjected to SUMOylation (Small Ubiquitin-like Modifier), which contributes to their ability to occupy gene promoters (Ng et al., 2015, Nadel et al., 2019, Oeser et al., 2016). My data indicate that Tup1 may be post-translationally modified in nutrient-rich conditions (marked by asterisk in Chapter 3: Figure 15A). Whether protein modifications regulate binding of Tup1-Cyc8 and its recruiting transcription factors at the *IME1* promoter remains to be investigated. Future work can address this question by detecting for modified transcription factors in nutrient-rich and nutrient-depleted conditions using specific antibodies in western blotting, or mass spectrometry.

Finally, it is worth noting that nutrients may differentially regulate Tup1 and Cyc8 binding at the *IME1* promoter. When cells are growing exponentially in nutrient-rich medium, Tup1 and Cyc8 are both strongly bound to the *IME1* promoter (Chapter 3: Figure 15). Eventually, when cells reach saturation, Tup1 remains strongly bound to the *IME1* promoter. In contrast, ChIP signals for Cyc8 reduced markedly at the *IME1* promoter in cells grown to saturation. Changes in Cyc8 protein abundance may in part contribute to the decreased ChIP signals (Chapter 3: Figure 14). Yet, the reduction in Cyc8 signals in cells grown to saturation does not correlate with loss of Cyc8 binding at the *IME1* promoter. Depletion of Cyc8 leads to rapid and complete de-repression of *IME1* transcription (Chapter 3: Figure 17), but *IME1* is not transcribed in cells grown to saturation (van Werven et al., 2012). It is possible that the interaction between Cyc8 and the *IME1* promoter was not detected by ChIP in cells grown to saturation. For example, Tup1-Cyc8 may undergo conformational changes so that Cyc8 becomes more distant from the chromatin. In addition, Cyc8 is a relatively large protein in budding yeast (966 residues, >100 kDa) (Redd et al.,

1997, Tartas et al., 2017, Warringer and Blomberg, 2006). Thus, Cyc8 may be more prone to protein degradation during the sonication step in the ChIP protocol (Pchelintsev et al., 2016). Consequently, ChIP signals for Cyc8 may be weaker, especially if less copies of Cyc8 are bound at the *IME1* promoter.

7.7 Tup1-Cyc8 modulates plasticity of *IME1* expression

Plasticity of gene expression describes the ability of a gene to be activated or repressed to adapt to changes in the environment. I propose that *IME1* is a highly flexible gene, and Tup1-Cyc8 plays a pivotal role in modulating its plasticity. My data demonstrate that the *IME1* promoter is poised for activation under repressive conditions, so that *IME1* transcription can occur rapidly once repression is relieved. When nutrients are replete, Tup1-Cyc8 binding at the *IME1* promoter ensures that *IME1* is quickly repressed by inhibiting activation of *IME1* transcription. Functional analyses of the *IME1* promoter also suggest that DNA sequences are designed to allow quick responses to changes in nutrient availability in the environment. My data demonstrate that Tup1-Cyc8 binds from 750 to 1400 bp upstream of the *IME1* start codon, which is exactly the same region that contains the regulatory elements important for *IME1* activation (Chapter 3: Figure 13, Chapter 6: Figure 39B) (Weidberg et al., 2016). Finer dissection of the Tup1-Cyc8 binding sites also reveals that Tup1-Cyc8 binds to *IME1* activating elements (Chapter 6: Figure 40, Figure 41, and Figure 43). In addition, previous study showed that the IREu sequence in the *IME1* promoter (1122 to 1153 upstream of the start codon) serves as a repressive element in the presence of glucose, but switch into an activating element in acetate-containing medium (Shenhar and Kassir, 2001). These evidence suggest that Tup1-Cyc8 and the *IME1* promoter sequences co-ordinate rapid activation and repression of *IME1* transcription to adapt to changes in nutrient availability.

Why is *IME1* expression plasticity biologically important in yeast? *IME1* is the transcription factor that dictates entry into meiosis, and thus its expression governs a major fate decision in yeast. In harsh environments such as nutrient stress, it is crucial that cells promptly make a decision to undergo meiosis and generate stress-resistant progenies to protect cell content from further damages. Transcription plasticity may allow *IME1* to be rapidly expressed to promote swift entry into meiosis when nutrients are depleted in the environment. In yeast, it is not uncommon for promoters to have overlapping repressive and activating elements to regulate gene expression. One example is *DIT1*, which is exclusively expressed during the late stages of sporulation and encodes for an enzyme required for spore wall maturation. The *DIT1* promoter contains a sequence element called NRE^{DIT} that mediates *DIT1*

repression during vegetative growth, and switches to an activating element of *DIT1* during sporulation (Friesen et al., 1997). Interestingly, transcription plasticity of many genes in yeast, including *IME1* and *DIT1*, is modulated by the binding of Tup1-Cyc8 in the promoters. In a study published by Rizzo et al., Tup1 binding was reported to be significantly correlated with genes that alter their expression when challenged with 13 different types of environmental changes (Rizzo et al., 2011). Thus, Tup1-Cyc8 binding is linked with plasticity in gene expression. Furthermore, Tup1-Cyc8 bound promoters exhibit a wider nucleosome depleted region near the transcription start site and have a broader distribution of conserved transcription factor compared to unbound promoters (Rizzo et al., 2011). These features likely allow promoters to be rapidly activated once Tup1-Cyc8 dissociates.

In *Drosophila*, the Groucho repressor protein is structurally similar to Tup1 and is considered a functional homologue of Tup1. Similar to Tup1, Groucho is also a global repressor that mediates multiple signalling pathways important for *Drosophila* development (Jennings and Ish-Horowicz, 2008). The Groucho repressor has also been linked with modulating gene expression plasticity in *Drosophila*. ChIP-seq studies revealed that Groucho binding in the genome allows fast activation of genes under permissive conditions. Groucho often co-localises with RNA polymerase II at the target promoters, and attenuates gene transcription by inducing proximal RNA polymerase II pausing (Kaul et al., 2014). Thus, genes that are muted by Groucho can be re-activated immediately as Groucho dissociates from the promoters. Tup1 and repressors of the Groucho/TLE family may have conserved functions in controlling genes that need to be flexibly expressed depending on the stage of development and environmental changes. In higher eukaryotes, genes with high expression plasticity generally regulate processes triggered by certain stimuli, such as inflammatory response, immune response, and drug responses (Xiao et al., 2019). Moreover, genes that demonstrate higher expression plasticity in humans are more likely to be implicated in diseases including cancer (Xiao et al., 2019). Understanding how Tup1-Cyc8 mediates gene expression plasticity in yeast may illuminate how gene are regulated to adapt to challenges in higher eukaryotes.

7.8 The *IME1* promoter displays some features of developmentally regulated enhancers found in mammalian genome

In this thesis, I showed that an unusually large complex of transcription factors binds to the *IME1* promoter at 1000 bp upstream of the start codon. My data demonstrate that at least 14 transcription factors (Tup1, Cyc8, Cup9, Yap6, Sok2, Phd1, Sut1, Mot3, Sko1, Nrg1, Nrg2, Pog1, Fkh1, Fkh2) are bound in nutrient-rich condition (Chapter 3: Figure 14 and Figure 19, Chapter 4: Figure 22). The unusually high density of transcription factors found at the *IME1* promoter is reminiscent of developmentally regulated enhancers found in mammalian cells (Sabari et al., 2018). Developmentally regulated enhancers are clusters of enhancers, which are short *cis*-regulatory DNA elements that recruit transcriptional activators and can mediate long range gene activation by contacting gene promoters. As a result, developmentally regulated enhancers are characterised by binding of high levels of transcription factors and the Mediator, and stimulate higher transcriptional activity (Whyte et al., 2013). Notably, clusters of enhancers frequently regulate genes encoding transcription factors that are responsible for establishing cell identity. In humans, developmentally regulated enhancers promote expression of embryonic stem cell transcription factors including Oct4, Sox2, and Nanog, which play important roles in maintaining stem cell pluripotency (Whyte et al., 2013). My data demonstrate that the *IME1* promoter exhibits two characteristics that resemble developmentally regulated enhancers in mammalian cells. First, the *IME1* promoter is bound by a large number of transcription factors that bind to DNA sequence motifs (Hnisz et al., 2013). Second, transcriptional activators are bound at the *IME1* promoter such that gene expression can be driven under appropriate conditions.

Given the similarities between the *IME1* promoter and developmentally regulated enhancers, it would be interesting to investigate whether mechanisms that regulate enhancers in the mammalian genome are applied to the *IME1* promoter in yeast. For example, genes that are driven by enhancers reinforce their own expression by forming a positive feedback loop. Specifically, transcription factors produced from these genes have binding sites enriched in the enhancer cluster domain, suggesting that they regulate their own expression (Whyte et al., 2013). Ime1 is a transcriptional activator that does not have sequence specificity. However,

when sporulation is induced, Ime1 partners with Ume6 which guides the heterodimer to target promoters by binding the URS1 motif. The YeTFaSCo database predicts a Ume6 binding site in the *IME1* promoter from 1095 to 1104 bp upstream of the start codon. Future work can dissect whether Ime1 promotes its own expression by binding to this Ume6 site upon induction of sporulation. More recently, a phenomenon known as phase separation has been suggested to regulate developmentally regulated enhancers in mammalian cells. Phase separation describes the formation of liquid-like condensates from the high density of transcriptional activators present at enhancer cluster domains (Sabari et al., 2018). Such condensates compartmentalise and concentrate transcriptional components and co-factors at genes involved in establishing cell identity (Sabari et al., 2018). Proteins with intrinsically disordered regions (or low complexity regions) can assemble into phase-separated droplets (Lin et al., 2015). Interestingly, I found that Tup1, Cyc8, Yap6, Sok2, and Phd1 contain intrinsically disordered regions by analysing their amino acid sequences with the PONDR tool (Predictor Of Naturally Disordered Regions, www.pondr.com). Future work can be done to investigate whether the large complex of transcription factors bound at the *IME1* promoter in nutrient-rich condition is concentrated by phase-separated liquid droplet. For example, binding of transcription factors at the *IME1* promoter may be examined after treating cells with 1,6-hexanediol, an aliphatic alcohol that disrupts formation of phase-separated liquid droplets (Kroschwald et al., 2017). Furthermore, the intrinsically disordered regions in the transcription factors may be purified to investigate their abilities to form phase-separated liquid droplets *in vitro* (Sabari et al., 2018).

IME1 governs entry into meiosis, an important cell fate decision in yeast. The *IME1* promoter is bound by a transcription factor assembly that displays common features with developmentally regulated enhancers in the mammalian genome. Hence, large transcription factor assemblies may be conserved throughout eukaryotes to control particular genes that are pivotal in making developmental decisions and establishing cell identity. In this thesis, I gained important insights into how signal integration and gene expression plasticity is achieved by co-ordinating binding of transcription factors at the *IME1* promoter. These findings may extend to

developmental genes in other eukaryotes to understand how transcriptional regulation controls fate decisions throughout development.

Chapter 8. Supplementary figures and tables

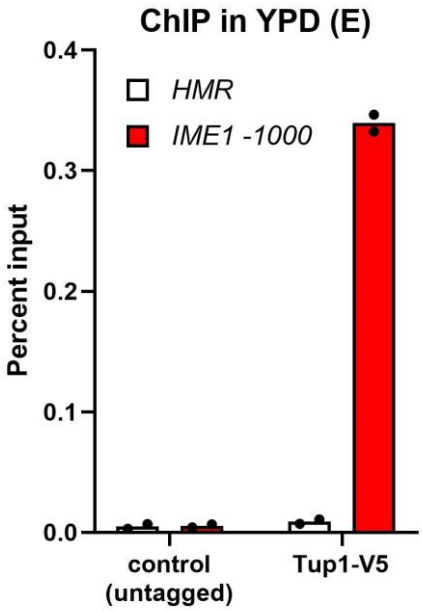

Supplementary figure 1. Tup1 binding detected by ChIP at the silent mating type cassette *HMR* and *IME1* upstream region.

ChIP-qPCR of V5 epitope-tagged Tup1 (FW3456) in exponentially growing cells (YPD (E)). For qPCR, primer pairs that amplify the silent mating type cassette *HMR* and 1000 bp upstream of the *IME1* start codon (*IME1 -1000*) were used. As negative control, ChIP signals from exponentially growing wild-type untagged cells (FW1511) were included. The signals are presented as a percentage of the input signal. Bars represent mean and dots indicate individual biological replicates.

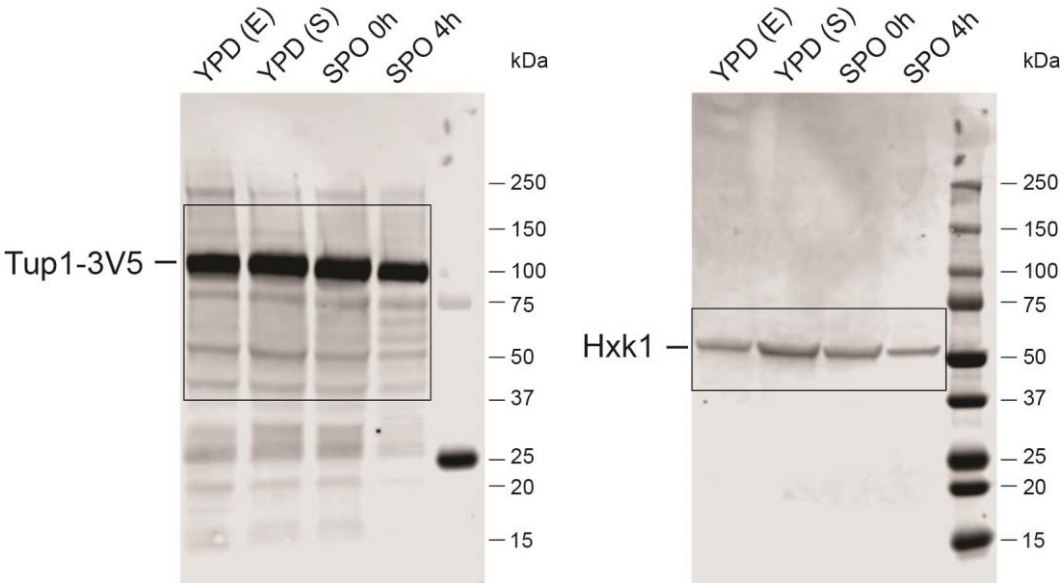

Supplementary figure 2. Uncropped western blot for Tup1-V5 and loading control Hxk1.

Uncropped western blot for Figure 15. *TUP1-V5* cells (FW3456) in exponential growth phase (YPD (E)), grown to saturation (YPD (S)), at 0h (SPO 0h) and 4h (SPO 4h) after sporulation induction were harvested. Total proteins were extracted and separated by SDS-PAGE. Tup1-V5 and Hxk1 were detected by antibodies specific to the V5 epitope and Hxk1 respectively. The cropped regions presented in the main figure are denoted by the boxes.

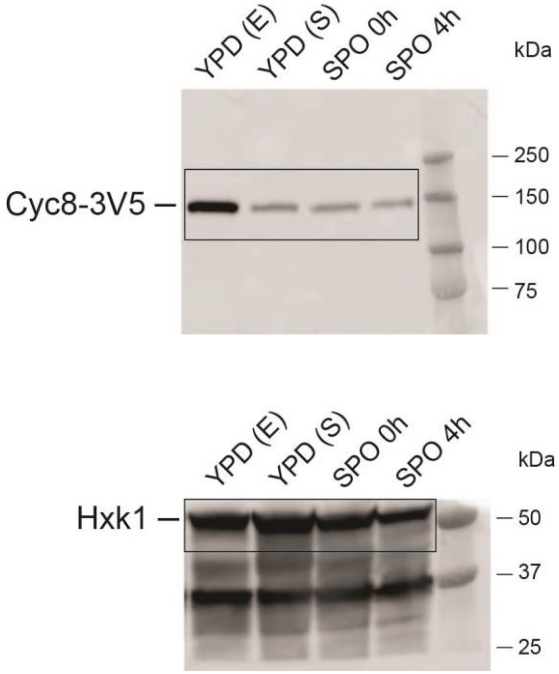

Supplementary figure 3. Uncropped western blot for Cyc8-V5 and loading control Hxk1.

Uncropped western blot for Figure 15. *CYC8-V5* cells (FW6381) in exponential growth phase (YPD (E)), grown to saturation (YPD (S)), at 0h (SPO 0h) and 4h (SPO 4h) after sporulation induction were harvested. Total proteins were extracted and separated by SDS-PAGE. Cyc8-V5 and Hxk1 were detected by antibodies specific to the V5 epitope and Hxk1 respectively. The cropped regions presented in the main figure are denoted by the boxes.

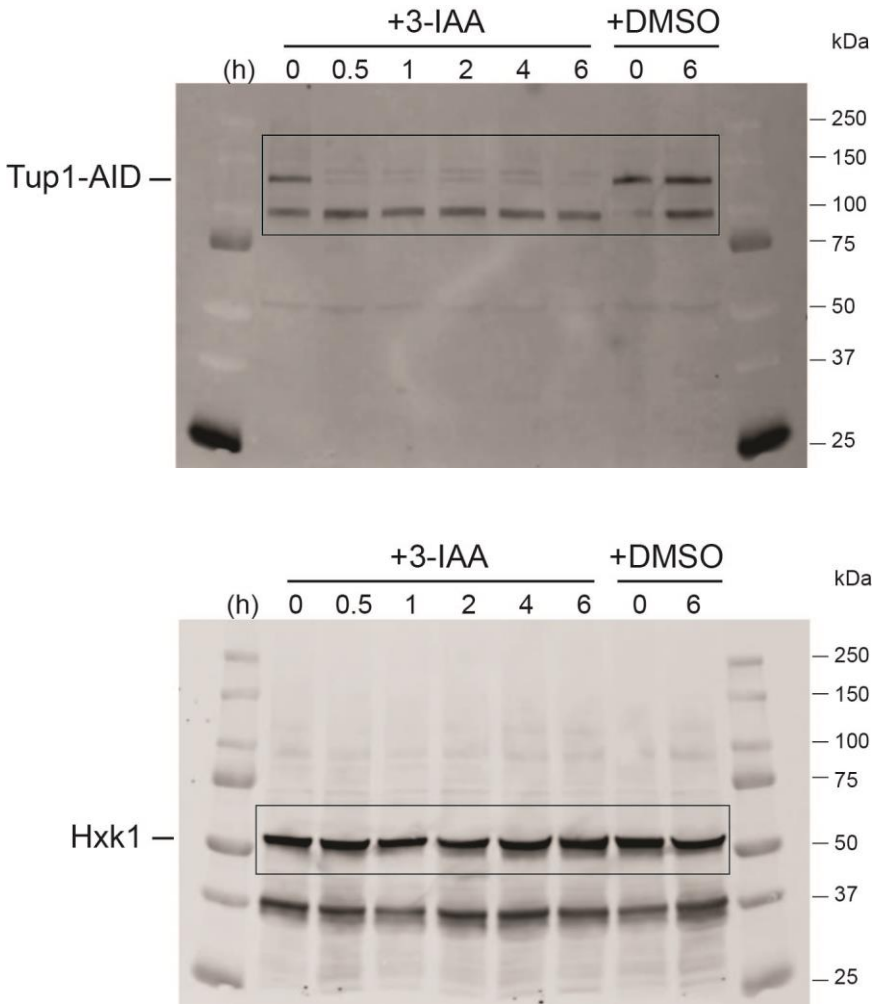

Supplementary figure 4. Uncropped western blot for Tup1-AID and loading control Hxk1 (Figure 17).

Uncropped western blot for Figure 17. *TUP1-AID* cells (FW5057) were treated with 3-IAA and DMSO respectively in nutrient-rich YPD medium, and harvested at the indicated time points. Total proteins were extracted and separated by SDS-PAGE. Tup1-AID and Hxk1 were detected by antibodies specific to the V5 epitope and Hxk1 respectively. The cropped regions presented in the main figure are denoted by the boxes.

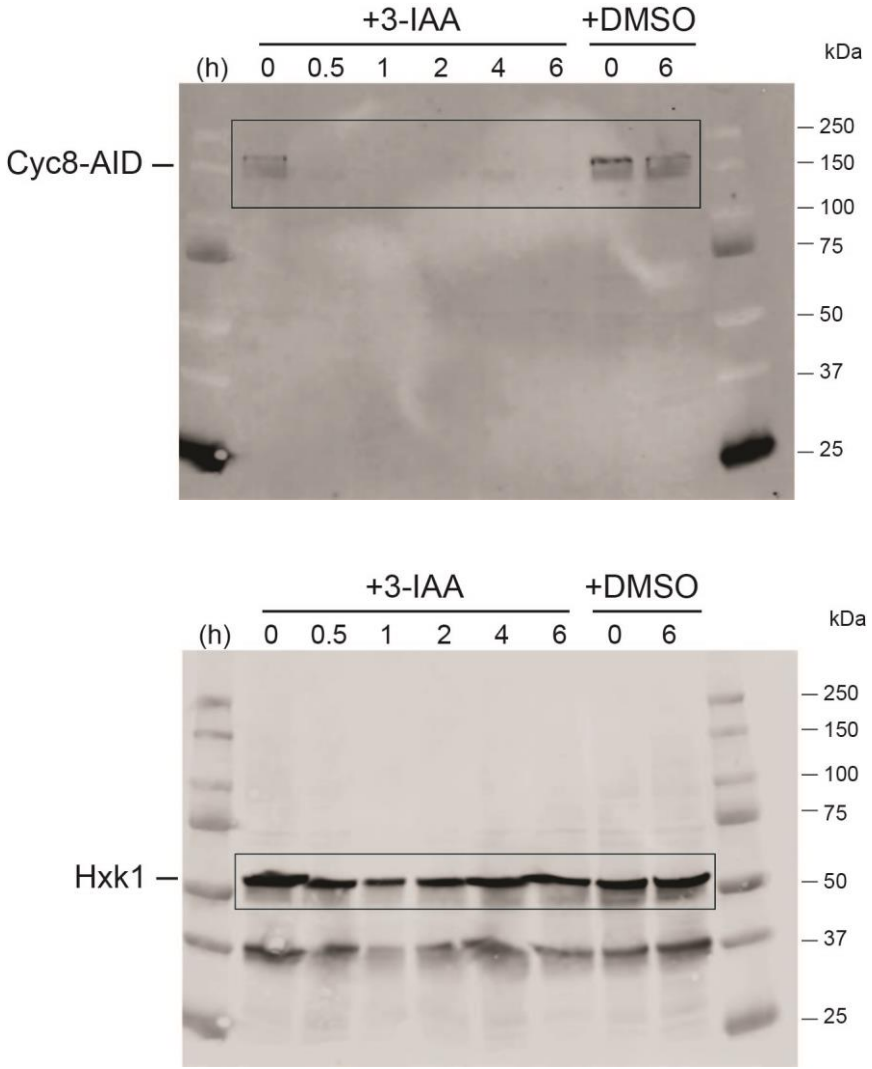

Supplementary figure 5. Uncropped western blot for Cyc8-AID and loading control Hxk1.

Uncropped western blot for Figure 17. *CYC8-AID* cells (FW6371) were treated with 3-IAA and DMSO respectively in nutrient-rich YPD medium, and harvested at the indicated time points. Total proteins were extracted and separated by SDS-PAGE. Cyc8-AID and Hxk1 were detected by antibodies specific to the V5 epitope and Hxk1 respectively. The cropped regions presented in the main figure are denoted by the boxes.

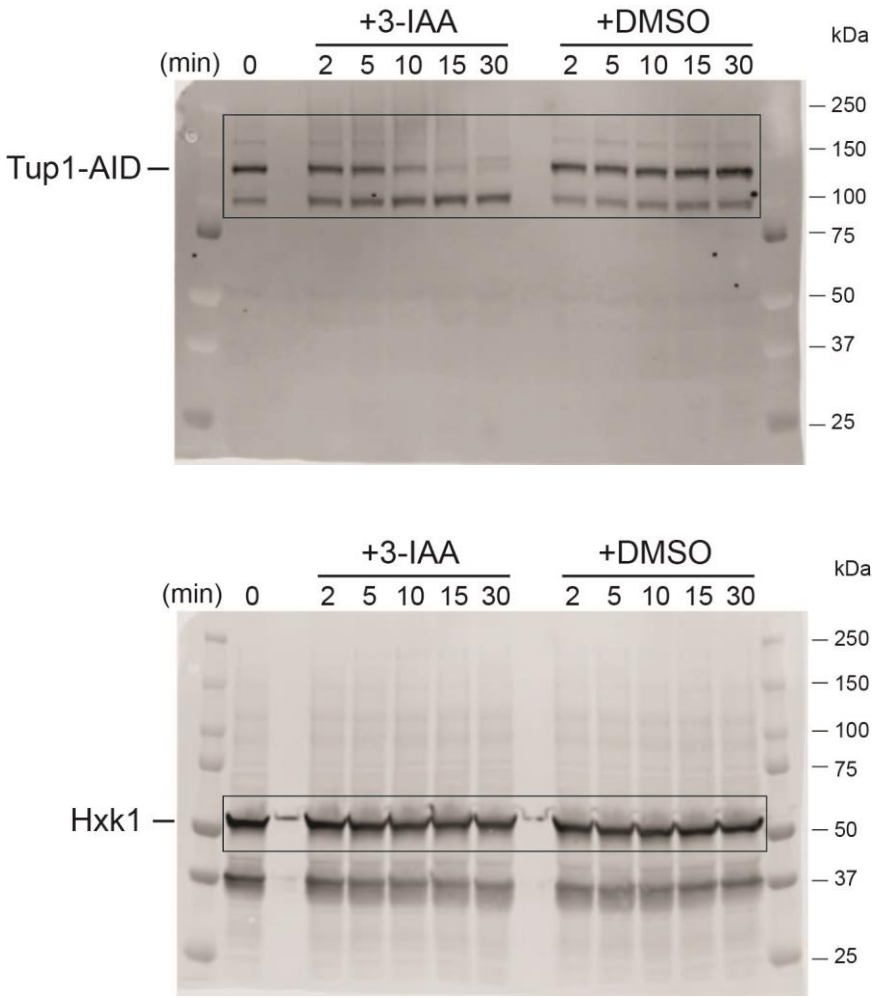

Supplementary figure 6. Uncropped western blot for Tup1-AID and loading control Hxk1 (Figure 18).

Uncropped western blot for Figure 18. *TUP1-AID* cells (FW5057) were treated with 3-IAA and DMSO respectively in nutrient-rich YPD medium, and harvested at indicated time points. Total proteins were extracted and separated by SDS-PAGE. Tup1-AID and Hxk1 were detected by antibodies specific to the V5 epitope and Hxk1 respectively. The cropped regions presented in the main figure are denoted by the boxes.

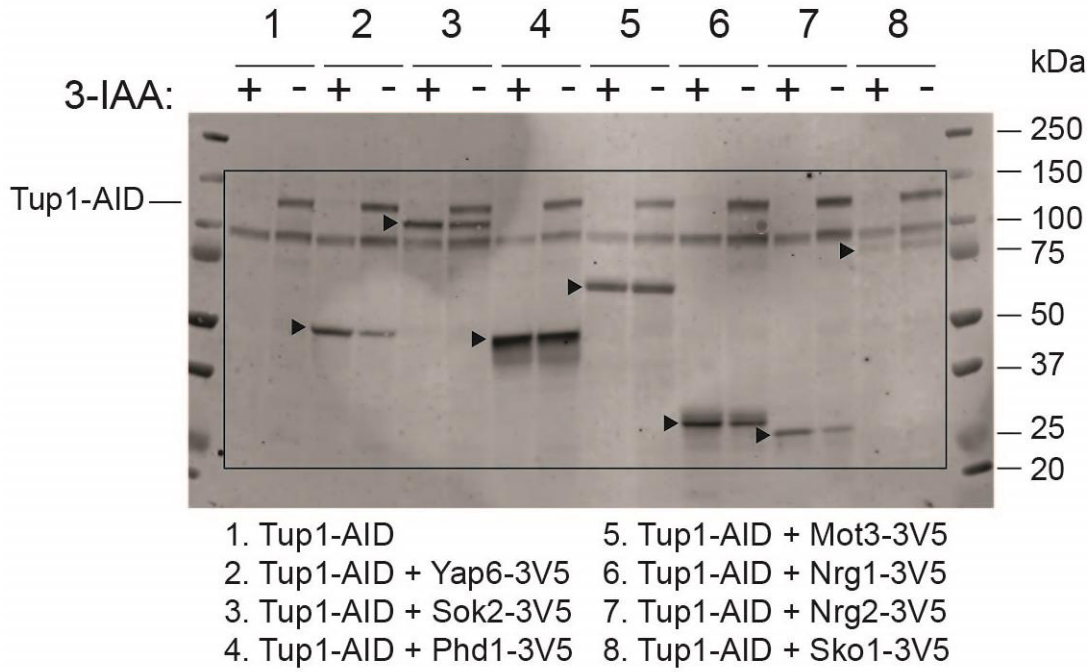

Supplementary figure 7. Uncropped western blot for Tup1-AID and V5-tagged transcription factors with Tup1-AID.

Uncropped western blot for Figure 24. *TUP1-AID* cells (FW5057) and *TUP1-AID* cells carrying V5-tagged Yap6 (FW4214), Sok2 (FW4218), Phd1 (FW5056), Mot3 (FW4229), Nrg1 (FW4230), Nrg2 (FW5055), and Sko1 (FW4224) were treated with 3-IAA and DMSO respectively in nutrient-rich YPD medium. Cells were harvested four hours after treatment. Total proteins were extracted and separated by SDS-PAGE. Tup1-AID and V5-tagged transcription factors were detected using an antibody specific to the V5 epitope. The band representing Tup1-AID is labelled in the figure and the black arrows indicate the V5-tagged transcription factors detected in the strains. The proteins detected in each strain are listed below the figure. The cropped region presented in the main figure is denoted by the box.

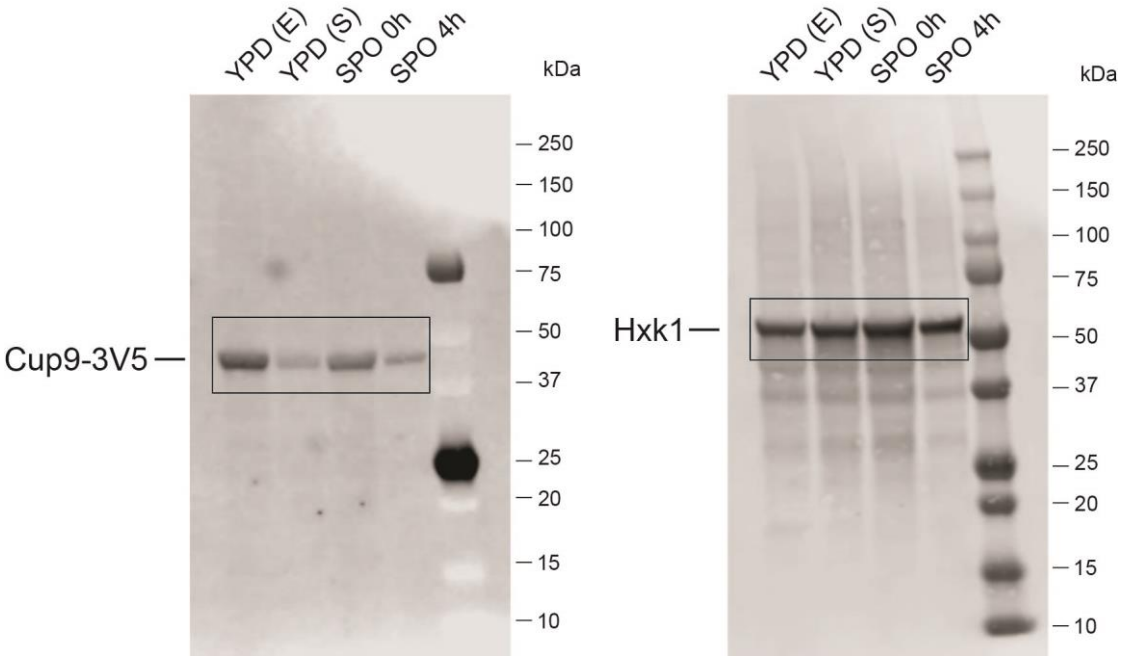

Supplementary figure 8. Uncropped western blot for Cup9-V5 and loading control Hxk1.

Uncropped western blot for Figure 27A. *CUP9-V5* cells (FW6976) in exponential growth phase (YPD (E)), grown to saturation (YPD (S)), at 0h (SPO 0h) and 4h (SPO 4h) after sporulation induction were harvested. Total proteins were extracted and separated by SDS-PAGE. Cup9-V5 and Hxk1 were detected by antibodies specific to the V5 epitope and Hxk1 respectively. The cropped regions presented in the main figure are denoted by the boxes.

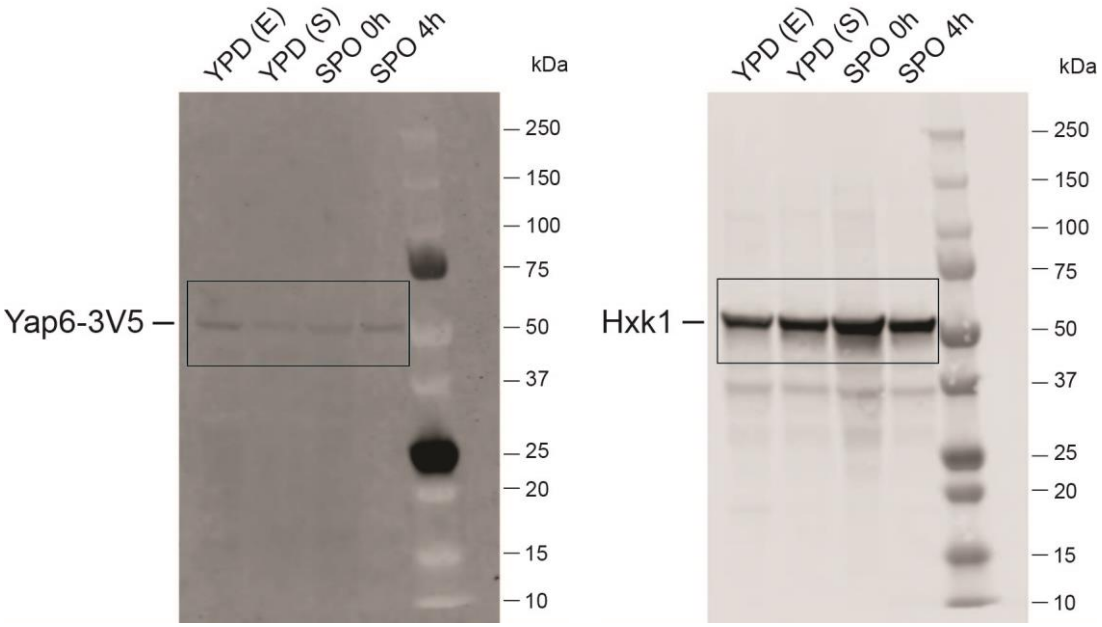

Supplementary figure 9. Uncropped western blot for Yap6-V5 and loading control Hxk1.

Uncropped western blot for Figure 27B. *YAP6-V5* cells (FW3833) in exponential growth phase (YPD (E)), grown to saturation (YPD (S)), at 0h (SPO 0h) and 4h (SPO 4h) after sporulation induction were harvested. Total proteins were extracted and separated by SDS-PAGE. Yap6-V5 and Hxk1 were detected by antibodies specific to the V5 epitope and Hxk1 respectively. The cropped regions presented in the main figure are denoted by the boxes.

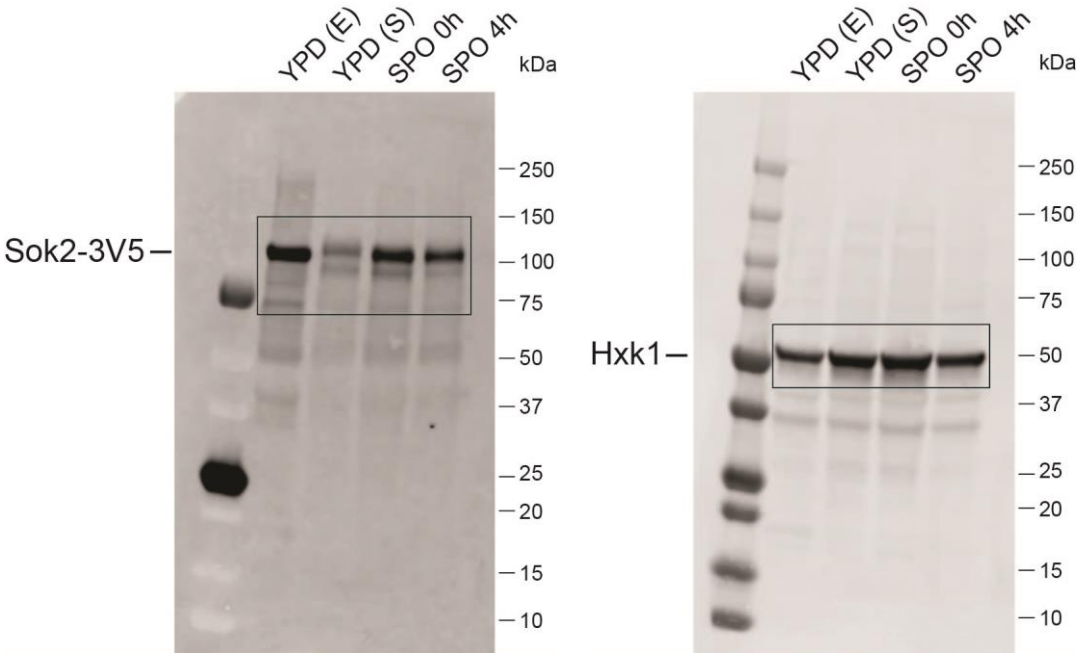

Supplementary figure 10. Uncropped western blot for Sok2-V5 and loading control Hxk1.

Uncropped western blot for Figure 27C. *SOK2-V5* cells (FW5638) in exponential growth phase (YPD (E)), grown to saturation (YPD (S)), at 0h (SPO 0h) and 4h (SPO 4h) after sporulation induction were harvested. Total proteins were extracted and separated by SDS-PAGE. Sok2-V5 and Hxk1 were detected by antibodies specific to the V5 epitope and Hxk1 respectively. The cropped regions presented in the main figure are denoted by the boxes.

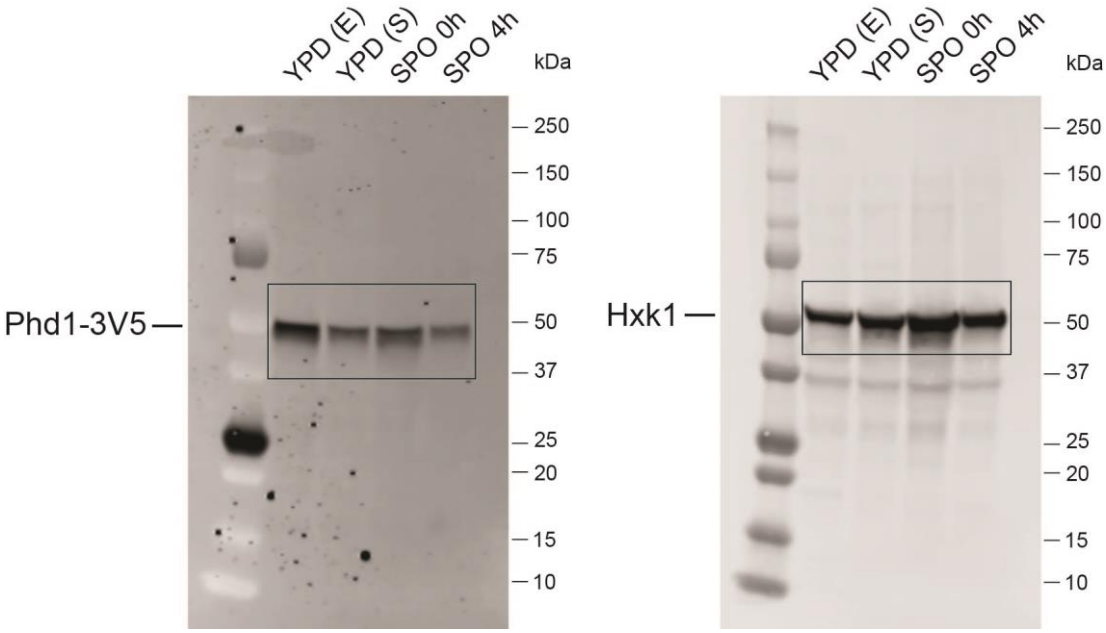

Supplementary figure 11. Uncropped western blot for Phd1-V5 and loading control Hxk1.

Uncropped western blot for Figure 27D. *PHD1-V5* cells (FW4466) in exponential growth phase (YPD (E)), grown to saturation (YPD (S)), at 0h (SPO 0h) and 4h (SPO 4h) after sporulation induction were harvested. Total proteins were extracted and separated by SDS-PAGE. Phd1-V5 and Hxk1 were detected by antibodies specific to the V5 epitope and Hxk1 respectively. The cropped regions presented in the main figure are denoted by the boxes.

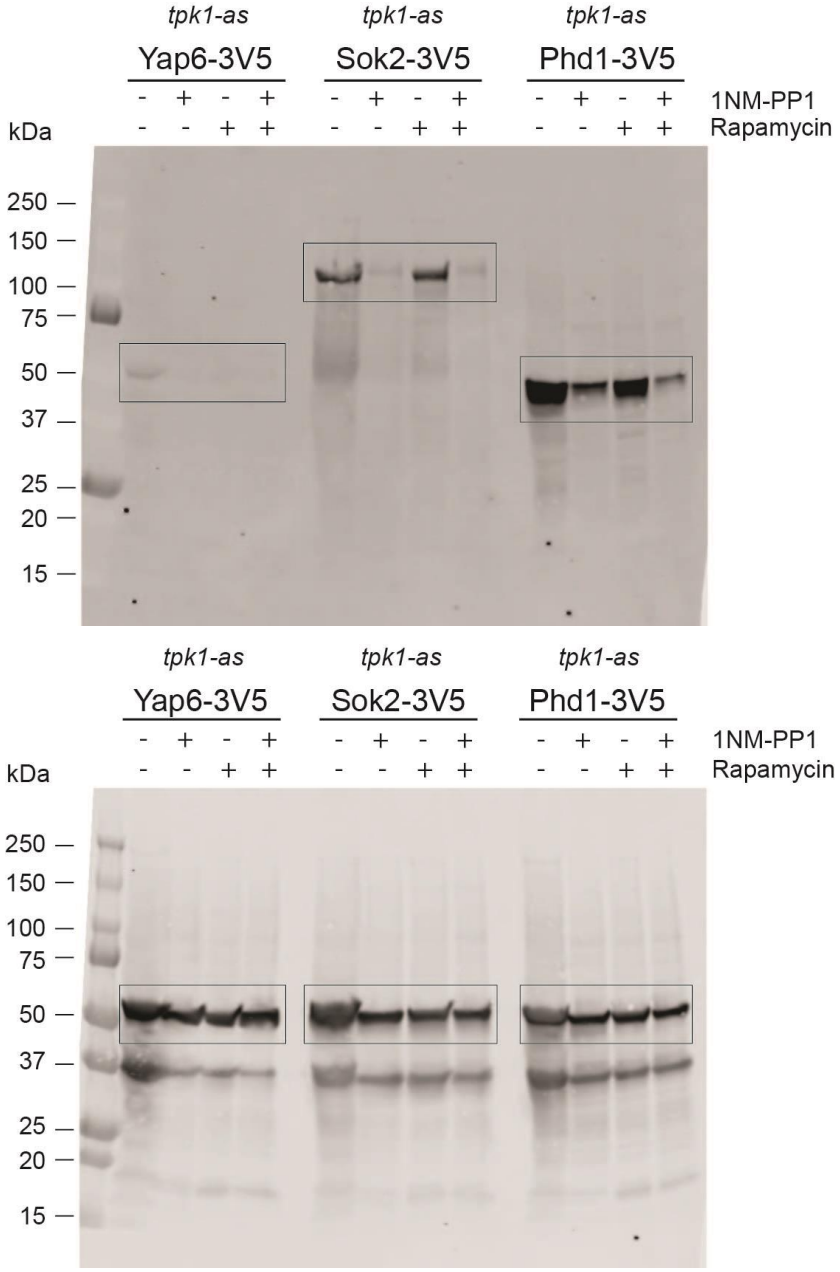

Supplementary figure 12. Uncropped western blot for Yap6-V5, Sok2-V5, and Phd1-V5 with PKA and TORC1 inhibition and loading control Hxk1.

Uncropped western blot for Figure 37. Cells with *tpk1-as* allele expressing Yap6-V5 (FW5453), Sok2-V5 (FW5454), and Phd1-V5 (FW5528) were treated with 1NM-PP1, rapamycin, or both. Total proteins were extracted and separated by SDS-PAGE. V5-tagged transcription factors and Hxk1 were detected by antibodies specific to the V5 epitope and Hxk1 respectively. The cropped regions presented in the main figure are denoted by the boxes.

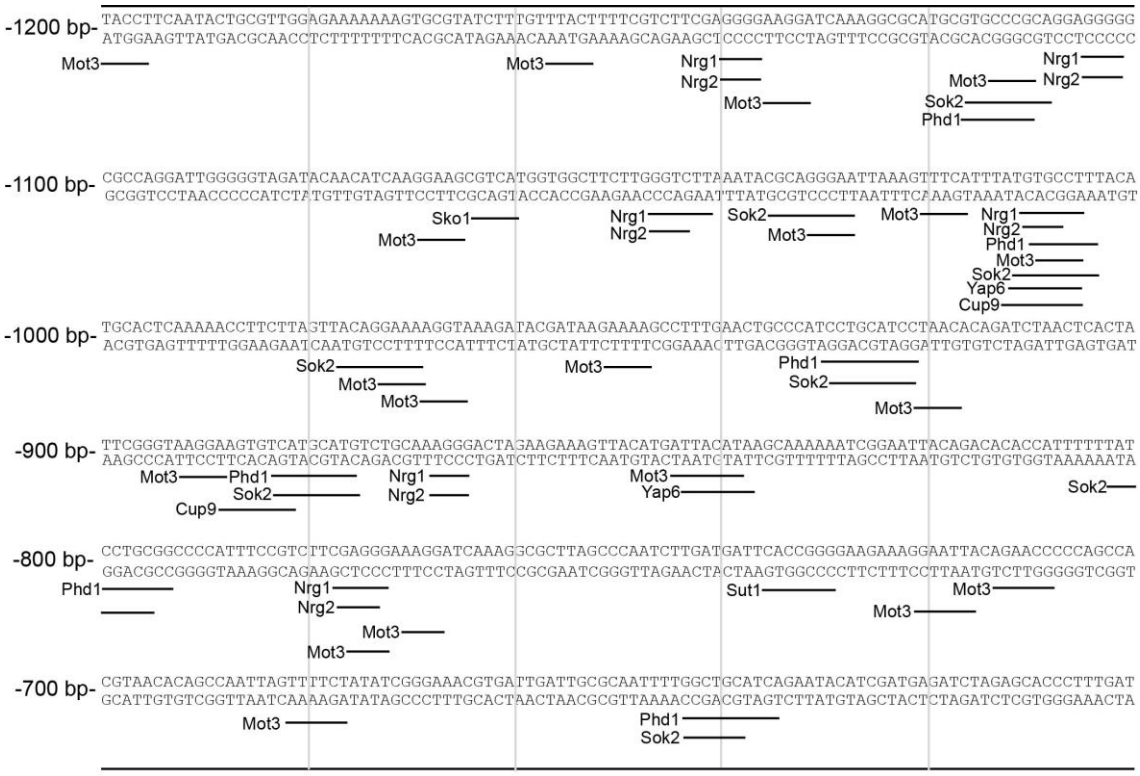

Supplementary figure 13. Sequence of the *IME1* promoter between 600 and 1200 bp upstream of the *IME1* start codon, with transcription factor binding sites labelled.

Sequence of the *IME1* promoter between 600 and 1200 bp upstream of the *IME1* start codon. Predicted binding motifs are displayed for the nine Tup1-Cyc8 interacting transcription factors that bind to the *IME1* promoter. Transcription factor binding motifs were predicted by the YeTFaSCo database with at least 70% of the maximum possible score (de Boer and Hughes, 2012), except for the Sko1 and Nrg2 binding sites which were labelled manually.

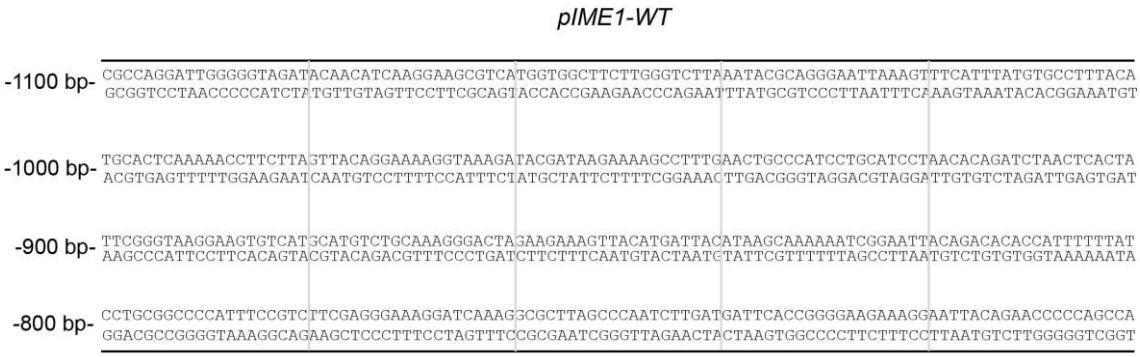

Supplementary figure 14. Sequence of the *pIME1-WT* promoter, between 700 and 1100 bp upstream of the *IME1* start codon.

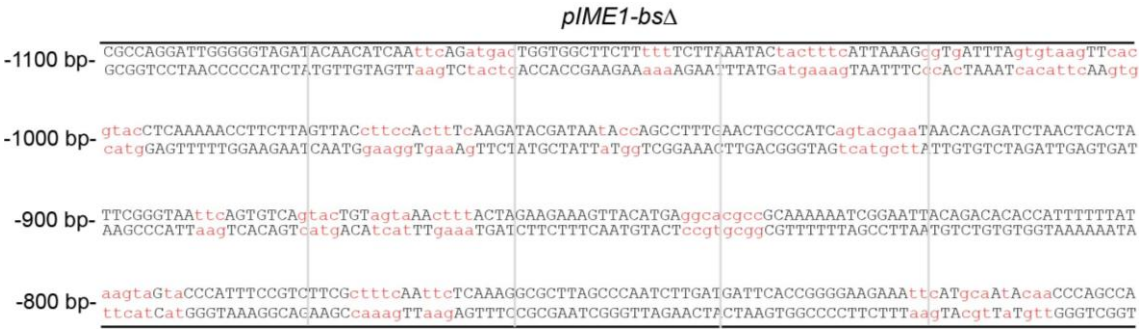

Supplementary figure 15. Sequence of the *pIME1-bs*Δ promoter, between 700 and 1100 bp upstream of the *IME1* start codon.

The *pIME1-bs*Δ sequence that was inserted into the single copy integration plasmid, and subsequently integrated into the yeast genome. The *pIME1-bs*Δ promoter carried mutations of the predicted binding sites of Yap6, Sok2, Phd1, Mot3, Sko1, Nrg1, and Nrg2 between 700 and 1100 bp upstream of the *IME1* start codon. Mutated sites (103 bp) are represented in red lowercase.

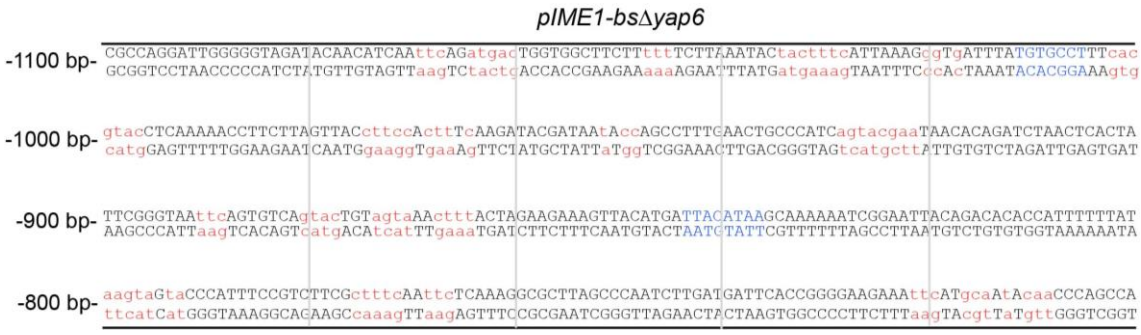

Supplementary figure 16. Sequence of the *pIME1-bsΔyap6* promoter, between 700 and 1100 bp upstream of the *IME1* start codon.

The *pIME1-bsΔyap6* sequence that was inserted into the single copy integration plasmid, and subsequently integrated into the yeast genome. Two binding sites (15 bp) predicted for Yap6 were restored from the *pIME1-bsΔ* promoter. Mutated sites are represented in red lowercase, and restored sites are indicated by blue uppercase.

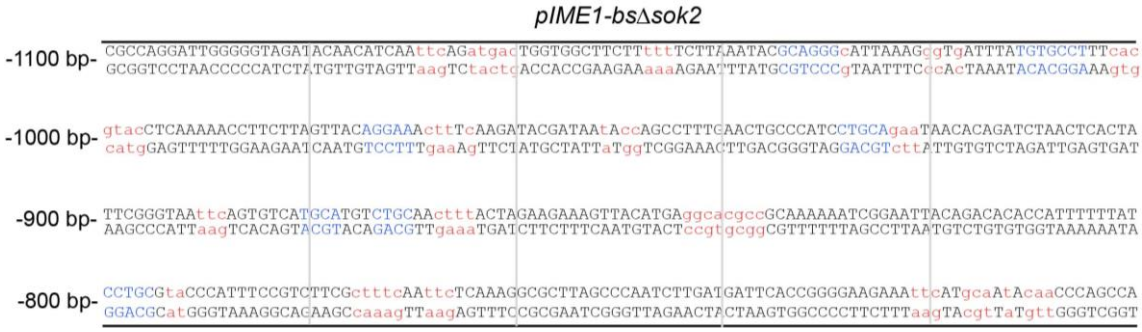

Supplementary figure 17. Sequence of the *pIME1-bsΔsok2* promoter, between 700 and 1100 bp upstream of the *IME1* start codon.

The *pIME1-bsΔsok2* sequence that was inserted into the single copy integration plasmid, and subsequently integrated into the yeast genome. Seven binding sites (36 bp) predicted for Sok2 were restored from the *pIME1-bsΔ* promoter. Mutated sites are represented in red lowercase, and restored sites are indicated by blue uppercase.

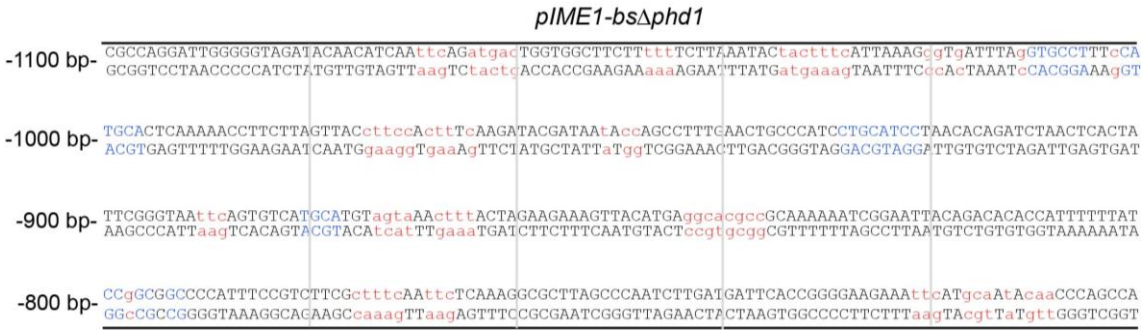

Supplementary figure 18. Sequence of the *pIME1-bsΔphd1* promoter, between 700 and 1100 bp upstream of the *IME1* start codon.

The *pIME1-bsΔphd1* sequence that was inserted into the single copy integration plasmid, and subsequently integrated into the yeast genome. Five binding sites (30 bp) predicted for Phd1 were restored from the *pIME1-bsΔ* promoter. Mutated sites are represented in red lowercase, and restored sites are indicated by blue uppercase.

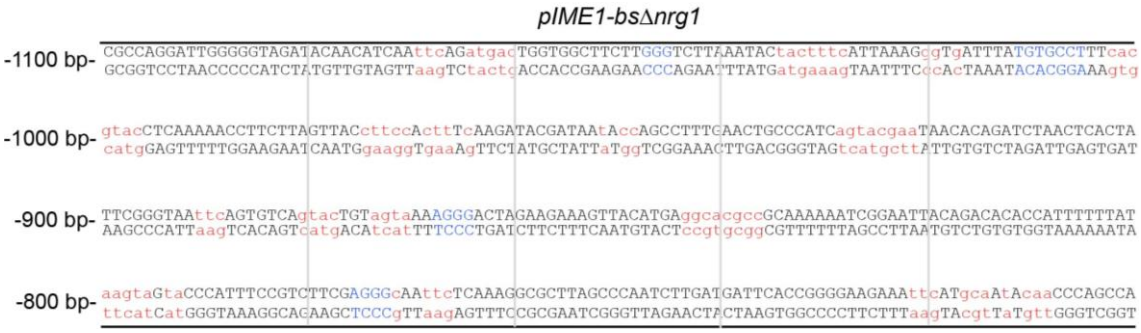

Supplementary figure 19. Sequence of the *pIME1-bsΔnrg1* promoter, between 700 and 1100 bp upstream of the *IME1* start codon.

The *pIME1-bsΔnrg1* sequence that was inserted into the single copy integration plasmid, and subsequently integrated into the yeast genome. Four binding sites (18 bp) predicted for Nrg1 were restored from the *pIME1-bsΔ* promoter. The *pIME1-bsΔnrg1* predicts a promoter that binds both Nrg1 and Nrg2, since the paralogues target opposite strands of the same motif. Mutated sites are represented in red lowercase, and restored sites are indicated by blue uppercase.

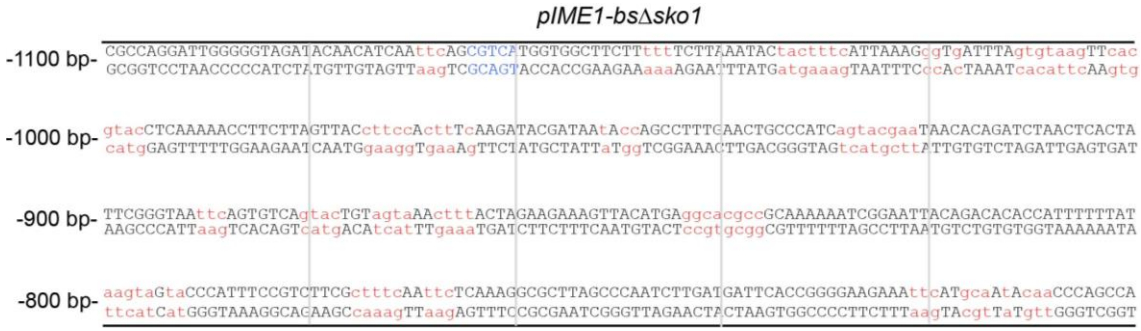

Supplementary figure 20. Sequence of the *pIME1-bsΔsko1* promoter, between 700 and 1100 bp upstream of the *IME1* start codon.

The *pIME1-bsΔsko1* sequence that was inserted into the single copy integration plasmid, and subsequently integrated into the yeast genome. One binding site (5 bp) predicted for Sko1 was restored from the *pIME1-bsΔ* promoter. Mutated sites are represented in red lowercase, and restored sites are indicated by blue uppercase.

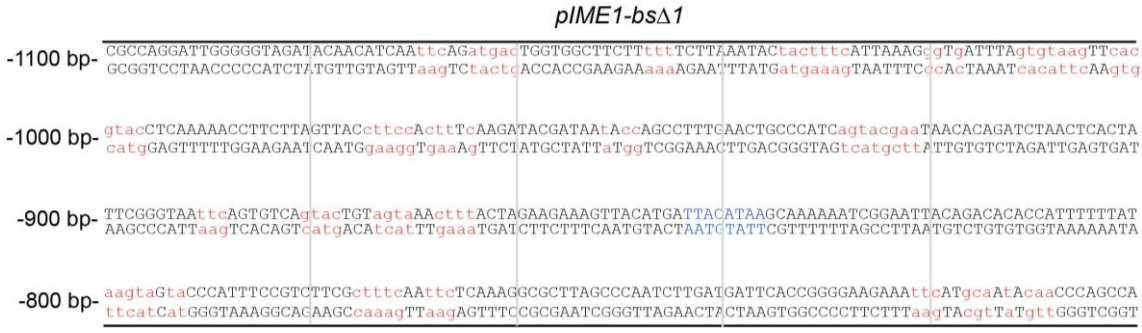

Supplementary figure 21. Sequence of the *pIME1-bsΔ1* promoter, between 700 and 1100 bp upstream of the *IME1* start codon.

The *pIME1-bsΔ1* sequence that was inserted into the single copy integration plasmid, and subsequently integrated into the yeast genome. Only one of the two binding sites predicted for Yap6 from 837 to 844 bp (8 bp) upstream of the *IME1* start codon was restored from the *pIME1-bsΔ* promoter. Mutated sites are represented in red lowercase, and restored sites are indicated by blue uppercase.

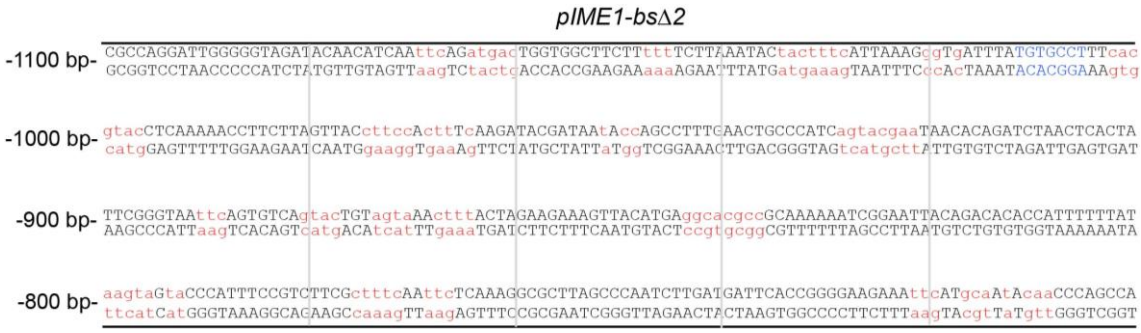

Supplementary figure 22. Sequence of the *pIME1-bsΔ2* promoter, between 700 and 1100 bp upstream of the *IME1* start codon.

The *pIME1-bsΔ2* sequence that was inserted into the single copy integration plasmid, and subsequently integrated into the yeast genome. Only one of the two binding sites predicted for Yap6 from 1006 to 1012 bp (7 bp) upstream of the *IME1* start codon was restored from the *pIME1-bsΔ* promoter. Mutated sites are represented in red lowercase, and restored sites are indicated by blue uppercase.

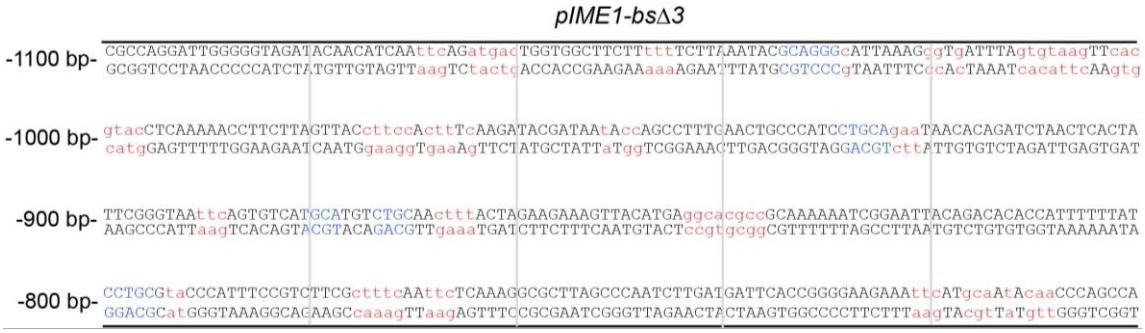

Supplementary figure 23. Sequence of the *pIME1-bsΔ3* promoter, between 700 and 1100 bp upstream of the *IME1* start codon.

The *pIME1-bsΔ3* sequence that was inserted into the single copy integration plasmid, and subsequently integrated into the yeast genome. Only binding sites predicted for Sok2 that match the MTGCA motif were restored from the *pIME1-bsΔ* promoter. Five sites were restored at 1030 to 1035, 925 to 929, 878 to 881, 871 to 874, 796 to 800 bp upstream of the *IME1* start codon (24 bp in total). Mutated sites are represented in red lowercase, and restored sites are indicated by blue uppercase.

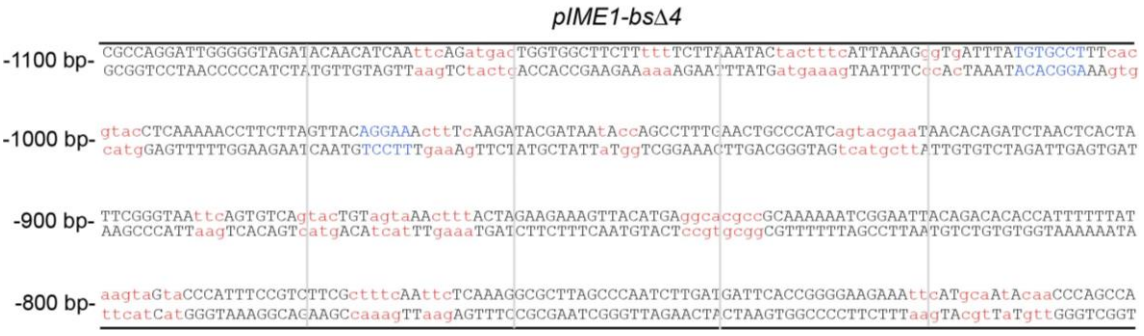

Supplementary figure 24. Sequence of the *pIME1-bsΔ4* promoter, between 700 and 1100 bp upstream of the *IME1* start codon.

The *pIME1-bsΔ4* sequence that was inserted into the single copy integration plasmid, and subsequently integrated into the yeast genome. Only binding sites predicted for Sok2 that match the AGGCAM motif were restored from the *pIME1-bsΔ* promoter. Two sites were restored at 1006 to 1012 and 971 to 975 bp upstream of the *IME1* start codon (12 bp in total). Mutated sites are represented in red lowercase, and restored sites are indicated by blue uppercase.

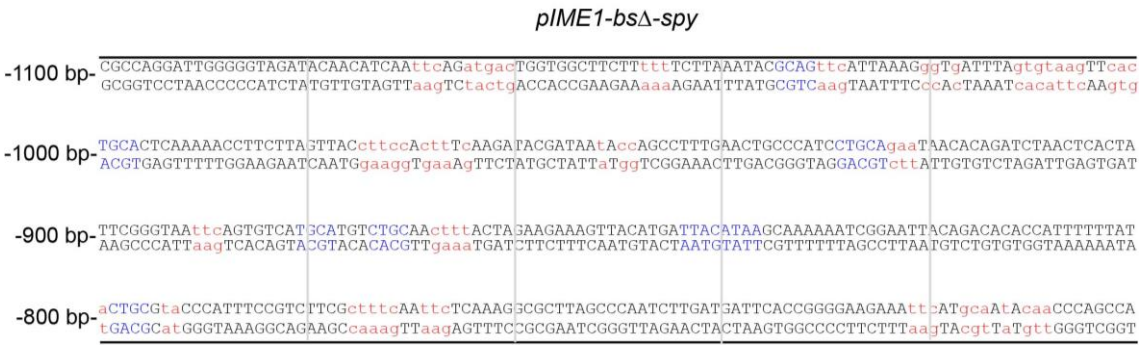

Supplementary figure 25. Sequence of the *pIME1-bsΔ-spy* promoter, between 700 and 1100 bp upstream of the *IME1* start codon.

The *pIME1-bsΔ-spy* sequence that was inserted into the single copy integration plasmid, and subsequently integrated into the yeast genome. The TTATGTAA (-837-844) motif and six motifs matching MTGCA were restored from the *pIME1-bsΔ* promoter. Seven sites were restored at 1032 to 1035, 997 to 1000, 925 to 928, 878 to 881, 871 to 874, 837 to 844, 796 to 799 bp upstream of the *IME1* start codon (33 bp in total). Mutated sites are represented in red lowercase, and restored sites are indicated by blue uppercase.

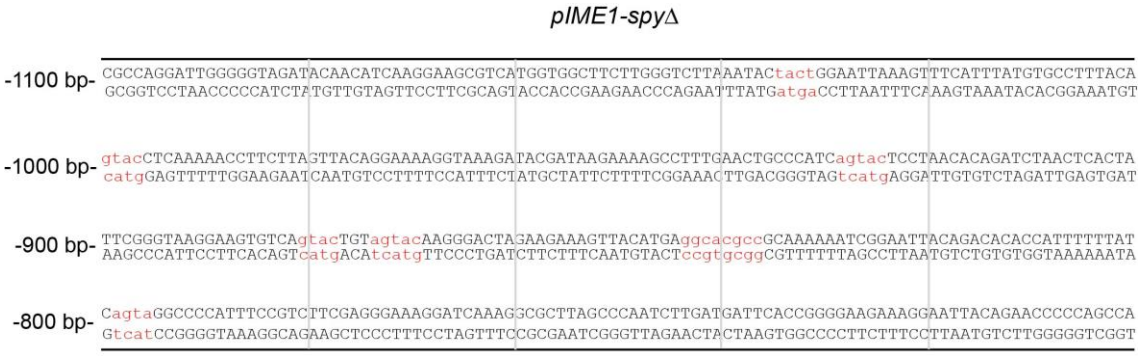

Supplementary figure 26. Sequence of the *pIME1-spy*Δ promoter, between 700 and 1100 bp upstream of the *IME1* start codon.

The *pIME1-spy*Δ sequence that was inserted into the single copy integration plasmid, and subsequently integrated into the yeast genome. The TTATGTAA (-837-844) motif and six motifs matching MTGCA were mutated from the *pIME1-WT* promoter. Seven sites were mutated at 1032 to 1035, 997 to 1000, 925 to 928, 878 to 881, 870 to 874, 837 to 844, 796 to 799 bp upstream of the *IME1* start codon (34 bp in total). Mutated sites are represented in red lowercase.

Yeast strain	Genotype	Source
FW1511 (*WT*)	*MAT**a**, ho::LYS2, lys2, ura3, leu2::hisG, his3::hisG, trp1::hisG* *MATα, ho::LYS2, lys2, ura3, leu2::hisG, his3::hisG, trp1::hisG*	Lab collection
FW968	*MAT**a**, ho::LYS2, ura3, leu2::hisG, his3::hisG, trp1::hisG, POG1-3V5::HIS3* *MATα, ho::LYS2, ura3, leu2::hisG, his3::hisG, trp1::hisG, POG1-3V5::HIS3*	Lab collection
FW969	*MAT**a**, ho::LYS2, ura3, leu2::hisG, his3::hisG, trp1::hisG, FKH2-3V5::HIS* *MATα, ho::LYS2, ura3, leu2::hisG, his3::hisG, trp1::hisG, FKH2-3V5::HIS*	Lab collection
FW1908	*MAT**a**, ho::LYS2, lys2, ura3, leu2::hisG, trp1::hisG, his3::pTEF1-osTIR::HIS3* *MATα, ho::LYS2, lys2, ura3, leu2::hisG, trp1::hisG, his3::pTEF1-osTIR::HIS3*	Lab collection
FW3456	*MAT**a**, ho::LYS2, lys2, ura3, leu2::hisG, his3::hisG, trp1::hisG, TUP1-3V5::HIS3* *MATα, ho::LYS2, lys2, ura3, leu2::hisG, his3::hisG, trp1::hisG, TUP1-3V5::HIS3*	This thesis
FW3603	*MAT**a**, ho::LYS2, lys2, ura3, leu2::hisG, his3::hisG, trp1::hisG, yap6::NatMX, TUP1-3V5::HIS3* *MATα, ho::LYS2, lys2, ura3, leu2::hisG, his3::hisG, trp1::hisG, yap6::NatMX, TUP1-3V5::HIS3*	This thesis
FW3833	*MAT**a**, ho::LYS2, lys2, ura3, leu2::hisG, his3::hisG, trp1::hisG, YAP6-3V5::KanMX* *MATα, ho::LYS2, lys2, ura3, leu2::hisG, his3::hisG, trp1::hisG, YAP6-3V5::KanMX*	This thesis
FW3944	*MAT**a**, ho::LYS2, lys2, ura3, leu2::hisG, his3::hisG, trp1::hisG, pIME1(-800-2315Δ)::HIS3MX* *MATα, ho::LYS2, lys2, ura3, leu2::hisG, his3::hisG, trp1::hisG, ime1::HISMX6*	This thesis
FW3946	*MAT**a**, ho::LYS2, lys2, ura3, leu2::hisG, his3::hisG, trp1::hisG, pIME1(-1600-2315Δ)::KanMX* *MATα, ho::LYS2, lys2, ura3, leu2::hisG, his3::hisG, trp1::hisG, ime1::HISMX6*	This thesis
FW3947	*MAT**a**, ho::LYS2, lys2, ura3, leu2::hisG, his3::hisG, trp1::hisG, pIME1(-1400-2315Δ)::KanMX* *MATα, ho::LYS2, lys2, ura3, leu2::hisG, his3::hisG, trp1::hisG, ime1::HISMX6*	This thesis
FW3948	*MAT**a**, ho::LYS2, lys2, ura3, leu2::hisG, his3::hisG, trp1::hisG, pIME1(-1200-2315Δ)::KanMX* *MATα, ho::LYS2, lys2, ura3, leu2::hisG, his3::hisG, trp1::hisG, ime1::HISMX6*	This thesis
FW3949	*MAT**a**, ho::LYS2, lys2, ura3, leu2::hisG, his3::hisG, trp1::hisG, pIME1(-1000-2315Δ)::KanMX* *MATα, ho::LYS2, lys2, ura3, leu2::hisG, his3::hisG, trp1::hisG, ime1::HISMX6*	This thesis

FW3950	*MAT**a**, ho::LYS2, lys2, ura3, leu2::hisG, his3::hisG, trp1::hisG, pIME1(-800-2315Δ)::KanMX* *MATα, ho::LYS2, lys2, ura3, leu2::hisG, his3::hisG, trp1::hisG, ime1::HISMX6*	This thesis
FW3951	*MAT**a**, ho::LYS2, lys2, ura3, leu2::hisG, his3::hisG, trp1::hisG, pIME1(-600-2315Δ)::KanMX* *MATα, ho::LYS2, lys2, ura3, leu2::hisG, his3::hisG, trp1::hisG, ime1::HISMX6*	This thesis
FW3979	*MAT**a**, ho::LYS2, lys2, ura3, leu2::hisG, his3::hisG, trp1::hisG, sok2::NatMX, TUP1-3V5::HIS3* *MATα, ho::LYS2, lys2, ura3, leu2::hisG, his3::hisG, trp1::hisG, sok2::NATMX, TUP1-3V5::HIS3*	This thesis
FW3991	*MAT**a**, ho::LYS2, lys2, ura3, leu2::hisG, his3::hisG, trp1::hisG, phd1::KanMX, TUP1-3V5::his3* *MATα, ho::LYS2, lys2, ura3, leu2::hisG, his3::hisG, trp1::hisG, phd1::KanMX, TUP1-3V5::his3*	This thesis
FW4010	*MAT**a**, ho::LYS2, lys2, ura3, leu2::hisG, his3::hisG, trp1::hisG, sok2::NATMX, phd1::KanMX, yap6::NATMX, TUP1-3V5::HIS3* *MATα, ho::LYS2, lys2, ura3, leu2::hisG, his3::hisG, trp1::hisG, sok2::NATMX, phd1::KanMX, yap6::NATMX, TUP1-3V5::HIS3*	This thesis
FW4128	*MAT**a**, ho::LYS2, lys2, ura3, leu2::hisG, his3::hisG, trp1::hisG* *MATα, ho::LYS2, lys2, ura3, leu2::hisG, his3::hisG, trp1::hisG, ime1::HISMX6*	This thesis
FW4214	*MAT**a**, ho::LYS2, lys2, ura3, leu2::hisG, trp1::hisG, his3::pTEF1-osTIR::HIS3, TUP1-3V5-IAA7::KanMX6, YAP6-3V5::KanMX* *MATα, ho::LYS2, lys2, ura3, leu2::hisG, trp1::hisG, his3::pTEF1-osTIR::HIS3, TUP1-3V5-IAA7::KanMx6, YAP6-3V5::KanMX*	This thesis
FW4218	*MAT**a**, ho::LYS2, lys2, ura3, leu2::hisG, trp1::hisG, his3::pTEF1-osTIR::HIS3, TUP1-3V5-IAA7::KanMX6, SOK2-3V5::HIS3* *MATα, ho::LYS2, lys2, ura3, leu2::hisG, trp1::hisG, his3::pTEF1-osTIR::HIS3, TUP1-3V5-IAA7::KanMX6, SOK2-3V5::HIS3*	This thesis
FW4224	*MAT**a**, ho::LYS2, lys2, ura3, leu2::hisG, trp1::hisG, his3::pTEF1-osTIR::HIS3, TUP1-3V5-IAA7::KanMX6, SKO1-3V5::KanMX* *MATα, ho::LYS2, lys2, ura3, leu2::hisG, trp1::hisG, his3::pTEF1-osTIR::HIS3, TUP1-3V5-IAA7::KanMX6, SKO1-3V5::KanMX*	This thesis
FW4229	*MAT**a**, ho::LYS2, lys2, ura3, leu2::hisG, trp1::hisG, his3::pTEF1-osTIR::HIS3, TUP1-3V5-IAA7::KanMX6, MOT3-3V5::KanMX* *MATα, ho::LYS2, lys2, ura3, leu2::hisG, trp1::hisG, his3::pTEF1-osTIR::HIS3, TUP1-3V5-IAA7::KanMX6, MOT3-3V5::KanMX*	This thesis
FW4230	*MAT**a**, ho::LYS2, lys2, ura3, leu2::hisG, trp1::hisG, his3::pTEF1-osTIR::HIS3, TUP1-3V5-IAA7::KanMX6, NRG1-3V5::KanMX* *MATα, ho::LYS2, lys2, ura3, leu2::hisG, trp1::hisG, his3::pTEF1-osTIR::HIS3, TUP1-3V5-IAA7::KanMX6, NRG1-3V5::KanMX*	This thesis

FW4239	*MAT**a**, ho::LYS2, lys2, ura3, leu2::hisG, his3::hisG, trp1::hisG, sok2::NatMX, yap6::NatMX, TUP1-3V5::HIS3* *MATα, ho::LYS2, lys2, ura3, leu2::hisG, his3::hisG, trp1::hisG, sok2::NatMX, yap6::NatMX, TUP1-3V5::HIS3*	This thesis
FW4383	*MAT**a**, ho::LYS2, lys2, ura3, leu2::hisG, his3::hisG, trp1::hisG, MOT3-3V5::KanMX* *MATα, ho::LYS2, lys2, ura3, leu2::hisG, his3::hisG, trp1::hisG, MOT3-3V5::KanMX*	This thesis
FW4386	*MAT**a**, ho::LYS2, lys2, ura3, leu2::hisG, his3::hisG, trp1::hisG, RGT1-3V5::KanMX* *MATα, ho::LYS2, lys2, ura3, leu2::hisG, his3::hisG, trp1::hisG, RGT1-3V5::KanMX*	This thesis
FW4389	*MAT**a**, ho::LYS2, lys2, ura3, leu2::hisG, his3::hisG, trp1::hisG, SKO1-3V5::KanMX* *MATα, ho::LYS2, lys2, ura3, leu2::hisG, his3::hisG, trp1::hisG, SKO1-3V5::KanMX*	This thesis
FW4393	*MAT**a**, ho::LYS2, lys2, ura3, leu2::hisG, his3::hisG, trp1::hisG, NRG1-3V5::KanMX* *MATα, ho::LYS2, lys2, ura3, leu2::hisG, his3::hisG, trp1::hisG, NRG1-3V5::KanMX*	This thesis
FW4396	*MAT**a**, ho::LYS2, lys2, ura3, leu2::hisG, his3::hisG, trp1::hisG, NRG2-3V5::KanMX* *MATα, ho::LYS2, lys2, ura3, leu2::hisG, his3::hisG, trp1::hisG, NRG2-3V5::KanMX*	This thesis
FW4399	*MAT**a**, ho::LYS2, lys2, ura3, leu2::hisG, his3::hisG, trp1::hisG, SKN7-3V5::KanMX* *MATα, ho::LYS2, lys2, ura3, leu2::hisG, his3::hisG, trp1::hisG, SKN7-3V5::KanMX*	This thesis
FW4406	*MAT**a**, ho::LYS2, lys2, ura3, leu2::hisG, his3::hisG, trp1::hisG, phd1::KanMX, yap6::NatMX, TUP1-3V5::HIS3* *MATα, ho::LYS2, lys2, ura3, leu2::hisG, his3::hisG, trp1::hisG, phd1::KanMX, yap6::NatMX, TUP1-3V5::HIS3*	This thesis
FW4466	*MAT**a**, ho::LYS2, lys2, ura3, leu2::hisG, his3::hisG, trp1::hisG, PHD1-3V5::KanMX* *MATα, ho::LYS2, lys2, ura3, leu2::hisG, his3::hisG, trp1::hisG, PHD1-3V5::KanMX*	This thesis
FW4665	*MAT**a**, ho::LYS2, lys2, ura3, leu2::hisG, his3::hisG, trp1::hisG, MIG1-3V5::KanMX* *MATα, ho::LYS2, lys2, ura3, leu2::hisG, his3::hisG, trp1::hisG, MIG1-3V5::KanMX*	This thesis
FW4710	*MAT**a**, ho::LYS2, lys2, ura3, leu2::hisG, his3::hisG, trp1::hisG, sok2::NatMX, phd1::KanMX, TUP1-3V5::HIS3* *MATα, ho::LYS2, lys2, ura3, leu2::hisG, his3::hisG, trp1::hisG, sok2::NatMX, phd1::KanMX, TUP1-3V5::HIS3*	This thesis
FW4777	*MAT**a**, ho::LYS2, lys2, ura3, leu2::hisG, his3::hisG, trp1::hisG, pIME1(-850-2315Δ)::HIS3MX* *MATα, ho::LYS2, lys2, ura3, leu2::hisG, his3::hisG, trp1::hisG, ime1::HISMX6*	This thesis

FW4778	*MAT**a**, ho::LYS2, lys2, ura3, leu2::hisG, his3::hisG, trp1::hisG, pIME1(-900-2315Δ)::HIS3MX* *MATα, ho::LYS2, lys2, ura3, leu2::hisG, his3::hisG, trp1::hisG, ime1::HISMX6*	This thesis
FW4779	*MAT**a**, ho::LYS2, lys2, ura3, leu2::hisG, his3::hisG, trp1::hisG, pIME1(-950-2315Δ)::HIS3MX* *MATα, ho::LYS2, lys2, ura3, leu2::hisG, his3::hisG, trp1::hisG, ime1::HISMX6*	This thesis
FW4780	*MAT**a**, ho::LYS2, lys2, ura3, leu2::hisG, his3::hisG, trp1::hisG, pIME1(-1250-2315Δ)::HIS3MX* *MATα, ho::LYS2, lys2, ura3, leu2::hisG, his3::hisG, trp1::hisG, ime1::HISMX6*	This thesis
FW4781	*MAT**a**, ho::LYS2, lys2, ura3, leu2::hisG, his3::hisG, trp1::hisG, pIME1(-1350-2315Δ)::HIS3MX* *MATα, ho::LYS2, lys2, ura3, leu2::hisG, his3::hisG, trp1::hisG, ime1::HISMX6*	This thesis
FW5055	*MAT**a**, ho::LYS2, lys2, ura3, leu2::hisG, trp1::hisG, his3::pTEF1-osTIR::HIS3, TUP1-3V5-IAA7::KanMX6, NRG2-3V5::KanMX* *MATα, ho::LYS2, lys2, ura3, leu2::hisG, trp1::hisG, his3::pTEF1-osTIR::HIS3, TUP1-3V5-IAA7::KanMX6, NRG2-3V5::KanMX*	This thesis
FW5056	*MAT**a**, ho::LYS2, lys2, ura3, leu2::hisG, trp1::hisG, his3::pTEF1-osTIR::HIS3, TUP1-3V5-IAA7::KanMX6, PHD1-3V5::KanMX* *MATα, ho::LYS2, lys2, ura3, leu2::hisG, trp1::hisG, his3::pTEF1-osTIR::HIS3, TUP1-3V5-IAA7::KanMX6, PHD1-3V5::KanMX*	This thesis
FW5057	*MAT**a**, ho::LYS2, lys2, ura3, leu2::hisG, trp1::hisG, his3::pTEF1-osTIR::HIS3, TUP1-3V5-IAA7::KanMX6* *MATα, ho::LYS2, ura3, leu2::hisG, his3::hisG, trp1::hisG, his3::pTEF1-osTIR::HIS3, TUP1-3V5-IAA7::KanMX6*	This thesis
FW5199	*MAT**a**, ho::LYS2, lys2, ura3, leu2::hisG, his3::hisG, trp1::hisG, pRS306-pCTS1-2xmCherry-SV40NLS* *MATα, ho::LYS2, lys2, ura3, leu2::hisG, his3::hisG, trp1::hisG, pRS306-pCTS1-2xmCherry-SV40NLS*	Lab collection
FW5370	*MAT**a**, ho::LYS2, lys2, ura3, leu2::hisG, his3::hisG, trp1::hisG, pIME1-ime1::KanMX, TUP1-3V5::HIS3, trp1::pNH604-pIME1(WT)-sfGFP-IME1::TRP1* *MATα, ho::LYS2, lys2, ura3, leu2::hisG, his3::hisG, trp1::hisG, pIME1-ime1::KanMX, TUP1-3V5::HIS3, trp1::pNH604-pIME1(WT)-sfGFP-IME1::TRP1*	This thesis
FW5372	*MAT**a**, ho::LYS2, lys2, ura3, leu2::hisG, his3::hisG, trp1::hisG, pIME1-ime1::KanMX, TUP1-3V5::HIS3, trp1::pNH604-pIME1(bsΔ)-sfGFP-IME1::TRP1* *MATα, ho::LYS2, lys2, ura3, leu2::hisG, his3::hisG, trp1::hisG, pIME1-ime1::KanMX, TUP1-3V5::HIS3, trp1::pNH604-pIME1(bsΔ)-sfGFP-IME1::TRP1*	This thesis

FW5453	*MAT**a**, ho::LYS2, lys2, ura3, leu2::hisG, his3::hisG, trp1::hisG, tpk1:: tpk1M164G, tpk3::TRP1, tpk2::KanMX6, YAP6-3V5::KanMX* *MATα, ho::LYS2, lys2, ura3, leu2::hisG, his3::hisG, trp1::hisG, tpk1:: tpk1M164G, tpk3::TRP1, tpk2::KanMX6, YAP6-3V5::KanMX*	This thesis
FW5454	*MAT**a**, ho::LYS2, lys2, ura3, leu2::hisG, his3::hisG, trp1::hisG, tpk1:: tpk1M164G, tpk3::TRP1, tpk2::KanMX6, SOK2-3V5::HIS3* *MATα, ho::LYS2, lys2, ura3, leu2::hisG, his3::hisG, trp1::hisG, tpk1:: tpk1M164G, tpk3::TRP1, tpk2::KanMX6, SOK2-3V5::HIS3*	This thesis
FW5528	*MAT**a**, ho::LYS2, lys2, ura3, leu2::hisG, his3::hisG, trp1::hisG, tpk1:: tpk1M164G, tpk3::TRP1, tpk2::KanMX6, PHD1-3V5::KanMX* *MATα, ho::LYS2, lys2, ura3, leu2::hisG, his3::hisG, trp1::hisG, tpk1:: tpk1M164G, tpk3::TRP1, tpk2::KanMX6, PHD1-3V5::KanMX*	This thesis
FW5638	*MAT**a**, ho::LYS2, ura3, leu2::hisG, his3::hisG, trp1::hisG, SOK2-3V5::HIS3* *MATα, ho::LYS2, ura3, leu2::hisG, his3::hisG, trp1::hisG, SOK2-3V5::HIS3*	This thesis
FW5657	*MAT**a**, ho::LYS2, lys2, ura3, leu2::hisG, his3::hisG, trp1::hisG, nrg1::KanMX, sok2::NatMX, phd1::KanMX, yap6::NatMX, TUP1-3V5::HIS3* *MATα, ho::LYS2, lys2, ura3, leu2::hisG, his3::hisG, trp1::hisG, nrg1::KanMX, sok2::NatMX, phd1::KanMX, yap6::NatMX, TUP1-3V5::HIS3*	This thesis
FW5694	*MAT**a**, ho::LYS2, lys2, ura3, leu2::hisG, his3::hisG, trp1::hisG, pIME1-ime1::KanMX, TUP1-3V5::HIS3, trp1::pNH604-pIME1(bs∆yap6)-sfGFP-IME1::TRP1* *MATα, ho::LYS2, lys2, ura3, leu2::hisG, his3::hisG, trp1::hisG, pIME1-ime1::KanMX, TUP1-3V5::HIS3, trp1::pNH604-pIME1(bs∆yap6)-sfGFP-IME1::TRP1*	This thesis
FW5696	*MAT**a**, ho::LYS2, lys2, ura3, leu2::hisG, his3::hisG, trp1::hisG, pIME1-ime1::KanMX, TUP1-3V5::HIS3, trp1::pNH604-pIME1(bs∆phd1)-sfGFP-IME1::TRP1* *MATα, ho::LYS2, lys2, ura3, leu2::hisG, his3::hisG, trp1::hisG, pIME1-ime1::KanMX, TUP1-3V5::HIS3, trp1::pNH604-pIME1(bs∆phd1)-sfGFP-IME1::TRP1*	This thesis
FW5800	*MAT**a**, ho::LYS2, lys2, ura3, leu2::hisG, his3::hisG, trp1::hisG, pIME1-ime1::KanMX, TUP1-3V5::HIS3, trp1::pNH604-pIME1(bs∆sok2)-sfGFP-IME1::TRP1* *MATα, ho::LYS2, lys2, ura3, leu2::hisG, his3::hisG, trp1::hisG, pIME1-ime1::KanMX, TUP1-3V5::HIS3, trp1::pNH604-pIME1(bs∆sok2)-sfGFP-IME1::TRP1*	This thesis

FW5890	*MAT**a**, ho::LYS2, lys2, ura3, leu2::hisG, his3::hisG, trp1::hisG, yap6::NatMX, sok2::NatMX, phd1::KanMX, nrg1::KanMX, nrg2::HIS3MX, TUP1-3V5::HIS3* *MATα, ho::LYS2, lys2, ura3, leu2::hisG, his3::hisG, trp1::hisG, yap6::NatMX, sok2::NatMX, phd1::KanMX, nrg1::KanMX, nrg2::HIS3MX, TUP1-3V5::HIS3*	This thesis
FW6371	*MAT**a**, ho::LYS2, lys2, ura3, leu2::hisG, his3::hisG, trp1::hisG, his3::pTEF1-osTIR::HIS3 , CYC8-3V5-IAA7::KanMX6* *MATα, ho::LYS2, lys2, ura3, leu2::hisG, his3::hisG, trp1::hisG, his3::pTEF1-osTIR::HIS3, CYC8-3V5-IAA7::KanMX6*	This thesis
FW6377	*MAT**a**, ho::LYS2, lys2, ura3, leu2::hisG, his3::hisG, trp1::hisG, GTS1-3V5::KanMX* *MATα, ho::LYS2, lys2, ura3, leu2::hisG, his3::hisG, trp1::hisG, GTS1-3V5::KanMX*	This thesis
FW6379	*MAT**a**, ho::LYS2, lys2, ura3, leu2::hisG, his3::hisG, trp1::hisG, cup9::NatMX, TUP1-3V5::HIS3* *MATα, ho::LYS2, lys2, ura3, leu2::hisG, his3::hisG, trp1::hisG, cup9::NatMX, TUP1-3V5::HIS3*	This thesis
FW6381	*MAT**a**, ho::LYS2, lys2, ura3, leu2::hisG, his3::hisG, trp1::hisG, CYC8-3V5::KanMX* *MATα, ho::LYS2, lys2, ura3, leu2::hisG, his3::hisG, trp1::hisG, CYC8-3V5::KanMX*	This thesis
FW6974	*MAT**a**, ho::LYS2, lys2, ura3, leu2::hisG, his3::hisG, trp1::hisG, SUT1-3V5::KanMX* *MATα, ho::LYS2, lys2, ura3, leu2::hisG, his3::hisG, trp1::hisG, SUT1-3V5::KanMX*	This thesis
FW6976	*MAT**a**, ho::LYS2, lys2, ura3, leu2::hisG, his3::hisG, trp1::hisG, CUP9-3V5::KanMX* *MATα, ho::LYS2, lys2, ura3, leu2::hisG, his3::hisG, trp1::hisG, CUP9-3V5::KanMX*	This thesis
FW7068	*MAT**a**, ho::LYS2, lys2, ura3, leu2::hisG, his3::hisG, trp1::hisG, SMP1-3V5::KanMX* *MATα, ho::LYS2, lys2, ura3, leu2::hisG, his3::hisG, trp1::hisG, SMP1-3V5::KanMX*	This thesis
FW7070	*MAT**a**, ho::LYS2, lys2, ura3, leu2::hisG, his3::hisG, trp1::hisG, SFL1-3V5::KanMX* *MATα, ho::LYS2, lys2, ura3, leu2::hisG, his3::hisG, trp1::hisG, SFL1-3V5::KanMX*	This thesis
FW7072	*MAT**a**, ho::LYS2, lys2, ura3, leu2::hisG, his3::hisG, trp1::hisG, CIN5-3V5::KanMX* *MATα, ho::LYS2, lys2, ura3, leu2::hisG, his3::hisG, trp1::hisG, CIN5-3V5::KanMX*	This thesis
FW7074	*MAT**a**, ho::LYS2, lys2, ura3, leu2::hisG, his3::hisG, trp1::hisG, pIME1-ime1::KanMX, TUP1-3V5::HIS3, trp1::pNH604-pIME1(bsΔsko1)-sfGFP-IME1::TRP1* *MATα, ho::LYS2, lys2, ura3, leu2::hisG, his3::hisG, trp1::hisG, pIME1-ime1::KanMX, TUP1-3V5::HIS3, trp1::pNH604-pIME1(bsΔsko1)-sfGFP-IME1::TRP1*	This thesis

FW7084	*MAT**a**, ho::LYS2, lys2, ura3, leu2::hisG, his3::hisG, trp1::hisG, pIME1-ime1::KanMX, TUP1-3V5::HIS3, trp1::pNH604-pIME1(bsΔ1)-sfGFP-IME1::TRP1* *MATα, ho::LYS2, lys2, ura3, leu2::hisG, his3::hisG, trp1::hisG, pIME1-ime1::KanMX, TUP1-3V5::HIS3, trp1::pNH604-pIME1(bsΔ1)-sfGFP-IME1::TRP1*	This thesis
FW7086	*MAT**a**, ho::LYS2, lys2, ura3, leu2::hisG, his3::hisG, trp1::hisG, pIME1-ime1::KanMX, TUP1-3V5::HIS3, trp1::pNH604-pIME1(bsΔ3)-sfGFP-IME1::TRP1* *MATα, ho::LYS2, lys2, ura3, leu2::hisG, his3::hisG, trp1::hisG, pIME1-ime1::KanMX, TUP1-3V5::HIS3, trp1::pNH604-pIME1(bsΔ3)-sfGFP-IME1::TRP1*	This thesis
FW7092	*MAT**a**, ho::LYS2, lys2, ura3, leu2::hisG, his3::hisG, trp1::hisG, pIME1-ime1::KanMX, TUP1-3V5::HIS3, trp1::pNH604-pIME1(bsΔnrg1)-sfGFP-IME1::TRP1* *MATα, ho::LYS2, lys2, ura3, leu2::hisG, his3::hisG, trp1::hisG, pIME1-ime1::KanMX, TUP1-3V5::HIS3, trp1::pNH604-pIME1(bsΔnrg1)-sfGFP-IME1::TRP1*	This thesis
FW7094	*MAT**a**, ho::LYS2, lys2, ura3, leu2::hisG, his3::hisG, trp1::hisG, pIME1-ime1::KanMX, TUP1-3V5::HIS3, trp1::pNH604-pIME1(bsΔ2)-sfGFP-IME1::TRP1* *MATα, ho::LYS2, lys2, ura3, leu2::hisG, his3::hisG, trp1::hisG, pIME1-ime1::KanMX, TUP1-3V5::HIS3, trp1::pNH604-pIME1(bsΔ2)-sfGFP-IME1::TRP1*	This thesis
FW7096	*MAT**a**, ho::LYS2, lys2, ura3, leu2::hisG, his3::hisG, trp1::hisG, pIME1-ime1::KanMX, TUP1-3V5::HIS3, trp1::pNH604-pIME1(bsΔ4)-sfGFP-IME1::TRP1* *MATα, ho::LYS2, lys2, ura3, leu2::hisG, his3::hisG, trp1::hisG, pIME1-ime1::KanMX, TUP1-3V5::HIS3, trp1::pNH604-pIME1(bsΔ4)-sfGFP-IME1::TRP1*	This thesis
FW7430	*MAT**a**, ho::LYS2, lys2, ura3, leu2::hisG, his3::hisG, trp1::hisG, yap6::NatMX, sok2::NatMX, phd1::KanMX, sko1::NatMX, TUP1-3V5::HIS3* *MATα, ho::LYS2, lys2, ura3, leu2::hisG, his3::hisG, trp1::hisG, yap6::NatMX, sok2::NatMX, phd1::KanMX, sko1::NatMX, TUP1-3V5::HIS3*	This thesis
FW7473	*MAT**a**, ho::LYS2, lys2, ura3, leu2::hisG, his3::hisG, trp1::hisG, pRS306-pCTS1-2xmCherry-SV40NLS, YAP6-mNeongreen(Yeast Optimized)::NatMX* *MATα, ho::LYS2, lys2, ura3, leu2::hisG, his3::hisG, trp1::hisG, pRS306-pCTS1-2xmCherry-SV40NLS, YAP6-mNeongreen(Yeast Optimized)::NatMX*	This thesis
FW7475	*MAT**a**, ho::LYS2, lys2, ura3, leu2::hisG, his3::hisG, trp1::hisG, pRS306-pCTS1-2xmCherry-SV40NLS, SOK2-mNeongreen(Yeast Optimized)::NatMX* *MATα, ho::LYS2, lys2, ura3, leu2::hisG, his3::hisG, trp1::hisG, pRS306-pCTS1-2xmCherry-SV40NLS, SOK2-mNeongreen(Yeast Optimized)::NatMX*	This thesis

FW7477	*MAT**a**, ho::LYS2, lys2, ura3, leu2::hisG, his3::hisG, trp1::hisG, pRS306-pCTS1-2xmCherry-SV40NLS, PHD1-mNeongreen(Yeast Optimized)::NatMX* *MATα, ho::LYS2, lys2, ura3, leu2::hisG, his3::hisG, trp1::hisG, pRS306-pCTS1-2xmCherry-SV40NLS, PHD1-mNeongreen(Yeast Optimized)::NatMX*	This thesis
FW7544	*MAT**a**, ho::LYS2, lys2, ura3, leu2::hisG, his3::hisG, trp1::hisG, sok2::NatMX, phd1::KanMX, yap6::NatMX, cup9::NatMX, TUP1-3V5::HIS3* *MATα, ho::LYS2, lys2, ura3, leu2::hisG, his3::hisG, trp1::hisG, sok2::NatMX, phd1::KanMX, yap6::NatMX, cup9::NatMX, TUP1-3V5::HIS3*	This thesis
FW7642	*MAT**a**, ho::LYS2, lys2, ura3, leu2::hisG, his3::hisG, trp1::hisG, pRS306-pCTS1-2xmCherry-SV40NLS, CYC8-mNeongreen(Yeast Optimized)::NatMX* *MATα, ho::LYS2, lys2, ura3, leu2::hisG, his3::hisG, trp1::hisG, pRS306-pCTS1-2xmCherry-SV40NLS, CYC8-mNeongreen(Yeast Optimized)::NatMX*	This thesis
FW7644	*MAT**a**, ho::LYS2, lys2, ura3, leu2::hisG, his3::hisG, trp1::hisG, pRS306-pCTS1-2xmCherry-SV40NLS, TUP1-mNeongreen(Yeast Optimized)::NatMX* *MATα, ho::LYS2, lys2, ura3, leu2::hisG, his3::hisG, trp1::hisG, pRS306-pCTS1-2xmCherry-SV40NLS, TUP1-mNeongreen(Yeast Optimized)::NatMX*	This thesis
FW7646	*MAT**a**, ho::LYS2, lys2, ura3, leu2::hisG, his3::hisG, trp1::hisG, pRS306-pCTS1-2xmCherry-SV40NLS, CUP9-mNeongreen(Yeast Optimized)::NatMX* *MATα, ho::LYS2, lys2, ura3, leu2::hisG, his3::hisG, trp1::hisG, pRS306-pCTS1-2xmCherry-SV40NLS, CUP9-mNeongreen(Yeast Optimized)::NatMX*	This thesis
FW7650	*MAT**a**, ho::LYS2, lys2, ura3, leu2::hisG, his3::hisG, trp1::hisG, sok2::NatMX, yap6::NatMX, phd1::KanMX, pIME1-ime1::KanMX, TUP1-3V5::HIS3, trp1::pNH604-pIME1(WT)-sfGFP-IME1::TRP1* *MATα, ho::LYS2, lys2, ura3, leu2::hisG, his3::hisG, trp1::hisG, sok2::NatMX, yap6::NatMX, phd1::KanMX, pIME1-ime1::KanMX, TUP1-3V5::HIS3, trp1::pNH604-pIME1(WT)-sfGFP-IME1::TRP1*	This thesis
FW7731	*MAT**a**, ho::LYS2, lys2, ura3, leu2::hisG, his3::hisG, trp1::hisG, pIME1-ime1::KanMX, TUP1-3V5::HIS3, trp1::pNH604-pIME1(spyΔ)-sfGFP-IME1::TRP1* *MATα, ho::LYS2, lys2, ura3, leu2::hisG, his3::hisG, trp1::hisG, pIME1-ime1::KanMX, TUP1-3V5::HIS3, trp1::pNH604-pIME1(spyΔ)-sfGFP-IME1::TRP1*	This thesis
FW7733	*MAT**a**, ho::LYS2, lys2, ura3, leu2::hisG, his3::hisG, trp1::hisG, pIME1-ime1::KanMX, TUP1-3V5::HIS3, trp1::pNH604-pIME1(bsΔ-spy)-sfGFP-IME1::TRP1* *MATα, ho::LYS2, lys2, ura3, leu2::hisG, his3::hisG, trp1::hisG, pIME1-ime1::KanMX, TUP1-3V5::HIS3, trp1::pNH604-pIME1(bsΔ-spy)-sfGFP-IME1::TRP1*	This thesis

FW8079	*MAT**a**, ho::LYS2, lys2, ura3, leu2::hisG, his3::hisG, trp1::hisG, pIME1-ime1::KanMX, YAP6-3V5::KanMX, trp1::pNH604-pIME1(WT)-sfGFP-IME1::TRP1* *MATα, ho::LYS2, lys2, ura3, leu2::hisG, his3::hisG, trp1::hisG, pIME1-ime1::KanMX, YAP6-3V5::KanMX, trp1::pNH604-pIME1(WT)-sfGFP-IME1::TRP1*	This thesis
FW8081	*MAT**a**, ho::LYS2, lys2, ura3, leu2::hisG, his3::hisG, trp1::hisG, pIME1-ime1::KanMX, SOK2-3V5::HIS3, trp1::pNH604-pIME1(WT)-sfGFP-IME1::TRP1* *MATα, ho::LYS2, lys2, ura3, leu2::hisG, his3::hisG, trp1::hisG, pIME1-ime1::KanMX, SOK2-3V5::HIS3, trp1::pNH604-pIME1(WT)-sfGFP-IME1::TRP1*	This thesis
FW8083	*MAT**a**, ho::LYS2, lys2, ura3, leu2::hisG, his3::hisG, trp1::hisG, pIME1-ime1::KanMX, PHD1-3V5::KanMX, trp1::pNH604-pIME1(WT)-sfGFP-IME1::TRP1* *MATα, ho::LYS2, lys2, ura3, leu2::hisG, his3::hisG, trp1::hisG, pIME1-ime1::KanMX, PHD1-3V5::KanMX, trp1::pNH604-pIME1(WT)-sfGFP-IME1::TRP1*	This thesis
FW8085	*MAT**a**, ho::LYS2, lys2, ura3, leu2::hisG, his3::hisG, trp1::hisG, pIME1-ime1::KanMX, YAP6-3V5::KanMX, trp1::pNH604-pIME1(bsΔ)-sfGFP-IME1::TRP1* *MATα, ho::LYS2, lys2, ura3, leu2::hisG, his3::hisG, trp1::hisG, pIME1-ime1::KanMX, YAP6-3V5::KanMX, trp1::pNH604-pIME1(bsΔ)-sfGFP-IME1::TRP1*	This thesis
FW8087	*MAT**a**, ho::LYS2, lys2, ura3, leu2::hisG, his3::hisG, trp1::hisG, pIME1-ime1::KanMX, SOK2-3V5::HIS3, trp1::pNH604-pIME1(bsΔ)-sfGFP-IME1::TRP1* *MATα, ho::LYS2, lys2, ura3, leu2::hisG, his3::hisG, trp1::hisG, pIME1-ime1::KanMX, SOK2-3V5::HIS3, trp1::pNH604-pIME1(bsΔ)-sfGFP-IME1::TRP1*	This thesis
FW8089	*MAT**a**, ho::LYS2, lys2, ura3, leu2::hisG, his3::hisG, trp1::hisG, pIME1-ime1::KanMX, PHD1-3V5::KanMX, trp1::pNH604-pIME1(bsΔ)-sfGFP-IME1::TRP1* *MATα, ho::LYS2, lys2, ura3, leu2::hisG, his3::hisG, trp1::hisG, pIME1-ime1::KanMX, PHD1-3V5::KanMX, trp1::pNH604-pIME1(bsΔ)-sfGFP-IME1::TRP1*	This thesis
FW8091	*MAT**a**, ho::LYS2, lys2, ura3, leu2::hisG, his3::hisG, trp1::hisG, pIME1-ime1::KanMX, YAP6-3V5::KanMX, trp1::pNH604-pIME1(bsΔ-spy)-sfGFP-IME1::TRP1* *MATα, ho::LYS2, lys2, ura3, leu2::hisG, his3::hisG, trp1::hisG, pIME1-ime1::KanMX, YAP6-3V5::KanMX, trp1::pNH604-pIME1(bsΔ-spy)-sfGFP-IME1::TRP1*	This thesis
FW8093	*MAT**a**, ho::LYS2, lys2, ura3, leu2::hisG, his3::hisG, trp1::hisG, pIME1-ime1::KanMX, SOK2-3V5::HIS3, trp1::pNH604-pIME1(bsΔ-spy)-sfGFP-IME1::TRP1* *MATα, ho::LYS2, lys2, ura3, leu2::hisG, his3::hisG, trp1::hisG, pIME1-ime1::KanMX, SOK2-3V5::HIS3, trp1::pNH604-pIME1(bsΔ-spy)-sfGFP-IME1::TRP1*	This thesis

FW8095	*MAT**a**, ho::LYS2, lys2, ura3, leu2::hisG, his3::hisG, trp1::hisG, pIME1-ime1::KanMX, PHD1-3V5::KanMX, trp1::pNH604-pIME1(bsΔ-spy)-sfGFP-IME1::TRP1* *MATα, ho::LYS2, lys2, ura3, leu2::hisG, his3::hisG, trp1::hisG, pIME1-ime1::KanMX, PHD1-3V5::KanMX, trp1::pNH604-pIME1(bsΔ-spy)-sfGFP-IME1::TRP1*	This thesis
FW8097	*MAT**a**, ho::LYS2, lys2, ura3, leu2::hisG, his3::hisG, trp1::hisG, pIME1-ime1::KanMX, YAP6-3V5::KanMX, trp1::pNH604-pIME1(spyΔ)-sfGFP-IME1::TRP1* *MATα, ho::LYS2, lys2, ura3, leu2::hisG, his3::hisG, trp1::hisG, pIME1-ime1::KanMX, YAP6-3V5::KanMX, trp1::pNH604-pIME1(spyΔ)-sfGFP-IME1::TRP1*	This thesis
FW8098	*MAT**a**, ho::LYS2, lys2, ura3, leu2::hisG, his3::hisG, trp1::hisG, pIME1-ime1::KanMX, SOK2-3V5::HIS3, trp1::pNH604-pIME1(spyΔ)-sfGFP-IME1::TRP1* *MATα, ho::LYS2, lys2, ura3, leu2::hisG, his3::hisG, trp1::hisG, pIME1-ime1::KanMX, SOK2-3V5::HIS3, trp1::pNH604-pIME1(spyΔ)-sfGFP-IME1::TRP1*	This thesis
FW8100	*MAT**a**, ho::LYS2, lys2, ura3, leu2::hisG, his3::hisG, trp1::hisG, pIME1-ime1::KanMX, PHD1-3V5::KanMX, trp1::pNH604-pIME1(spyΔ)-sfGFP-IME1::TRP1* *MATα, ho::LYS2, lys2, ura3, leu2::hisG, his3::hisG, trp1::hisG, pIME1-ime1::KanMX, PHD1-3V5::KanMX, trp1::pNH604-pIME1(spyΔ)-sfGFP-IME1::TRP1*	This thesis
FW8102	*MAT**a**, ho::LYS2, lys2, ura3, leu2::hisG, his3::hisG, trp1::hisG, rpd3::HIS3MX, TUP1-3V5::HIS3* *MATα, ho::LYS2, lys2, ura3, leu2::hisG, his3::hisG, trp1::hisG, rpd3::HIS3MX, TUP1-3V5::HIS3*	This thesis
FW8103	*MAT**a**, ho::LYS2, lys2, ura3, leu2::hisG, his3::hisG, trp1::hisG, hos2:HIS3MX, TUP1-3V5::HIS3* *MATα, ho::LYS2, lys2, ura3, leu2::hisG, his3::hisG, trp1::hisG, hos2:HIS3MX, TUP1-3V5::HIS3*	This thesis
FW8171	*MAT**a**, ho::LYS2, lys2, ura3, leu2::hisG, his3::hisG, trp1::hisG, rpd3::HIS3MX, hos2:HIS3MX, TUP1-3V5::HIS3* *MATα, ho::LYS2, lys2, ura3, leu2::hisG, his3::hisG, trp1::hisG, rpd3::HIS3MX, hos2:HIS3MX, TUP1-3V5::HIS3*	This thesis
FW8177	*MAT**a**, ho::LYS2, lys2, ura3, leu2::hisG, his3::hisG, trp1::hisG, yap6::NatMX, sok2::NatMX, phd1::KanMX, pIME1-ime1::KanMX, TUP1-3V5::HIS3, trp1::pNH604-pIME1(bsΔ-spy)-sfGFP-IME1::TRP1* *MATα, ho::LYS2, lys2, ura3, leu2::hisG, his3::hisG, trp1::hisG, yap6::NatMX, sok2::NatMX, phd1::KanMX, pIME1-ime1::KanMX, TUP1-3V5::HIS3, trp1::pNH604-pIME1(bsΔ-spy)-sfGFP-IME1::TRP1*	This thesis

FW8420	*MAT**a**, ho::LYS2, lys2, ura3, leu2::hisG, his3::hisG, trp1::hisG, sok2::NatMX, yap6::NatMX, phd1::KanMX, pIME1-ime1::KanMX, TUP1-3V5::HIS3, trp1::pNH604-pIME1(bsΔ)-sfGFP-IME1::TRP1* *MATα, ho::LYS2, lys2, ura3, leu2::hisG, his3::hisG, trp1::hisG, sok2::NatMX, yap6::NatMX, phd1::KanMX, pIME1-ime1::KanMX, TUP1-3V5::HIS3, trp1::pNH604-pIME1(bsΔ)-sfGFP-IME1::TRP1*	This thesis
FW8426	*MAT**a**, ho::LYS2, lys2, ura3, leu2::hisG, his3::hisG, trp1::hisG, hda1::KanMX, TUP1-3V5::HIS3* *MATα, ho::LYS2, lys2, ura3, leu2::hisG, his3::hisG, trp1::hisG, hda1::KanMX, TUP1-3V5::HIS3*	This thesis
FW8428	*MAT**a**, ho::LYS2, lys2, ura3, leu2::hisG, his3::hisG, trp1::hisG, hos1::NatMX, rpd3::HIS3MX, TUP1-3V5::HIS3* *MATα, ho::LYS2, lys2, ura3, leu2::hisG, his3::hisG, trp1::hisG, hos1::NatMX, rpd3::HIS3MX, TUP1-3V5::HIS3*	This thesis
FW8430	*MAT**a**, ho::LYS2, lys2, ura3, leu2::hisG, his3::hisG, trp1::hisG, hos1::NatMX, TUP1-3V5::HIS3* *MATα, ho::LYS2, lys2, ura3, leu2::hisG, his3::hisG, trp1::hisG, hos1::NatMX, TUP1-3V5::HIS3*	This thesis
FW8432	*MAT**a**, ho::LYS2, lys2, ura3, leu2::hisG, his3::hisG, trp1::hisG, FKH1-3V5::KanMX* *MATα, ho::LYS2, lys2, ura3, leu2::hisG, his3::hisG, trp1::hisG, FKH1-3V5::KanMX*	This thesis
FW8457	*MAT**a**, ho::LYS2, lys2, ura3, leu2::hisG, his3::hisG, trp1::hisG, hda1::KanMX, rpd3::HIS3MX, TUP1-3V5::HIS3* *MATα, ho::LYS2, lys2, ura3, leu2::hisG, his3::hisG, trp1::hisG, hda1::KanMX, rpd3::HIS3MX, TUP1-3V5::HIS3*	This thesis
FW8473	*MAT**a**, ho::LYS2, lys2, ura3, leu2::hisG, his3::hisG, trp1::hisG, COM2-3V5::KanMX* *MATα, ho::LYS2, lys2, ura3, leu2::hisG, his3::hisG, trp1::hisG, COM2-3V5::KanMX*	This thesis

Supplementary table 1. *S. cerevisiae* strains used in this thesis.

Plasmid	Description	Parent plasmid	Insert sequence
pFW506	*pIME1-WT*	*pNH604*	Full length *IME1* promoter and *IME1* gene tagged with *sfGFP* at the 5' end.
pFW575	*pIME1-bs∆*	*pFW506*	701 to 1100 bp upstream of *IME1* start codon with mutated nucleotides at Yap6, Sok2, Phd1, Mot3, Sko1, Nrg1, and Nrg2 sites.
pFW576	*pIME1-bs∆yap6*	*pFW506*	*pIME1-bs∆* insert with wild-type Yap6 sites.
pFW577	*pIME1-bs∆sok2*	*pFW506*	*pIME1-bs∆* insert with wild-type Sok2 sites.
pFW578	*pIME1-bs∆phd1*	*pFW506*	*pIME1-bs∆* insert with wild-type Phd1 sites.
pFW600	*pIME1-bs∆nrg1*	*pFW506*	*pIME1-bs∆* insert with wild-type Nrg1 sites.
pFW602	*pIME1-bs∆sko1*	*pFW506*	*pIME1-bs∆* insert with wild-type Sko1 site.
pFW604	*pIME1-bs∆1*	*pFW506*	*pIME1-bs∆* insert with wild-type Yap6 site from 837 to 844 bp upstream of *IME1* start codon.
pFW606	*pIME1-bs∆2*	*pFW506*	*pIME1-bs∆* insert with wild-type Yap6 site from 1006 to 1012 bp upstream of *IME1* start codon.
pFW608	*pIME1-bs∆3*	*pFW506*	*pIME1-bs∆* insert with wild-type Sok2 motifs that match the MTGCA motif.
pFW610	*pIME1-bs∆4*	*pFW506*	*pIME1-bs∆* insert with wild-type Sok2 motifs that match the AGGCAM motif.
pFW669	*pIME1-bs∆-spy*	*pFW506*	*pIME1-bs∆* insert with wild-type Yap6 site from 837 to 844 bp upstream of *IME1* start codon, and five wild-type Sok2/Phd1 sites that match the MTGCA motif.
pFW675	*pIME1-spy∆*	*pFW506*	701 to 1100 bp upstream of *IME1* start codon with mutated nucleotides at Yap6 site from 837 to 844 bp upstream of *IME1* start codon, and five Sok2/Phd1 sites that match the MTGCA motif.

Supplementary table 2. Single-copy integration plasmids used in this thesis.

Primer	Oligo sequence (5' to 3')	Targeted region	Source
oFW43	acgatccccgtccaagttatg	*HMR1* (forward)	van Werven lab collection
oFW50	cttcaaaggagtcttaatttccctg	*HMR1* (reverse)	van Werven lab collection
oFW106	gtaccaccatgttcccaggtatt	*ACT1* (forward)	van Werven lab collection
oFW268	agatggaccactttcgtcgt	*ACT1* (reverse)	van Werven lab collection
oFW493	gatggagggttggcataaaa	2310 bp upstream of *IME1* ORF (forward)	van Werven lab collection
oFW494	tgacggtgacgtacgatctcta	2310 bp upstream of *IME1* ORF (reverse)	van Werven lab collection
oFW248	ccgtatggtgttggagtaatttg	2100 bp upstream of *IME1* ORF (forward)	van Werven lab collection
oFW249	tgccatttagtggacttcttgag	2100 bp upstream of *IME1* ORF (reverse)	van Werven lab collection
oFW481	atttttagcgactgccgaaa	1950 bp upstream of *IME1* ORF (forward)	van Werven lab collection
oFW482	atgcaacgcctacttgtttt	1950 bp upstream of *IME1* ORF (reverse)	van Werven lab collection
oFW127	gccaacttggagaaagaatgtg	1700 bp upstream of *IME1* ORF (forward)	van Werven lab collection
oFW128	cggaggtactagtcatcggaat	1700 bp upstream of *IME1* ORF (reverse)	van Werven lab collection
oFW254	agaaacgcaaatgctcagagag	1400 bp upstream of *IME1* ORF (forward)	van Werven lab collection
oFW255	gaggtaatagcggatgacatcaa	1400 bp upstream of *IME1* ORF (reverse)	van Werven lab collection
oFW539	gggtcttaaatacgcagggaat	1000 bp upstream of *IME1* ORF (forward)	van Werven lab collection
oFW540	ggcagttcaaaggcttttctta	1000 bp upstream of *IME1* ORF (reverse)	van Werven lab collection
oFW2685	aggattgggggtagatacaacatc	1000 bp upstream of *IME1* ORF (forward) for *IME1* promoter at *TRP1* locus	This thesis
oFW2688	gatgggcagttcaaaggct	1000 bp upstream of *IME1* ORF (reverse) for *IME1* promoter at *TRP1* locus	This thesis
oFW333	cttcgagggaaaggatcaaag	750 bp upstream of *IME1* ORF (forward)	van Werven lab collection
oFW334	ggctgggggttctgtaattc	750 bp upstream of *IME1* ORF (reverse)	van Werven lab collection

oFW161	taaacaacaacaacaacgcaca	400 bp upstream of *IME1* ORF (forward)	van Werven lab collection
oFW162	ggcaaggaacaagatcaaaaac	400 bp upstream of *IME1* ORF (reverse)	van Werven lab collection
oFW463	caacgcctccgataatgtatatg	*IME1* (forward)	van Werven lab collection
oFW464	acgtcgaaggcaatttctaatg	*IME1* (reverse)	van Werven lab collection

Supplementary table 3. Primers used for qPCR reactions in this thesis.

Reference List

Agatep, R., Kirkpatrick, R. D., Parchaliuk, D. L., Woods, R. A. & Gietz, R. D. (1998) Transformation of *Saccharomyces cerevisiae* by the lithium acetate/single-stranded carrier DNA/polyethylene glycol protocol. *Technical Tips Online,* 3**,** 133-137.

Ahmadpour, D., Geijer, C., Tamás, M. J., Lindkvist-Petersson, K. & Hohmann, S. (2014) Yeast reveals unexpected roles and regulatory features of aquaporins and aquaglyceroporins. *Biochimica et Biophysica Acta (BBA) - General Subjects,* 1840**,** 1482-1491.

Alves-Rodrigues, I., Ferreira, P. G., Moldón, A., Vivancos, A. P., Hidalgo, E., Guigó, R. & Ayté, J. (2016) Spatiotemporal control of forkhead binding to DNA regulates the meiotic gene expression program. *Cell Reports,* 14**,** 885-895.

An, Z., Tassa, A., Thomas, C., Zhong, R., Xiao, G., Fotedar, R., Tu, B. P., Klionsky, D. J. & Levine, B. (2014) Autophagy is required for G_1/G_0 quiescence in response to nitrogen starvation in *Saccharomyces cerevisiae*. *Autophagy,* 10**,** 1702-1711.

Anderson, E. L., Baltus, A. E., Roepers-Gajadien, H. L., Hassold, T. J., de Rooij, D. G., van Pelt, A. M. M. & Page, D. C. (2008) *Stra8* and its inducer, retinoic acid, regulate meiotic initiation in both spermatogenesis and oogenesis in mice. *Proceedings of the National Academy of Sciences,* 105**,** 14976-14980.

Argüello-Miranda, O., Liu, Y., Wood, N. E., Kositangool, P. & Doncic, A. (2018) Integration of multiple metabolic signals determines cell fate prior to commitment. *Molecular Cell,* 71**,** 733-744.e11.

Averbeck, N., Sunder, S., Sample, N., Wise, J. A. & Leatherwood, J. (2005) Negative control contributes to an extensive program of meiotic splicing in fission yeast. *Molecular Cell,* 18**,** 491-498.

Badis, G., Chan, E. T., van Bakel, H., Pena-Castillo, L., Tillo, D., Tsui, K., Carlson, C. D., Gossett, A. J., Hasinoff, M. J., Warren, C. L., Gebbia, M., Talukder, S., Yang, A., Mnaimneh, S., Terterov, D., Coburn, D., Li Yeo, A., Yeo, Z. X., Clarke, N. D., Lieb, J. D., Ansari, A. Z., Nislow, C. & Hughes, T. R. (2008) A library of yeast transcription factor motifs reveals a widespread function for Rsc3 in targeting nucleosome exclusion at promoters. *Molecular Cell,* 32**,** 878-887.

Baidyaroy, D., Brosch, G., Ahn, J. H., Graessle, S., Wegener, S., Tonukari, N. J., Caballero, O., Loidl, P. & Walton, J. D. (2001) A gene related to yeast *HOS2* histone deacetylase affects extracellular depolymerase expression and virulence in a plant pathogenic fungus. *The Plant Cell,* 13**,** 1609-1624.

Bannister, A. J. & Kouzarides, T. (2011) Regulation of chromatin by histone modifications. *Cell Research,* 21**,** 381-395.

Barnes, C. E., English, D. M. & Cowley, S. M. (2019) Acetylation & Co: an expanding repertoire of histone acylations regulates chromatin and transcription. *Essays in Biochemistry,* 63**,** 97-107.

Barnes, P. J., Adcock, I. M. & Ito, K. (2005) Histone acetylation and deacetylation: importance in inflammatory lung diseases. *European Respiratory Journal,* 25**,** 552-563.

Baron, J. A., Laws, K. M., Chen, J. S. & Culotta, V. C. (2013) Superoxide triggers an acid burst in *Saccharomyces cerevisiae* to condition the environment of glucose-starved cells. *Journal of Biological Chemistry,* 288**,** 4557-4566.

Beck, T. & Hall, M. N. (1999) The TOR signalling pathway controls nuclear localization of nutrient-regulated transcription factors. *Nature,* 402**,** 689-692.

Berkey, C. D., Vyas, V. K. & Carlson, M. (2004) Nrg1 and Nrg2 transcriptional repressors are differently regulated in response to carbon source. *Eukaryotic Cell,* 3**,** 311-317.

Bernstein, B. E., Humphrey, E. L., Erlich, R. L., Schneider, R., Bouman, P., Liu, J. S., Kouzarides, T. & Schreiber, S. L. (2002) Methylation of histone H3 Lys 4 in coding regions of active genes. *Proceedings of the National Academy of Sciences,* 99**,** 8695-8700.

Bertram, P. G., Choi, J. H., Carvalho, J., Chan, T.-F., Ai, W. & Zheng, X. F. S. (2002) Convergence of TOR-nitrogen and Snf1-glucose signaling pathways onto Gln3. *Molecular and Cellular Biology,* 22**,** 1246-1252.

Boorsma, A., Lu, X.-J., Zakrzewska, A., Klis, F. M. & Bussemaker, H. J. (2008) Inferring condition-specific modulation of transcription factor activity in yeast through regulon-based analysis of genomewide expression. *PLOS One,* 3**,** e3112.

Botstein, D. & Fink, G. R. (2011) Yeast: an experimental organism for 21st Century biology. *Genetics,* 189**,** 695-704.

Bowdish, K. S., Yuan, H. E. & Mitchell, A. P. (1995) Positive control of yeast meiotic genes by the negative regulator UME6. *Molecular and Cellular Biology,* 15**,** 2955-2961.

Brahma, S., Udugama, M. I., Kim, J., Hada, A., Bhardwaj, S. K., Hailu, S. G., Lee, T.-H. & Bartholomew, B. (2017) INO80 exchanges H2A.Z for H2A by translocating on DNA proximal to histone dimers. *Nature Communications,* 8.

Broach, J. R. (2012) Nutritional control of growth and development in yeast. *Genetics,* 192**,** 73-105.

Broach, J. R. & Deschenes, R. J. (1990) The function of *Ras* genes in Saccharomyces cerevisiae. *Advances in Cancer Research,* 54**,** 79-139.

Byrne, K. P. & Wolfe, K. H. (2005) The Yeast Gene Order Browser: combining curated homology and syntenic context reveals gene fate in polyploid species. *Genome Research,* 15**,** 1456-1461.

Carlson, M. (1997) Genetics of transcriptional regulation in yeast: connections to the RNA polymerase II CTD. *Annual Review of Cell and Developmental Biology,* 13**,** 1-23.

Cavallin, M., Maillard, C., Hully, M., Philbert, M., Boddaert, N., Reilly, M. L., Nitschke, P., Bery, A. & Bahi-Buisson, N. (2018) *TLE1*, a key player in neurogenesis, a new candidate gene for autosomal recessive postnatal microcephaly. *European Journal of Medical Genetics,* 61**,** 729-732.

Celis, J. E., Fink, M. & Kaltoft, K. (1976) On the use of ultraviolet light to study protein-DNA crosslinking. *Nucleic Acids Research,* 3**,** 1065-1071.

Chen, G. & Courey, A. J. (2000) Groucho/TLE family proteins and transcriptional repression. *Gene,* 249**,** 1-16.

Chen, K., Wilson, M. A., Hirsch, C., Watson, A., Liang, S., Lu, Y., Li, W. & Dent, S. Y. (2013) Stabilization of the promoter nucleosomes in nucleosome-free regions by the yeast Cyc8-Tup1 corepressor. *Genome Research,* 23**,** 312-322.

Chen, S., West, R. W., Jr., Johnson, S. L., Gans, H., Kruger, B. & Ma, J. (1993) TSF3, a global regulatory protein that silences transcription of yeast *GAL* genes, also mediates repression by α2 repressor and is identical to SIN4. *Molecular and Cellular Biology,* 13**,** 831-840.

Chen, X., Guo, L., Fan, Z. & Jiang, T. (2008) W-AlignACE: an improved Gibbs sampling algorithm based on more accurate position weight matrices learned from sequence and gene expression/ChIP-chip data. *Bioinformatics,* 24**,** 1121-1128.

Cherry, J. M., Hong, E. L., Amundsen, C., Balakrishnan, R., Binkley, G., Chan, E. T., Christie, K. R., Costanzo, M. C., Dwight, S. S., Engel, S. R., Fisk, D. G., Hirschman, J. E., Hitz, B. C., Karra, K., Krieger, C. J., Miyasato, S. R., Nash, R. S., Park, J., Skrzypek, M. S., Simison, M., Weng, S. & Wong, E. D. (2012)

Saccharomyces Genome Database: the genomics resource of budding yeast. *Nucleic Acids Research,* 40**,** D700-D705.

Chia, M. & van Werven, F. J. (2016) Temporal Expression of a Master Regulator Drives Synchronous Sporulation in Budding Yeast. *G3: Genes|Genomes|Genetics,* 6**,** 3553-3560.

Chu, S., DeRisi, J., Eisen, M., Mulholland, J., Botstein, D., Brown, P. O. & Herskowitz, I. (1998) The transcriptional program of sporulation in budding yeast. *Science,* 282**,** 699-705.

Chu, S. & Herskowitz, I. (1998) Gametogenesis in yeast is regulated by a transcriptional cascade dependent on Ndt80. *Molecular Cell,* 1**,** 685-696.

Clapier, C. R., Iwasa, J., Cairns, B. R. & Peterson, C. L. (2017) Mechanisms of action and regulation of ATP-dependent chromatin-remodelling complexes. *Nature Reviews Molecular Cell Biology,* 18**,** 407-422.

Clifford, D. M., Marinco, S. M. & Brush, G. S. (2004) The meiosis-specific protein kinase Ime2 directs phosphorylation of replication protein A. *Journal of Biological Chemistry,* 279**,** 6163-6170.

Coelho, M. C., Pinto, R. M. & Murray, A. W. (2019) Heterozygous mutations cause genetic instability in a yeast model of cancer evolution. *Nature,* 566**,** 275-278.

Colomina, N., Liu, Y., Aldea, M. & Garí, E. (2003) TOR regulates the subcellular localization of Ime1, a transcriptional activator of meiotic development in budding yeast. *Molecular and Cellular Biology,* 23**,** 7415-7424.

Conlan, R. S., Gounalaki, N., Hatzis, P. & Tzamarias, D. (1999) The Tup1-Cyc8 protein complex can shift from a transcriptional co-repressor to a transcriptional co-activator. *Journal of Biological Chemistry,* 274**,** 205-210.

Conlan, R. S. & Tzamarias, D. (2001) Sfl1 functions via the co-repressor Ssn6-Tup1 and the cAMP-dependent protein kinase Tpk2. *Journal of Molecular Biology,* 309**,** 1007-1015.

Conrad, M., Schothorst, J., Kankipati, H. N., Van Zeebroeck, G., Rubio-Texeira, M. & Thevelein, J. M. (2014) Nutrient sensing and signaling in the yeast *Saccharomyces cerevisiae*. *FEMS Microbiology Reviews,* 38**,** 254-299.

Covitz, P. A., Herskowitz, I. & Mitchell, A. P. (1991) The yeast *RME1* gene encodes a putative zinc finger protein that is directly repressed by a1-α2. *Genes & Development,* 5**,** 1982-1989.

Covitz, P. A. & Mitchell, A. P. (1993) Repression by the yeast meiotic inhibitor RME1. *Genes & Development,* 7**,** 1598-1608.

Crick, F. (1970) Central dogma of molecular biology. *Nature,* 227**,** 561-563.

Das, P. M., Ramachandran, K., vanWert, J. & Singal, R. (2004) Chromatin immunoprecipitation assay. *BioTechniques,* 37**,** 961-969.

Dastidar, R. G., Hooda, J., Shah, A., Cao, T. M., Henke, R. M. & Zhang, L. (2012) The nuclear localization of SWI/SNF proteins is subjected to oxygen regulation. *Cell & Bioscience,* 2**,** 30.

Davie, J. K., Edmondson, D. G., Coco, C. B. & Dent, S. Y. (2003) Tup1-Ssn6 interacts with multiple class I histone deacetylases *in vivo*. *Journal of Biological Chemistry,* 278**,** 50158-50162.

de Boer, C. G. & Hughes, T. R. (2012) YeTFaSCo: a database of evaluated yeast transcription factor sequence specificities. *Nucleic Acids Research,* 40**,** D169-D179.

De Nadal, E., Zapater, M., Alepuz, P. M., Sumoy, L., Mas, G. & Posas, F. (2004) The MAPK Hog1 recruits Rpd3 histone deacetylase to activate osmoresponsive genes. *Nature,* 427**,** 370-374.

de Nobel, H., Ruiz, C., Martin, H., Morris, W., Brul, S., Molina, M. & Klis, F. M. (2000) Cell wall perturbation in yeast results in dual phosphorylation of the Slt2/Mpk1

MAP kinase and in an Slt2-mediated increase in *FKS2-lacZ* expression, glucanase resistance and thermotolerance. *Microbiology,* 146**,** 2121-2132.

Denoth Lippuner, A., Julou, T. & Barral, Y. (2014) Budding yeast as a model organism to study the effects of age. *FEMS Microbiology Reviews,* 38**,** 300-325.

Dokmanovic, M., Clarke, C. & Marks, P. A. (2007) Histone deacetylase inhibitors: overview and perspectives. *Molecular Cancer Research,* 5**,** 981-989.

Ducker, C. E. & Simpson, R. T. (2000) The organized chromatin domain of the repressed yeast a cell-specific gene *STE6* contains two molecules of the corepressor Tup1p per nucleosome. *The EMBO Journal,* 19**,** 400-409.

Duina, A. A., Miller, M. E. & Keeney, J. B. (2014) Budding yeast for budding geneticists: a primer on the *Saccharomyces cerevisiae* model system. *Genetics,* 197**,** 33-48.

Dujon, B. (1996) The yeast genome project: what did we learn? *Trends in Genetics,* 12**,** 263-270.

Edmondson, D. G., Smith, M. M. & Roth, S. Y. (1996) Repression domain of the yeast global repressor Tup1 interacts directly with histones H3 and H4. *Genes & Development,* 10**,** 1247-1259.

Fagerström-Billai, F. & Wright, A. P. H. (2005) Functional comparison of the Tup11 and Tup12 transcriptional corepressors in fission yeast. *Molecular and Cellular Biology,* 25**,** 716-727.

Fan, X., Lamarre-Vincent, N., Wang, Q. & Struhl, K. (2008) Extensive chromatin fragmentation improves enrichment of protein binding sites in chromatin immunoprecipitation experiments. *Nucleic Acids Research,* 36**,** e125.

Farooq, Z., Banday, S., Pandita, T. K. & Altaf, M. (2016) The many faces of histone H3K79 methylation. *Mutation Research. Reviews in Mutation Research,* 768**,** 46-52.

Fernandes, L., Rodrigues-Pousada, C. & Struhl, K. (1997) Yap, a novel family of eight bZIP proteins in Saccharomyces cerevisiae with distinct biological functions. *Molecular and Cellular Biology,* 17**,** 6982-6993.

Fisher, A. L. & Caudy, M. (1998) Groucho proteins: transcriptional corepressors for specific subsets of DNA-binding transcription factors in vertebrates and invertebrates. *Genes & Development,* 12**,** 1931-1940.

Fleming, A. B., Beggs, S., Church, M., Tsukihashi, Y. & Pennings, S. (2014) The yeast Cyc8–Tup1 complex cooperates with Hda1p and Rpd3p histone deacetylases to robustly repress transcription of the subtelomeric *FLO1* gene. *Biochimica et Biophysica Acta (BBA) - Gene Regulatory Mechanisms,* 1839**,** 1242-1255.

Folco, H. D., Chalamcharla, V. R., Sugiyama, T., Thillainadesan, G., Zofall, M., Balachandran, V., Dhakshnamoorthy, J., Mizuguchi, T. & Grewal, S. I. S. (2017) Untimely expression of gametogenic genes in vegetative cells causes uniparental disomy. *Nature,* 543**,** 126-130.

Fowell, R. R. 1969. Sporulation and hybridization of yeasts. *In:* ROSE, A. H. & HARRISON, J. S. (eds.) *The Yeasts.* New York: Academic Press, Inc.

Freese, E. B., Chu, M. I. & Freese, E. (1982) Initiation of yeast sporulation of partial carbon, nitrogen, or phosphate deprivation. *Journal of Bacteriology,* 149**,** 840-851.

Friesen, H., Hepworth, S. R. & Segall, J. (1997) An Ssn6-Tup1-Dependent Negative Regulatory Element Controls Sporulation-Specific Expression of DIT1 and DIT2 in Saccharomyces cerevisiae. *Molecular and Cellular Biology,* 17**,** 123-134.

Fujii, Y., Shimizu, T., Toda, T., Yanagida, M. & Hakoshima, T. (2000) Structural basis for the diversity of DNA recognition by bZIP transcription factors. *Nature Structural Biology,* 7**,** 889-893.

Futai, E., Maeda, T., Sorimachi, H., Kitamoto, K., Ishiura, S. & Suzuki, K. (1999) The protease activity of a calpain-like cysteine protease in *Saccharomyces cerevisiae*

is required for alkaline adaptation and sporulation. *Molecular and General Genetics MGG,* 260**,** 559-568.

Gailus-Durner, V., Chintamaneni, C., Wilson, R., Brill, S. J. & Vershon, A. K. (1997) Analysis of a meiosis-specific URS1 site: sequence requirements and involvement of replication protein A. *Molecular and Cellular Biology,* 17**,** 3536-3546.

Gantchev, J., Martínez Villarreal, A., Xie, P., Lefrançois, P., Gunn, S., Netchiporouk, E., Sasseville, D. & Litvinov, I. V. (2019) The Ectopic Expression of Meiosis Regulatory Genes in Cutaneous T-Cell Lymphomas (CTCL). *Frontiers in Oncology,* 9.

Gaston, K. & Jayaraman, P. S. (2003) Transcriptional repression in eukaryotes: repressors and repression mechanisms. *Cellular and Molecular Life Sciences,* 60**,** 721-741.

Gilmour, D. S. & Lis, J. T. (1984) Detecting protein-DNA interactions *in vivo*: Distribution of RNA polymerase on specific bacterial genes. *Proceedings of the National Academy of Sciences,* 81**,** 4275-4279.

Gimeno, C. J. & Fink, G. R. (1994) Induction of pseudohyphal growth by overexpression of PHD1, a Saccharomyces cerevisiae gene related to transcriptional regulators of fungal development. *Molecular and Cellular Biology,* 14**,** 2100-2112.

Gimeno, C. J., Ljungdahl, P. O., Styles, C. A. & Fink, G. R. (1992) Unipolar cell divisions in the yeast S. cerevisiae lead to filamentous growth: regulation by starvation and *RAS*. *Cell,* 68**,** 1077-1090.

Gligoris, T., Thireos, G. & Tzamarias, D. (2007) The Tup1 corepressor directs Htz1 deposition at a specific promoter nucleosome marking the *GAL1* gene for rapid activation. *Molecular and Cellular Biology,* 27**,** 4198-4205.

Godard, P., Urrestarazu, A., Vissers, S., Kontos, K., Bontempi, G., van Helden, J. & André, B. (2007) Effect of 21 different nitrogen sources on global gene expression in the yeast *Saccharomyces cerevisiae*. *Molecular and Cellular Biology,* 27**,** 3065-3086.

Goffeau, A., Barrell, B. G., Bussey, H., Davis, R. W., Dujon, B., Feldmann, H., Galibert, F., Hoheisel, J. D., Jacq, C., Johnston, M., Louis, E. J., Mewes, H. W., Murakami, Y., Philippsen, P., Tettelin, H. & Oliver, S. G. (1996) Life with 6000 genes. *Science,* 274**,** 546, 563-567.

Goldstein, R. E., Jiménez, G., Cook, O., Gur, D. & Paroush, Z. (1999) Huckebein repressor activity in Drosophila terminal patterning is mediated by Groucho. *Development,* 126**,** 3747-3755.

González, A. & Hall, M. N. (2017) Nutrient sensing and TOR signaling in yeast and mammals. *The EMBO Journal,* 36**,** 397-408.

Gounalaki, N., Tzamarias, D. & Vlassi, M. (2000) Identification of residues in the TPR domain of Ssn6 responsible for interaction with the Tup1 protein. *FEBS Letters,* 473**,** 37-41.

Goutte, C. & Johnson, A. D. (1988) a1 protein alters the DNA binding specificity of α2 repressor. *Cell,* 52**,** 875-882.

Gray, J. V., Petsko, G. A., Johnston, G. C., Ringe, D., Singer, R. A. & Werner-Washburne, M. (2004) "Sleeping Beauty": Quiescence in *Saccharomyces cerevisiae*. *Microbiology and Molecular Biology Reviews,* 68**,** 187-206.

Grbavec, D., Lo, R., Liu, Y., Greenfield, A. & Stifani, S. (1999) Groucho/transducin-like enhancer of split (TLE) family members interact with the yeast transcriptional co-repressor SSN6 and mammalian SSN6-related proteins: implications for evolutionary conservation of transcription repression mechanisms. *Biochemical Journal,* 337**,** 13-17.

Gurevich, V. & Kassir, Y. (2010) A switch from a gradient to a threshold mode in the regulation of a transcriptional cascade promotes robust execution of meiosis in budding yeast. *PLOS One,* 5**,** e11005.

Guttmann-Raviv, N., Martin, S. & Kassir, Y. (2002) Ime2, a meiosis-specific kinase in yeast, is required for destabilization of its transcriptional activator, Ime1. *Molecular and Cellular Biology,* 22**,** 2047-2056.

Hall, M. & Johnson, A. (1987) Homeo domain of the yeast repressor α2 is a sequence-specific DNA-binding domain but is not sufficient for repression. *Science,* 237**,** 1007-1012.

Hanlon, S. E., Rizzo, J. M., Tatomer, D. C., Lieb, J. D. & Buck, M. J. (2011) The stress response factors Yap6, Cin5, Phd1, and Skn7 direct targeting of the conserved co-repressor Tup1-Ssn6 in *S. cerevisiae*. *PLOS One,* 6**,** e19060.

Harbison, C. T., Gordon, D. B., Lee, T. I., Rinaldi, N. J., Macisaac, K. D., Danford, T. W., Hannett, N. M., Tagne, J. B., Reynolds, D. B., Yoo, J., Jennings, E. G., Zeitlinger, J., Pokholok, D. K., Kellis, M., Rolfe, P. A., Takusagawa, K. T., Lander, E. S., Gifford, D. K., Fraenkel, E. & Young, R. A. (2004) Transcriptional regulatory code of a eukaryotic genome. *Nature,* 431**,** 99-104.

Heitman, J., Movva, N. R., Hiestand, P. C. & Hall, M. N. (1991) FK 506-binding protein proline rotamase is a target for the immunosuppressive agent FK 506 in *Saccharomyces cerevisiae*. *Proceedings of the National Academy of Sciences,* 88**,** 1948-1952.

Herschbach, B. M., Arnaud, M. B. & Johnson, A. D. (1994) Transcriptional repression directed by the yeast α2 protein *in vitro*. *Nature,* 370**,** 309-311.

Herskowitz, I. (1988) Life cycle of the budding yeast *Saccharomyces cerevisiae*. *Microbiological Reviews,* 52**,** 536-553.

Hnisz, D., Abraham, Brian J., Lee, Tong I., Lau, A., Saint-André, V., Sigova, Alla A., Hoke, Heather A. & Young, Richard A. (2013) Super-enhancers in the control of cell identity and disease. *Cell,* 155**,** 934-947.

Hoffman, E. A., Frey, B. L., Smith, L. M. & Auble, D. T. (2015) Formaldehyde crosslinking: a tool for the study of chromatin complexes. *Journal of Biological Chemistry,* 290**,** 26404-26411.

Hollenhorst, P. C., Bose, M. E., Mielke, M. R., Müller, U. & Fox, C. A. (2000) Forkhead genes in transcriptional silencing, cell morphology and the cell cycle: overlapping and distinct functions for *FKH1* and *FKH2* in *Saccharomyces cerevisiae*. *Genetics,* 154**,** 1533-1548.

Honigberg, S. M. & Lee, R. H. (1998) Snf1 kinase connects nutritional pathways controlling meiosis in *Saccharomyces cerevisiae*. *Molecular and Cellular Biology,* 18**,** 4548-4555.

Honigberg, S. M. & Purnapatre, K. (2003) Signal pathway integration in the switch from the mitotic cell cycle to meiosis in yeast. *Journal of Cell Science,* 116**,** 2137-2147.

Husain, J., Lo, R., Grbavec, D. & Stifani, S. (1996) Affinity for the nuclear compartment and expression during cell differentiation implicate phosphorylated Groucho/TLE1 forms of higher molecular mass in nuclear functions. *The Biochemical Journal,* 317**,** 523-531.

Hyun, K., Jeon, J., Park, K. & Kim, J. (2017) Writing, erasing and reading histone lysine methylations. *Experimental & Molecular Medicine,* 49**,** e324.

Imai, S., Armstrong, C. M., Kaeberlein, M. & Guarente, L. (2000) Transcriptional silencing and longevity protein Sir2 is an NAD-dependent histone deacetylase. *Nature,* 403**,** 795-800.

Iñigo, S., Giraldez, A. N., Chory, J. & Cerdán, P. D. (2012) Proteasome-mediated turnover of Arabidopsis MED25 is coupled to the activation of *FLOWERING LOCUS T* transcription. *Plant Physiology,* 160**,** 1662-1673.

Jackson, V. (1978) Studies on histone organization in the nucleosome using formaldehyde as a reversible cross-linking agent. *Cell,* 15**,** 945-954.

Jambhekar, A. & Amon, A. (2008) Control of meiosis by respiration. *Current Biology,* 18**,** 969-975.

Jennings, B. H. & Ish-Horowicz, D. (2008) The Groucho/TLE/Grg family of transcriptional co-repressors. *Genome Biology,* 9**,** 205.

Jennings, B. H., Pickles, L. M., Wainwright, S. M., Roe, S. M., Pearl, L. H. & Ish-Horowicz, D. (2006) Molecular recognition of transcriptional repressor motifs by the WD domain of the Groucho/TLE corepressor. *Molecular Cell,* 22**,** 645-655.

Jiang, Y. W. & Kang, C. M. (2003) Induction of *S. cerevisiae* filamentous differentiation by slowed DNA synthesis involves Mec1, Rad53 and Swe1 checkpoint proteins. *Molecular Biology of the Cell,* 14**,** 5116-5124.

Kachroo, A. H., Laurent, J. M., Yellman, C. M., Meyer, A. G., Wilke, C. O. & Marcotte, E. M. (2015) Systematic humanization of yeast genes reveals conserved functions and genetic modularity. *Science,* 348**,** 921-925.

Kahana-Edwin, S., Stark, M. & Kassir, Y. (2013) Multiple MAPK cascades regulate the transcription of *IME1*, the master transcriptional activator of meiosis in *Saccharomyces cerevisiae*. *PLOS One,* 8**,** e78920.

Kahana, S., Pnueli, L., Kainth, P., Sassi, H. E., Andrews, B. & Kassir, Y. (2010) Functional dissection of *IME1* transcription using quantitative promoter-reporter screening. *Genetics,* 186**,** 829-841.

Kalejs, M. & Erenpreisa, J. (2005) Cancer/testis antigens and gametogenesis: a review and "brain-storming" session. *Cancer Cell International,* 5**,** 4.

Kanhere, A. & Bansal, M. (2005) Structural properties of promoters: similarities and differences between prokaryotes and eukaryotes. *Nucleic Acids Research,* 33**,** 3165-3175.

Kassir, Y., Adir, N., Boger-Nadjar, E., Raviv, N. G., Rubin-Bejerano, I., Sagee, S. & Shenhar, G. (2003) Transcriptional regulation of meiosis in budding yeast. *International Review of Cytology,* 224**,** 111-171.

Kassir, Y., Granot, D. & Simchen, G. (1988) *IME1*, a positive regulator gene of meiosis in S. cerevisiae. *Cell,* 52**,** 853-862.

Kaul, A., Schuster, E. & Jennings, B. H. (2014) The Groucho co-repressor is primarily recruited to local target sites in active chromatin to attenuate transcription. *PLOS Genetics,* 10**,** e1004595.

Keleher, C. A., Goutte, C. & Johnson, A. D. (1988) The yeast cell-type-specific repressor α2 acts cooperatively with a non-cell-type-specific protein. *Cell,* 53**,** 927-936.

Keleher, C. A., Redd, M. J., Schultz, J., Carlson, M. & Johnson, A. D. (1992) Ssn6-Tup1 is a general repressor of transcription in yeast. *Cell,* 68**,** 709-719.

Kemmeren, P., Sameith, K., van de Pasch, L. A., Benschop, J. J., Lenstra, T. L., Margaritis, T., O'Duibhir, E., Apweiler, E., van Wageningen, S., Ko, C. W., van Heesch, S., Kashani, M. M., Ampatziadis-Michailidis, G., Brok, M. O., Brabers, N. A., Miles, A. J., Bouwmeester, D., van Hooff, S. R., van Bakel, H., Sluiters, E., Bakker, L. V., Snel, B., Lijnzaad, P., van Leenen, D., Groot Koerkamp, M. J. & Holstege, F. C. (2014) Large-scale genetic perturbations reveal regulatory networks and an abundance of gene-specific repressors. *Cell,* 157**,** 740-752.

Kennedy-Darling, J. & Smith, L. M. (2014) Measuring the formaldehyde protein-DNA cross-link reversal rate. *Analytical Chemistry,* 86**,** 5678-5681.

Khan, J., Ezan, F., Crémet, J. Y., Fautrel, A., Gilot, D., Lambert, M., Benaud, C., Troadec, M. B. & Prigent, C. (2011) Overexpression of active Aurora-C kinase results in cell transformation and tumour formation. *PLOS One,* 6**,** e26512.

Komachi, K. & Johnson, A. D. (1997) Residues in the WD repeats of Tup1 required for interaction with alpha2. *Molecular and Cellular Biology,* 17**,** 6023-6028.

Komachi, K., Redd, M. J. & Johnson, A. D. (1994) The WD repeats of Tup1 interact with the homeo domain protein α2. *Genes & Development,* 8**,** 2857-2867.

Kroschwald, S., Maharana, S. & Simon, A. (2017) Hexanediol: a chemical probe to investigate the material properties of membrane-less compartments. *Matters***,** doi: 10.19185/matters.201702000010.

Kuchin, S., Vyas, V. K. & Carlson, M. (2002) Snf1 protein kinase and the repressors Nrg1 and Nrg2 regulate *FLO11*, haploid invasive growth, and diploid pseudohyphal differentiation. *Molecular and Cellular Biology,* 22**,** 3994-4000.

Kumar, R., Reynolds, D. M., Shevchenko, A., Shevchenko, A., Goldstone, S. D. & Dalton, S. (2000) Forkhead transcription factors, Fkh1p and Fkh2p, collaborate with Mcm1p to control transcription required for M-phase. *Current Biology,* 10**,** 896-906.

Kuo, D., Licon, K., Bandyopadhyay, S., Chuang, R., Luo, C., Catalana, J., Ravasi, T., Tan, K. & Ideker, T. (2010) Coevolution within a transcriptional network by compensatory *trans* and *cis* mutations. *Genome Research,* 20**,** 1672-1678.

Kuras, L. & Struhl, K. (1999) Binding of TBP to promoters *in vivo* is stimulated by activators and requires Pol II holoenzyme. *Nature,* 399**,** 609-613.

Kurdistani, S. K. & Grunstein, M. (2003) Histone acetylation and deacetylation in yeast. *Nature Reviews Molecular Cell Biology,* 4**,** 276-284.

Lardenois, A., Stuparevic, I., Liu, Y., Law, M. J., Becker, E., Smagulova, F., Waern, K., Guilleux, M.-H., Horecka, J., Chu, A., Kervarrec, C., Strich, R., Snyder, M., Davis, R. W., Steinmetz, L. M. & Primig, M. (2015) The conserved histone deacetylase Rpd3 and its DNA binding subunit Ume6 control dynamic transcript architecture during mitotic growth and meiotic development. *Nucleic Acids Research,* 43**,** 115-128.

Lelli, K. M., Slattery, M. & Mann, R. S. (2012) Disentangling the many layers of eukaryotic transcriptional regulation. *Annual Review of Genetics,* 46**,** 43-68.

Leza, M. A. & Elion, E. A. (1999) *POG1*, a novel yeast gene, promotes recovery from pheromone arrest via the G1 cyclin *CLN2*. *Genetics,* 151**,** 531-543.

Liebman, S. W. & Chernoff, Y. O. (2012) Prions in yeast. *Genetics,* 191**,** 1041-1072.

Lin, X., Zhang, C. Y., Bai, X. W., Song, H. Y. & Xiao, D. G. (2014) Effects of *MIG1*, *TUP1* and *SSN6* deletion on maltose metabolism and leavening ability of baker's yeast in lean dough. *Microbial Cell Factories,* 13.

Lin, Y., Gill, M. E., Koubova, J. & Page, D. C. (2008) Germ cell-intrinsic and -extrinsic factors govern meiotic initiation in mouse embryos. *Science,* 322**,** 1685-1687.

Lin, Y., Protter, D. S. W., Rosen, M. K. & Parker, R. (2015) Formation and maturation of phase-separated liquid droplets by RNA-binding proteins. *Molecular Cell,* 60**,** 208-219.

Loewith, R. & Hall, M. N. (2011) Target of rapamycin (TOR) in nutrient signaling and growth control. *Genetics,* 189**,** 1177-1201.

Loewith, R., Jacinto, E., Wullschleger, S., Lorberg, A., Crespo, J. L., Bonenfant, D., Oppliger, W., Jenoe, P. & Hall, M. N. (2002) Two TOR complexes, only one of which is rapamycin sensitive, have distinct roles in cell growth control. *Molecular Cell,* 10**,** 457-468.

Loidl, J. 2000. Meiosis in budding yeast and in multicellular eukaryotes - similarities and differences. *In:* OLMO, E. & REDI, C. A. (eds.) *Chromosomes Today.* Switzerland: Birkhäuser Verlag.

Longtine, M. S., McKenzie, A., III, Demarini, D. J., Shah, N. G., Wach, A., Brachat, A., Philippsen, P. & Pringle, J. R. (1998) Additional modules for versatile and economical PCR-based gene deletion and modification in *Saccharomyces cerevisiae*. *Yeast,* 14**,** 953-961.

Lorenz, M. C., Cutler, N. S. & Heitman, J. (2000) Characterization of alcohol-induced filamentous growth in *Saccharomyces cerevisiae*. *Molecular Biology of the Cell,* 11**,** 183-199.

Ma, H. T., Niu, C. M., Xia, J., Shen, X. Y., Xia, M. M., Hu, Y. Q. & Zheng, Y. (2018) Stimulated by retinoic acid gene 8 (Stra8) plays important roles in many stages of spermatogenesis. *Asian Journal of Andrology,* 20**,** 479-487.

MacIsaac, K. D., Wang, T., Gordon, D. B., Gifford, D. K., Stormo, G. D. & Fraenkel, E. (2006) An improved map of conserved regulatory sites for *Saccharomyces cerevisiae*. *BMC Bioinformatics,* 7**,** 113.

Madhani, H. D. (2000) Interplay of intrinsic and extrinsic signals in yeast differentiation. *Proceedings of the National Academy of Sciences,* 97**,** 13461-13463.

Madlung, A., Tyagi, A. P., Watson, B., Jiang, H., Kagochi, T., Doerge, R. W., Martienssen, R. & Comai, L. (2005) Genomic changes in synthetic Arabidopsis polyploids. *The Plant Journal,* 41**,** 221-230.

Malcher, M., Schladebeck, S. & Mösch, H. U. (2011) The Yak1 protein kinase lies at the center of a regulatory cascade affecting adhesive growth and stress resistance in *Saccharomyces cerevisiae*. *Genetics,* 187**,** 717-730.

Mathias, J. R., Hanlon, S. E., O'Flanagan, R. A., Sengupta, A. M. & Vershon, A. K. (2004) Repression of the yeast *HO* gene by the MATα2 and MATa1 homeodomain proteins. *Nucleic Acids Research,* 32**,** 6469-6478.

Matsumura, H., Kusaka, N., Nakamura, T., Tanaka, N., Sagegami, K., Uegaki, K., Inoue, T. & Mukai, Y. (2012) Crystal structure of the N-terminal domain of the yeast general corepressor Tup1p and its functional implications. *Journal of Biological Chemistry,* 287**,** 26528-26538.

McCarroll, R. M. & Esposito, R. E. (1994) SPO13 negatively regulates the progression of mitotic and meiotic nuclear division in Saccharomyces cerevisiae. *Genetics,* 138**,** 47-60.

Mennella, T. A., Klinkenberg, L. G. & Zitomer, R. S. (2003) Recruitment of Tup1-Ssn6 by yeast hypoxic genes and chromatin-independent exclusion of TATA binding protein. *Eukaryotic Cell,* 2**,** 1288-1303.

Merlini, L., Dudin, O. & Martin, S. G. (2013) Mate and fuse: how yeast cells do it. *Open Biology,* 3**,** 130008.

Metz, B., Kersten, G. F., Hoogerhout, P., Brugghe, H. F., Timmermans, H. A., de Jong, A., Meiring, H., ten Hove, J., Hennink, W. E., Crommelin, D. J. & Jiskoot, W. (2004) Identification of formaldehyde-induced modifications in proteins: reactions with model peptides. *Journal of Biological Chemistry,* 279**,** 6235-6243.

Miccio, A., Wang, Y., Hong, W., Gregory, G. D., Wang, H., Yu, X., Choi, J. K., Shelat, S., Tong, W., Poncz, M. & Blobel, G. A. (2010) NuRD mediates activating and repressive functions of GATA-1 and FOG-1 during blood development. *The EMBO Journal,* 29**,** 442-456.

Miller-Fleming, L., Giorgini, F. & Outeiro, T. F. (2008) Yeast as a model for studying human neurodegenerative disorders. *Biotechnology Journal,* 3**,** 325-338.

Miller, J. J. (1957) Metabolism of yeast sporulation. II. Stimulation and inhibition by monosaccharides. *Canadian Journal of Microbiology,* 3**,** 81-90.

Mitchell, A. P. & Bowdish, K. S. (1992) Selection for early meiotic mutants in yeast. *Genetics,* 131**,** 65-72.

Mitchell, A. P., Driscoll, S. E. & Smith, H. E. (1990) Positive control of sporulation-specific genes by the *IME1* and *IME2* products in *Saccharomyces cerevisiae*. *Molecular and Cellular Biology,* 10**,** 2104-2110.

Mizuno, T., Nakazawa, N., Remgsamrarn, P., Kunoh, T., Oshima, Y. & Harashima, S. (1998) The Tup1-Ssn6 general repressor is involved in repression of *IME1* encoding a transcriptional activator of meiosis in *Saccharomyces cerevisiae*. *Current Genetics,* 33**,** 239-247.

Mora, A., Sandve, G. K., Gabrielsen, O. S. & Eskeland, R. (2016) In the loop: promoter-enhancer interactions and bioinformatics. *Briefings in Bioinformatics,* 17**,** 980-995.

Moretto, F., Wood, N. E., Kelly, G., Doncic, A. & van Werven, F. J. (2018) A regulatory circuit of two lncRNAs and a master regulator directs cell fate in yeast. *Nature Communications,* 9**,** 780.

Muhr, J., Andersson, E., Persson, M., Jessell, T. M. & Ericson, J. (2001) Groucho-mediated transcriptional repression establishes progenitor cell pattern and neuronal fate in the ventral neural tube. *Cell,* 104**,** 861-873.

Nadel, C. M., Mackie, T. D. & Gardner, R. G. (2019) Osmolyte accumulation regulates the SUMOylation and inclusion dynamics of the prionogenic Cyc8-Tup1 transcription corepressor. *PLOS Genetics,* 15**,** e1008115.

Nakazawa, N., Abe, K., Koshika, Y. & Iwano, K. (2010) Cln3 blocks *IME1* transcription and the Ime1-Ume6 interaction to cause the sporulation incompetence in a sake yeast, Kyokai no. 7. *Journal of Bioscience and Bioengineering,* 110**,** 1-7.

Ng, C. H., Akhter, A., Yurko, N., Burgener, J. M., Rosonina, E. & Manley, J. L. (2015) Sumoylation controls the timing of Tup1-mediated transcriptional deactivation. *Nature Communications,* 6**,** 6610.

Ni, L., Bruce, C., Hart, C., Leigh-Bell, J., Gelperin, D., Umansky, L., Gerstein, M. B. & Snyder, M. (2009) Dynamic and complex transcription factor binding during an inducible response in yeast. *Genes & Development,* 2**3,** 1351-1363.

Nicastro, R., Tripodi, F., Gaggini, M., Castoldi, A., Reghellin, V., Nonnis, S., Tedeschi, G. & Coccetti, P. (2015) Snf1 phosphorylates adenylate cyclase and negatively regulates protein kinase A-dependent transcription in *Saccharomyces cerevisiae*. *Journal of Biological Chemistry,* 290**,** 24715-24726.

Nishimura, K., Fukagawa, T., Takisawa, H., Kakimoto, T. & Kanemaki, M. (2009) An auxin-based degron system for the rapid depletion of proteins in nonplant cells. *Nature Methods,* 6**,** 917-922.

Oeser, M. L., Amen, T., Nadel, C. M., Bradley, A. I., Reed, B. J., Jones, R. D., Gopalan, J., Kaganovich, D. & Gardner, R. G. (2016) Dynamic sumoylation of a conserved transcription corepressor prevents persistent inclusion formation during hyperosmotic stress. *PLOS Genetics,* 12**,** e1005809.

Oshiro, S. & Takagi, H. (2014) The transcriptional activator Pog1 controls cell cycle, and its phosphorylated form is downregulated by the ubiquitin ligase Dma2 in *Saccharomyces cerevisiae*. *FEMS Yeast Research,* 14**,** 1015-1027.

Pan, X. & Heitman, J. (2000) Sok2 regulates yeast pseudohyphal differentiation via a transcription factor cascade that regulates cell-cell adhesion. *Molecular and Cellular Biology,* 20**,** 8364-8372.

Papamichos-Chronakis, M., Conlan, R. S., Gounalaki, N., Copf, T. & Tzamarias, D. (2000) Hrs1/Med3 is a Cyc8-Tup1 corepressor target in the RNA polymerase II holoenzyme. *Journal of Biological Chemistry,* 275**,** 8397-8403.

Papamichos-Chronakis, M., Gligoris, T. & Tzamarias, D. (2004) The Snf1 kinase controls glucose repression in yeast by modulating interactions between the Mig1 repressor and the Cyc8-Tup1 co-repressor. *EMBO Reports,* 5**,** 368-372.

Papamichos-Chronakis, M., Watanabe, S., Rando, O. J. & Peterson, C. L. (2011) Global regulation of H2A.Z localization by the INO80 chromatin-remodeling enzyme is essential for genome integrity. *Cell,* 144**,** 200-213.

Park, S. H., Koh, S. S., Chun, J. H., Hwang, H. J. & Kang, H. S. (1999) Nrg1 is a transcriptional repressor for glucose repression of *STA1* gene expression in *Saccharomyces cerevisiae*. *Molecular and Cellular Biology,* 19**,** 2044-2050.

Pascual-Ahuir, A., Posas, F., Serrano, R. & Proft, M. (2001) Multiple levels of control regulate the yeast cAMP-response element-binding protein repressor Sko1p in response to stress. *Journal of Biological Chemistry,* 276**,** 37373-37378.

Pchelintsev, N. A., Adams, P. D. & Nelson, D. M. (2016) Critical parameters for efficient sonication and improved chromatin immunoprecipitation of high molecular weight proteins. *PLOS One,* 11**,** e0148023.

Pereira, J., Pimentel, C., Amaral, C., Menezes, R. A. & Rodrigues-Pousada, C. (2009) Yap4 PKA- and GSK3-dependent phosphorylation affects its stability but not its nuclear localization. *Yeast,* 26**,** 641-653.

Peterson, T. A., Park, D. & Kann, M. G. (2013) A protein domain-centric approach for the comparative analysis of human and yeast phenotypically relevant mutations. *BMC Genomics,* 14 Suppl 3**,** S5.

Phatnani, H. P. & Greenleaf, A. L. (2006) Phosphorylation and functions of the RNA polymerase II CTD. *Genes & Development,* 20**,** 2922-2936.

Piñon, R. (1978) Folded chromosomes in non-cycling yeast cells: evidence for a characteristic g_0 form. *Chromosoma,* 67**,** 263-274.

Pokholok, D. K., Harbison, C. T., Levine, S., Cole, M., Hannett, N. M., Lee, T. I., Bell, G. W., Walker, K., Rolfe, P. A., Herbolsheimer, E., Zeitlinger, J., Lewitter, F., Gifford, D. K. & Young, R. A. (2005) Genome-wide map of nucleosome acetylation and methylation in yeast. *Cell,* 122**,** 517-527.

Pokholok, D. K., Zeitlinger, J., Hannett, N. M., Reynolds, D. B. & Young, R. A. (2006) Activated signal transduction kinases frequently occupy target genes. *Science,* 313**,** 533-536.

Polish, J. A., Kim, J. H. & Johnston, M. (2005) How the Rgt1 transcription factor of *Saccharomyces cerevisiae* is regulated by glucose. *Genetics,* 169**,** 583-594.

Proft, M., Pascual-Ahuir, A., de Nadal, E., Ariño, J., Serrano, R. & Posas, F. (2001) Regulation of the Sko1 transcriptional repressor by the Hog1 MAP kinase in response to osmotic stress. *The EMBO Journal,* 20**,** 1123-1133.

Proft, M. & Struhl, K. (2002) Hog1 kinase converts the Sko1-Cyc8-Tup1 repressor complex into an activator that recruits SAGA and SWI/SNF in response to osmotic stress. *Molecular Cell,* 9**,** 1307-1317.

Ptacek, J., Devgan, G., Michaud, G., Zhu, H., Zhu, X., Fasolo, J., Guo, H., Jona, G., Breitkreutz, A., Sopko, R., McCartney, R. R., Schmidt, M. C., Rachidi, N., Lee, S.-J., Mah, A. S., Meng, L., Stark, M. J. R., Stern, D. F., De Virgilio, C., Tyers, M., Andrews, B., Gerstein, M., Schweitzer, B., Predki, P. F. & Snyder, M. (2005) Global analysis of protein phosphorylation in yeast. *Nature,* 438**,** 679-684.

Quievryn, G. & Zhitkovich, A. (2000) Loss of DNA-protein crosslinks from formaldehyde-exposed cells occurs through spontaneous hydrolysis and an active repair process linked to proteosome function. *Carcinogenesis,* 21**,** 1573-1580.

Raithatha, S., Su, T. C., Lourenco, P., Goto, S. & Sadowski, I. (2012) Cdk8 regulates stability of the transcription factor Phd1 to control pseudohyphal differentiation of *Saccharomyces cerevisiae*. *Molecular and Cellular Biology,* 32**,** 664-674.

Raj, A., van den Bogaard, P., Rifkin, S. A., van Oudenaarden, A. & Tyagi, S. (2008) Imaging individual mRNA molecules using multiple singly labeled probes. *Nature Methods,* 5**,** 877-879.

Rajvanshi, P. K., Arya, M. & Rajasekharan, R. (2017) The stress-regulatory transcription factors Msn2 and Msn4 regulate fatty acid oxidation in budding yeast. *Journal of Biological Chemistry,* 292**,** 18628-18643.

Redd, M. J., Arnaud, M. B. & Johnson, A. D. (1997) A complex composed of Tup1 and Ssn6 represses transcription *in vitro*. *Journal of Biological Chemistry,* 272**,** 11193-11197.

Redd, M. J., Stark, M. R. & Johnson, A. D. (1996) Accessibility of α2-repressed promoters to the activator Gal4. *Molecular and Cellular Biology,* 16**,** 2865-2869.

Reddy, T. E., DeLisi, C. & Shakhnovich, B. E. (2007) Binding site graphs: a new graph theoretical framework for prediction of transcription factor binding sites. *PLOS Computational Biology,* 3**,** e90.

Régnacq, M., Alimardani, P., El Moudni, B. & Bergès, T. (2001) SUT1p interaction with Cyc8p(Ssn6p) relieves hypoxic genes from Cyc8p-Tup1p repression in *Saccharomyces cerevisiae*. *Molecular Microbiology,* 40**,** 1085-1096.

Reynolds, N., O'Shaughnessy, A. & Hendrich, B. (2013) Transcriptional repressors: multifaceted regulators of gene expression. *Development,* 140**,** 505-512.

Rine, J., Sprague, G. F., Jr. & Herskowitz, I. (1981) *rme1* mutation of *Saccharomyces cerevisiae*: map position and bypass of mating type locus control of sporulation. *Molecular and Cellular Biology,* 1**,** 958-960.

Rizzo, J. M., Mieczkowski, P. A. & Buck, M. J. (2011) Tup1 stabilizes promoter nucleosome positioning and occupancy at transcriptionally plastic genes. *Nucleic Acids Research,* 39**,** 8803-8819.

Robyr, D., Suka, Y., Xenarios, I., Kurdistani, S. K., Wang, A., Suka, N. & Grunstein, M. (2002) Microarray deacetylation maps determine genome-wide functions for yeast histone deacetylases. *Cell,* 109**,** 437-446.

Rodrigues-Pousada, C., Devaux, F., Caetano, S. M., Pimentel, C., da Silva, S., Cordeiro, A. C. & Amaral, C. (2019) Yeast AP-1 like transcription factors (Yap) and stress response: a current overview. *Microbial Cell,* 6**,** 267-285.

Rodríguez, A., De La Cera, T., Herrero, P. & Moreno, F. (2001) The hexokinase 2 protein regulates the expression of the *GLK1*, *HXK1* and *HXK2* genes of *Saccharomyces cerevisiae*. *The Biochemical Journal,* 355**,** 625-631.

Roeder, R. G. (1996) The role of general initiation factors in transcription by RNA polymerase II. *Trends in Biochemical Sciences,* 21**,** 327-335.

Roelants, F. M., Leskoske, K. L., Martinez Marshall, M. N., Locke, M. N. & Thorner, J. (2017) The TORC2-dependent signaling network in the yeast *Saccharomyces cerevisiae*. *Biomolecules,* 7**,** pii: E66.

Roy, A., Shin, Y. J., Cho, K. H. & Kim, J. H. (2013) Mth1 regulates the interaction between the Rgt1 repressor and the Ssn6-Tup1 corepressor complex by modulating PKA-dependent phosphorylation of Rgt1. *Molecular Biology of the Cell,* 24**,** 1493-1503.

Rubin-Bejerano, I., Mandel, S., Robzyk, K. & Kassir, Y. (1996) Induction of meiosis in *Saccharomyces cerevisiae* depends on conversion of the transcriptional represssor Ume6 to a positive regulator by its regulated association with the transcriptional activator Ime1. *Molecular and Cellular Biology,* 16**,** 2518-2526.

Rubin-Bejerano, I., Sagee, S., Friedman, O., Pnueli, L. & Kassir, Y. (2004) The in vivo activity of Ime1, the key transcriptional activator of meiosis-specific genes in *Saccharomyces cerevisiae*, is inhibited by the cyclic AMP/protein kinase A signal pathway through the glycogen synthase kinase 3-β homolog Rim11. *Molecular and Cellular Biology,* 24**,** 6967-6979.

Rundlett, S. E., Carmen, A. A., Kobayashi, R., Bavykin, S., Turner, B. M. & Grunstein, M. (1996) HDA1 and RPD3 are members of distinct yeast histone deacetylase complexes that regulate silencing and transcription. *Proceedings of the National Academy of Sciences,* 93**,** 14503-14508.

Rupp, S., Summers, E., Lo, H.-J., Madhani, H. & Fink, G. (1999) MAP kinase and cAMP filamentation signaling pathways converge on the unusually large promoter of the yeast *FLO11* gene. *The EMBO Journal,* 18**,** 1257-1269.

Rutledge, M. T., Russo, M., Belton, J.-M., Dekker, J. & Broach, J. R. (2015) The yeast genome undergoes significant topological reorganization in quiescence. *Nucleic Acids Research,* 43**,** 8299-8313.

Sabari, B. R., Dall'Agnese, A., Boija, A., Klein, I. A., Coffey, E. L., Shrinivas, K., Abraham, B. J., Hannett, N. M., Zamudio, A. V., Manteiga, J. C., Li, C. H., Guo, Y. E., Day, D. S., Schuijers, J., Vasile, E., Malik, S., Hnisz, D., Lee, T. I., Cisse, I. I., Roeder, R. G., Sharp, P. A., Chakraborty, A. K. & Young, R. A. (2018) Coactivator condensation at super-enhancers links phase separation and gene control. *Science,* 361**,** pii: eaar3958.

Sagee, S., Sherman, A., Shenhar, G., Robzyk, K., Ben-Doy, N., Simchen, G. & Kassir, Y. (1998) Multiple and distinct activation and repression sequences mediate the regulated transcription of *IME1*, a transcriptional activator of meiosis-specific genes in *Saccharomyces cerevisiae*. *Molecular and Cellular Biology,* 18**,** 1985-1995.

Salghetti, S. E., Muratani, M., Wijnen, H., Futcher, B. & Tansey, W. P. (2000) Functional overlap of sequences that activate transcription and signal ubiquitin-mediated proteolysis. *Proceedings of the National Academy of Sciences,* 97**,** 3118-3123.

Sanada, M., Kuroda, K. & Ueda, M. (2011) *GTS1* induction causes derepression of Tup1-Cyc8-repressing genes and chromatin remodeling through the interaction of Gts1p with Cyc8p. *Bioscience, Biotechnology, and Biochemistry,* 75**,** 740-747.

Santangelo, G. M. (2006) Glucose signaling in *Saccharomyces cerevisiae*. *Microbiology and Molecular Biology Reviews,* 70**,** 253-282.

Sapio, L., Di Maiolo, F., Illiano, M., Esposito, A., Chiosi, E., Spina, A. & Naviglio, S. (2014) Targeting protein kinase A in cancer therapy: an update. *EXCLI Journal,* 13**,** 843-855.

Schäfer, G., McEvoy, C. R. E. & Patterton, H.-G. (2008) The *Saccharomyces cerevisiae* linker histone Hho1p is essential for chromatin compaction in stationary phase and is displaced by transcription. *Proceedings of the National Academy of Sciences,* 105**,** 14838-14843.

Schindelin, J., Rueden, C. T., Hiner, M. C. & Eliceiri, K. W. (2015) The ImageJ ecosystem: An open platform for biomedical image analysis. *Molecular Reproduction and Development,* 82**,** 518-529.

Serra-Cardona, A., Petrezsélyová, S., Canadell, D., Ramos, J. & Ariño, J. (2014) Coregulated expression of the Na+/phosphate Pho89 transporter and Ena1 Na+-ATPase allows their functional coupling under high-pH stress. *Molecular and Cellular Biology,* 34**,** 4420-4435.

Shankar, C. S., Ramakrishnan, M. S. & Umesh-Kumar, S. (1996) *MIG1* overexpression causes flocculation in *Saccharomyces cerevisiae*. *Microbiology,* 142**,** 2663-2667.

Shaywitz, A. J. & Greenberg, M. E. (1999) CREB: A stimulus-induced transcription factor activated by a diverse array of extracellular signals. *Annual Review of Biochemistry,* 68**,** 821-861.

Shefer-Vaida, M., Sherman, A., Ashkenazi, T., Robzyk, K. & Kassir, Y. (1995) Positive and negative feedback loops affect the transcription of *IME1*, a positive regulator of meiosis in *Saccharomyces cerevisiae*. *Developmental Genetics,* 16**,** 219-228.

Shenhar, G. & Kassir, Y. (2001) A positive regulator of mitosis, Sok2, functions as a negative regulator of meiosis in *Saccharomyces cerevisiae*. *Molecular and Cellular Biology,* 21**,** 1603-1612.

Sherman, A., Shefer, M., Sagee, S. & Kassir, Y. (1993) Post-transcriptional regulation of *IME1* determines initiation of meiosis in *Saccharomyces cerevisiae*. *Molecular and General Genetics MGG,* 237**,** 375-384.

Siggers, T., Reddy, J., Barron, B. & Bulyk, M. L. (2014) Diversification of transcription factor paralogs via noncanonical modularity in C2H2 zinc finger DNA binding. *Molecular Cell,* 55**,** 640-648.

Simon, J. A., Szankasi, P., Nguyen, D. K., Ludlow, C., Dunstan, H. M., Roberts, C. J., Jensen, E. L., Hartwell, L. H. & Friend, S. H. (2000) Differential toxicities of anticancer agents among DNA repair and checkpoint mutants of *Saccharomyces cerevisiae*. *Cancer Research,* 60**,** 328-333.

Smith, A., Ward, M. P. & Garrett, S. (1998) Yeast PKA represses Msn2p/Msn4p-dependent gene expression to regulate growth, stress response and glycogen accumulation. *The EMBO Journal,* 17**,** 3556-3564.

Smith, H. E., Su, S. S., Neigeborn, L., Driscoll, S. E. & Mitchell, A. P. (1990) Role of *IME1* expression in regulation of meiosis in *Saccharomyces cerevisiae*. *Molecular and Cellular Biology,* 10**,** 6103-6113.

Smith, R. L. & Johnson, A. D. (2000) Turning genes off by Ssn6-Tup1: a conserved system of transcriptional repression in eukaryotes. *Trends in Biochemical Sciences,* 25**,** 325-330.

Smith, R. L., Redd, M. J. & Johnson, A. D. (1995) The tetratricopeptide repeats of Ssn6 interact with the homeo domain of α2. *Genes & Development,* 9**,** 2903-2910.

Snoek, I. S., Tai, S. L., Pronk, J. T., Yde Steensma, H. & Daran, J. M. (2010) Involvement of Snf7p and Rim101p in the transcriptional regulation of *TIR1* and other anaerobically upregulated genes in *Saccharomyces cerevisiae*. *FEMS Yeast Research,* 10**,** 367-384.

Solomon, M. J. & Varshavsky, A. (1985) Formaldehyde-mediated DNA-protein crosslinking: a probe for *in vivo* chromatin structures. *Proceeding of the National Academy of Sciences,* 82**,** 6470-6474.

Sood, V., Cajigas, I., D'Urso, A., Light, W. H. & Brickner, J. H. (2017) Epigenetic transcriptional memory of *GAL* genes depends on growth in glucose and the Tup1 transcription factor in *Saccharomyces cerevisiae*. *Genetics,* 206**,** 1895-1907.

Sopko, R., Raithatha, S. & Stuart, D. (2002) Phosphorylation and maximal activity of *Saccharomyces cerevisiae* meiosis-specific transcription factor Ndt80 is dependent on Ime2. *Molecular and Cellular Biology,* 22**,** 7024-7040.

Soulard, A., Cremonesi, A., Moes, S., Schütz, F., Jenö, P. & Hall, M. N. (2010) The rapamycin-sensitive phosphoproteome reveals that TOR controls protein kinase A toward some but not all substrates. *Molecular Biology of the Cell,* 21**,** 3475-3486.

Spencer, V. A., Sun, J. M., Li, L. & Davie, J. R. (2003) Chromatin immunoprecipitation: a tool for studying histone acetylation and transcription factor binding. *Methods,* 31**,** 67-75.

Spoel, S. H., Mou, Z., Tada, Y., Spivey, N. W., Genschik, P. & Dong, X. (2009) Proteasome-mediated turnover of the transcription coactivator NPR1 plays dual roles in regulating plant immunity. *Cell,* 137**,** 860-872.

Stanhill, A., Schick, N. & Engelberg, D. (1999) The yeast Ras/cyclic AMP pathway induces invasive growth by suppressing the cellular stress response. *Molecular and Cellular Biology,* 19**,** 7529-7538.

Stracka, D., Jozefczuk, S., Rudroff, F., Sauer, U. & Hall, M. N. (2014) Nitrogen source activates TOR (target of rapamycin) complex 1 via glutamine and independently of Gtr/Rag proteins. *Journal of Biological Chemistry,* 289**,** 25010-25020.

Strich, R., Surosky, R. T., Steber, C., Dubois, E., Messenguy, F. & Esposito, R. E. (1994) *UME6* is a key regulator of nitrogen repression and meiotic development. *Genes & Development,* 8**,** 796-810.

Su, S. S. & Mitchell, A. P. (1993) Identification of functionally related genes that stimulate early meiotic gene expression in yeast. *Genetics,* 133**,** 67-77.

Sumrada, R. A. & Cooper, T. G. (1987) Ubiquitous upstream repression sequences control activation of the inducible arginase gene in yeast. *Proceedings of the National Academy of Sciences,* 84**,** 3997-4001.

Swaney, D. L., Beltrao, P., Starita, L., Guo, A., Rush, J., Fields, S., Krogan, N. J. & Villén, J. (2013) Global analysis of phosphorylation and ubiquitylation cross-talk in protein degradation. *Nature Methods,* 10**,** 676-682.

Swinnen, E., Wanke, V., Roosen, J., Smets, B., Dubouloz, F., Pedruzzi, I., Cameroni, E., De Virgilio, C. & Winderickx, J. (2006) Rim15 and the crossroads of nutrient signalling pathways in *Saccharomyces cerevisiae*. *Cell Division,* 1**,** 3.

Takeshige, K., Baba, M., Tsuboi, S., Noda, T. & Ohsumi, Y. (1992) Autophagy in yeast demonstrated with proteinase-deficient mutants and conditions for its induction. *Journal of Cell Biology,* 119**,** 301-311.

Tamaki, H. (2007) Glucose-stimulated cAMP-protein kinase A pathway in yeast *Saccharomyces cerevisiae*. *Journal of Bioscience and Bioengineering,* 104**,** 245-250.

Tan, K., Feizi, H., Luo, C., Fan, S. H., Ravasi, T. & Ideker, T. G. (2008) A systems approach to delineate functions of paralogous transcription factors: role of the Yap family in the DNA damage response. *Proceedings of the National Academy of Sciences,* 105**,** 2934-2939.

Tanaka, N. & Mukai, Y. (2015) Yeast Cyc8p and Tup1p proteins function as coactivators for transcription of Stp1/2p-dependent amino acid transporter genes. *Biochemical and Biophysical Research Communications,* 468**,** 32-38.

Tartas, A., Zarkadas, C., Palaiomylitou, M., Gounalaki, N., Tzamarias, D. & Vlassi, M. (2017) Ssn6-Tup1 global transcriptional co-repressor: Role of the N-terminal glutamine-rich region of Ssn6. *PLOS One,* 12**,** e0186363.

Tate, J. J., Rai, R. & Cooper, T. G. (2018) More than one way in: three Gln3 sequences required to relieve negative Ure2 regulation and support nuclear Gln3 import in *Saccharomyces cerevisiae*. *Genetics,* 208**,** 207-227.

Tedesco, M., La Sala, G., Barbagallo, F., De Felici, M. & Farini, D. (2009) STRA8 shuttles between nucleus and cytoplasm and displays transcriptional activity. *Journal of Biological Chemistry,* 284**,** 35781-35793.

ter Schure, E. G., van Riel, N. A. W. & Verrips, C. T. (2000) The role of ammonia metabolism in nitrogen catabolite repression in *Saccharomyces cerevisiae*. *FEMS Microbiology Reviews,* 24**,** 67-83.

The *C. elegans* Sequencing Consortium (1998) Genome Sequence of the Nematode *C. elegans*: A Platform for Investigating Biology. *Science,* 282**,** 2012-2018.

Toda, T., Cameron, S., Sass, P., Zoller, M. & Wigler, M. (1987) Three different genes in S. cerevisiae encode the catalytic subunits of the cAMP-dependent protein kinase. *Cell,* 50**,** 277-287.

Tomás-Cobos, L. & Sanz, P. (2002) Active Snf1 protein kinase inhibits expression of the *Saccharomyces cerevisiae HXT1* glucose transporter gene. *Biochemical Journal,* 368**,** 657-663.

Treitel, M. A. & Carlson, M. (1995) Repression by SSN6-TUP1 is directed by MIG1, a repressor/activator protein. *Proceedings of the National Academy of Sciences,* 92**,** 3132-3136.

Trumbly, R. J. (1992) Glucose repression in the yeast *Saccharomyces cerevisiae*. *Molecular Microbiology,* 6**,** 15-21.

Tsou, J. H., Chang, K. C., Chang-Liao, P. Y., Yang, S. T., Lee, C. T., Chen, Y. P., Lee, Y. C., Lin, B. W., Lee, J. C., Shen, M. R., Chuang, C. K., Chang, W. C., Wang, J. M. & Hung, L. Y. (2011) Aberrantly expressed AURKC enhances the transformation and tumourigenicity of epithelial cells. *Journal of Pathology,* 225**,** 243-254.

Tsuchiya, D., Yang, Y. & Lacefield, S. (2014) Positive feedback of *NDT80* expression ensures irreversible meiotic commitment in budding yeast. *PLOS Genetics,* 10**,** e1004398.

Türeci, Ö., Sahin, U., Zwick, C., Koslowski, M., Seitz, G. & Pfreundschuh, M. (1998) Identification of a meiosis-specific protein as a member of the class of cancer/testis antigens. *Proceedings of the National Academy of Sciences,* 95**,** 5211-5216.

Tzamarias, D. & Struhl, K. (1994) Functional dissection of the yeast Cyc8-Tup1 transcriptional co-repressor complex. *Nature,* 369**,** 758-761.

Tzamarias, D. & Struhl, K. (1995) Distinct TPR motifs of Cyc8 are involved in recruiting the Cyc8-Tup1 corepressor complex to differentially regulated promoters. *Genes & Development,* 9**,** 821-831.

van der Voorn, L. & Ploegh, H. L. (1992) The WD-40 repeat. *FEBS Letters,* 307**,** 131-134.

van Werven, F. J. & Amon, A. (2011) Regulation of entry into gametogenesis. *Philosophical Transactions of the Royal Society B Biological Sciences,* 366**,** 3521-3531.

van Werven, F. J., Neuert, G., Hendrick, N., Lardenois, A., Buratowski, S., van Oudenaarden, A., Primig, M. & Amon, A. (2012) Transcription of two long non-coding RNAs mediates mating type control of gametogenesis in budding yeast. *Cell,* 150**,** 1170-1181.

Varanasi, U. S., Klis, M., Mikesell, P. B. & Trumbly, R. J. (1996) The Cyc8 (Ssn6)-Tup1 corepressor complex is composed of one Cyc8 and four Tup1 subunits. *Molecular and Cellular Biology,* 16**,** 6707-6714.

Venters, B. J. & Pugh, B. F. (2009) How eukaryotic genes are transcribed. *Critical Reviews in Biochemistry and Molecular Biology,* 44**,** 117-141.

Vershon, A. K. & Pierce, M. (2000) Transcriptional regulation of meiosis in yeast. *Current Opinion in Cell Biology,* 12**,** 334-339.

Wagstaff, J. E., Klapholz, S. & Esposito, R. E. (1982) Meiosis in haploid yeast. *Proceedings of the National Academy of Sciences,* 79**,** 2986-2990.

Wahi, M. & Johnson, A. D. (1995) Identification of genes required for alpha 2 repression in Saccharomyces cerevisiae. *Genetics,* 140**,** 79-90.

Wang, A., Kurdistani, S. K. & Grunstein, M. (2002) Requirement of Hos2 histone deacetylase for gene activity in yeast. *Science,* 298**,** 1412-1414.

Wang, W., Li, P., Schettino, A., Peng, Z. & McLeod, M. (1998) Characterization of functional regions in the *Schizosaccharomyces pombe mei3* developmental activator. *Genetics,* 150**,** 1007-1018.

Ward, M. P., Gimeno, C. J., Fink, G. R. & Garrett, S. (1995) SOK2 may regulate cyclic AMP-dependent protein kinase-stimulated growth and pseudohyphal development by repressing transcription. *Molecular and Cellular Biology,* 15**,** 6854-6863.

Warringer, J. & Blomberg, A. (2006) Evolutionary constraints on yeast protein size. *BMC Evolutionary Biology,* 6**,** 61.

Wasserstrom, L., Dünkler, A., Walther, A. & Wendland, J. (2017) The APSES protein Sok2 is a positive regulator of sporulation in *Ashbya gossypii*. *Molecular Microbiology,* 106**,** 949-960.

Watson, A. D., Edmondson, D. G., Bone, J. R., Mukai, Y., Yu, Y., Du, W., Stillman, D. J. & Roth, S. Y. (2000) Ssn6-Tup1 interacts with class I histone deacetylases required for repression. *Genes & Development,* 14**,** 2737-2744.

Weidberg, H., Moretto, F., Spedale, G., Amon, A. & van Werven, F. J. (2016) Nutrient control of yeast gametogenesis is mediated by TORC1, PKA and energy availability. *PLOS Genetics,* 12**,** e1006075.

Whyte, Warren A., Orlando, David A., Hnisz, D., Abraham, Brian J., Lin, Charles Y., Kagey, Michael H., Rahl, Peter B., Lee, Tong I. & Young, Richard A. (2013) Master transcription factors and Mediator establish super-enhancers at key cell identity genes. *Cell,* 153**,** 307-319.

Williams, F. E., Varanasi, U. & Trumbly, R. J. (1991) The CYC8 and TUP1 proteins involved in glucose repression in Saccharomyces cerevisiae are associated in a protein complex. *Molecular and Cellular Biology,* 11**,** 3307-3316.

Winter, E. (2012) The Sum1/Ndt80 transcriptional switch and commitment to meiosis in *Saccharomyces cerevisiae*. *Microbiology and Molecular Biology Reviews,* 76**,** 1-15.

Wolfe, K. H. (2015) Origin of the yeast whole-genome duplication. *PLOS Biology,* 13**,** e1002221.

Wong, K. H. & Struhl, K. (2011) The Cyc8-Tup1 complex inhibits transcription primarily by masking the activation domain of the recruiting protein. *Genes & Development,* 25**,** 2525-2539.

Wood, V., Gwilliam, R., Rajandream, M. A., Lyne, M., Lyne, R., Stewart, A., Sgouros, J., Peat, N., Hayles, J., Baker, S., Basham, D., Bowman, S., Brooks, K., Brown, D., Brown, S., Chillingworth, T., Churcher, C., Collins, M., Connor, R., Cronin, A., Davis, P., Feltwell, T., Fraser, A., Gentles, S., Goble, A., Hamlin, N., Harris, D., Hidalgo, J., Hodgson, G., Holroyd, S., Hornsby, T., Howarth, S., Huckle, E. J., Hunt, S., Jagels, K., James, K., Jones, L., Jones, M., Leather, S., McDonald, S., McLean, J., Mooney, P., Moule, S., Mungall, K., Murphy, L., Niblett, D., Odell, C., Oliver, K., O'Neil, S., Pearson, D., Quail, M. A., Rabbinowitsch, E., Rutherford, K., Rutter, S., Saunders, D., Seeger, K., Sharp, S., Skelton, J., Simmonds, M., Squares, R., Squares, S., Stevens, K., Taylor, K., Taylor, R. G., Tivey, A., Walsh, S., Warren, T., Whitehead, S., Woodward, J., Volckaert, G., Aert, R., Robben, J., Grymonprez, B., Weltjens, I., Vanstreels, E., Rieger, M., Schäfer, M., Müller-Auer, S., Gabel, C., Fuchs, M., Fritzc, C., Holzer, E., Moestl, D., Hilbert, H., Borzym, K., Langer, I., Beck, A., Lehrach, H., Reinhardt, R., Pohl, T. M., Eger, P., Zimmermann, W., Wedler, H., Wambutt, R., Purnelle, B., Goffeau, A., Cadieu, E., Dréano, S., Gloux, S., Lelaure, V., et al. (2002) The genome sequence of *Schizosaccharomyces pombe*. *Nature,* 415**,** 871-880.

Wu, J., Suka, N., Carlson, M. & Grunstein, M. (2001) TUP1 utilizes histone H3/H2B-specific HDA1 deacetylase to repress gene activity in yeast. *Molecular Cell,* 7**,** 117-126.

Xia, Z., Turner, G. C., Hwang, C. S., Byrd, C. & Varshavsky, A. (2008) Amino acids induce peptide uptake via accelerated degradation of CUP9, the transcriptional repressor of the PTR2 peptide transporter. *Journal of Biological Chemistry,* 283**,** 28958-28968.

Xiao, L., Zhao, Z., He, F. & Du, Z. (2019) Multivariable regulation of gene expression plasticity in metazoans. *bioRxiv***,** doi: 10.1101/692863.

Xie, J., Wang, X. & Proud, C. G. (2016) mTOR inhibitors in cancer therapy. *F1000Research,* 5**,** pii: F1000 Faculty Rev-2078.

Xu, L., Ajimura, M., Padmore, R., Klein, C. & Kleckner, N. (1995) NDT80, a meiosis-specific gene required for exit from pachytene in Saccharomyces cerevisiae. *Molecular and Cellular Biology,* 15**,** 6572-6581.

Yaguchi, S., Mitsui, K., Kawabata, K., Xu, Z. & Tsurugi, K. (1996) The pleiotropic effect of the *GTS1* gene product on heat tolerance, sporulation and the life span of *Saccharomyces cerevisiae*. *Biochemical and Biophysical Research Communications,* 218**,** 234-237.

Yamamoto, M. (1996) Regulation of meiosis in fission yeast. *Cell Structure and Function,* 21**,** 431-436.

Youk, H. & Lim, W. A. (2014) Secreting and sensing the same molecule allows cells to achieve versatile social behaviors. *Science,* 343**,** 1242782.

Zaman, Z., Ansari, A. Z., Koh, S. S., Young, R. & Ptashne, M. (2001) Interaction of a transcriptional repressor with the RNA polymerase II holoenzyme plays a crucial role in repression. *Proceedings of the National Academy of Sciences,* 98**,** 2550-2554.

Zeytuni, N. & Zarivach, R. (2012) Structural and functional discussion of the tetra-trico-peptide repeat, a protein interaction module. *Structure,* 20**,** 397-405.

Zhang, Z. & Reese, J. C. (2004a) Redundant mechanisms are used by Ssn6–Tup1 in repressing chromosomal gene transcription in *Saccharomyces cerevisiae*. *Journal of Biological Chemistry,* 279**,** 39240-39250.

Zhang, Z. & Reese, J. C. (2004b) Ssn6-Tup1 requires the ISW2 complex to position nucleosomes in *Saccharomyces cerevisiae*. *The EMBO Journal,* 23**,** 2246-2257.
Zhao, H., Wang, Q., Liu, C., Shang, Y., Wen, F., Wang, F., Liu, W., Xiao, W. & Li, W. (2018) A role for the respiratory chain in regulating meiosis initiation in *Saccharomyces cerevisiae*. *Genetics,* 208**,** 1181-1194.
Zhao, Y., Granas, D. & Stormo, G. D. (2009) Inferring binding energies from selected binding sites. *PLOS Computational Biology,* 5**,** e1000590.